ON THE SECRECY ANALYSIS OF COGNITIVE RADIO NETWORKS

Abstract: The increasing number of connected devices represents a major challenge for broadband wireless networks that would require a paradigm shift towards the development of key enabling technologies for the fifth-generation wireless networks. One of the key challenges towards realizing the next-generation wireless networks, however, is the scarcity of spectrum, owing to the unprecedented broadband penetration rate in recent years. Cognitive radio has emerged as a promising solution to the current spectrum crunch. Assuming a spectrum sharing scenario, the unlicensed users, also known as secondary users, opportunistically access the spectrum of primary (licensed) users under the constraint of not causing harmful interference to them.

Similarly to traditional wireless networks, cognitive radio networks (CRNs) could be vulnerable to several attacks that could disrupt their operation. Eavesdropping attack is one of the security threats that can occur at the physical layer. Therein, unauthorized users try to overhear the communication between legitimate users. Since the SUs have to continuously adapt their transmit power to avoid causing harmful interference to the PUs, ensuring the security at the physical layer becomes a challenging task. Although several research works have investigated physical layer security (PLS) of wireless communication networks, secrecy analysis of CRNs is among the hottest research topics that are in their infancy. Therefore, in this thesis, the PLS of several cognitive radio-based wireless communication systems has been investigated and some main techniques such as friendly jammer, space diversity, and energy harvesting have been considered for security enhancement purposes.

The first phase of work focused on investigating the impact of exploiting a multi-antenna relay to forward the message from a source to the intended destination. Indeed, secrecy metrics have been derived by considering a generalized fading model namely, Nakagami-*m*. The second phase of investigation consisted in performing secrecy analysis of different EH-based CRNs. Specifically, focus was placed on deriving closed-form and asymptotic expressions for the secrecy outage probability, based on which the impact of different key parameters of the network was investigated and new insights were gained. Finally, we focused our efforts on investigating the impact of a friendly jammer on the secrecy performance of CRNs. Indeed, our aim was to continuously send an artificial noise that could be added to the eavesdroppers' signal and thus decrease his signal-to-noise ratio. However, given the power adaption constraint of secondary users, we were uncertain whether a friendly jammer would contribute to the enhancement of the secrecy performance of CRNs. Therefore, secrecy metrics were derived based on which we were able to conclude meaningful insights as to when a friendly jammer could improve the secrecy of a given communication system. Moreover, another main contribution consisted in deriving a new and generalized expression for the intercept probability representing communication between two nodes, through the aid of a relay performing decode-and-forward protocol, in the presence of two eavesdroppers at the first and second hop.

Keywords: Cognitive radio networks, dual-hop based satellite communication, eavesdropping, energy harvesting, fading channels, friendly jammer, intercept probability, maximum tolerated interference power, physical layer security, power-splitting, secrecy capacity, secrecy outage probability, time-switching.

Mounia BOUABDELLAH
ON THE SECRECY ANALYSIS OF COGNITIVE RADIO NETWORKS
N° thèse : 197/ST2I
Année : 2021

Année : 2021

Thèse N° : 197/ST2I

École Nationale Supérieure d'Informatique et d'Analyse des Systèmes
Centre d'Études Doctorales en Sciences des Technologies de l'Information et de l'Ingénieur

THÈSE DE DOCTORAT

ON THE SECRECY ANALYSIS OF COGNITIVE RADIO NETWORKS

Présentée par

Mounia BOUABDELLAH

Le 20/01/2021

Formation doctorale : Informatique
Structure de recherche : Équipe Information, Communication and Embedded Systems (ICES)

JURY

Professeur Mohamed ESSAAIDI PES, ENSIAS, Université Mohammed V de Rabat	**Président**
Professeur Faissal EL BOUANANI PH, ENSIAS, Université Mohammed V de Rabat	**Directeur de thèse**
Professeur Ana García ARMADA Full Professor, Universidad Carlos III de Madrid, Spain	**Rapporteur**
Professeur Osamah BADARNEH Professor, German-Jordanian University, Jordan	**Rapporteur**
Professeur Fouad AYOUB PH, CRMEF, Kénitra	**Rapporteur**
Professeur Mohamed-Slim ALOUINI Full Professor, KAUST, Kingdom of Saudi Arabia	**Examinateur**
Professeur Sami MUHAIDAT Full Professor, Khalifa University, United of Arab Emirates	**Examinateur**
Professeur Hussain BEN-AZZA PH, ENSAM, Université Moulay Ismail, Meknès	**Examinateur**

Abstract

The increasing number of connected devices represents a major challenge for broadband wire less networks that would require a paradigm shift towards the development of key enabling technologies for the fifth-generation wireless networks. One of the key challenges towards realizing the next-generation wireless networks, however, is the scarcity of spectrum, owing to the unprecedented broadband penetration rate in recent years. Cognitive radio has emerged as a promising solution to the current spectrum crunch. Assuming a spectrum sharing scenario, the unlicensed users, also known as secondary users, opportunistically access the spectrum of primary (licensed) users under the constraint of not causing harmful interference to them.

Similarly to traditional wireless networks, cognitive radio networks (CRNs) could be vulnerable to several attacks that could disrupt their operation. Eavesdropping attack is one of the security threats that can occur at the physical layer. Therein, unauthorized users try to overhear the communication between legitimate users. Since the SUs have to continuously adapt their transmit power to avoid causing harmful interference to the PUs, ensuring the security at the physical layer becomes a challenging task. Although several research works have investigated physical layer security (PLS) of wireless communication networks, secrecy analysis of CRNs is among the hottest research topics that are in their infancy. Therefore, in this thesis, the PLS of several cognitive radio-based wireless communication systems has been investigated and some main techniques such as friendly jammer, space diversity, and energy harvesting have been considered for security enhancement purposes.

The first phase of work focused on investigating the impact of exploiting a multi-antenna relay to forward the message from a source to the intended destination. Indeed, secrecy metrics have been derived by considering a generalized fading model namely, Nakagami-m. The second phase of investigation consisted in performing secrecy analysis of different EH-based CRNs. Specifically, focus was placed on deriving closed-form and asymptotic expressions for the secrecy outage probability, based on which the impact of different key parameters of the network was investigated and new insights were gained. Finally, we focused our efforts on investigating the impact of a friendly jammer on the secrecy performance of CRNs. Indeed, our aim was to continuously send an artificial noise that could be added to the eavesdroppers signal and thus

decrease his signal-to-noise ratio. However, given the power adaption constraint of secondary users, we were uncertain whether a friendly jammer would contribute to the enhancement of the secrecy performance of CRNs. Therefore, secrecy metrics were derived based on which we were able to conclude meaningful insights as to when a friendly jammer could improve the secrecy of a given communication system. Moreover, another main contribution consisted in deriving a new and generalized expression for the intercept probability representing communication between two nodes, through the aid of a relay performing decode-and-forward protocol, in the presence of two eavesdroppers at the first and second hop.

Keywords: Cognitive radio networks, dual-hop based satellite communication, eavesdropping, energy harvesting, fading channels, friendly jammer, intercept probability, maximum tolerated interference power, physical layer security, power-splitting, secrecy capacity, secrecy outage probability, time-switching.

Contents

List of Figures

List of Tables

Acknowledgment

I am grateful to my thesis supervisor professor Faissal El Bouanani for his continuous help and support during all these years of the Ph.D. program. I would like to express my gratitude to him for his availability in supervising and helping me improve my research performance. Without his valuable feedback, permanent guidance, and encouragement this work would not have been successfully completed. I cannot find the words to thank him enough for everything he has done and he is doing to help me achieve my goals and succeed in my research career.

I would like to pay my special regards to professor Hussain Ben-azza for his assistance and to the Ph.D. committee members for their time in reviewing this work and for their valuable remarks. I am also thankful to my family, friends, colleagues, and all the people at ENSIAS, Mohammed V University in Rabat whose assistance was a milestone in the completion of this thesis. Especially, I wish to acknowledge the support and encouragement of my parents which helped me overcome all the hurdles and successfully complete my thesis.

Nomenclature

Acronyms

Acronym	Meaning	Acronym	Meaning
AF	Amplify-and-forward	MIMO	Multiple-input multiple-output
AWGN	Additive white Gaussian noise	MRC	Maximal-ratio combining
CDF	Cumulative distribution function	MTIP	Maximum tolerated interference power
CRN	Cognitive radio network	NLOS	Non-line of sight
DSA	Dynamic spectrum allocation	OGS	Optical ground station
DF	Decode-and-forward	PDF	Probability density function
EH	Energy harvesting	PLS	Physical layer security
FSA	Fixed spectrum allocation	PS	Power splitting
FSO	free space optics	PU	Primary user
FSPL	Free space path-loss	RF	Radio-frequency
HSTCN	Hybrid satellite-terrestrial cognitive network	RV	Random variable
i.i.d	Independent and identically distributed	SU	Secondary user
i.n.i.d	Independent and non-identically distributed	SC	Selection combining
IP	Intercept probability	SNR	Signal-to-noise ratio
LOS	Line-of-sight	SOP	Secrecy outage probability
MC	Monte-Carlo	TS	Time switching

List of symbols

Symbol	Meaning
C_s	Secrecy capacity
$f_{.}(z)$	Probability density function
$F_{.}(z)$	Cumulative distribution function
γ_Z	SNR at Z
$\Gamma(.)$	Gamma function
$\Gamma(.,.)$	Upper incomplete Gamma function
$\gamma_{inc}(.,.)$	Lower incomplete Gamma function
$\Psi(.)$	Digamma function
$\mathbb{E}_X[.]$	Expectation operator with respect to X
$G_{p,q}^{m,n}\left(z\middle\vert \begin{matrix}(a_v)_{v\leq p}\\(b_w)_{w\leq q}\end{matrix}\right)$	Meijer's G-function
$G_{p,q}^{m,n}\left(z\middle\vert \begin{matrix}(a_l,\alpha_l)_{l\leq p}\\(b_r,\beta_r)_{r\leq q}\end{matrix}\right)$	Incomplete Meijer's G-function
$G_{p_1,q_1:p_2,q_2:p_3,q_3}^{0,n_1:m_2,n_2:m_3,n_3}$	Bivariate Meijer's G-function
$\|h\|_F$	Frobenius norm of a vector h
h_l	Fading amplitude of link l
$g_l = \|h_l\|^2$	Channel gain of link l
m_l	Fading severity parameter of link l
α_l, β_l	Turbulence-induced fading parameters
P_{Tx}	Transmit power of node Tx
$P_{Tx}^{\max}$	Maximum transmit power at node Tx
x_{Tx}	Transmitted signal from node Tx
y_{Rx}	received signal at node Rx
P_I	Maximum tolerated interference power at PU receiver
n_Z	Additive white Gaussian noise(AWGN) at node Z
d_Z	Distance between the satellite and the node Z
b_X	Half average power of the multi-path component
Ω_X	Average power of LOS component
r	Detection technique parameter
ϕ	Path-loss exponent
γ_{th}	Decoding threshold SNR
$K_v(.)$	Modified Bessel function of the second kind
${}_1F_1(.;.;.)$	Confluent hypergeometric function
j	$\sqrt{-1}$

General Introduction

In recent years, the proliferation of mobile devices has led to unprecedented demand for wireless spectrum and energy-efficient solutions [1–4]. In this regard, cognitive radio and energy harvesting (EH) paradigms have emerged as promising solutions to ensure spectrum and energy efficiency. Specifically, cognitive radio allows effective utilization of the spectrum [5, 6], while EH enables devices to harvest energy from ambient RF signals [7, 8]. In underlay cognitive radio networks (CRNs), the issue of radio-frequency spectrum scarcity is alleviated by allowing the secondary users (SUs) to share the spectrum with primary users (PUs) under the condition of not causing any harmful interference to them [9–11]. Consequently, the SUs are required to continuously adjust their transmit powers in order to meet the PUs' quality of service (QoS).

Under the conditions of spectrum and energy efficiency constraints, ensuring the physical layer security (PLS) of multi-hop CRNs becomes a challenge of utmost importance. It has been demonstrated by Wyner in his seminal work [12] that a system is secure if the capacity of the legitimate user is higher than that of the wiretap channel. However, in practical scenarios, the main channel does not always have a higher capacity. Therefore, in order to achieve secure communication, one can either increase the capacity of the main link or decrease the one of eavesdropping channel. To do so, several techniques have been proposed in the literature, including exploiting (i) a friendly jammer to transmit artificial noise to malicious eavesdroppers [13–16], (ii) cooperative transmission through one or multiple relays [17–21], (iii) space diversity [22–26], (iv) employing zero-forcing precoding techniques [27–30], etc.

Problematic and contributions

The deployment of CRNs requires the consideration of more realistic scenarios and investigating the joint impact of multiple key parameters of the network. Although several research works

have investigated the PLS of CRNs, many system setups (e.g., presence of multiple eavesdroppers, uplink communication system in the presence of multiple users, harvesting energy from SU signals instead of PU signals, etc.) have not been considered yet in the literature due to the complexity of the analytical approaches. For instance, several works such as [31–35] investigated the PLS of EH-based systems by considering that the energy-constrained node is harvesting energy from PU signals. On the other hand, the impact of a jamming signal on the system's security has been extensively investigated for traditional wireless networks [13–16], whereas few research works have dealt with jamming signal in the case of CRNs.

Therefore, the main objectives of this thesis are as follows

- To fill the existent gap in the literature with regard to the PLS of dual-hop CRNs, we aimed at considering more realistic scenarios such as the presence of multiple eavesdroppers, uplink communication system in the presence of multiple users, etc.

- Differently from the existing works, we aim to investigate the secrecy performance of EH-based CRNs where the energy is harvested from the SU signals which added another layer of complexity to assess the security of the system.

- To the best of our knowledge, few research works have investigated the impact of jamming signals on the physical layer security of CRNs [36, 37]. Therefore, our aim was to investigate the impact of jamming-signal on the overall system's security under the condition of power adaptation constraint of an SU friendly jammer.

The main contributions of this thesis are

- We inspect the impact of space diversity on the secrecy performance of a dual-hop CRNs over a generalized fading model, namely Nakagami-m [38].

- Investigate the PLS of EH-based CRNs by considering that SU relay is harvesting energy from the SU source. The analytical expressions for the considered secrecy metric are derived over independent and non-identically distributed (i.n.id) and independent and identically distributed Rayleigh fading models [39, 40].

- We investigate the PLS of jamming-based CRNs along with space diversity and we attempt to answer the following question: Can better secrecy be achieved without jamming

by considering a single antenna at eavesdroppers and multiple-ones at the legitimate users (i.e., relay and end-user) rather than sending permanently an artificial noise and considering that both the relay and the destination are equipped with a single antenna, while multiple antennas are used by the eavesdroppers? [41–44].

- We provide a new framework for the IP of a dual-hop decode-and-forward (DF) relaying in the presence of eavesdroppers at each hop based on which we investigate the PLS of a hybrid satellite-terrestrial cognitive network (HSTCN) and attempt to answer the following question: could a friendly jammer further enhance the security of a system even in a low SNR regime? [44].

Structure

The remainder of this dissertation is organized as follows: Chapter 1 depicts a state of art, while Chapter 2 represents our contribution dealing with the impact of space diversity on the CRN security. Chapter 3 depicts our contributions dealing with the performance analysis of EH-based underlay CRN, while in Chapter 4, our contributions related to the secrecy performance of jamming-based underlay CRN are presented. Finally, several conclusions and perspectives are provided.

Chapter 1

State of Art

In this chapter, a review of the wireless communication in the form of either radio frequency (RF) signals or optical light waves along with the channel impairments is presented. Techniques such as diversity, jamming-based communication, EH are also introduced and their impact on improving the security is highlighted.

1.1 Wireless Communications

In this section, technologies allowing for an efficient spectrum utilization are introduced. Although these technologies allow mitigating spectrum scarcity issue, they can be subject to several channel impairments that could degrade the performance of a communication system. Therefore, the main channel impairments for both RF and free space optics (FSO) along with some corresponding mitigation techniques are also provided in this section.

1.1.1 RF and visible spectrum

Wireless communication is ensured through electromagnetic waves that are transmitted in the free space. The wireless transmission can be performed by either using radio waves in the range 300 kHz and 300 GHz or optical light waves which accounts for the visible spectrum ranging from 300 GHz to 3000 THz.

1.1.2 Cognitive radio networks

The proliferation of mobile users over the last decade resulted in an unprecedented demand for radio spectrum resources leading to a spectrum scarcity issue [45,46]. Since the radio spectrum is a very limited resource, its allocation policy is controlled by some authorities such as the national agency for the legalization of communications (ANRT) in Morocco and the federal communications commission (FCC) in the US. The main role of these authorities is to assign the radio spectrum to some users for specific technologies and services using static spectrum allocation policies. Recent studies revealed that, under this fixed spectrum allocation (FSA) policy, certain channels can be heavily occupied while others are rarely used [47, 48]. In this regard, developing new techniques for spectrum allocation becomes mandatory in order to achieve and efficient spectrum utilization and alleviate the spectrum scarcity issue.

Since the allocated spectrum is not always exploited by their owners called primary users (PUs), a new spectrum allocation policy could be established to mitigate the spectrum scarcity problem. In contrast to FSA, a dynamic spectrum allocation (DSA) policy can be used to achieve a better exploitation of the spectrum by allowing unlicensed users also called secondary users (SUs) to share spectrum with PUs [49, 50]. In order to perform DSA, several solutions have been proposed, including cognitive radio [49–53]. Indeed, cognitive radio can be defined as intelligent radio frequency transmitter/receiver able to detect available channels and adjust its transmission parameters to use these channels. Therefore, this new paradigm allows the SUs to opportunistically access the radio spectrum assigned to PUs under the condition of not causing harmful interference to existing traffics. Depending on the knowledge that is required to access the spectrum of the primary network, cognitive radio approaches fall into three distinct categories namely, underlay, overlay, and interweave [54].

Underlay cognitive radio

This mode is known to be efficient in terms of spectrum utilization as it allows the SUs to simultaneously share the spectrum with the active PUs (i.e., the PUs are also using the spectrum) [54]. This can be performed under the condition of not causing harmful interference to the primary network. Therefore, the main functions to achieve a better performance in underlay CRN are spectrum sharing and spectrum mobility. The former allows multiple SUs

to coordinate with the PUs and transmit their data simultaneously with them. The latter deals with the changeover channels when spectrum access policies are violated (i.e. harmful interference is introduced to the PU signals). In order to avoid interfering with PU signals, the SU node has to adapt his transmit power as [39]

$$P_S = \min\left(P_S^{\max}, \frac{P_I}{g_{SP}}\right), \tag{1.1}$$

where $P_S^{\max}$ is the maximal transmit power of the SU, P_I accounts for the maximum tolerated interference power (MTIP) at the PU receiver, and $g_{SP} = |h_{SP}|^2$ with h_{SP} standing for the fading amplitude of the link between SU transmitter and the PU receiver.

Interweave cognitive radio

In this mode, the SUs access the spectrum only when it is not used by the PUs. To do so, the SUs are required to continuously perform spectrum sensing in order to detect available spectrum holes that are unoccupied by the PUs. It has been reported by several research works (e.g. [55], [56]) that the network's performance can be deteriorate by an imperfect spectrum sensing. Spectrum decision is another important function that is used to select the best available channels. Similarity to underlay mode, spectrum mobility is of utmost importance as it allows vacating some frequency bands when the PUs start using them.

Overlay cognitive radio

Differently from the two previous modes, the overlay mode allows the SUs to share the spectrum with the PUs under the condition to act as a relay to PUs' messages [57]. Therefore, the SU has to continuously adapt its transmit power as in (1.1).

1.1.3 FSO communication

Similarly to CRNs, FSO technology could be also used as an alternative solution to overcome the spectrum scarcity issue and provide high data rate. Indeed, high-speed communication (i.e., Tbps per optical beam) can be achieved by employing FSO technology [58] where the data is transmitted with the help of an optical source emitting light beams in either visible (400-800 nm) or infrared (1500-1550 nm) spectrum bands [59, 60]. Besides providing high data rate,

FSO communication is most immune to the interference and provide a high level of security against wiretapping attacks due to its narrow beamwidth. Despite the advantages of the FSO technology, the optical feeder is vulnerable to several critical issues, such as the atmospheric turbulence, and pointing error loss due to beam wandering [61].

Atmospheric turbulence

Optical light wave propagation in the atmosphere is subject to random fluctuations due to atmospheric turbulence. Such impairment is caused mainly by the rapid changes in the temperature, pressure, as well as the refractive index change in the propagation environment [62]. This latter factor leads to creating several turbulent cells with different indices of refraction, called *eddies*. To this end, the refractive index structure parameter and the Rytov variance are the two key parameters that describe the turbulence effect. In the context of vertical optical links, the altitude-dependent refractive structure index parameter in $\mathrm{m}^{-\frac{2}{3}}$ can be expressed for the uplink using the Hufnagel-Valley Boundary model as [63, Eq. (10)]

$$C_n^2(h) = 0.00594 \left(\frac{V_w}{27}\right)^2 \left(10^{-5}h\right)^{10} e^{-\frac{h}{1000}} + 2.7 \times 10^{-10} e^{-\frac{h}{1500}} + A e^{-\frac{h}{100}}, \tag{1.2}$$

with h is the altitude in meters, V_w stands for the wind speed in m/s, and A is the measured value of the refractive index structure parameter at the ground (i.e., $h = 0$). A mostly common value for A is to $A = 1.7 \times 10^{-14}$ $\mathrm{m}^{-\frac{2}{3}}$ for $V_w = 21$ m/s [64]. Based on the above result, the Rytov variance is given as [65]

$$\sigma_R^2 = 8.70 \int_{h_0}^{d_\upsilon} C_n^2(h) \left(\left[\frac{L\lambda\vartheta^2(h)}{\pi W_L^2} + i\vartheta\left(h\right)\left(1 + \frac{L\vartheta(h)}{F}\right)\right]^{\frac{5}{6}} - \left(\frac{L\lambda}{\pi W_L^2}\right)^{\frac{5}{6}} \vartheta^{\frac{5}{3}}\left(h\right) \right) dh, \tag{1.3}$$

where $\vartheta\left(h\right) = \frac{d_\upsilon - h}{d_\upsilon - h_0}$, d_υ and h_0 are the satellite and optical ground station (OGS) altitudes with respect to the sea level, $L = \frac{d_\upsilon - h_0}{\cos(\theta_0)}$ with θ_0 referring to the satellite's zenith angle with respect to the OGS, λ is the operating wavelength, and [65, 66]

$$F = d_\upsilon - h_0 + \frac{z_0}{d_\upsilon - h_0}, \tag{1.4}$$

$$W_L^2 = W_0^2 \left(1 + \frac{\left(d_\upsilon - h_0\right)^2}{z_0^2}\right) + 2\left(\frac{2\lambda\left(d_\upsilon - h_0\right)}{\pi r_{0,s}}\right)^2, \tag{1.5}$$

denote the radius of curvature and the square of the beam waist at the satellite altitude, with W_0 stands for the beam waist at the origin, $z_0 = \frac{\pi W_0^2}{\lambda}$ is the Rayleigh distance, and [66]

$$r_{0,s} = \left[0.42\left(\frac{2\pi}{\lambda}\right)^2 \int_0^{d_v - h_0} C_n^2(h)\left(1 - \frac{h}{d_v - h_0}\right)^{\frac{5}{3}} dh\right]^{-\frac{3}{5}}, \tag{1.6}$$

refers to the coherence diameter.

Gamma-Gamma model, proposed by [64], considers that the light propagation through a turbulent medium consists of small-scale (i.e., scattering) and large-scale (i.e., refraction) effect. The PDF of the normalized received irradiance I_a subject to atmospheric turbulence is given by [62]

$$f_{I_a}(x) = \frac{2\left(\alpha\beta\right)^{\frac{\alpha+\beta}{2}}}{\Gamma\left(\alpha\right)\Gamma\left(\beta\right)} x^{\frac{\alpha+\beta}{2}-1} K_{\alpha-\beta}\left(2\sqrt{\alpha\beta x}\right), x \geq 0, \tag{1.7}$$

where $K_v\left(.\right)$ is the modified Bessel function of the second kind and v-th order [67, Eq. (8.432.1)]. Importantly, the turbulence-induced fading parameters $\alpha > 0$ and $\beta > 0$ are expressed in terms of the Rytov variance σ_R^2 given in (1.2) as follows [63, 68]

$$\alpha = \left[\exp\left(\frac{0.49\sigma_R^2}{\left(1 + 1.11\sigma_R^{\frac{12}{5}}\right)^{\frac{7}{6}}}\right) - 1\right]^{-1}, \tag{1.8}$$

$$\beta = \left[\exp\left(\frac{0.51\sigma_R^2}{\left(1 + 0.69\sigma_R^{\frac{12}{5}}\right)^{\frac{5}{6}}}\right) - 1\right]^{-1}. \tag{1.9}$$

Remark 1. *It can be noticed from (1.8) and (1.9) that α and β increase with the increasing of the Rytov variance. Therefore, it can be seen from (1.2) and (1.3) that the greater the wind speed V_w is, the stronger is the turbulence.*

Beam wandering and pointing error

The beam wandering is a phenomenon which occurs when the size of turbulence eddies are larger than the beam size. This results in a random deflection of the beam from its propagating direction by several hundreds of meters, and thus results in pointing error issue [69]. In such an instance, the pointing error strength, which is the ratio between the equivalent beam waist at the satellite altitude and the beam wander displacement variance, is the key parameter that

quantifies the pointing error loss severity, given as [70]

$$\xi = \frac{W_{eq}}{2\sigma_s^2}, \tag{1.10}$$

where σ_s^2 and W_{eq} are the random beam wander displacement variance as well as the equivalent beam waist, being expressed as [65, 70]

$$\sigma_s^2 = \mathcal{B}_w \left[1 - \frac{\frac{\pi^2 W_0^2}{r_{0,s}}}{1 + \frac{\pi^2 W_0^2}{r_{0,s}}} \right], \tag{1.11}$$

$$W_{eq} = W_L \sqrt{\operatorname{erf}\left(\sqrt{\frac{\pi R}{2W_L}} \right) \sqrt{\frac{W_L}{2R}} \exp\left(\frac{\pi R}{4W_L} \right)}, \tag{1.12}$$

respectively, with erf(.) is the error function [67, Eq. (8.250.1)], R is the receiver's aperture radius, $\mathcal{B}_w = 0.54 \left(d_v - h_0\right)^2 \left(\frac{\lambda}{2W_0}\right)^2 \left(\frac{2W_0}{r_{0,s}}\right)^{\frac{5}{3}}$ denotes the beam wander displacement in meters. A widely used statistical model for representing the PDF of the normalized received irradiance I_p subject to pointing error impairment is given as [70]

$$f_{I_p}(x) = \frac{\xi^2}{A_0^{\xi^2}} x^{\xi^2 - 1}; \quad 0 \leq x \leq A_0, \tag{1.13}$$

where $A_0 = \left(\operatorname{erf}\left(\sqrt{\frac{\pi R}{2W_L}}\right)\right)^2$ is the fraction of the collected power at $\rho = 0$ such that ρ is the distance between the bean footprint and the receiver photoelectric center.

Notwithstanding that in the context of pointing loss impairment, tracking and pointing algorithms are among the key solutions the reduction of the pointing error impact [69].

Free-space path-loss

Similarly to the RF communication, its FSO counterpart can be impaired by FSPL, which is a deterministic phenomenon that arises from the atmosphere and layers particles absorption and scattering. Herein, the propagating photons either lose their energy through absorption or get deflected through scattering. A general expression for the normalized received light irradiance

is given as [69]

$$\begin{aligned} I_l &= \frac{I_r}{I_0} \\ &= \exp\left[-\sec(\theta_0)\int_{h_0}^{d_v} c(\lambda,h)\,dh\right], \theta_0 \neq \frac{\pi}{2}, \end{aligned} \tag{1.14}$$

with $\sec(.) = \frac{1}{\cos(.)}$ is the secant function, θ_0 refers to the satellite's zenith angle with respect to the OGS, I_0 and I_r are the transmit and receive irradiances in $\mathrm{W/m^2}$, respectively, and $c(\lambda,h)$ stands for the wavelength and altitude-dependent attenuation coefficient, and is given by [69]

$$c(\lambda,h) = a_m(\lambda,h) + a_e(\lambda,h) + b_m(\lambda,h) + b_e(\lambda,h), \tag{1.15}$$

with $a_m(\lambda,h)$, $a_e(\lambda,h)$, $b_m(\lambda,h)$, $b_e(\lambda,h)$ denote the molecular, aerosol absorption coefficients and their scattering counterparts, respectively which are depending on both frequency and altitude.

SNR statistical representation

Capitalizing on the PDF expressions in (1.7) and (1.13) alongside [71, Eq. (03.04.26.0008.01)] and some algebraic manipulations, the respective PDF and CDF of the SNR $\gamma_Z = \frac{(\eta I)^r}{\sigma_N^2}$ can be obtained as [60]

$$f_{\gamma_Z}(z) = \frac{\mathcal{O}_Z}{rz} G_{1,3}^{3,0}\left(\Upsilon_Z \sqrt[r]{\frac{z}{\mu_r^{(Z)}}}\,\middle|\, \begin{matrix} -;\xi_Z^2+1 \\ \xi_Z^2,\alpha_Z,\beta_Z;- \end{matrix}\right), \tag{1.16}$$

$$F_{\gamma_Z}(z) = \frac{r^{\alpha_Z+\beta_Z-2}\mathcal{O}_Z}{(2\pi)^{r-1}} G_{r+1,3r+1}^{3r,1}\left(\frac{\Upsilon_Z^r z}{r^{2r}\mu_r^{(Z)}}\,\middle|\, \begin{matrix} 1;\kappa_1^{(Z)} \\ \kappa_2^{(Z)};0 \end{matrix}\right), \tag{1.17}$$

where $\sqrt[r]{.}$ denotes the rth root, $\mathcal{O}_Z = \frac{\xi_Z^2}{\Gamma(\alpha_Z)\Gamma(\beta_Z)}$, $\mu_r^{(Z)} = \mathbb{E}[\gamma_Z]$, $\Upsilon_Z = \frac{\xi_Z^2\alpha_Z\beta_Z}{\xi_Z^2+1}$, $\kappa_1^{(Z)} = \left\{\frac{\xi_Z^2+i}{r}\right\}_{i=1:r}$, $\kappa_2^{(Z)} = \left\{\frac{\xi_Z^2+i}{r}, \frac{\alpha_Z+i}{r}, \frac{\beta_Z+i}{r}\right\}_{i=0:r-1}$, $G_{p,q}^{m,n}\left(.\,\middle|\, \begin{matrix}(a_k)_{k\leq p}\\(b_k)_{k\leq q}\end{matrix}\right)$ denotes the Meijer G-function [67, Eq. (9.301)], and r is a detection technique depending-parameter (i.e., $r = 1$ refers to coherent detection, and $r = 2$ accounts for the direct detection).

1.1.4 Wireless channel impairments

To design reliable wireless communication systems, it is imperative to understand how propagating radio waves are attenuated. Indeed, the propagation of electromagnetic waves in the free-space (wireless channel) is susceptible to several impairments including channel impediments, interference, and noise that are unpredictably changing over time [72]. These impairments could result in a variation in received signal power due to free-space path loss, shadowing, and multipath fading [72, 73].

Free-space path-loss

The free-space path-loss (FSPL) represents a deterministic attenuation of the signal strength between the transmitter and receiver over a communication channel free from obstacles. Since variation in the signal strength occurs over large distances (100-1000 meters), this attenuation is sometimes termed to as large-scale propagation effects [72]. The FSPL can be modeled as [74]

$$\frac{P_r}{P_t} = G_t G_r \left(\frac{\lambda}{4\pi d_{ref}}\right)^2 \left(\frac{d_{ref}}{d}\right)^{\phi}. \tag{1.18}$$

where P_t and P_r are the transmitted and received powers, respectively, G_t and G_r are the transmitter and the receiver antenna gains, respectively, λ is the wavelength, d_{ref} and d is a reference distance for the antenna far-field and the distance between the transmitter and the receiver, and ϕ is the environment-dependent path-loss exponent.

Shadowing

Shadowing phenomena occurs when the transmitted signal encounters obstructing large-scale objects (e.g., buildings, trees, etc) throughout the communication channel which results in random fluctuations of the signal envelope and thus attenuation of the signal power [75, 76].

Fading

In a typical wireless communication environment, the transmitted signal encounters multiple objects throughout the communication channel which creates reflected, diffracted, or scattered copies of the signal [72] as shown in Figure 1.1. These copies, also called multipath signal

components, reach the receiver with random delays, magnitudes, and phases. The summation of these components at the receiver results in a distortion of the signal(i.e., fading) [72, 76].

Generally, one can distinguish between two types of fading, namely fast and slow fading. In the former, the channel impulse response changes rapidly during a symbol duration T_s, while in the latter no change occurs over time [77].

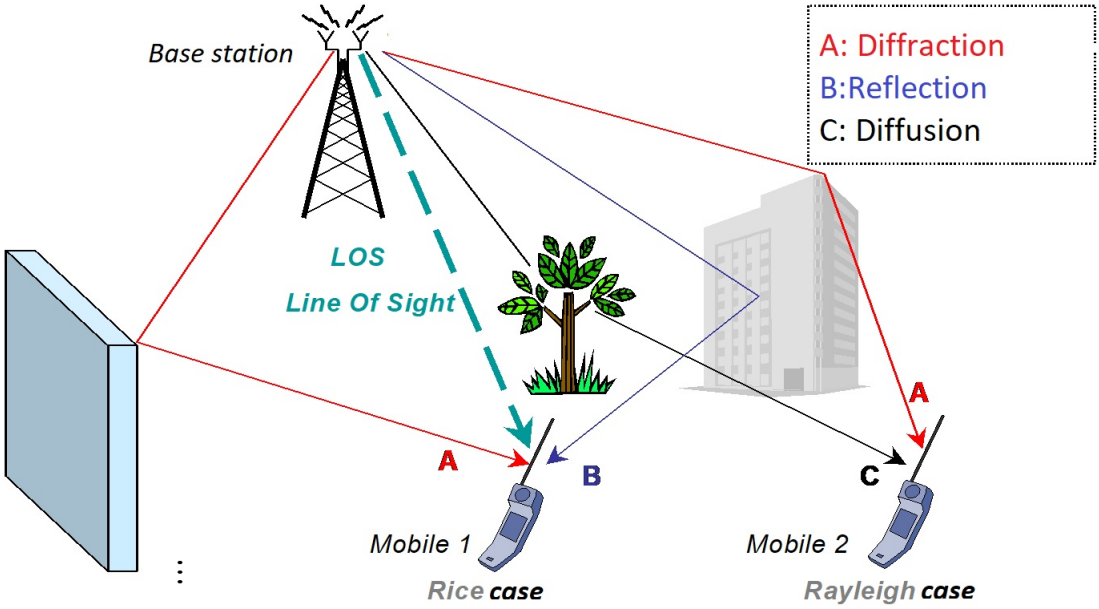

Figure 1.1: Multipath wireless propagation.

1.1.5 RF fading models

Given the random variation of the signal strength due to fading phenomena, several statistical models have been proposed in the literature to characterize the fading. In the sequel, we will present exclusively the RF fading models considered in our research works.

Rayleigh fading

Rayleigh distribution is used to characterize the propagation of a transmitted signal through a communication channel where no line-of-sight (LOS) exists [72]. The probability density function (PDF) of the fading amplitude h is expressed as [73, Eq.(2.6)]

$$f_h(x) = \frac{2x}{\Omega} \exp\left(\frac{-x^2}{\Omega}\right), x \geq 0, \tag{1.19}$$

where $\Omega = \mathbb{E}_h[h^2]$ represents the average fading power, and $\mathbb{E}_X[.]$ denotes expectation operator with respect to the random variable (RV) X.

Nakagami-m fading

Nakagami-m fading is generally suitable for land-mobile and indoor mobile multipath propagation [73]. The PDF of Nakagami-m distribution is given as [73, Eq. (2.20)]

$$f_h(x) = \frac{2m^m x^{2m-1}}{\Gamma(m)\,\Omega^m} \exp\left(-\frac{mx^2}{\Omega}\right), x \geq 0, \tag{1.20}$$

where $\Gamma(.)$ denotes the Euler Gamma function [67, Eq. (8.310)], $\Omega = \mathbb{E}_h[h^2]$, with $m \geq 0.5$ denotes the fading severity parameter. It is worth mentioning that when $m = 1$, Nakagami-m is reduced to Rayleigh model.

Shadowed Rician fading

Shadowed Rician fading model perfectly describes the land mobile satellite (LMS) channel. The PDF of the channel gain corresponding to a link l can be characterized as

$$\begin{aligned} f_{g_l}(x) &= \Delta_l e^{-\beta_l x}\ {}_1F_1(m_l; 1; \delta_l x) \\ &\overset{(a)}{=} \Delta_l e^{-\upsilon_l x} \sum_{n=0}^{m_l-1} \phi_l^{(n)} x^n, \end{aligned} \tag{1.21}$$

where $\Delta_l = \frac{1}{2b_l}\left(\frac{2b_l m_l}{2b_l m_l+\Omega_l}\right)^{m_l}$, $\upsilon_l = \beta_l - \delta_l$, $\beta_l = \frac{1}{2b_l}$, $\delta_l = \frac{\beta_l \Omega_l}{2b_l m_l+\Omega_l}$, $\phi_l^{(n)} = \frac{(m_l-1)!\delta_l^n}{(m_l-1-n)!(n!)^2}$, ${}_1F_1(.;.;.)$ denotes the confluent hypergeometric function [67, Eq. (9.210)], and step (a) follows by assuming that m_l is a positive-valued number and by using jointly Eqs. (06.10.02.0003.01) and (07.20.03.0025.01) of [71]. The corresponding cumulative distribution function (CDF) can be straightforwardly obtained from the above PDF as

$$\begin{aligned} F_{g_l}(x) &= \Delta_l \sum_{n=0}^{m_l-1} \phi_l^{(n)} \int_0^x t^n e^{-\upsilon_l t} dt \\ &= \Delta_l \sum_{n=0}^{m_l-1} \frac{\phi_l^{(n)}}{\upsilon_l^{n+1}} \gamma_{inc}(n+1, \upsilon_l x), \end{aligned} \tag{1.22}$$

where $\gamma_{inc}(.,.)$ denotes the lower incomplete Gamma function [67, Eq. (8.350.1)].

1.2 Diversity Systems

To mitigate the destructive effect of multipath fading and enhance the reliability of a communication system, diversity techniques had been proposed as an effective solution by combining constructively multiple replicas of the transmitted signal at the receiver. Indeed, it has been suggested that these replicas would experience independent fading, which would reduce the probability that all paths could fade simultaneously. Diversity can be achieved using multiples approaches, namely [73]

- **Time Diversity:** Consists in sending multiple copies of the signal over different time slots. To circumvent the intersymbol interference, the time slots have to be separated by the channel coherence time [72].
- **Frequency Diversity:** Multiple copies of the signal are transmitted at the same time using different carrier frequencies. In a similar manner, these frequencies have to be separated by the coherence bandwidth so as to experience independent fading scenario [73].
- **Space Diversity:** Consists in transmitting the signal over different propagation paths. This could be achieved by using multiple transmit and/or receive antennas [76]. In order to avoid fading correlation, the antennas have to be separated by at least half the wavelength [72].
- **Intelligent reflecting surfaces (IRSs):** Consists of matrix of small reflecting elements able to reflect smartly the transmitted signal towards the end-user, regardless of its position [78].

Among combining techniques that have been proposed in the literature, one can highlight the most practical ones:

- **Maximal-ratio combining (MRC):** with the help of such a receiver, the received copies are linearly combined together after removing the phase shift and using optimal weights equal to the fading amplitudes [72, 79]. Therefore, the combined SNR at the receiver can be expressed as

$$\gamma = \sum_{i=1}^{L} \gamma_i, \tag{1.23}$$

where L is the number of diversity branches.

- **Equal-gain combining (EGC):** Differently from MRC, this receiver corrects the phase shift of the received signals and then combines them with equal gain [73, 80]. Hence, the combined SNR is given by

$$\gamma = \frac{\left(\sum_{i=1}^{L} \sqrt{\gamma_i}\right)^2}{L}. \tag{1.24}$$

- **Selection combining (SC):** This technique consists in selecting the antenna with the highest SNR [73, 80]. Therefore, the SNR can be expressed as

$$\gamma = \max_{i \leq L} \gamma_i. \tag{1.25}$$

1.3 Energy Harvesting

The rapid increase of internet of things (IoT) devices with limited power constraints has led to unprecedented demand for energy efficient solutions. Indeed, prolonging the lifetime of energy-constrained nodes is the key factor towards achieving self-sustaining futuristic wireless networks. In this regard, harvesting energy from radio-frequency (RF) signals has gained considerable attention during the past years [81–89]. Besides, environmental sources of energy (e.g., thermal, vibration, and solar), energy-constrained nodes could scavenge energy from ambient radio sources such as TV broadcast and cellular networks so as to ensure a long-term functioning and sustainability of mobile communication.

1.3.1 Wireless EH protocols

In the literature, as it can be seen in Fig. 1.2 one can distinguish three main wireless EH protocols:

1. Wireless power transfer (WPT): Consists of transferring only energy signals to the energy-constrained node without sending information signals [86, 87].

2. Wireless-powered communication network (WPCN): EH is carried out in a first time slot by the energy-constrained node following information transfer in a second time slot [88].

3. Simultaneous wireless information and power transfer (SWIPT): The concept of SWIPT was first introduced in [89] where both EH and information processing could be carried out simultaneously.

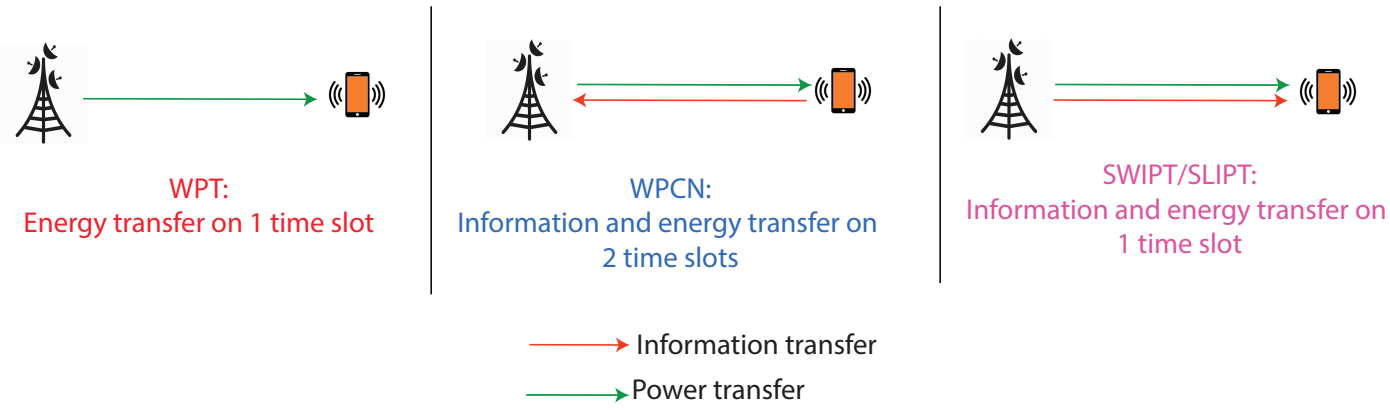

Figure 1.2: Wireless EH protocols.

1.3.2 Variants of SWIPT protocol

Due to the robustness of SWIPT protocol, compared to the two other aforementioned ones, it has been considered in our contributions in Chapter 3. Indeed, two SWIPT variants have been presented in the literature, namely, time switching (TS) and power splitting (PS) [84, 85].

Time Switching

TS protocol allocates portion of the time to EH and dedicates the rest to information processing. As illustrated in Fig. 1.3a, the energy-constrained relay node performs information processing during αT_0, $0 \leq \alpha \leq 1$ and harvests energy during $(1-\alpha)T_0$ where T_0 stands for the dedicated time slot for S-R communication. Therefore, the harvested energy at the relay is given by

$$E_H = \eta(1-\alpha)P_S \left|h_{SR}\right|^2 T_0, \tag{1.26}$$

where η, P_S, and h_R denote the energy conversion efficiency ($0 < \eta < 1$), the source's transmit power, and fading coefficient, respectively.

Power Splitting

The PS protocol splits the received signal into two streams, one for EH and the other one for information decoding. As depicted in Fig. 1.3b, the relay uses a fraction of power αP_S to carry out the information processing, while the remaining power $(1-\alpha)\,P_S$ is used to harvest energy. Therefore, the harvested energy is given by

$$E_H \;=\; \eta P_S(1-\alpha)\,|h_{SR}|^2\,T_0. \tag{1.27}$$

Importantly, the harvested energy by the relay R is assumed to be used for forwarding the information signal to its destination during a time slot T_1. Therefore, the transmit power at the relay is

$$P_R = \frac{E_H}{T_1} = \frac{\eta P_S\,|h_{SR}|^2\,(1-\alpha)T_0}{T_1}, \tag{1.28}$$

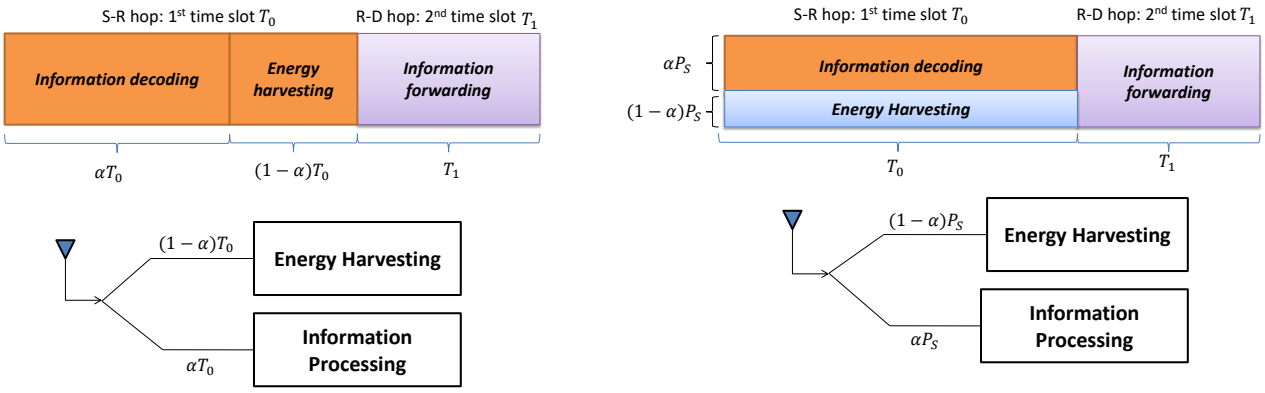

(a) TS scheme (b) PS scheme

Figure 1.3: Variants of SWIPT protocol.

1.4 Jamming-based systems

Jamming-based communication systems consists in exploiting, in addition to the transmitter S, a legitimate node J to transmit an artificial noise and thus cause interference at the eavesdropper node E. Therefore, the SNR at E can be expressed as

$$\gamma_E = \frac{P_S g_{SE}}{P_J g_{JE} + N}, \tag{1.29}$$

with P_S and P_J are the transmit powers of the source and friendly jammer, respectively, g_{SE} and g_{JE} represent the channel gains of the link S-E and J-E, respectively, and N is the noise power..

One can see from (1.29) that increasing the transmit power of a friendly jammer decreases the SNR at the eavesdropper and therefore this techniques allows reducing the capacity of the eavesdropping link, which contributes to the enhancement of the communication system's security.

It is worth mentioning that in this dissertation, we assumed that the legitimate node is able to cancel out the artificial noise, whereas the eavesdropper cannot cancel it. Indeed, this can be achieved by generating an artificial noise using a pseudo-random sequence that is known to the legitimate nodes which allows them to cancel out this noise, while this sequence remains unknown to the illegitimate ones. Since our main aim is to investigate the PLS of CRNs under different system setups, noise cancellation techniques are out of the scope in this thesis.

1.5 Physical layer security performance metrics

The broadcast nature of wireless transmission gives the possibility to malicious users to overhear the communication channel. Indeed, eavesdropping attack occurs when a malicious user intercepts the communication of the legitimate users. Traditionally, security can be ensured using cryptographic techniques that rely on using secret keys to encrypt messages at upper layers. Although a good security level of the transmitted messages could be achieved using these cryptographic techniques, they are performed at the cost of computational overhead as well as additional system complexity for secret key management and distribution. Therefore, PLS, which leverages the characteristics of the wireless communication channels, gained a sig-

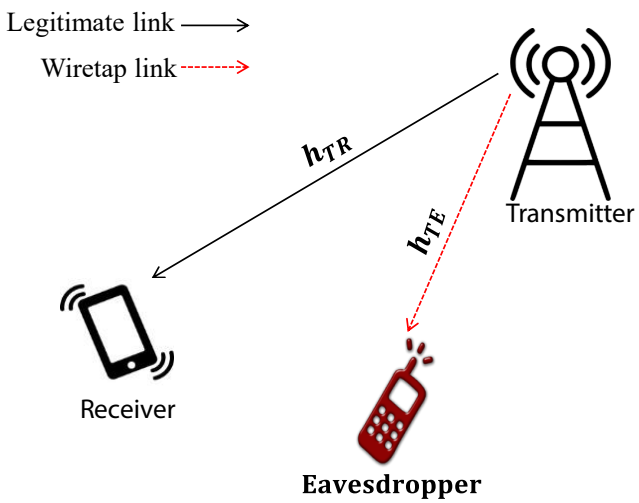

Figure 1.4: Eavesdropping attack of an RF transmission.

nificant attention as an enhancing security technique complementary to cryptography. In this context, it has been pioneeringly demonstrated by Wyner in his seminal work [12] that perfect secrecy can be achieved when the capacity of the legitimate channel, i.e., the link between the source and the destination is better than the one of the eavesdropping channel. Therefore, the secrecy capacity emerged as a new paradigm measuring the difference between the capacities of the main and eavesdropping channels so as to investigate the secrecy performance of a wireless communication system. Mathematically speaking, such a metric is defined as

$$C_s = \left[C_L - C_E\right]^+, \tag{1.30}$$

where $C_L = \log_2(1+\gamma_L)$ and $C_E = \log_2(1+\gamma_E)$ represent the capacities of the main and wiretap links, respectively, γ_L and γ_E refer to the SNR of the legitimate and eavesdropping links, respectively, and $[x]^+ = \max(x, 0)$.

For a dual-hop communication system, the secrecy capacity of the end-to-end communication system is given by

$$C_S = \min(C_{1S}, C_{2S}), \tag{1.31}$$

with C_{qS} denotes the secrecy capacities at the qth hop which is defined as

$$C_{1S} = \begin{cases} \log_2\left(\dfrac{1+\gamma_R}{1+\gamma_{1E}}\right) & , \ \gamma_R > \gamma_{1E} \\ 0 & , \ \text{elsewhere} \end{cases} \tag{1.32}$$

and

$$C_{2S} = \begin{cases} \log_2\left(\dfrac{1+\gamma_D}{1+\gamma_{2E}}\right) & , \ \gamma_D > \gamma_{2E} \\ 0 & , \ \text{elsewhere} \end{cases} \tag{1.33}$$

where γ_R, γ_{qE}, γ_D, account for the SNR at the relay R, eavesdropper when intercepting communication at the qth hop, and destination D, respectively.

1.5.1 Secrecy outage probability

The secrecy outage probability (SOP) can be used as a key performance metric to assess the secrecy level of a given communication system. This metric accounts for the probability that the secrecy capacity falls below a predefined secrecy rate R_s [90]

$$\text{SOP} = \Pr\left(C_s \leq R_s\right), \tag{1.34}$$

1.5.2 Intercept probability

The intercept probability (IP) is another secrecy performance metric that stands for the probability that the capacity of the legitimate link is smaller than the eavesdropping link's one. Therefore, the IP can be expressed as [91]

$$P_{int} = \Pr\left(C_s \leq 0\right), \tag{1.35}$$

1.5.3 Average secrecy capacity

The average secrecy capacity (ASC) is another PLS metric quantifying the average behavior of the gap between the legitimate and wiretapper capacities, irrespective of time. Explicitly, the ASC can be expressed as [92]

$$\overline{C}_s = \mathbb{E}_{\gamma_L,\gamma_E}\left[C_s\right]. \tag{1.36}$$

Particularly, the metrics given in (1.34)-(1.36) for a direct communication link, can be expressed, respectively, as

$$\text{SOP} = \int_0^\infty F_{\gamma_L}\left(2^R\left(z+1\right)-1\right) f_{\gamma_E}(z)dz, \tag{1.37}$$

$$P_{int} = \int_0^\infty F_{\gamma_L}\left(z\right) f_{\gamma_E}(z)dz, \tag{1.38}$$

and

$$\overline{C}_s = \frac{1}{\ln(2)}\int_0^\infty \frac{F_{\gamma_{SE}}(z)}{1+z} F^c_{\gamma_{eq}}\left(z\right) dz, \tag{1.39}$$

With $F^c_{\cdot}$ is the complementary CDF.

It is worth mentioning that neither the SOP nor the IP have been derived in the literature for a decode-and-forward (DF) dual-hop communication system in the presence of two eavesdroppers. Therefore, a contribution of this thesis is to provide a framework for IP evaluation when two eavesdroppers are intercepting communication at both hops.

Remark 2. *One can see from (1.34) and (1.35) that a perfect secrecy can be achieved by maximizing C_s. This can be attained by either maximizing the capacity of the legitimate link (i.e., increasing γ_L) or minimizing the one of the eavesdropping link (i.e., decreasing γ_E). To do so, multiple techniques can be used such as exploiting (i) a friendly jammer to send an artificial noise and consequently degrade the SNR at the eavesdropper, (ii) MIMO techniques to enhance the SNR at legitimate nodes, (iii) EH to provide the relay with maximal power for transmission, etc.*

Chapter 2

PLS of CRNs assisted MIMO

2.1 Introduction

2.1.1 Motivation

Space diversity such as MIMO managed by diversity combining techniques, e.g. MRC or SC, can be used in practice to overcome the challenge of unreliable communications by strengthening the combined SNR of the legitimate user.

In CRN, the PLS using multi-antenna techniques has been investigated by considering either (i) the presence of a direct communication link between the source and destination [93–96] or (ii) a cooperative relaying technique [97–101]. Secrecy metrics have been derived, in the presence of a direct communication link, by considering diverse scenarios namely, single-input multi-output (SIMO) channels with SC at both the legitimate receiver and the eavesdropper [93–95], MIMO systems with transmit antenna selection and different receiver combining schemes [96]. On the other hand, cooperative relaying technique received much interests as it could extend the wireless coverage while improving the secrecy performance of a given communication system. The PLS of a cooperative CRN has been investigated by considering multiple relays such that only one relay is selected to forward the message to its intended destination [97–100]. The secrecy performance over Rayleigh fading channels of a multi-antenna relay has been investigated in [101].

Although the above works have added new insights to the research field, they have mainly focused on direct-link communication system or on the case of cooperative relaying with multiple

relays. Few research works considered the case of a multi-antenna relaying system. To fill this gap, we focused our efforts on investigating the impact of spatial diversity on a dual-hop CRN by considering a more generalized fading, namely Nakagami-m model.

2.1.2 Contribution

The main contributions of this chapter can be summarized as follows

- The exact expression for the SOP is derived by considering a dual-hop CRN where the information is forwarded to its intended destination through a multi-antenna relay and under the attempt of the eavesdropper to intercept the transmitted information at both communication hops.
- Based on the derived expression for the SOP, the impact of different key parameters of the network are investigated. Meaningful insights are gained in terms of the impact of spatial diversity on the system's security.

2.1.3 Chapter's structure

The remainder of this chapter is organized as follows. In Section II, the system and channel models are presented. The closed-form expression for the SOP is derived in Section III. In Section IV, we provide and discuss the numerical and simulation results. Finally, Section V concludes this chapter.

2.2 System and channel model

The considered CR communication system represented in Fig. 2.1 consists of one SU source S that communicates with one SU destination D through one SU relay R in the presence of one eavesdropper E. This eavesdropper is intercepting the transmitted information at both communication hops (i.e. S -R and R-D). The SUs are opportunistically accessing the spectrum of the primary network consisting of one PU transmitter PU_{Tx}, and one PU receiver PU_{Rx}. The relay is assumed to be equipped with multiple antennas and performs MRC technique to combine the multiple copies of the signal received on its L branches. On the other hand, all other nodes are supposed to be equipped with single antenna namely, S, E, D, PU_{Tx}, and

PU_{Rx}. As the SUs in CRN share the spectrum with the PUs hence their transmission power is constrained by the MTIP P_I at the PU receiver. These powers are expressed as

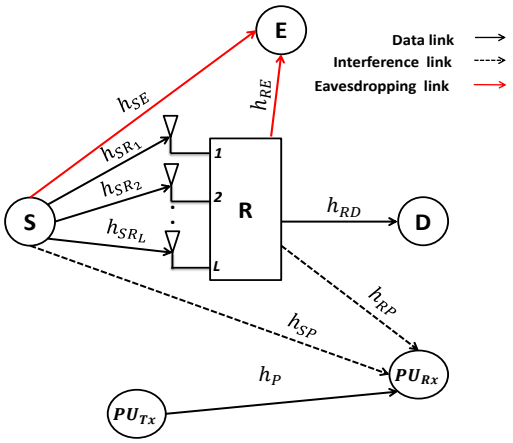

Figure 2.1: The considered CR communication system.

$$P_S = \min\left(P_S^{\max}, \frac{P_I}{g_{SP}}\right), \tag{2.1}$$

and

$$P_R = \min\left(P_R^{\max}, \frac{P_I}{g_{RP}}\right), \tag{2.2}$$

where $P_S^{\max}$ and $P_R^{\max}$ denote the maximal transmit power at S and R, respectively, and P_I accounts for the MTIP at the primary receiver.

For the sake of simplicity, we consider that the fading amplitudes of all channels are Nakagami-m distributed. Let m_i and Ω_i denote the fading severity and the average channel power gain, respectively, where $i \in \{SP, SR_k, RP, RD, RE\}$. For the sake of simplicity, we denote the channel power gains as $g_i = |h_i|^2$. As $|h_i|$ is Nakagami-m distributed, the channel power gains are Gamma distributed with shape and scale parameters m_i and $\lambda_i = \frac{m_i}{\Omega_i}$.

The PDF as well as the CDF of the channel power gains are given as

$$f_{g_i}(x) = \frac{\lambda_i^{m_i}}{\Gamma(m_i)} x^{m_i - 1} e^{-\lambda_i x}, \tag{2.3}$$

$$F_{g_i}(x) = \frac{\gamma(m_i, \lambda_i x)}{\Gamma_{inc}(m_i)}. \tag{2.4}$$

For a positive number m_i, the above CDF can be written in terms of finite simple series

as [67, Eq. (8.352.1)]

$$F_{g_i}(x) = 1 - e^{-\lambda_i x} \sum_{k=0}^{m_i-1} \frac{\lambda_i^k x^k}{k!}. \tag{2.5}$$

According to [97], the combined signal at the MRC output of R can be expressed as

$$y_R = \sqrt{P_S} \parallel \mathbf{h}_{SR} \parallel x_s + w_R n_R, \tag{2.6}$$

where $\parallel . \parallel$ accounts for the Frobenius norm , $\mathbf{h}_{SR}$ is the $L \times 1$ channel vector from the S to R, x_s is the transmitted signal from S, and n_R stands for the additive white Gaussian noise (AWGN) $L \times 1$ channel vector with variance N_R and zero mean. The MRC weight vector is $w_R = \frac{\mathbf{h}_{SR}^{\dagger}}{||\mathbf{h}_{SR}||}$, where the symbol † denotes the transpose conjugate.

Moreover, the received signal at D can be also expressed as

$$y_D = \sqrt{P_R} h_{RD} x_r + n_D, \tag{2.7}$$

where x_r is the transmitted signal of R and n_D is the AWGN of mean zero and variance N_D. The received signals at the eavesdropper from the source and from the relay are given as

$$y_{jE} = \sqrt{P_j} h_{jE} x_j + n_E, j \in \{S, R\}, \tag{2.8}$$

where n_E represents the additive noise assumed to be AWGN with zero mean and variance N_E. Without loss of generality, we assume, in what follows, that all noise powers are equal, that is $N_E = N_R = N_D = N$.

2.3 Secrecy outage probability

The secrecy capacity of the considered system is defined as in (1.31), where

- γ_R is the combined SNR at R

$$\gamma_R = \min\left(\overline{\gamma}_s, \frac{\overline{\gamma}_P}{g_{SP}}\right) \sum_{l=1}^{L} g_{SR_l}, \tag{2.9}$$

with $\overline{\gamma}_s = \frac{P_S^{max}}{N}$ and $\overline{\gamma}_P = \frac{P_I}{N}$.

We assume that the fading amplitudes of all links between S and the L branches of R are independent and identically Nakagami-m distributed (i.i.d) (i.e, $\lambda_{SR_k} = \lambda_{SR}$). Hence, the sum of all the channel gains $\sum_{l=1}^{L} g_{SR_l}$ is Gamma distributed with the shape and scale parameters $m_{SR} = \sum_{l=0}^{L} m_{SR_i}$ and λ_{SR}, respectively.

- γ_D is the SNR at D and can be expressed as

$$\gamma_D = \min\left(\overline{\gamma}_R, \frac{\overline{\gamma}_P}{g_{RP}}\right) g_{RD}, \tag{2.10}$$

with $\overline{\gamma}_R = \frac{P_R^{max}}{N}$.

- γ_{qE} denotes the SNR at the eavesdropper and can be expressed as

$$\gamma_{qE} = \min\left(\overline{\gamma}_{A_q}, \frac{\overline{\gamma}_P}{g_{A_qP}}\right) g_{A_qE}, \tag{2.11}$$

where $A_1 = S$ and $A_2 = R$.

Now, substituting (1.31) into (1.34), the SOP can be expressed as

$$\begin{aligned} \text{SOP} &= \Pr\left(\min(C_{S1}, C_{S2}) < R_S\right) \\ &= 1 - \left[1 - \text{SOP}_1\right]\left[1 - \text{SOP}_2\right], \end{aligned} \tag{2.12}$$

with $\text{SOP}_q = \Pr\left(C_{Sq} < R_S\right)$ denotes the SOP at the qth hop.

Theorem 2.3.1. *The expressions of* SOP_1 *and* SOP_2 *under Nakagami-m fading channels assumption are expressed as*

$$\text{SOP}_1 = 1 - \frac{\lambda_{SE}^{m_{SE}}}{\Gamma(m_{SE})} \sum_{k=0}^{m_{SR}-1} \frac{\lambda_{SR}^k}{k!} \sum_{j=0}^{k} \psi_{k,j}^{(1)} \left[\frac{\alpha_1\delta_1}{\overline{\gamma}_s^k \chi_S^{m_{SE}+j}} + \frac{\theta_1 \Theta_{j,k}^{(1)}}{\overline{\gamma}_P^k}\right]. \tag{2.13}$$

and

$$\text{SOP}_2 = 1 - \frac{\lambda_{RE}^{m_{RE}}}{\Gamma(m_{RE})} \sum_{k=0}^{m_{RD}-1} \frac{\lambda_{RD}^k}{k!} \sum_{j=0}^{k} \psi_{k,j}^{(2)} \left(\frac{\alpha_2\delta_2}{\overline{\gamma}_R^k \chi_R^{m_{RE}+j}} + \frac{\theta_2 \Theta_{j,k}^{(2)}}{\overline{\gamma}_P^k}\right). \tag{2.14}$$

where

$$\psi_{k,j}^{(q)} = \binom{k}{j} \gamma^j \left(\gamma - 1\right)^{k-j} \Gamma\left(m_{B_qE} + j\right), \; B_1 = S, \; B_2 = R \tag{2.15}$$

$$\alpha_q = \frac{\gamma\left(m_{B_qP}, \frac{\lambda_{B_qP}\overline{\gamma}_P}{\overline{\gamma}_{B_q}}\right)}{\Gamma\left(m_{B_qP}\right)}, \tag{2.16}$$

$$\delta_1 = \frac{e^{-\frac{\lambda_{SR}(\gamma-1)}{\overline{\gamma}_S}}}{\overline{\gamma}_S^{m_{SE}}}, \tag{2.17}$$

$$\chi_S = \frac{\lambda_{SR}\gamma + \lambda_{SE}}{\overline{\gamma}_S}, \tag{2.18}$$

$$\theta_q = \frac{\lambda_{B_qP}^{m_{B_qP}}}{\Gamma(m_{B_qP})\overline{\gamma}_P^{m_{B_qE}}}, \tag{2.19}$$

$$\Theta_{j,k}^{(1)} = \frac{\left(\frac{\overline{\gamma}_P}{\lambda_{SE}+\lambda_{SR}\gamma}\right)^{m_{SE}+j}\Gamma\left(\zeta_{SP}, \frac{\beta_1\overline{\gamma}_P}{\overline{\gamma}_S}\right)}{\beta_1^{m_{SP}+k-j}}, \tag{2.20}$$

$$\Theta_{j,k}^{(2)} = \frac{\left(\frac{\overline{\gamma}_P}{\lambda_{RE}+\lambda_{RD}\gamma}\right)^{m_{RE}+j}\Gamma\left(\zeta_{RP}, \frac{\beta_2\overline{\gamma}_P}{\overline{\gamma}_R}\right)}{\beta_2^{m_{RP}+k-j}}, \tag{2.21}$$

$$\zeta_q = m_{B_qP} + k - j, \tag{2.22}$$

$$\beta_1 = \lambda_{SP} + \frac{\lambda_{SR}(\gamma-1)}{\overline{\gamma}_P}. \tag{2.23}$$

$$\chi_R = \frac{\lambda_{RD}\gamma + \lambda_{RE}}{\overline{\gamma}_R}, \tag{2.24}$$

$$\delta_2 = \frac{e^{-\frac{\lambda_{RD}(\gamma-1)}{\overline{\gamma}_R}}}{\overline{\gamma}_R^{m_{RE}}}, \tag{2.25}$$

and

$$\beta_2 = \lambda_{RP} + \frac{\lambda_{RD}(\gamma-1)}{\overline{\gamma}_P}. \tag{2.26}$$

Proof.

- **SOP at the first hop**

Using (1.32), we have

$$\mathrm{SOP}_1 = \Pr(\ \gamma_R \leq \gamma_{1E}) + \left[\Pr(\gamma_R > \gamma_{1E})\Pr(C_{S1} < R_S|\gamma_R > \gamma_{1E})\right]. \tag{2.27}$$

According to [95, Eq. (12)], SOP_1 can be expressed as

$$\mathrm{SOP}_1 = \int_{x=0}^{\infty} \int_{y=0}^{\infty} F_{\gamma_R|g_{SP}=x}\left(\gamma y + \gamma - 1\right) f_{\gamma_{1E}|g_{SP}=x}(y) f_{g_{SP}}(x) dy dx, \tag{2.28}$$

where and $\gamma = 2^{R_s}$.

It is clear from (2.28) the we have to start first by deriving the CDF of $\gamma_R|g_{SP} = x$ and the PDF of $\gamma_{1E}|g_{SP} = x$ in order to derive SOP_1.

Using (2.9), the conditional CDF of γ_R given g_{SP} can be evaluated as

$$\begin{aligned} F_{\gamma_R|g_{SP}=x}(z) &= \Pr\left(\gamma_R \leq z | g_{SP} = x\right) \\ &= \Pr\left(\min\left(\overline{\gamma}_s, \frac{\overline{\gamma}_P}{x}\right) Y_{SR} \leq z\right), \end{aligned} \tag{2.29}$$

where $Y_{SR} = \sum_{l=1}^{L} g_{SR_l}$.

Now using (2.11), the conditional CDF of γ_{1E} given g_{SP} can be expressed as

$$\begin{aligned} F_{\gamma_{1E}|g_{SP}=x}(y) &= \Pr\left(\gamma_{1E} \leq y | g_{SP} = x\right) \\ &= \Pr\left(\min\left(\overline{\gamma}_s, \frac{\overline{\gamma}_P}{x}\right) g_{SE} \leq y\right). \end{aligned} \tag{2.30}$$

It is obvious that if $x \leq \frac{\overline{\gamma}_P}{\overline{\gamma}_S}$ then

$$F_{\gamma_R|g_{SP}=x}(z) = F_{Y_{SR}}\left(\frac{z}{\overline{\gamma}_s}\right), \tag{2.31}$$

and

$$f_{\gamma_{1E}|g_{SP}=x}(y) = \frac{f_{g_{SE}}\left(\frac{y}{\overline{\gamma}_s}\right)}{\overline{\gamma}_s}. \tag{2.32}$$

Otherwise, the above two expressions become

$$F_{\gamma_R|g_{SP}=x}(z) = F_{Y_{SR}}\left(\frac{xz}{\overline{\gamma}_P}\right), \tag{2.33}$$

and

$$f_{\gamma_{1E}|g_{SP}=x}(y) = \frac{x}{\overline{\gamma}_P} f_{g_{SE}}\left(\frac{xy}{\overline{\gamma}_P}\right). \tag{2.34}$$

Replacing (2.31)-(2.34) into (2.28), the expression of SOP_1 can be expressed as

$$\begin{aligned}\mathrm{SOP}_1 &= \underbrace{\frac{1}{\overline{\gamma}_s}\int_{x=0}^{\frac{\overline{\gamma}_P}{\overline{\gamma}_s}} f_{g_{SP}}(x)\int_{y=0}^{\infty} F_{Y_{SR}}\left(\frac{\gamma y+\gamma-1}{\overline{\gamma}_s}\right) f_{g_{SE}}\left(\frac{y}{\overline{\gamma}_s}\right) dydx}_{\mathcal{I}_1} \\ &\quad + \underbrace{\frac{1}{\overline{\gamma}_P}\int_{x=\frac{\overline{\gamma}_P}{\overline{\gamma}_s}}^{\infty} x f_{g_{SP}}(x)\int_{y=0}^{\infty} F_{Y_{SR}}\left(\frac{x\left(\gamma y+\gamma-1\right)}{\overline{\gamma}_P}\right) f_{g_{SE}}\left(\frac{xy}{\overline{\gamma}_P}\right) dydx.}_{\mathcal{I}_2} \end{aligned} \quad (2.35)$$

Now, by using (2.3) and (2.5), and performing some algebraic manipulations we obtain

$$\mathcal{I}_1 = \alpha_1\left(1-\frac{\lambda_{SE}^{m_{SE}}\delta_1}{\Gamma(m_{SE})}\sum_{k=0}^{m_{SR}-1}\frac{\lambda_{SR}^k}{\overline{\gamma}_s^k k!}\sum_{j=0}^{k}\frac{\psi_{k,j}^{(1)}}{\chi_S^{m_{SE}+j}}\right) \quad (2.36)$$

where $\psi_{k,j}^{(1)}$, α_1, and δ_1 are given in (2.15), (2.16), and (2.17), respectively.

On the other side, the second term $\mathcal{I}_2$ can be written as

$$\mathcal{I}_2 = 1-\alpha_1-\frac{\lambda_{SE}^{m_{SE}}\theta_1}{\Gamma(m_{SE})}\sum_{k=0}^{m_{SR}-1}\frac{\lambda_{SR}^k}{\overline{\gamma}_P^k k!}\sum_{j=0}^{k}\Phi_{k,j}^{(1)}, \quad (2.37)$$

where $\Phi_{k,j}^{(1)} = \psi_{k,j}^{(1)}\Theta_{j,k}^{(1)}$, θ_1, and $\Theta_{j,k}^{(1)}$ are defined in (2.19) and (2.20), respectively.

Finally, by incorporating (2.36) and (2.37) into (2.35), we obtain the expression of SOP_1 given in (2.13).

- **SOP at the second hop**

Similarly to (2.27) and (2.28), the expression of SOP_2 can be written as

$$\mathrm{SOP}_2 = \int_{x=0}^{\infty}\int_{y=0}^{\infty} F_{\gamma_D|g_{RP}=x}\left(\gamma y+\gamma-1\right) f_{\gamma_{2E}|g_{RP}=x}(y) f_{g_{RP}}(x) dydx. \quad (2.38)$$

Analogously to (2.29) and (2.30), we have

$$F_{\gamma_D|g_{RP}=x}(\gamma y+\gamma-1) = F_{g_{RD}}\left(\frac{\gamma y+\gamma-1}{\overline{\gamma}_R}\right), \quad (2.39)$$

and

$$f_{\gamma_{2E}|g_{RP}=x}(y) = \frac{1}{\overline{\gamma}_R} f_{g_{RE}}\left(\frac{y}{\overline{\gamma}_R}\right). \quad (2.40)$$

Pointedly, when $x \leq \frac{\overline{\gamma}_P}{\overline{\gamma}_R}$

$$F_{\gamma_D|g_{RP}=x}(\gamma y+\gamma-1) = F_{g_{RD}}\left(\frac{x\left(\gamma y+\gamma-1\right)}{\overline{\gamma}_P}\right), \tag{2.41}$$

and elsewhere,

$$f_{\gamma_{2E}|g_{RP}=x}(y) = \frac{x}{\overline{\gamma}_P} f_{g_{RE}}\left(\frac{xy}{\overline{\gamma}_P}\right). \tag{2.42}$$

By substituting Eqs. (2.39)-(2.42) into (2.38), yields

$$\begin{aligned} \mathrm{SOP}_2 \;=\; & \underbrace{\frac{1}{\overline{\gamma}_R}\int_{x=0}^{\frac{\overline{\gamma}_P}{\overline{\gamma}_R}} f_{g_{RP}}(x)\int_{y=0}^{\infty} F_{g_{RD}}\left(\frac{\gamma y+\gamma-1}{\overline{\gamma}_R}\right) f_{g_{RE}}\left(\frac{y}{\overline{\gamma}_R}\right) dydx}_{\mathcal{I}_3} \\ & \underbrace{+\frac{1}{\overline{\gamma}_P}\int_{x=\frac{\overline{\gamma}_P}{\overline{\gamma}_R}}^{\infty} x f_{g_{RP}}(x)\int_{y=0}^{\infty} F_{g_{RD}}\left(\frac{x\left(\gamma y+\gamma-1\right)}{\overline{\gamma}_P}\right) f_{g_{RE}}\left(\frac{xy}{\overline{\gamma}_P}\right) dydx.}_{\mathcal{I}_4} \end{aligned} \tag{2.43}$$

The first term in (2.43) can be expressed as

$$\mathcal{I}_3 = \alpha_2\left(1-\frac{\lambda_{RE}^{m_{RE}}\delta_2}{\Gamma(m_{RE})}\sum_{k=0}^{m_{RD}-1}\frac{\lambda_{RD}^k}{k!\overline{\gamma}_R^k}\sum_{j=0}^{k}\frac{\psi_{k,j}^{(2)}}{\chi_R^{m_{RE}+j}}\right), \tag{2.44}$$

where $\psi_{k,j}^{(2)}$, α_2, and δ_2 are given in (2.15), (2.16), and (2.25), respectively.

While, the second term $\mathcal{I}_4$ is given as

$$\mathcal{I}_4 = 1-\alpha_2-\frac{\lambda_{RE}^{m_{RE}}\theta_2}{\Gamma(m_{RE})}\sum_{k=0}^{m_{RD}-1}\frac{\lambda_{RD}^k}{\overline{\gamma}_P^k k!}\sum_{j=0}^{k}\Phi_{j,k}^{(2)}, \tag{2.45}$$

where $\Phi_{j,k}^{(2)} = \psi_{k,j}^{(2)}\Theta_{j,k}^{(2)}$, θ_2 and $\Theta_{j,k}^{(2)}$ are given in (2.19) and (2.21), respectively.

Finally, by substituting (2.44) and (2.45) into (2.43), (2.14) is attained which concludes the proof of Theorem 2.3.1. ■

2.4 Numerical results and discussions

In this section, the derived analytical expression for the SOP is validated through Monte-Carlo simulation by generating 10^6 Gamma distributed random values. Several parameters have been considered in order to show their impact on the security performance of the considered

communication system. The simulation parameters settings are summarized in Table 2.1.

Table 2.1: Simulation parameters of contribution 1.

Parameter	λ_i	m_i	R_S(bit/s/Hz)	$\bar{\gamma}_P$(dB)	$\bar{\gamma}_S$ (dB)	$\bar{\gamma}_R$(dB)
value	0.5	2	1	10	6	6

Fig. 2.2 depicts the SOP as a function of the secrecy rate R_s for various numbers of the relay's antennas L. It is obvious that the system's security is improved by increasing L. Moreover, when R_s increases, the SOP increases as well. In fact, and as it can be noticed from (1.34), when the SU adopts a high secrecy rate for better throughput performance, a secrecy outage is most likely happening.

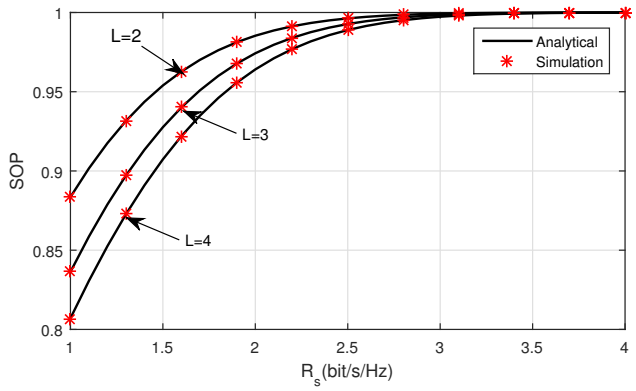

Figure 2.2: SOP versus secrecy rate for various numbers of the MRC branches.

Fig. 2.3 shows the SOP as a function of $\overline{\gamma}_P$ for various numbers the relay's antennas. As it can be seen the greater $\overline{\gamma}_P$ the smaller the SOP. From (2.1) and (2.2), it is obvious that when the MTIP at the PU receiver becomes higher, the SU source and the relay are allowed to use their maximum transmission power which improves the system's security. Additionally, and as expected, using a multi-antenna relay enhances the security performances.

Fig. 2.4 presents the SOP versus $\overline{\gamma}_S$ for different values of the relay's antennas. As it can be noticed, the SOP becomes smaller as the values of $\overline{\gamma}_S$ increase. Also, as long as the transmission power of the SUs is increased, the security of the system gets enhanced.

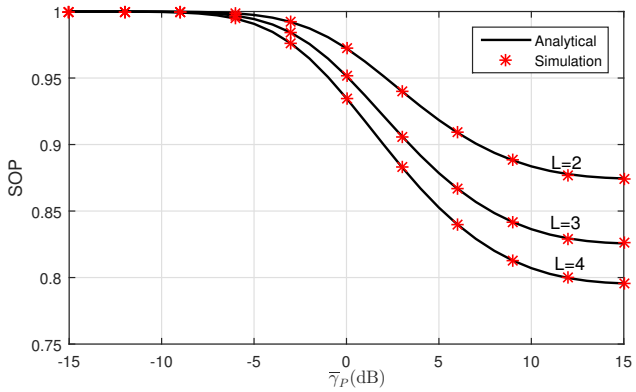

Figure 2.3: SOP versus $\overline{\gamma}_P$ for various numbers the relay's antennas.

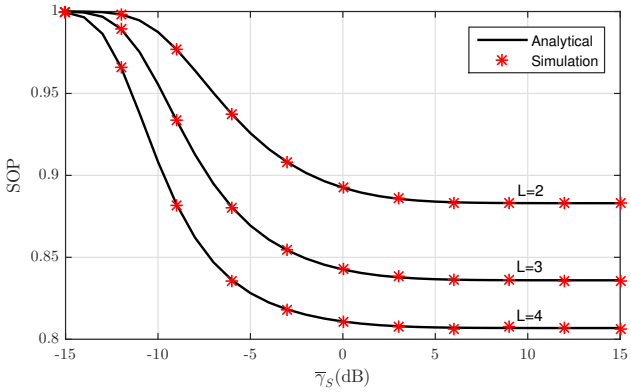

Figure 2.4: SOP versus $\overline{\gamma}_S$ for various numbers the relay's antennas
.

2.5 Concluding remarks

In this chapter, we investigated the PLS of a dual-hop CR communication system, under the constraint of interfering with the PU's signals. By considering a more generalized fading, namely Nakagami-m, and by considering a multi-antenna relay, we derived the SOP as a performance metric, based on which, new insights were gained. The obtained results show that the security is enhanced with the increase of number of the relay's antennas. The next chapter investigates the impact of both spatial diversity and energy harvesting on the secrecy performance of a dual-hop CRN.

Chapter 3

On the Secrecy Performance of EH-based Underlay CRN

3.1 Introduction

3.1.1 Motivation

In a cooperative CRN, the information is forwarded to its intended destination through the aid of one or multiple relays. However, in some cases, the relay nodes can be energy-constrained, which leads to degraded network performance. To deal with this issue, EH has been recently proposed as an effective emerging technology that makes use of RF energy. However, it is noted that despite the promising advantages of a cooperative EH-CRN, securing data transmission in such complex environment becomes a critical and challenging task.

Considerable research analyses have investigated the PLS of CRNs under different system setups [31–34, 93–103]. In general, two types of CRNs have been considered in the literature, namely (i) a system that assumes the existence of a direct communication link between the source and the destination; and (ii) a cooperative system where the source communicates with the intended destination with the aid of multiple relays. Specifically, the secrecy performance of cooperative EH-CRNs has been investigated in [31–34]. In [31], lower bounds for the probability of strictly positive secrecy capacity were derived by assuming that the destination receives via a direct link both confidential information and a sub-frame used for EH purposes. The harvested energy is then exploited to broadcast jamming signal towards an eavesdropper so as to achieve

secure communication. By considering that the SUs harvest energy from the PU's signals, the SOP has been derived over Rayleigh fading channels in [32], while the authors in [33] investigated the corresponding IP. In [34], the SOP is derived by considering a dual-hop overlay EH-CRN in which the SUs act as relays to forward the PU's data to its intended PU destination. The SUs, in this case, harvest energy from the received signals of the PU source. On the other hand, the authors of [93–96] derived both a closed-form and asymptotic expressions for the SOP metric by considering either Rayleigh or Nakagami-m fading conditions. In [93–95], the source node was equipped with one antenna, whereas in [96] a multi-antenna source was considered and analyzed. Also, the receivers (i.e., destination and eavesdropper), were assumed to be equipped with multiple antennas. Additionally, in [94] the authors assumed the existence of two eavesdroppers, in which one is intercepting the communication of the primary network whereas the other is eavesdropping the secondary user. In [97–99], the PLS of a cooperative CRN using multiple relays was investigated. Closed-form and asymptotic expressions for the SOP were derived under the optimal relay selection technique. In [97] and [99], the SOP expressions were derived under Nakagami-m and Rayleigh fading channels, respectively. Moreover, the IP was derived in [98] over Rayleigh fading conditions.

Despite the usefulness of the above scenarios, they do not embrace all the practical cases that are encountered in realistic communication scenarios involving cognitive radio systems. For instance, a direct communication link does not typically exist between the source and the destination. Moreover, the case of multiple relays seems to be also impractical as, in some cases, only one relay can be available to forward the data from the source to the destination. Likewise, the corresponding energy consumption and computational complexity can be increased dramatically when the number of cooperative nodes is high, which can render the required computation and processing unsustainable. Additionally, the available relay may not always have sufficient energy to forward the received information to its intended destination. Motivated by the above, the main objective of this chapter is to investigate the PLS by combining both diversity as well as EH at the relay.

3.1.2 Contributions

The main contributions of this chapter are given as:

- Secrecy performance analysis of a dual-hop EH-CRN with single antenna relay over Rayleigh fading channel is investigated. Precisely, closed-form expression for the SOP was derived by considering a single-antenna relay that is not causing any interference to the PU.
- The PLS of a dual-hop EH-CRN is investigated by assuming that the relay is equipped with multiple antennas and causing interference to the PU signals. Mainly,
  - Closed-form and asymptotic expressions for the SOP are derived by considering both i.n.i.d as well as i.i.d flat Rayleigh fading channels.
  - Impact of key parameters such as the MTIP at the PU, maximum transmit power of both relay and source, power splitting ratio, and the number of MRC branches at the relay on the overall system's security are investigated.

3.1.3 Chapter's structure

The remainder of this chapter is organized as follows: Sections 2 and 3 present contributions on the secrecy performance analysis of two various setups, namely (i) a dual-hop EH-CRN with a single antenna relay located in a far-field area of the PU (i.e. not causing any interference to the PU signals), and (ii) a dual-hop EH-CRN where the relay is equipped with multiple antennas and continuously adapting its transmit power to avoid interfering with the PU. For each setup, system and channel model, secrecy performance metrics, and numerical results are presented. Lastly, Section 5 concludes this chapter.

3.2 Contribution 2: Cooperative EH-based CRNs with a single-antenna relay

3.2.1 System and channel model

We consider the EH-CRN system illustrated in Fig. 3.1 where the SUs share the same spectrum with PUs under the requirement of respecting the PUs' quality of service (QoS). Therefore, node S has to continuously adapt its transmission power in order to avoid interfering with PUs. For the considered system, the communication is carried out in two phases as follows:

- Phase 1: The source S transmits data with power P_S. In order to avoid interference with the PU signal, the transmit power P_S should fall below the MTIP at PU_{Rx} (i.e., P_I). It follows that the transmission power of S is constrained by its maximum transmit power $P_S^{\max}$ and the tolerated P_I as given in (1.1).

- Phase 2: The relay R harvests energy from RF signals transmitted by S. In the considered setup, it is assumed that the relay performs PS protocol. Hence, R harvests a fraction of power θ (i.e., $0 \leq \theta \leq 1$), from the received signal. The remaining power $(1-\theta)P_S$ is used to carry out information processing. If R harvests energy from the received signal for a duration of T, then the harvested energy at R is

$$E_H = T\eta\theta P_S g_{SR}, \tag{3.1}$$

  where η denotes the energy conversion efficiency coefficient ($0 \leq \eta \leq 1$). Importantly, all the harvested energy by R is assumed to be used for forwarding the information to its destination during the same time slot considered at the first hop. Therefore, the transmission power of R is given by

$$P_R = \frac{E_H}{T} = \eta\theta P_S g_{SR}. \tag{3.2}$$

Without loss of generality, we assume that the relay is located far away from the primary network. Therefore, it is not required that the relay uses the power adaption policy as it does not impact the PU's QoS.

Also, all fading amplitudes are assumed to be Rayleigh distributed. Consequently, the channel power gains $g_q = |h_q|^2$, with $q = \{SR, SE, RD, RE\}$, are exponentially distributed with parameters λ_q that are inversely proportional to the average SNRs of the associated links. Accordingly, the received signal at R and D are given by

$$y_R = \sqrt{(1-\theta)P_S}h_{SR}x_s + n_R, \tag{3.3}$$

and

$$y_D = \sqrt{P_R}h_{RD}x_r + n_D, \tag{3.4}$$

respectively, where n_R and n_D denote the AWGN of zero mean and variance N_R and N_D, respectively. Likewise, x_s and x_r stand for the transmitted signals from S and R, respectively.

The received signals at the eavesdropper at the first and the second hop, respectively, are expressed as

$$y_{1E} = \sqrt{(1-\theta)P_S}h_{SE}x_s + n_E, \tag{3.5}$$

and

$$y_{2E} = \sqrt{P_R}h_{RE}x_r + n_E, \tag{3.6}$$

where n_E is the AWGN with zero mean and variance N_E. For the sake of simplicity, we also consider that all noise powers are identical, i.e., $N_E = N_R = N_D = N$.

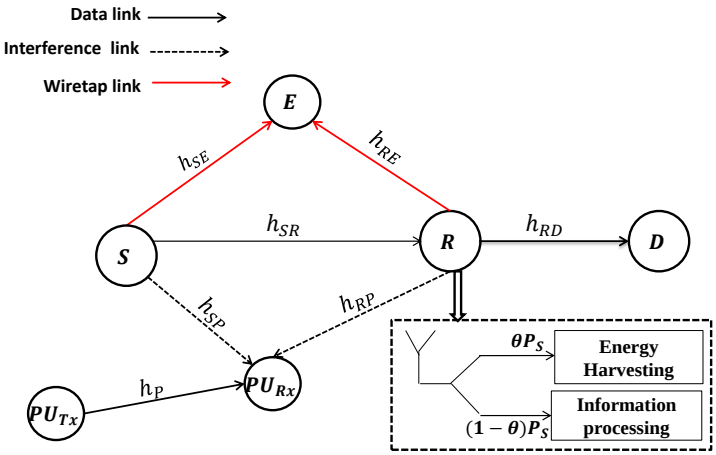

Figure 3.1: The considered EH-CRN system.

3.2.2 Secrecy performance analysis

In this section, the SOP is derived as performance metric for the considered communication system. In the considered EH-CRN system, the eavesdropper is assumed to be intercepting communication at both hops i.e., S-R and R-D. The secrecy capacity of the considered system

is defined as in (1.31) such that the SNR γ_R at the relay R is given by

$$\gamma_R = (1-\theta)\min\left(\overline{\gamma}_s, \frac{\overline{\gamma}_P}{g_{SP}}\right) g_{SR}. \tag{3.7}$$

Likewise, the SNR γ_D at D can be expressed as $\gamma_D = \rho_R g_{RD}$, with

$$\rho_R = \eta\theta \min\left(\overline{\gamma}_s, \frac{\overline{\gamma}_P}{g_{SP}}\right) g_{SR}, \tag{3.8}$$

and $\overline{\gamma}_s = P_S^{max}/N$, and $\overline{\gamma}_P = P_I/N$.

Finally, the SNRs at the eavesdropper γ_{1E} and γ_{2E} of the links S-E and R-E, are given by

$$\gamma_{1E} = (1-\theta)\min\left(\overline{\gamma}_s, \frac{\overline{\gamma}_P}{g_{SP}}\right) g_{SE}, \tag{3.9}$$

and $\gamma_{2E} = \rho_R g_{RE}$, respectively.

Closed-form expression for the SOP

The closed-form expression for the SOP is derived in Theorem 3.2.1.

Theorem 3.2.1. *The SOP of the considered EH-CRN system subject to flat Rayleigh fading channels is given by*

$$\text{SOP} = 1 - \frac{1}{\delta}\left[\frac{e^{-\frac{\rho}{\overline{\gamma}_S}}}{\chi+1}\left(1 - e^{-\phi} + \frac{e^{-\phi}}{\frac{\rho}{\overline{\gamma}_P\lambda_{SP}}+1}\right)\right]\left[\left(1-e^{-\phi}\right) G_{0,2}^{2,0}\left(\omega_S\xi \left| \begin{matrix} -;- \\ 0,1;- \end{matrix}\right.\right) + \frac{\lambda_{SP}e^{-\phi}}{\xi\omega_P}\left[\xi^2\Xi_1 - \Omega\right]\right]. \tag{3.10}$$

where

$$\chi = \lambda_{SR}\gamma/\lambda_{SE}, \tag{3.11}$$

$$\rho = \lambda_{SR}(\gamma-1)/(1-\theta), \tag{3.12}$$

$$\phi = \lambda_{SP}\overline{\gamma}_P/\overline{\gamma}_S, \tag{3.13}$$

$$\omega_v = \lambda_{SR}/(\eta\theta\overline{\gamma}_s),\ v \in \{S,P\}, \tag{3.14}$$

$$\xi = \lambda_{RD}(\gamma-1), \tag{3.15}$$

$$\Xi_1 = \xi^{-2} G_{2,1}^{1,2}\left(\frac{\lambda_{SP}}{\omega_P \xi}\middle| \begin{matrix} -1, 0; - \\ 0; - \end{matrix}\right), \tag{3.16}$$

and

$$\Omega = G_{0,1:1,1:1,2}^{1,0:1,1:1,1}\left(\frac{\omega_P \xi}{\lambda_{SP}}, \xi\omega_S\middle| \begin{matrix} -; - : 1; - : 1; - \\ 2; - : 1; - : 1; 0 \end{matrix}\right). \tag{3.17}$$

Proof.

Substituting (1.31) into (1.34), the SOP becomes

$$\begin{aligned} \text{SOP} &= 1 - \Pr\left(C_{1S} > R_s\right) \Pr\left(C_{2S} > R_s\right) \\ &= 1 - \left[1 - \text{SOP}_1\right]\left[1 - \text{SOP}_2\right], \end{aligned} \tag{3.18}$$

where SOP_1 and SOP_2 denote the SOP of either the first or the second hop.

Expression of SOP_1

By using (1.32), SOP_1 can be expressed as

$$\text{SOP}_1 = \Pr\left(\gamma_R \leq \gamma_{1E}\right) + \Pr\left(\gamma_R > \gamma_{1E}\right) \Pr\left(C_{1S} < R_s \,|\gamma_R > \gamma_{1E}\right). \tag{3.19}$$

Utilizing [67, Eq. (12)], one can obtain

$$\text{SOP}_1 = \int_{x=0}^{\infty}\int_{y=0}^{\infty} F_{\gamma_R|g_{SP}=x}\left(\gamma y + \gamma - 1\right) f_{\gamma_{1E}|g_{SP}=x}(y) f_{g_{SP}}(x) dy dx. \tag{3.20}$$

The CDFs of γ_R and γ_{1E} for a given g_{SP} are expressed as

$$\begin{aligned} F_{\gamma_R|g_{SP}=x}\left(z\right) &= \Pr\left(\gamma_R \leq z \,|g_{SP} = x\right) \\ &= F_{g_{SR}}\left(\frac{z}{\left(1-\theta\right)\Phi\left(x\right)}\right), \end{aligned} \tag{3.21}$$

and

$$\begin{aligned} F_{\gamma_{1E}|g_{SP}=x}(y) &= \Pr\left(\gamma_{1E} \leq y | g_{SP} = x\right) \\ &= F_{g_{SE}}\left(\frac{y}{\left(1-\theta\right)\Phi\left(x\right)}\right). \end{aligned} \tag{3.22}$$

respectively, with

$$\Phi(x) = \begin{cases} \overline{\gamma}_S, x \leq \overline{\gamma}_P/\overline{\gamma}_S \\ \overline{\gamma}_P/x, x > \overline{\gamma}_P/\overline{\gamma}_S \end{cases}. \tag{3.23}$$

Hence, substituting the derivative of (3.22) alongside (3.21) yields

$$\begin{aligned} \mathrm{SOP}_1 &= \int_0^\infty \frac{f_{g_{SP}}(x)}{(1-\theta)\,\Phi(x)} \int_0^\infty F_{g_{SR}}\left(\frac{\gamma y + \gamma - 1}{(1-\theta)\,\Phi(x)}\right) f_{g_{SE}}\left(\frac{y}{(1-\theta)\,\Phi(x)}\right) dydx \\ &= \int_{x=0}^\infty f_{g_{SP}}(x)\left(1 - \frac{e^{-\frac{\rho}{\Phi(x)}}}{\chi+1}\right) dx. \end{aligned} \tag{3.24}$$

Now, using (3.23), we obtain

$$\begin{aligned} \mathrm{SOP}_1 &= \left(1 - \frac{e^{-\frac{\rho}{\overline{\gamma}_S}}}{\chi+1}\right) \int_{x=0}^{\frac{\overline{\gamma}_P}{\overline{\gamma}_S}} f_{g_{SP}}(x)dx + \int_{x=\frac{\overline{\gamma}_P}{\overline{\gamma}_S}}^\infty f_{g_{SP}}(x)\left(1 - \frac{e^{-\frac{\rho x}{\overline{\gamma}_P}}}{\chi+1}\right) dx \\ &= 1 - \frac{e^{-\frac{\rho}{\overline{\gamma}_S}}}{\chi+1}\left(1 - e^{-\phi} + \frac{e^{-\phi}}{\frac{\rho}{\overline{\gamma}_P \lambda_{SP}} + 1}\right). \end{aligned} \tag{3.25}$$

Expression of SOP_2

Similarly, using (1.33), SOP_2 can be expressed as

$$\mathrm{SOP}_2 = \Pr(\gamma_D \leq \gamma_{2E}) + \Pr(\gamma_D > \gamma_{2E}) \Pr(C_{2S} < R_s \,|\gamma_D > \gamma_{2E}). \tag{3.26}$$

To this effect, using [95, Eq. (12)], yields

$$\mathrm{SOP}_2 = \int_{x=0}^\infty \int_{y=0}^\infty F_{\gamma_D|\rho_R=x}(\gamma y + \gamma - 1)\, f_{\gamma_{2E}|\rho_R=x}(y) f_{\rho_R}(x) dydx. \tag{3.27}$$

Analogously, the CDFs of γ_D and γ_{2E} for a given ρ_R can be expressed as

$$F_{\gamma_D|\rho_R=x}(z) = \Pr(\gamma_D \leq z \,|\rho_R = x) = F_{g_{RD}}\left(\frac{z}{x}\right), \tag{3.28}$$

and

$$F_{\gamma_{2E}|\rho_R=x}(z) = \Pr(\gamma_{2E} \leq z \,|\rho_R = x) = F_{g_{RE}}\left(\frac{z}{x}\right), \tag{3.29}$$

respectively. Based on this, the CDF of ρ_R is given by

$$\begin{aligned} F_{\rho_R}(z) &= \Pr\left(\min\left(\overline{\gamma}_s, \frac{\overline{\gamma}_P}{g_{SP}}\right) g_{SR} \leq \frac{z}{\eta\theta}\right) \\ &= \underbrace{\Pr\left(g_{SR} \leq \frac{z}{\eta\theta\overline{\gamma}_s}, \frac{\overline{\gamma}_P}{g_{SP}} \geq \overline{\gamma}_s\right)}_{\mathcal{I}_1} + \underbrace{\Pr\left(\frac{g_{SR}}{g_{SP}} \leq \frac{z}{\eta\theta\overline{\gamma}_P}, \frac{\overline{\gamma}_P}{g_{SP}} \leq \overline{\gamma}_s\right)}_{\mathcal{I}_2}, \end{aligned} \tag{3.30}$$

where the two terms $\mathcal{I}_1$ and $\mathcal{I}_2$ can be rewritten as

$$\mathcal{I}_1 = F_{g_{SR}}\left(\frac{z}{\eta\theta\overline{\gamma}_s}\right) F_{g_{SP}}\left(\frac{\overline{\gamma}_P}{\overline{\gamma}_s}\right), \tag{3.31}$$

and

$$\begin{aligned} \mathcal{I}_2 &= \int_{\frac{\overline{\gamma}_P}{\overline{\gamma}_s}}^{\infty} F_{g_{SR}}\left(\frac{z}{\eta\theta\overline{\gamma}_P} y\right) f_{g_{SP}}(y)\, dy \\ &= \lambda_{SP} \int_{\frac{\overline{\gamma}_P}{\overline{\gamma}_s}}^{\infty} \left(1 - e^{-\omega_P z y}\right) e^{-\lambda_{SP} y} dy \\ &= e^{-\phi} - \frac{\lambda_{SP} e^{-(\omega_S z + \phi)}}{\omega_P z + \lambda_{SP}}. \end{aligned} \tag{3.32}$$

Then, replacing (3.31) and (3.32) into (3.30), yields

$$F_{\rho_R}(z) = 1 - e^{-\omega_S z}\left(1 - e^{-\phi}\right) - \frac{\lambda_{SP} e^{-(\omega_S z + \phi)}}{\omega_P z + \lambda_{SP}}, \tag{3.33}$$

whereas by differentiating (3.33), it follows that

$$f_{\rho_R}(z) = \left(1 - e^{-\phi}\right) \omega_S e^{-\omega_S z} + \frac{\lambda_{SP} e^{-\phi}}{\omega_P} \left(\frac{\omega_S e^{-\omega_S z}}{z + \frac{\lambda_{SP}}{\omega_P}} + \frac{e^{-\omega_S z}}{\left(z + \frac{\lambda_{SP}}{\omega_P}\right)^2}\right). \tag{3.34}$$

Based on the above, substituting (3.28), (3.34), and the derivative of (3.29) into (3.27), yields

$$\begin{aligned} \mathrm{SOP}_2 &= 1 - \frac{1}{\delta} \int_{x=0}^{\infty} f_{\rho_R}(x) e^{-\frac{\xi}{x}} dx \\ &= 1 - \frac{1}{\delta}\left[\left(1 - e^{-\phi}\right)\Phi_1 + \frac{\lambda_{SP} e^{-\phi}}{\omega_P}\left(\Phi_2 + \Phi_3\right)\right], \end{aligned} \tag{3.35}$$

where

$$\Phi_1 = \omega_S \int_0^\infty e^{-\left(\frac{\xi}{x}+\omega_S x\right)} dx, \tag{3.36}$$

$$\Phi_2 = \omega_S \int_0^\infty \frac{e^{-\left(\omega_S x+\frac{\xi}{x}\right)}}{x+\frac{\lambda_{SP}}{\omega_P}} dx, \tag{3.37}$$

and

$$\Phi_3 = \int_0^\infty \frac{e^{-\left(\omega_S x+\frac{\xi}{x}\right)}}{\left(x+\frac{\lambda_{SP}}{\omega_P}\right)^2} dx. \tag{3.38}$$

Using [67, Eq. (3.324.1)] alongside [71, Eq. (03.04.26.0006.01)], it follows that

$$\begin{aligned} \Phi_1 &= \omega_S \sqrt{\frac{\xi}{\omega_S}} G_{0,2}^{2,0}\left(\omega_S \xi \left| \begin{matrix} -;- \\ \frac{1}{2}, \frac{-1}{2};- \end{matrix} \right.\right) \\ &= G_{0,2}^{2,0}\left(\omega_S \xi \left| \begin{matrix} -;- \\ 0,1;- \end{matrix} \right.\right). \end{aligned} \tag{3.39}$$

By performing integration by parts, Φ_3 can rewritten as

$$\Phi_3 = \int_0^\infty \left(-\omega_S + \frac{\xi}{x^2}\right) \frac{e^{-\left(\omega_S x+\frac{\xi}{x}\right)}}{x+\frac{\lambda_{SP}}{\omega_P}} dx. \tag{3.40}$$

On the other hand, using [71, Eqs. (07.34.03.0271.01), (01.03.26.0007.01)] along with (3.40), yields $\Phi_2 + \Phi_3 = \xi\left[\Xi_1 - \Xi_2\right]$, where

$$\Xi_1 = \int_0^\infty y e^{-\xi y} G_{1,1}^{1,1}\left(\frac{\lambda_{SP}}{\omega_P} y \left| \begin{matrix} 0;- \\ 0;- \end{matrix} \right.\right) dy, \tag{3.41}$$

and

$$\Xi_2 = \int_0^\infty \frac{y}{e^{\xi y}} G_{1,1}^{1,1}\left(\frac{\lambda_{SP}}{\omega_P} y \left| \begin{matrix} 0;- \\ 0;- \end{matrix} \right.\right) G_{1,2}^{1,1}\left(\frac{\omega_S}{y} \left| \begin{matrix} 1;- \\ 1;0 \end{matrix} \right.\right) dy. \tag{3.42}$$

Now, using [71, Eq. (07.34.21.0088.01)], (3.16) is attained.

On the other hand, (3.42) can be rewritten using Mellin-Barnes integrals as

$$\Xi_2 = \frac{1}{(2\pi j)^2} \int_{\mathcal{C}_1} \Gamma(s)\Gamma(1-s) \left(\frac{\lambda_{SP}}{\omega_P}\right)^{-s} \int_{\mathcal{C}_2} \frac{\Gamma(1+v)\Gamma(-v)}{\Gamma(1-v)\omega_S^v} ds dv \int_0^\infty \frac{y^{v-s+1}}{e^{\xi y}} dy \tag{3.43}$$

which becomes $\Xi_2 = \Omega/\xi^2$, where $j = \sqrt{-1}$, and $\mathcal{C}_1$ and $\mathcal{C}_2$ are two complex contours of integration ensuring the convergence of the above bivariate Meijer G-function.

Next, substituting (3.16) and (3.43) into (3.2.2), yields

$$\Phi_2 + \Phi_3 = \frac{1}{\xi}\left[G_{2,1}^{1,2}\left(\frac{\lambda_{SP}}{\omega_P \xi}\middle| \begin{matrix} -1, 0; - \\ 0; - \end{matrix}\right) - \Omega\right]. \tag{3.44}$$

By also substituting (3.39) and (3.44) into (3.35), yields

$$\mathrm{SOP}_2 = 1 - \frac{1}{\delta}\left[\left(1 - e^{-\phi}\right)\Phi_1 + \frac{\lambda_{SP} e^{-\phi}}{\omega_P \xi}\left(G_{2,1}^{1,2}\left(\frac{\lambda_{SP}}{\omega_P \xi}\middle| \begin{matrix} -1, 0; - \\ 0; - \end{matrix}\right) - \Omega\right)\right]. \tag{3.45}$$

Finally, substituting (3.25) and (3.45) into (3.18), leads to (3.10) which concludes the proof of Theorem 3.2.1. ■

3.2.3 Numerical results and discussions

In this section, we evaluate the security performance of the considered EH-CRN setup. The derived SOP expression in (3.10) is validated through corresponding Monte-Carlo simulation by generating 10^6 exponentially distributed random values. The simulation parameters are depicted in Table 3.1.

Table 3.1: Simulation parameters of contribution 2.

Parameter	λ_q	$\bar{\gamma}_P$ (dB)	$\bar{\gamma}_S$ (dB)	R_S (bit/s/Hz)	θ
value	0.5	10	10	1	0.5

Fig. 3.2 illustrates the SOP as a function of $\overline{\gamma}_P$ for various values of η. It can be observed that SOP decreases with the increasing values of $\overline{\gamma}_P$ and η. Indeed, under the assumption that fading severity parameters of the legitimate links i.e., λ_{SR} and λ_{RD} are smaller than those of the wiretap channels, i.e., λ_{SE} and λ_{RE}, the greater $\overline{\gamma}_P$, the greater the SNRs γ_R and γ_{1D}. Consequently, the capacity of the legitimate links is greater than the one of the wiretap links, which ultimately leads to an enhanced system security.

Fig. 3.3 shows the SOP versus the EH ratio θ for different values of η. Clearly, the SOP is a concave function of θ. This behavior can be construed by the fact that as θ tends to 0

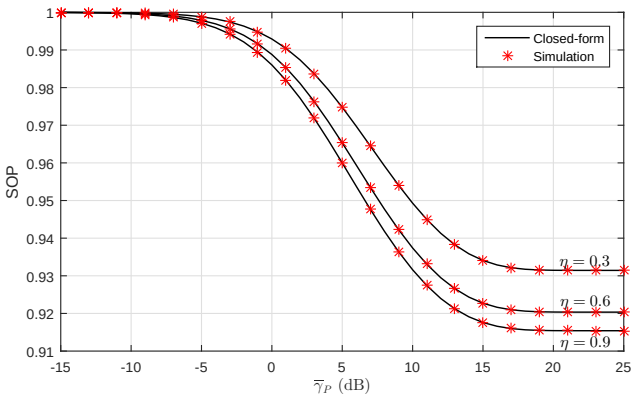

Figure 3.2: SOP versus $\overline{\gamma}_P$ for various values of η.

the instantaneous SNRs given in (3.2.2), also approach 0. Hence, C_S tends to 0 leading to the highest value of the SOP. Similarly, as θ tends to 1 the instantaneous SNRs given in (3.7) and (3.9) approach 0. Consequently, both C_{1S} and C_S approach 0, and thus the SOP increases accordingly.

Finally, Fig. 3.4 demonstrates the SOP versus both $\overline{\gamma}_P$ and θ. Evidently, the parameters $\overline{\gamma}_P$ and θ admit certain values for which a better security is achieved. For instance, one can infer that a higher secrecy is achieved for $0.4 \leq \theta \leq 0.6$ and $\overline{\gamma}_P \geq 15$dB.

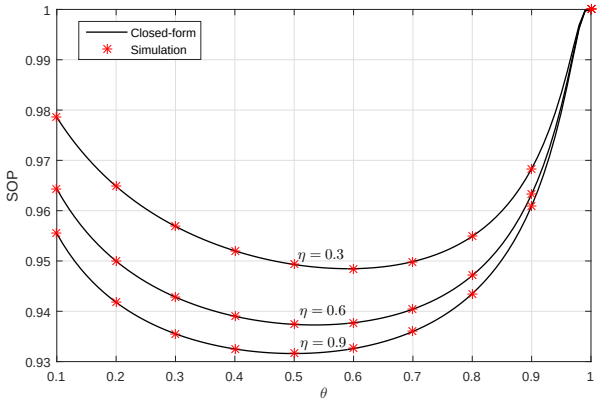

Figure 3.3: SOP versus θ for various values of η.

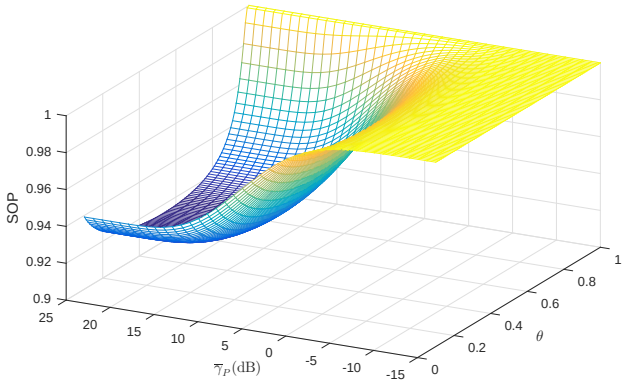

Figure 3.4: SOP versus θ and $\overline{\gamma}_P$ for $\eta = 0.9$.

3.3 Contribution 3: Cooperative EH-based CRN with multi-antennas relay

3.3.1 System and channel model

In this contribution, we consider a dual-hop cooperative DF EH-CRN system, as illustrated in Fig. 3.5. This system consists of one SU source node S who is transmitting data to one

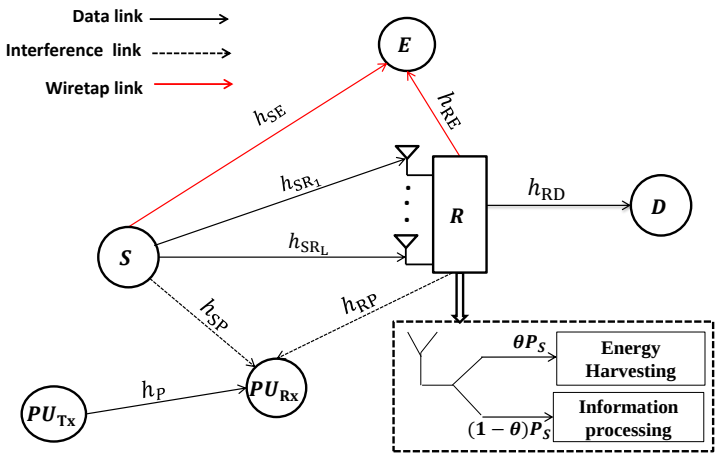

Figure 3.5: The considered cooperative EH-CRN.

SU destination node D through an energy-constrained SU relay R, under the eavesdropping attempt of E. The relay is assumed to be equipped with multiple antennas and an MRC diversity receiver in order to combine the received signals. Without loss of generality, all other nodes are assumed to be equipped with a single antenna. Additionally, R performs the PS-EH technique to mitigate the lack of energy constraint, whereas E is continuously listening to both communication hops. During the data transmission, the PU receiver is subject to the interference signals coming from both S and R. Under this constraint, only the node S has to adjust its transmit power in order to satisfy the PUs' quality of service. That is, the transmit power P_S is constrained by the maximum transmit power $P_S^{\max}$ and the MTIP P_I at PU receiver as given in (1.1).

On the contrary, according to [32] and under the PS variant, the relay harvests energy from the received information for a duration of T. Hence, the harvested energy at the relay can be

expressed as

$$E_H = T\eta\theta P_S \sum_{k=1}^{L} g_{\mathrm{SR}_k}, \tag{3.46}$$

where η accounts for the energy conversion efficiency coefficient that takes values in the interval $[0, 1]$. Also, θ denotes the fraction of power harvested by the relay from the received signal and it takes values also in the interval $[0, 1]$, whereas L is the number of diversity branches. To this effect, the maximum transmit power of R is given by

$$P_R^{\max} = \frac{E_H}{T} = \eta\theta P_S \sum_{k=1}^{L} g_{\mathrm{SR}_k}. \tag{3.47}$$

The transmit power allowing the relay to avoid any potential interference to the PU is given by

$$\begin{aligned} P_R &= \min\left(P_R^{\max}, \frac{P_I}{g_{\mathrm{RP}}}\right) \\ &= \min\left(\eta\theta P_S \sum_{k=1}^{L} g_{\mathrm{SR}_k}, \frac{P_I}{g_{\mathrm{RP}}}\right). \end{aligned} \tag{3.48}$$

One can ascertain from (1.1) and (3.48) that when P_I increases, the nodes S and R are able to use their maximum transmit powers, which results in increasing the SNR at both R and D, ultimately leading to the system's security enhancement.

Without loss of generality, the communication between the transmitters and the receivers is assumed to be established in a non-line-of-sight scenario. Therefore, the fading amplitudes of all links are Rayleigh distributed, i.e. the channel coefficients of links $S \to R_k$, $R \to D$, $S \to E$, $R \to E$, $P_{\mathrm{Tx}} \to P_{\mathrm{Rx}}$, $R \to P_{\mathrm{Rx}}$ are h_{SR_k}, h_{RD}, h_{SE}, h_{RE}, h_P, h_{RP}, respectively. For simplicity, we write the channel power gains as $g_{\mathrm{SR}_k} = |h_{\mathrm{SR}_k}|^2$, $g_{\mathrm{RD}} = |h_{\mathrm{RD}}|^2$, $g_{\mathrm{SE}} = |h_{\mathrm{SE}}|^2$, $g_{\mathrm{RE}} = |h_{\mathrm{RE}}|^2$, $g_P = |h_P|^2$, $g_{\mathrm{RP}} = |h_{\mathrm{RP}}|^2$. Evidently, all these gains are exponentially distributed with parameters λ_{SR_k}, λ_{RD}, λ_{SE}, λ_{RE}, λ_P, λ_{RP}, λ_{SP} that are inversely proportional to the average SNRs of the associated links. Moreover, each input signal at the relay arrives with a certain delay compared to the one received by its first branch. Since the considered receiver employs MRC, all these delays will be eliminated and the interference of these signals will be canceled out. It is worth mentioning that the delays, as well as the interference cancellation, are out of the scope of this contribution since the present contribution is devoted to the investigation of the impact of the

primary network, the EH, as well as the diversity techniques on the security performance of the system.

Additionally, the relay operates according to the PS scheme such that θP_S is dedicated to EH and $(1-\theta)P_S$ is used for information detection. Accordingly, the signal at the MRC output of R can be expressed as

$$y_R = \sqrt{(1-\theta)P_S}||\mathbf{h}_{\mathrm{SR}}||x_s + w_R n_R, \tag{3.49}$$

where $\| \, . \, \|$ denotes the Frobenius norm, $\mathbf{h}_{\mathrm{SR}}$ denotes the $L \times 1$ channel vector $(h_{\mathrm{SR}_k})_{1 \leq k \leq L}$, x_s is the transmitted signal from S, n_R stands for the additive white Gaussian noise (AWGN) with variance N_R and zero mean, whereas and $w_R = \frac{h_{\mathrm{SR}}^{\dagger}}{||h_{\mathrm{SR}}||}$, where $\dagger$ denotes the transpose conjugate.

On the other hand, the received signal at the destination D is given by

$$y_D = \sqrt{P_R} h_{\mathrm{RD}} x_r + n_D, \tag{3.50}$$

where x_r denotes the transmitted signal from R after performing both the relaying and the EH techniques, and n_D is an AWGN of zero mean and variance N_D.

The received signals arriving at the eavesdropper from the source and from the relay are, respectively, written as

$$y_{1E} = \sqrt{(1-\theta)P_S} h_{\mathrm{SE}} x_s + n_E, \tag{3.51}$$

and

$$y_{2E} = \sqrt{P_R} h_{\mathrm{RE}} x_r + n_E, \tag{3.52}$$

where n_E is the corresponding AWGN with zero mean and variance N_E. Without loss of generality, we also consider that all noise powers are identical, i.e. $N_E = N_R = N_D = N$.

3.3.2 Secrecy performance analysis

In this section, we derive the closed-form as well as the asymptotic expressions for the SOP by considering both i.i.d and i.n.i.d Rayleigh fading channels. The secrecy capacity of the considered communication system is defined as in (1.31) where

- γ_R is the combined SNR at the relay R, namely

$$\gamma_R = (1-\theta)\, W_k, \tag{3.53}$$

with

$$W_k = \min\left(\overline{\gamma}_s, \frac{\overline{\gamma}_P}{g_{\mathrm{SP}}}\right) Y_{SR,} \tag{3.54}$$

and $\overline{\gamma}_s = P_S^{max}/N$, $\overline{\gamma}_P = P_I/N$, $Y_{\mathrm{SR}} = \sum_{k=1}^{L} g_{\mathrm{SR}_k}$.

- γ_D denotes the SNR at the destination D, namely

$$\gamma_D = \rho_R g_{\mathrm{RD}}, \tag{3.55}$$

where

$$\rho_R = \min\left(\eta\theta W_k, \frac{\overline{\gamma}_P}{g_{\mathrm{RP}}}\right). \tag{3.56}$$

- γ_{1E} and γ_{2E} are the SNRs of the links S-E and R-E, respectively and are expressed as

$$\gamma_{1E} = (1-\theta)\min\left(\overline{\gamma}_s, \frac{\overline{\gamma}_P}{g_{\mathrm{SP}}}\right) g_{\mathrm{SE}}, \tag{3.57}$$

and

$$\gamma_{2E} = \rho_R g_{\mathrm{RE}}. \tag{3.58}$$

Remark 3.

- *From (1.31), it can be seen that improving the security of the system relies on increasing the two secrecy capacities at the same time. In other words, improving the secrecy of only one link will not enhance the system's reliability. In addition, it is noticed from (3.53) that the greater the number of branches L, the greater the γ_R, γ_1, C_{1S} and C_S. Consequently, the SOP metric decreases, which in turn leads to an overall system's security improvement.*

- *As the parameters λ_q are inversely proportional to the associated average SNR, it follows that the greater λ_{SE} and λ_{RE}, the smaller the first and the second wiretap link capacities, respectively. That is, the two secrecy capacities become greater which lead to the* SOP *reduction and consequently to enhanced system security.*

Closed-form expression for the SOP

Using (1.34) and (1.31), closed-form expressions for the SOP are derived in Theorem 3.3.1 for both i.n.i.d and i.i.d Rayleigh fading channels.

Theorem 3.3.1. *The* SOP *of the considered communication system subject to i.n.i.d and i.i.d flat Rayleigh fading channels can be expressed by (3.59) and (3.60), respectively,*

$$SOP_{i.n.i.d} = 1 - \frac{1}{\delta}\sum_{k=1}^{L}\frac{\Psi_k e^{-\frac{\iota_k}{\overline{\gamma}_S}}}{\chi_k+1}\left(1-e^{-\phi}+\frac{e^{-\phi}}{\frac{\iota_k}{\overline{\gamma}_P\lambda_{SP}}+1}\right)\sum_{k=1}^{L}\Psi_k\left[\left(1-e^{-\phi}\right)\Phi_1^{(k)}+e^{-\phi}\Phi_2^{(k)}\right], \tag{3.59}$$

and

$$\begin{aligned} SOP_{i.i.d} &= 1-\frac{\lambda_{SE}}{\delta\gamma\left(1-\theta\right)}\sum_{m=0}^{L-1}\frac{\mu^m}{m!\varrho^{m+1}}\left[\begin{array}{c}\left(1-e^{-\phi}\right)e^{-\frac{\varpi}{\overline{\gamma}_S}}\Gamma\left(m+1,\frac{(\gamma-1)\varrho}{\overline{\gamma}_S}\right)\\ +\left(\frac{1}{1+\frac{\varpi}{\overline{\gamma}_P\lambda_{SP}}}\right)G_{2,2}^{2,1}\left(\frac{(\gamma-1)\varrho}{\lambda_{SP}\overline{\gamma}_P+\varpi}\middle|\begin{array}{c}\left(0,\phi+\frac{\varpi}{\overline{\gamma}_S}\right);(1,0)\\ (0,0),(m+1,0);-\end{array}\right)\end{array}\right]\\ &\quad\times\left[1-\xi\left(\frac{1}{\beta}+\frac{\left(1-e^{-\phi}\right)\Omega_1+\Omega_2}{\Gamma\left(L\right)}\right)\right], \end{aligned} \tag{3.60}$$

where

$$\Psi_k = \prod_{\substack{j=1\\ j\neq k}}^{L}\left(\frac{\lambda_{\mathrm{SR}_j}}{\lambda_{\mathrm{SR}_j}-\lambda_{\mathrm{SR}_k}}\right), \tag{3.61}$$

$$\chi_k = \frac{\lambda_{\mathrm{SR}_k}\gamma}{\lambda_{\mathrm{SE}}}, \tag{3.62}$$

$$\gamma = 2^{R_s}, \tag{3.63}$$

$$\iota_k = \frac{\lambda_{\mathrm{SR}_k}\left(\gamma-1\right)}{1-\theta}, \tag{3.64}$$

$$\phi = \frac{\lambda_{\mathrm{SP}}\overline{\gamma}_P}{\overline{\gamma}_S}, \tag{3.65}$$

$$\delta = \frac{\lambda_{\mathrm{RD}}\gamma}{\lambda_{\mathrm{RE}}}+1, \tag{3.66}$$

$$\xi = \lambda_{\mathrm{RD}}\left(\gamma-1\right), \tag{3.67}$$

$$\omega_l^{(k)} = \frac{\lambda_{\mathrm{SR}_k}}{\eta\theta\overline{\gamma}_l}, \tag{3.68}$$

$$l = \{P, S\}, \tag{3.69}$$

$$\omega_l = \frac{\lambda_{\mathrm{SR}}}{\eta\theta\overline{\gamma}_l}, \tag{3.70}$$

$$\beta = \lambda_{\mathrm{RP}}\overline{\gamma}_P + \xi, \tag{3.71}$$

$$\varrho = \frac{\lambda_{\mathrm{SR}} + \frac{\lambda_{\mathrm{SE}}}{\gamma}}{1-\theta}, \tag{3.72}$$

$$\mu = \frac{\lambda_{\mathrm{SR}}}{1-\theta}, \tag{3.73}$$

$$\varpi = \frac{\lambda_{\mathrm{SE}}\left(\frac{1}{\gamma} - 1\right)}{1-\theta}, \tag{3.74}$$

$$\Phi_1^{(k)} = \mathcal{M}_1(\xi) - \frac{\xi}{\beta}\mathcal{M}_1(\beta), \tag{3.75}$$

$$\mathcal{M}_1(u) = G_{0,2}^{2,0}\left(\omega_k^{(S)}u \,\middle|\, \begin{matrix} -;- \\ 0,1;- \end{matrix}\right), \tag{3.76}$$

$$\Phi_2^{(k)} = \frac{\xi\lambda_{\mathrm{SP}}}{\omega_k^{(P)}}\left(\mathcal{Z}(\xi) - \mathcal{Z}(\beta)\right), \tag{3.77}$$

$$\mathcal{Z}(u) = \frac{1}{u^2}\left[G_{2,1}^{1,2}\left(\frac{\lambda_{\mathrm{SP}}}{\omega_k^{(P)}u} \,\middle|\, \begin{matrix} -1,0;- \\ 0;- \end{matrix}\right) - \Lambda_k(u)\right], \tag{3.78}$$

$$\Lambda_k(u) = G_{0,1:1,1:1,2}^{1,0:1,1:1,1}\left(\frac{\omega_k^{(P)}u}{\lambda_{\mathrm{SP}}}, \omega_k^{(S)}u \,\middle|\, \begin{matrix} -;-:1;-:1;- \\ 2;-:1;-:1;0 \end{matrix}\right), \tag{3.79}$$

$$\Omega_1 = \mathcal{M}_2(\xi) - \mathcal{M}_2(\beta), \tag{3.80}$$

$$\mathcal{M}_2(u) = \frac{1}{u}G_{1,3}^{2,1}\left(\omega_S u \,\middle|\, \begin{matrix} 1;- \\ L,1;0 \end{matrix}\right), \tag{3.81}$$

$$\Omega_2 = \mathcal{J}(\xi) - \mathcal{J}(\beta), \tag{3.82}$$

$$\mathcal{J}(u) = \frac{1}{u}G_{3,2}^{2,2}\left(\frac{\omega_P u}{\lambda_{\mathrm{SP}}} \,\middle|\, \begin{matrix} (1,0),(0,\phi);- \\ (L,0),(1,0);(0,0) \end{matrix}\right), \tag{3.83}$$

with u referring to either ξ or β.

Proof.

Substituting (1.31) into (1.34), the SOP can be rewritten as

$$\begin{aligned} \text{SOP} &= 1 - \Pr\left(C_{1S} > R_s\right).Pr\left(C_{2S} > R_s\right) \\ &= 1 - \left[1 - \text{SOP}_1\right]\left[1 - \text{SOP}_2\right], \end{aligned} \tag{3.84}$$

where

$$\text{SOP}_q = \Pr\left(C_{qS} < R_S\right),\ q = \{1,\ 2\}, \tag{3.85}$$

denotes the SOP of either the first or the second hop. Therefore, to derive the above SOP expression, it is sufficient to know both SOP_1 and SOP_2.

- **Expression of SOP_1**

Using (1.32), the expression of SOP_1 can be expressed as

$$\text{SOP}_1 = \Pr\left(\gamma_R \leq \gamma_{1E}\right) + \Pr\left(\gamma_R > \gamma_{1E}\right)\Pr\left(C_{1S} < R_s \,|\gamma_R > \gamma_{1E}\right). \tag{3.86}$$

According to [95, Eq. (12)], SOP_1 can be rewritten as

$$\text{SOP}_1 = \int_{x=0}^{\infty}\int_{y=0}^{\infty} F_{\gamma_R|g_{\text{SP}}=x}\left(\gamma y + \gamma - 1\right) f_{\gamma_{1E}|g_{\text{SP}}=x}(y) f_{g_{\text{SP}}}(x) dy dx. \tag{3.87}$$

The conditional CDF of γ_R given g_{SP} is expressed as

$$\begin{aligned} F_{\gamma_R|g_{\text{SP}}=x}\left(z\right) &= \Pr\left(\gamma_R \leq z \,|g_{\text{SP}} = x\right) \\ &= F_{\text{Y}_{\text{SR}}}\left(\frac{z}{\left(1-\theta\right)\Phi\left(x\right)}\right), \end{aligned} \tag{3.88}$$

with $\Phi\left(x\right)$ is defined in (3.23)

Similarly, the one of γ_{1E} given g_{SP} can be written as

$$\begin{aligned} F_{\gamma_{1E}|g_{\text{SP}}=x}(y) &= \Pr\left(\gamma_{1E} \leq y|g_{\text{SP}} = x\right) \\ &= F_{g_{\text{SE}}}\left(\frac{y}{\left(1-\theta\right)\Phi\left(x\right)}\right). \end{aligned} \tag{3.89}$$

Substituting the derivative of (3.89) alongside (3.88) into (3.87), yields

$$\mathrm{SOP}_1 = \frac{1}{1-\theta}\int_0^{\infty}\frac{f_{g_{\mathrm{SP}}}(x)}{\Phi(x)}\int_0^{\infty}F_{Y_{\mathrm{SR}}}\left(\frac{\gamma y+\gamma-1}{(1-\theta)\Phi(x)}\right)f_{g_{\mathrm{SE}}}\left(\frac{y}{(1-\theta)\Phi(x)}\right)dydx. \tag{3.90}$$

In the sequel, two different cases will be distinguished.

i.n.i.d Rayleigh fading channels of the link S-R

For i.n.i.d Rayleigh fading model, the CDF of Y_{SR} is given by [104]

$$F_{Y_{\mathrm{SR}}}(x) = \sum_{k=1}^{L}\Psi_k\left(1-e^{-\lambda_{\mathrm{SR}_k}x}\right). \tag{3.91}$$

Substituting (3.91) into (3.90) alongside the function $\Phi(x)$, and performing some algebraic manipulations, one can obtain

$$\begin{aligned}\mathrm{SOP}_{1,i.n.i.d} &= \sum_{k=1}^{L}\Psi_k\int_0^{\frac{\overline{\gamma}_P}{\overline{\gamma}_S}}f_{g_{\mathrm{SP}}}(x)\left(1-\frac{e^{-\frac{\iota_k}{\overline{\gamma}_S}}}{\beta_k}\right)dx+\sum_{k=1}^{L}\Psi_k\int_{\frac{\overline{\gamma}_P}{\overline{\gamma}_S}}^{\infty}f_{g_{\mathrm{SP}}}(x)\left(1-\frac{e^{-\frac{\iota_k x}{\overline{\gamma}_P}}}{\beta_k}\right)dx\\ &= 1-\sum_{k=1}^{L}\frac{\Psi_k e^{-\frac{\iota_k}{\overline{\gamma}_S}}}{\epsilon_k}\left(\ 1-e^{-\phi}+\frac{e^{-\phi}}{\frac{\iota_k}{\overline{\gamma}_P\lambda_{\mathrm{SP}}}+1}\ \right),\end{aligned} \tag{3.92}$$

where $\epsilon_k = \chi_k + 1$ and χ_k are defined in Theorem 3.3.1.

i.i.d Rayleigh fading channels of the link S-R

Under this assumption, it can be seen that Y_{SR} is chi square distributed of $2L$ degrees of freedom. That is, the CDF of Y_{SR} can be expressed as [67, Eq. (8.352.1)]

$$\begin{aligned}F_{Y_{\mathrm{SR}}}(y) &= \frac{\gamma_{inc}(L,\lambda_{\mathrm{SR}}y)}{\Gamma(L)},\\ &= 1-e^{-\lambda_{\mathrm{SR}}y}\sum_{m=0}^{L-1}\frac{(\lambda_{\mathrm{SR}}y)^m}{m!}.\end{aligned} \tag{3.93}$$

Incorporating (3.93) into (3.90), and by carrying out some algebraic manipulations, the term $\mathrm{SOP}_{1,i.i.d}$ can be expressed as

$$\mathrm{SOP}_{1,i.i.d} = \left(1-e^{-\phi}\right)\left(1-\frac{\lambda_{\mathrm{SE}}e^{-\frac{\varpi}{\overline{\gamma}_S}}}{\gamma(1-\theta)}\sum_{m=0}^{L-1}\frac{\mu^m}{m!}\frac{\Gamma\left(m+1,\frac{(\gamma-1)\varrho}{\overline{\gamma}_S}\right)}{\varrho^{m+1}}\right)+e^{-\phi}-\frac{\lambda_{\mathrm{SP}}\lambda_{\mathrm{SE}}}{\gamma(1-\theta)}\sum_{m=0}^{L-1}\frac{\mu^m}{m!}\frac{\digamma_1}{\varrho^{m+1}}, \tag{3.94}$$

where

$$\digamma_1 = \int_{\frac{\overline{\gamma}_P}{\overline{\gamma}_S}}^{\infty} e^{-\left(\frac{\varpi}{\overline{\gamma}_P}+\lambda_{\rm SP}\right)x}\Gamma\left(m+1,\frac{(\gamma-1)\,\varrho}{\overline{\gamma}_P}x\right)dx. \tag{3.95}$$

Using [71, Eq. (06.06.26.0005.01)], the term $\digamma_1$ can be expressed in terms of upper incomplete Meijer's G-function as follows:

$$\begin{aligned}
\digamma_1 &= \int_{\frac{\overline{\gamma}_P}{\overline{\gamma}_S}}^{\infty} G_{1,2}^{2,0}\left(\frac{(\gamma-1)\,\varrho x}{\overline{\gamma}_P}\,\middle|\,\begin{matrix}-;1\\ 0,m+1;-\end{matrix}\right)e^{-\nu x}dx\\
&= \frac{1}{\nu}\frac{1}{2\pi j}\int_{\mathcal{C}}\frac{\Gamma(s)\,\Gamma(m+1+s)\,\Gamma(1-s,\varsigma)}{\Gamma(1+s)}\left(\frac{(\gamma-1)\,\varrho}{\overline{\gamma}_P\nu}\right)^{-s}ds\\
&= \frac{1}{\nu}G_{2,2}^{2,1}\left(\frac{(\gamma-1)\,\varrho}{\overline{\gamma}_P\nu}\,\middle|\,\begin{matrix}(0,\varsigma);(1,0)\\ (0,0),(m+1,0);-\end{matrix}\right),
\end{aligned} \tag{3.96}$$

where $\mathcal{C}$ is a complex contour of integration ensuring the convergence of the above Meijer's G-function, $\varsigma = \phi + \frac{\varpi}{\overline{\gamma}_S}$, and $\nu = \lambda_{\rm SP} + \varpi/\overline{\gamma}_P$.

Replacing (3.96) into (3.94), yields

$$\mathrm{SOP}_{1,i.i.d} = 1 - \frac{\lambda_{\rm SE}}{\gamma\,(1-\theta)}\sum_{m=0}^{L-1}\frac{\mu^m}{m!\varrho^{m+1}}\left[\,\left(1-e^{-\phi}\right)e^{-\frac{\varpi}{\overline{\gamma}_S}}\Gamma\left(m+1,\tfrac{(\gamma-1)\varrho}{\overline{\gamma}_S}\right)+\tfrac{\Theta_m}{1+\frac{\varpi}{\overline{\gamma}_P\lambda_{\rm SP}}}\,\right], \tag{3.97}$$

where $\Theta_m = G_{2,2}^{2,1}\left(\frac{(\gamma-1)\varrho}{\overline{\gamma}_P\nu}\,\middle|\,\begin{matrix}(0,\varsigma);(1,0)\\ (0,0),(m+1,0);-\end{matrix}\right)$.

- **Expression of SOP_2**

In the same manner to SOP_1, the SOP_2 for the second hop can be expressed from (1.33) as follows:

$$\mathrm{SOP}_2 = \Pr\left(\gamma_D \le \gamma_{2E}\right) + \Pr\left(\gamma_D > \gamma_{2E}\right)\Pr\left(C_{2S} < R_s\,|\gamma_D > \gamma_{2E}\right). \tag{3.98}$$

Similarly to (3.87), SOP_2 can be expressed as

$$\mathrm{SOP}_2 = \int_{x=0}^{\infty}\int_{y=0}^{\infty} F_{\gamma_D|\rho_R=x}\left(\gamma y+\gamma-1\right)f_{\gamma_{2E}|\rho_R=x}(y)f_{\rho_R}(x)dydx. \tag{3.99}$$

The CDFs of γ_D and γ_{2E} for a given ρ_R are expressed as

$$\begin{aligned} F_{\gamma_D|\rho_R=x}(z) &= \Pr(\gamma_D \leq z \,|\rho_R = x) \\ &= F_{g_{\mathrm{RD}}}\left(\frac{z}{x}\right), \end{aligned} \tag{3.100}$$

and

$$\begin{aligned} F_{\gamma_{2E}|\rho_R=x}(z) &= \Pr(\gamma_{2E} \leq z \,|\rho_R = x) \\ &= F_{g_{\mathrm{RE}}}\left(\frac{z}{x}\right), \end{aligned} \tag{3.101}$$

respectively, while the one of ρ_R is given by

$$\begin{aligned} F_{\rho_R}(z) &= \Pr\left(\min\left(\eta\theta W_k, \frac{\overline{\gamma}_P}{g_{\mathrm{RP}}}\right) \leq z\right) \\ &= \underbrace{\Pr\left(\eta\theta W_k \leq z, \frac{\overline{\gamma}_P}{g_{\mathrm{RP}}} \geq \eta\theta W_k\right)}_{\mathcal{I}_1} + \underbrace{\Pr\left(\frac{\overline{\gamma}_P}{g_{\mathrm{RP}}} \leq z, \frac{\overline{\gamma}_P}{g_{\mathrm{RP}}} \leq \eta\theta W_k\right)}_{\mathcal{I}_2}. \end{aligned} \tag{3.102}$$

Likewise, the terms $\mathcal{I}_1$ and $\mathcal{I}_2$ can be expressed as

$$\begin{aligned} \mathcal{I}_1 &= \Pr\left(\eta\theta W_k \leq z, \frac{\overline{\gamma}_P}{g_{\mathrm{RP}}} \geq \eta\theta W_k\right) \\ &= \int_0^{\frac{z}{\eta\theta}} F_{g_{\mathrm{RP}}}\left(\frac{\overline{\gamma}_P}{\eta\theta y}\right) f_{W_k}(y)\, dy, \end{aligned} \tag{3.103}$$

and

$$\begin{aligned} \mathcal{I}_2 &= \Pr\left(\frac{\overline{\gamma}_P}{g_{\mathrm{RP}}} \leq z, \frac{\overline{\gamma}_P}{g_{\mathrm{RP}}} \leq \eta\theta W_k\right) \\ &= \int_{\frac{\overline{\gamma}_P}{z}}^{\infty} \left(1 - F_{W_k}\left(\frac{\overline{\gamma}_P}{\eta\theta y}\right)\right) f_{g_{\mathrm{RP}}}(y)\, dy. \end{aligned} \tag{3.104}$$

respectively. Substituting the two terms $\mathcal{I}_1$ and $\mathcal{I}_2$ into (3.102) and performing some algebraic operations, the CDF of ρ_R can be rewritten as

$$F_{\rho_R}(z) = 1 - F_{g_{\mathrm{RP}}}\left(\frac{\overline{\gamma}_P}{z}\right)\left[1 - F_{W_k}\left(\frac{z}{\eta\theta}\right)\right]. \tag{3.105}$$

On the other hand, the CDF of W_k is expressed by

$$\begin{aligned} F_{W_k}(y) &= \Pr\left(\min\left(\overline{\gamma}_s, \frac{\overline{\gamma}_P}{g_{\mathrm{SP}}}\right) Y_{\mathrm{SR}} \leq y\right) \\ &= \underbrace{\Pr\left(Y_{\mathrm{SR}} \leq \frac{y}{\overline{\gamma}_s}, \frac{\overline{\gamma}_P}{g_{\mathrm{SP}}} \geq \overline{\gamma}_s\right)}_{\mathcal{T}_1} + \underbrace{\Pr\left(\frac{Y_{\mathrm{SR}}}{g_{\mathrm{SP}}} \leq \frac{y}{\overline{\gamma}_P}, \frac{\overline{\gamma}_P}{g_{\mathrm{SP}}} \leq \overline{\gamma}_s\right)}_{\mathcal{T}_2}. \end{aligned} \tag{3.106}$$

The two terms $\mathcal{T}_1$ and $\mathcal{T}_2$ can be rewritten as

$$\mathcal{T}_1 = F_{Y_{\mathrm{SR}}}\left(\frac{y}{\overline{\gamma}_s}\right) F_{g_{\mathrm{SP}}}\left(\frac{\overline{\gamma}_P}{\overline{\gamma}_s}\right), \tag{3.107}$$

and

$$\mathcal{T}_2 = \int_{\frac{\overline{\gamma}_P}{\overline{\gamma}_s}}^{\infty} F_{Y_{\mathrm{SR}}}\left(\frac{y}{\overline{\gamma}_P} t\right) f_{g_{\mathrm{SP}}}(t)\, dt. \tag{3.108}$$

In the sequel, two cases will be distinguished.

i.n.i.d Rayleigh fading channels of the link S-R

With the aid of (3.91), the two terms $\mathcal{T}_1$ and $\mathcal{T}_2$ can be rewritten as

$$\mathcal{T}_1 = \left(1 - e^{-\phi}\right) \sum_{k=1}^{L} \Psi_k \left(1 - e^{-\alpha_S^{(k)} y}\right), \tag{3.109}$$

and

$$\mathcal{T}_2 = \sum_{k=1}^{L} \Psi_k \left(e^{-\phi} - \frac{e^{-\left(\alpha_S^{(k)} y + \phi\right)}}{\frac{\alpha_P^{(k)}}{\lambda_{\mathrm{SP}}} y + 1}\right), \tag{3.110}$$

where $\alpha_l^{(k)} = \lambda_{\mathrm{SR}_k}/\overline{\gamma}_l$, $l = \{S, P\}$.

Now, substituting (3.109) and (3.110) into (3.106), yields

$$F_{W_k}(y) = 1 - \left(1 - e^{-\phi}\right) \sum_{k=1}^{L} \Psi_k e^{-\alpha_S^{(k)} y} - e^{-\phi} \sum_{k=1}^{L} \Psi_k \frac{e^{-\alpha_S^{(k)} y}}{\frac{\alpha_P^{(k)}}{\lambda_{\mathrm{SP}}} y + 1}. \tag{3.111}$$

The CDF of ρ_R can be now rewritten as

$$F_{\rho_R}(z) = 1 - F_{g_{\mathrm{RP}}}\left(\frac{\overline{\gamma}_P}{z}\right) + F_{g_{\mathrm{RP}}}\left(\frac{\overline{\gamma}_P}{z}\right) e^{-\phi} \sum_{k=1}^{L} \Psi_k e^{-\omega_k^{(S)} z} \left[1 - \frac{1}{\frac{\omega_k^{(P)}}{\lambda_{\mathrm{SP}}} z + 1}\right]. \tag{3.112}$$

By substituting (3.100), (3.112), and the derivative of (3.101) into (3.99), along with some

algebraic manipulations, yields

$$\begin{aligned} \mathrm{SOP}_{2,i.n.i.d} &= 1-\frac{1}{\delta}\left[1-\xi\int_0^{\infty}\frac{e^{-\frac{\xi}{x}}}{x^2}F_{\rho_R}(x)dx\right] \\ &= 1-\frac{1}{\delta}\sum_{k=1}^{L}\Psi_k\left[\left(1-e^{-\phi}\right)\Phi_1^{(k)}+e^{-\phi}\Phi_2^{(k)}\right], \end{aligned} \tag{3.113}$$

where

$$\Phi_1^{(k)}=\xi\int_0^{\infty}\frac{e^{-\left(\omega_k^{(S)}x+\frac{\xi}{x}\right)}}{x^2}\left(1-e^{-\frac{\lambda_{\mathrm{RP}}\overline{\gamma}_P}{x}}\right)dx, \tag{3.114}$$

and

$$\begin{aligned} \Phi_2^{(k)} &= \xi\int_0^{\infty}\frac{e^{-\left(\omega_k^{(S)}x+\frac{\xi}{x}\right)}\left(1-e^{-\frac{\lambda_{\mathrm{RP}}\overline{\gamma}_P}{x}}\right)}{x^2\left(\frac{\omega_k^{(P)}}{\lambda_{\mathrm{SP}}}x+1\right)}dx \\ &= \frac{\xi\lambda_{\mathrm{SP}}}{\omega_k^{(P)}}\left[\mathcal{G}\left(\xi\right)-\mathcal{G}\left(\beta\right)\right], \end{aligned} \tag{3.115}$$

with

$$\mathcal{G}\left(u\right)=\int_0^{\infty}\frac{te^{-\left(\frac{\omega_k^{(S)}}{t}+ut\right)}}{1+\frac{\lambda_{\mathrm{SP}}}{\omega_k^{(P)}}t}dt, u=\{\xi,\beta\}, \tag{3.116}$$

where β is defined in Theorem 3.3.1. Using [67, Eq. (3.324.1)] alongside [71, Eq. (03.04.26.0006.01)], we obtain (3.75).

By also using Eqs. (07.34.03.0271.01) and (01.03.26.0007.01) of [71], (3.116) can be rewritten as

$$\mathcal{G}\left(u\right)=\Xi_1-\Xi_2, \tag{3.117}$$

where

$$\Xi_1=\int_0^{\infty}te^{-ut}G_{1,1}^{1,1}\left(\frac{\lambda_{\mathrm{SP}}}{\omega_k^{(P)}}t\,\middle|\,\begin{matrix}0;-\\0;-\end{matrix}\right)dt, \tag{3.118}$$

and

$$\Xi_2=\int_0^{\infty}te^{-ut}G_{1,1}^{1,1}\left(\frac{\lambda_{\mathrm{SP}}}{\omega_k^{(P)}}t\,\middle|\,\begin{matrix}0;-\\0;-\end{matrix}\right)G_{1,2}^{1,1}\left(\frac{\omega_k^{(S)}}{t}\,\middle|\,\begin{matrix}1;-\\1;0\end{matrix}\right)dt.$$

Using [71, Eq. (07.34.21.0088.01)], the term Ξ_1 can be rewritten as

$$\Xi_1 = u^{-2} G_{2,1}^{1,2}\left(\frac{\lambda_{\mathrm{SP}}}{\omega_k^{(P)} u}\middle| \begin{matrix} -1, 0; - \\ 0; - \end{matrix}\right). \tag{3.119}$$

On the other hand, the term Ξ_2 can be re-expressed as

$$\Xi_2 = \frac{1}{(2\pi j)^2}\int_{\mathcal{C}_s} \Gamma(-s)\,\Gamma(1+s)\left(\frac{\omega_k^{(P)}}{\lambda_{\mathrm{SP}}}\right)^{-s} \int_{\mathcal{C}_t} \frac{\Gamma(1+v)\,\Gamma(-v)}{\Gamma(1-v)\left(\omega_k^{(S)}\right)^v} ds dv \int_0^\infty \frac{t^{s+v+1}}{e^{ut}} dt, \tag{3.120}$$

which becomes $\Xi_2 = \Lambda_k(u)/\xi^2$, where $\Lambda_k(u)$ is being defined in (3.79), and $\mathcal{C}_s$ and $\mathcal{C}_t$ are two complex contours of integration ensuring the convergence of the above bivariate Meijer's G-functions.

Replacing (3.119) and (3.120) into (3.117) and then incorporating (3.117) into (3.115), one can obtain (3.77).

i.i.d Rayleigh fading channels of the link S-R

Subject to this case, (3.107) and (3.108) can be rewritten using (3.93) as

$$\mathcal{T}_1 = \frac{\left(1 - e^{-\phi}\right)}{\Gamma(L)} \gamma_{inc}(L, \alpha_S y). \tag{3.121}$$

Using (3.93) along with [71, Eq. (06.06.26.0004.01)], (3.108) can be expressed as

$$\begin{aligned} \mathcal{T}_2 &= \frac{1}{2\pi j}\int_{\mathcal{C}} \frac{\Gamma(L+s)\,\Gamma(-s)\,\Gamma(1-s,\phi)}{\Gamma(1-s)\,\Gamma(L)} \left(\frac{\alpha_P y}{\lambda_{\mathrm{SP}}}\right)^{-s} ds \\ &= \frac{1}{\Gamma(L)} G_{2,2}^{1,2}\left(\frac{\alpha_P y}{\lambda_{\mathrm{SP}}}\middle| \begin{matrix} (1,0), (0,\phi); - \\ (L,0); (0,0) \end{matrix}\right), \end{aligned} \tag{3.122}$$

where $\alpha_v = \lambda_{\mathrm{SR}}/\overline{\gamma}_v, v = \{S, P\}$. Now, substituting (3.121) and (3.122) into (3.106), yields

$$F_{W_k}(y) = \frac{\left(1 - e^{-\phi}\right)\gamma(L, \alpha_S y)}{\Gamma(L)} + \frac{1}{\Gamma(L)} G_{2,2}^{1,2}\left(\frac{\alpha_P y}{\lambda_{\mathrm{SP}}}\middle| \begin{matrix} (1,0), (0,\phi); - \\ (L,0); (0,0) \end{matrix}\right). \tag{3.123}$$

Substituting (3.123) into (3.105), one can obtain

$$F_{\rho_R}(z) = e^{-\frac{\lambda_{\mathrm{RP}}\overline{\gamma}_P}{z}} + \frac{\left(1-e^{-\frac{\lambda_{\mathrm{RP}}\overline{\gamma}_P}{z}}\right)}{\Gamma(L)} \left[\begin{array}{c} \left(1-e^{-\phi}\right)\gamma\left(L,\omega_S z\right) \\ +G_{1,2}^{1,1}\left(\omega_P z \left| \begin{array}{c} (1,0),(0,\phi);- \\ (L,0);(0,0) \end{array} \right. \right) \end{array} \right] \tag{3.124}$$

where ω_P is being defined in Theorem 3.3.1.

Similarly to (3.113), $\mathrm{SOP}_{2,i.i.d}$ can be expressed as

$$\begin{aligned} \mathrm{SOP}_{2,i.i.d} &= 1-\frac{1}{\delta}\left[1-\xi\int_0^\infty \frac{e^{-\frac{\xi}{x}}}{x^2}F_{\rho_R}(x)dx\right] \\ &= 1-\frac{1}{\delta}\left[1-\xi\left\{\frac{1}{\beta}+\frac{\left(1-e^{-\phi}\right)\Omega_1+\Omega_2}{\Gamma(L)}\right\}\right] \end{aligned} \tag{3.125}$$

where

$$\Omega_1 = \int_0^\infty \frac{e^{-\frac{\xi}{x}}}{x^2}\left(1-e^{-\frac{\lambda_{\mathrm{RP}}\overline{\gamma}_P}{x}}\right)\gamma\left(L,\omega_S x\right)dx, \tag{3.126}$$

and

$$\Omega_2 = \int_0^\infty \frac{e^{-\frac{\xi}{x}}}{x^2}\left(1-e^{-\frac{\lambda_{\mathrm{RP}}\overline{\gamma}_P}{x}}\right)G_{1,2}^{1,1}\left(\frac{\omega_S}{\lambda_{\mathrm{SP}}}x\left| \begin{array}{c} (1,0),(0,\phi);- \\ (L,0);(0,0) \end{array} \right.\right)dx. \tag{3.127}$$

By making a change of variable $t=1/x$ and using [71, Eq. (06.06.26.0004.01)], the term Ω_1 can be rewritten as

$$\Omega_1 = \int_0^\infty e^{-\xi t}G_{1,2}^{1,1}\left(\frac{\omega_S}{t}\left| \begin{array}{c} 1;- \\ L;0 \end{array} \right.\right)dt - \int_0^\infty e^{-\beta t}G_{1,2}^{1,1}\left(\frac{\omega_S}{t}\left| \begin{array}{c} 1;- \\ L;0 \end{array} \right.\right)dt, \tag{3.128}$$

while

$$\begin{aligned} G_{1,2}^{1,1}\left(\frac{\omega_S}{t}\left| \begin{array}{c} 1;- \\ L;0 \end{array} \right.\right) &= \int_{\mathcal{C}} \frac{\Gamma(L-s)\Gamma(s)}{\Gamma(1+s)}\left(\frac{t}{\omega_S}\right)^{-s}ds \\ &= G_{2,1}^{1,1}\left(\frac{t}{\omega_S}\left| \begin{array}{c} 1-L;1 \\ 0;- \end{array} \right.\right). \end{aligned} \tag{3.129}$$

Now, making use of [71, Eq. (07.34.21.0088.01)], one can obtain (3.80). On the contrary, the

term Ω_2 can be expressed as

$$\Omega_2 = \int_{\mathcal{C}} \frac{\Gamma(L+s)\,\Gamma(-s)\,\Gamma(1-s,\phi)}{2\pi j \Gamma(1-s)} \left(\frac{\omega_P}{\lambda_{\rm SP}}\right)^{-s} \left\{ \int_0^{\infty} e^{-\xi t} t^s dt ds - \int_0^{\infty} e^{-\beta t} t^s dt \right\} ds, \quad (3.130)$$

which leads to (3.82). Finally, replacing (3.75) and (3.77) into (3.113) and incorporating (3.92) along with the final expression for $\mathrm{SOP}_{2,i.n.i.d}$ into (3.84) yields (3.59). By also replacing (3.80) and (3.130) into (3.125), one can obtain the final expression for $\mathrm{SOP}_{2,i.i.d}$. Then, by substituting it alongside (3.97) into (3.84), we obtain (3.60), which concludes the proof of Theorem 3.3.1. ■

Asymptotic Secrecy Outage Probability

An asymptotic analysis is next carried out in order to obtain useful insights on the impact of the involved parameters on the overall system performance. Based on this, we quantify the impact of the MTIP at the PU receiver on the SOP behavior. Similarly to [95], we assume that the interference power P_I is proportional to the maximum transmit power of the source S. For the sake of simplicity, we define the positive constant $\sigma = \overline{\gamma}_P/\overline{\gamma}_S = P_I/P_S^{\max}$.

Proposition 1. *The Asymptotic* SOP *in high SNR regimes (i.e., $\overline{\gamma}_P \to \infty$) of the considered communication system subject to i.n.i.d as well as i.i.d flat Rayleigh fading channels for the S-R link can be expressed by (3.131) and (3.132), respectively, as*

$$\mathrm{SOP}_{i.n.i.d} \sim 1 - \frac{\mathcal{A}_1}{\delta} - \frac{\mathcal{A}_2}{\delta}\overline{\gamma}_P^{-1}, \quad (3.131)$$

and

$$\mathrm{SOP}_{i.i.d} \sim 1 - \frac{\mathcal{C}_1}{\delta} + \frac{\mathcal{C}_2 + \mathcal{D}_1}{\delta}\overline{\gamma}_P^{-1}, \quad (3.132)$$

where

$$\mathcal{A}_1 = \sum_{k=1}^{L} \frac{\Psi_k}{\chi_k + 1}, \quad (3.133)$$

$$\mathcal{A}_2 = \sum_{k=1}^{L} \frac{\Psi_k}{\chi_k + 1} \left\{ \iota_k \left(\sigma + \frac{e^{-\phi}}{\lambda_{\rm SP}}\right) - \frac{\xi}{\lambda_{\rm RP}} \right\}, \quad (3.134)$$

$$\mathcal{C}_1 = \frac{\lambda_{\rm SE}\left(\frac{1}{\varrho} + \sum_{m=1}^{L-1} \frac{\mu^m}{\varrho^{m+1}}\right)}{\gamma(1-\theta)}, \quad (3.135)$$

$$\mathcal{C}_2 = \frac{\lambda_{\mathrm{SE}}}{\gamma\left(1-\theta\right)}\left[\gamma - 1 + \varpi\left(\frac{1}{\varrho} + \sum_{m=1}^{L-1}\frac{\mu^m}{\varrho^{m+1}}\right)\right]\left[\left(1-e^{-\phi}\right)\sigma + \frac{\Gamma\left(2,\phi\right)}{\lambda_{\mathrm{SP}}}\right], \tag{3.136}$$

$$\mathcal{D}_1 = \frac{\xi C_1}{\lambda_{\mathrm{RP}}}\left[1 + \frac{\left(1-e^{-\phi}\right)}{\Gamma\left(L\right)}\left(\mathcal{B}_1 + \mathcal{B}_2\right) - \mathcal{B}_3\right], \tag{3.137}$$

$$\mathcal{B}_1 = \frac{\left(-a\right)^L}{L!}\left[\psi(1) + 2\psi(L) - \psi(1+L) - \log\left(a\right)\right], \tag{3.138}$$

$$\mathcal{B}_2 = \sum_{i=2}^{L-1}\frac{\Gamma\left(L-i\right)}{i!}\left(-a\right)^i, \tag{3.139}$$

$$\mathcal{B}_3 = \frac{1}{\Gamma\left(L\right)}G_{2,3}^{2,2}\left(\frac{a}{\lambda_{\mathrm{SP}}\sigma}\middle|\begin{matrix}\left(1,0\right),\left(0,\phi\right);-\\ \left(L,0\right),\left(1,0\right);\left(0,0\right)\end{matrix}\right) - \frac{a\Gamma\left(2,\phi\right)}{\left(L-1\right)\lambda_{\mathrm{SP}}\sigma}, \tag{3.140}$$

whereas $a = \frac{\sigma\lambda_{\mathrm{SR}}\lambda_{\mathrm{RP}}}{\eta\theta}$, and $\psi\left(.\right)$ stands for the Polygamma function [71, Eq. (06.14.02.0001.01)].

Proof.

- **Asymptotic expression for SOP at the first hop**

In order to find the asymptotic expression of SOP for both *i.n.i.d* and *i.i.d* cases, we use the Maclaurin series when $1/\overline{\gamma}_P$ approaches zero, to express the exponential function, the upper incomplete Gamma function, and the polynomial power function as well.

i.n.i.d Rayleigh fading channels of the link S-R

Armed by Maclaurin series of the exponential function and the polynomial power function, the approximate SOP can be expressed from (3.92) as

$$\mathrm{SOP}_{1,i.n.i.d} \sim 1 - \sum_{k=1}^{L}\frac{\Psi_k}{\chi_k+1} - \overline{\gamma}_P^{-1}\left(\sigma + \frac{e^{-\phi}}{\lambda_{\mathrm{SP}}}\right)\sum_{k=1}^{L}\frac{\Psi_k\iota_k}{\chi_k+1}, \tag{3.141}$$

i.i.d Rayleigh fading channels of the link S-R

Note that the upper incomplete Gamma can be asymptotically expressed, near $x = 0$ as

$$\Gamma\left(a,x\right) \sim \begin{cases} 1-x, & a = 1 \\ \Gamma\left(a\right), & a > 1 \end{cases} \tag{3.142}$$

By replacing (3.142) into (3.94), yields

$$\mathrm{SOP}_{1,i.i.d} \sim 1 - \frac{\left(1-e^{-\phi}\right)\lambda_{\mathrm{SE}}\left(1-\frac{\sigma\varpi}{\overline{\gamma}_P}\right)}{\gamma\left(1-\theta\right)}\left[\frac{1-\frac{\sigma(\gamma-1)\varrho}{\overline{\gamma}_P}}{\varrho}+\sum_{m=1}^{L-1}\frac{\mu^m}{\varrho^{m+1}}\right]-\frac{\lambda_{\mathrm{SP}}}{\gamma\left(1-\theta\right)}$$
$$\times\int_{\frac{\overline{\gamma}_P}{\overline{\gamma}_S}}^{\infty} e^{-\lambda_{\mathrm{SP}}x}\lambda_{\mathrm{SE}}\left(1-\frac{\varpi}{\overline{\gamma}_P}x\right)\left[\frac{1-\frac{(\gamma-1)\varrho}{\overline{\gamma}_P}x}{\varrho}+\sum_{m=1}^{L-1}\frac{\mu^m}{\varrho^{m+1}}\right]dx, \tag{3.143}$$

By performing some mathematical manipulations, we obtain

$$\mathrm{SOP}_{1,i.i.d} \sim 1-\mathcal{C}_1+\mathcal{C}_2\overline{\gamma}_P^{-1}, \tag{3.144}$$

where $\mathcal{C}_1$ and $\mathcal{C}_2$ are defined in (3.135) and (3.136), respectively.

- **Asymptotic expression for the SOP at the second hop**

In this part, the residues theorem will be used to derive the asymptotic expressions of both Meijer's and incomplete Meijer's G-functions.

i.n.i.d Rayleigh fading channels of the link S-R

The term $\Phi_2^{(k)}$ given in (3.115) can be approximated for high values of $\overline{\gamma}_P$ as

$$\Phi_2^{(k)} \sim \xi\left[\int_0^{\infty}\frac{e^{-\left(\omega_k^{(S)}x+\frac{\xi}{x}\right)}}{x^2}\left(1-\frac{\omega_k^{(P)}}{\lambda_{\mathrm{SP}}}x\right)dx-\int_0^{\infty}\frac{e^{-\left(\omega_k^{(S)}x+\frac{\beta}{x}\right)}}{x^2}\left(1-\frac{\omega_k^{(P)}}{\lambda_{\mathrm{SP}}}x\right)dx\right], \tag{3.145}$$

That is, this term becomes with the help of [105, Eq. (2.9.32)] as

$$\Phi_2^{(k)} \sim \xi\omega_k^{(P)}\left[\sigma\left(\mathcal{M}_3\left(\xi\right)-\mathcal{M}_3\left(\beta\right)\right)+\tfrac{1}{\lambda_{\mathrm{SP}}}\left(\mathcal{M}_4\left(\beta\right)-\mathcal{M}_4\left(\xi\right)\right)\right], \tag{3.146}$$

where $\mathcal{M}_3\left(u\right)=G_{0,2}^{2,0}\left(\sigma\omega_k^{(P)}u\,\middle|\,\begin{matrix}-;-\\0,-1;-\end{matrix}\right)$, $\mathcal{M}_4\left(u\right)=G_{0,2}^{2,0}\left(\sigma\omega_k^{(P)}u\,\middle|\,\begin{matrix}-;-\\0,0;-\end{matrix}\right)$, and $u=\{\xi,\beta\}$.

The term $\mathcal{M}_3\left(u\right)$ given in (3.146) can be written in terms of complex integral as

$$\mathcal{M}_3\left(u\right)=\frac{1}{2\pi j}\int_{\mathcal{C}}\frac{\Gamma^2\left(s\right)}{s-1}\left(\sigma\omega_k^{(P)}u\right)^{-s}ds, \tag{3.147}$$

That is, the above integrand function has

- Poles of second-order: $-l$, $l\in\mathbb{N}$.

- Simple pole (i.e., of first-order) at $l = 1$.

Hence, (3.147) can be expressed using the residue theorem [105, Theorem 1.5] as follows:

$$\mathcal{M}_3(u) = \lim_{s\to 1} \Gamma^2(s) \left(\sigma\omega_k^{(P)} u\right)^{-s} + \sum_{l=0}^{\infty} \lim_{s\to -l} \frac{\partial Q_1(s,u)}{\partial s}, \tag{3.148}$$

where

$$Q_1(s,u) = \mathcal{H}_1(s)\mathcal{H}_2(s) \left(\sigma\omega_k^{(P)} u\right)^{-s}, \tag{3.149}$$

$$\mathcal{H}_1(s) = (s+l)^2\Gamma^2(s), \tag{3.150}$$

and

$$\mathcal{H}_2(s) = \frac{1}{s-1}. \tag{3.151}$$

The partial derivative of (3.149) with respect to s is given by

$$\frac{\partial Q_1(s,u)}{\partial s} = \lim_{s\to -l} \left(\mathcal{U}_1 + \mathcal{U}_2 + \mathcal{U}_3\right), \tag{3.152}$$

where

$$\mathcal{U}_1 = -\mathcal{H}_1(s)\mathcal{H}_2(s) \left(\sigma\omega_k^{(P)} u\right)^{-s} \log\left(\sigma\omega_k^{(P)} u\right), \tag{3.153}$$

$$\mathcal{U}_2 = -\frac{\mathcal{H}_1(s)}{(s-1)^2} \left(\sigma\omega_k^{(P)} u\right)^{-s}, \tag{3.154}$$

$$\mathcal{U}_3 = 2(s+l)\Gamma^2(s)\left[1 + (s+l)\psi(s)\right] \mathcal{H}_2(s) \left(\sigma\omega_k^{(P)} u\right)^{-s}. \tag{3.155}$$

Using [71, Eq. (06.05.04.0004.01)], the limit of the terms $\mathcal{U}_1$ and $\mathcal{U}_2$ can be expressed as

$$\lim_{s\to -l} \mathcal{U}_1 = \frac{\left(\sigma\omega_k^{(P)} u\right)^{l} \log\left(\sigma\omega_k^{(P)} u\right)}{(l+1)!l!}, \tag{3.156}$$

and

$$\lim_{s\to -l} \mathcal{U}_2 = -\frac{\left(\sigma\omega_k^{(P)} u\right)^{l}}{[(l+1)!]^2}. \tag{3.157}$$

By considering $s = -l + \epsilon$ and making use of [71, Eq. (06.14.06.0026.01)], one can see that

$$\lim_{s\to -l} \mathcal{U}_3 = -\frac{2\psi(l+1)}{(l+1)!l!} \left(\sigma\omega_k^{(P)} u\right)^{l}. \tag{3.158}$$

Finally, substituting (3.156), (3.157), and (3.158) into (3.152), yields

$$\mathcal{M}_3(u) = \left(\sigma\omega_k^{(P)}u\right)^{-1} + \sum_{l=0}^{+\infty} \frac{\left(\sigma\omega_k^{(P)}u\right)^l}{l!\,(l+1)!}\left[\log\left(\sigma\omega_k^{(P)}u\right) - 2\psi(l+1) - \frac{1}{l+1}\right]. \tag{3.159}$$

In the same manner to $\mathcal{M}_3(u)$, it can be seen that the integrand associated with $\mathcal{M}_4(u)$ has only poles of second-order, namely $-l$, $l \in \mathbb{N}$. Thus, similarly to (4.182), the term $\mathcal{M}_4(u)$ can be expressed as

$$\mathcal{M}_4(u) = \sum_{l=0}^{+\infty} \frac{\left(\sigma\omega_k^{(P)}u\right)^l}{(l!)^2}\left[2\psi(l+1) - \log\left(\sigma\omega_k^{(P)}u\right)\right]. \tag{3.160}$$

On the other hand, one can notice that the integrand of the Mellin-Barnes integral associated with the Meijer's G-function $\mathcal{M}_1(u)$ defined in (3.76) has poles of second-order at $-l$, $l \in \mathbb{N}$. To this effect, it follows that

$$\mathcal{M}_1(u) = \sum_{l=0}^{+\infty} \frac{\left(\sigma\omega_k^{(P)}u\right)^l}{(l!)^2}\left[l\log\left(\sigma\omega_k^{(P)}u\right) - 2l\psi(1+l) + 1\right]. \tag{3.161}$$

Now, by substituting (3.159) and (3.160) into (3.146) and incorporating (3.161) into (3.75), then replacing $\Phi_1^{(k)}$ and the approximate expression of $\Phi_2^{(k)}$ into (3.113) and by considering only the first terms in the infinite series (i.e., $l = 0$ and $l = 1$), the asymptotic expression of $\mathrm{SOP}_{2,i.n.i.d}$ is obtained, namely

$$\mathrm{SOP}_{2,i.n.i.d} \sim 1 - \frac{1}{\delta}\left(1 - \frac{\xi}{\lambda_{\mathrm{RP}}\overline{\gamma}_P}\right). \tag{3.162}$$

i.i.d Rayleigh fading channels of the link S-R

One can notice that $\mathcal{M}_2(u)$ is given in (3.80) can be rewritten in terms of complex integral as

$$\mathcal{M}_2(u) = \frac{1}{u}\frac{1}{2\pi j}\int_{\mathcal{C}} \frac{\Gamma(1+s)\,\Gamma(L+s)\,\Gamma(-s)}{\Gamma(1-s)\,(\sigma\omega_P u)^s} ds, \tag{3.163}$$

It can be noticed that the integrand function given in (3.163) has poles of second-order at $-L-i, i \in \mathbb{N}$ and ones of simple order at $-i$, $1 \le i \le L-1$. That is

$$\mathcal{M}_2(u) = \frac{1}{u}\sum_{i=1}^{L-1} \lim_{s\to -i}(s+i)\,Q_2(s,u) + \frac{1}{u}\sum_{i=0}^{\infty} \lim_{s\to -(L+i)} \frac{\partial Q_3(s,u)}{\partial s}. \tag{3.164}$$

Based on this, it follows that

$$\lim_{s\to -i}\left(s+i\right)Q_2\left(s,u\right)=\frac{\left(-1\right)^{i-1}\Gamma\left(L-i\right)}{i!}\left(\sigma\omega_P u\right)^i, \tag{3.165}$$

and

$$Q_2\left(s,u\right)=\frac{\left(s+L+i\right)^2\Gamma\left(L+s\right)\Gamma\left(1+s\right)\Gamma\left(-s\right)}{\Gamma\left(1-s\right)\left(\sigma\omega_P u\right)^s}. \tag{3.166}$$

On the other hand, the partial derivative of $Q_3\left(s,u\right)$ with respect to s is given by

$$\frac{\partial Q_3\left(s,u\right)}{\partial s}=\mathcal{U}_4+\mathcal{U}_5+\mathcal{U}_6, \tag{3.167}$$

where

$$\mathcal{U}_4=-(s+L+i)^2\Gamma\left(L+s\right)\Gamma\left(1+s\right)\frac{\Gamma\left(-s\right)}{\Gamma\left(1-s\right)}\left(\sigma\omega_P u\right)^{-s}\log\left(\sigma\omega_P u\right), \tag{3.168}$$

$$\mathcal{U}_5=\left[2+\left(s+L+i\right)\left\{\psi(L+s)+\psi(1+s)\right\}\right]\frac{(s+L+i)\Gamma\left(L+s\right)\Gamma\left(1+s\right)\Gamma\left(-s\right)}{\Gamma\left(1-s\right)\left(\sigma\omega_P u\right)^s}, \tag{3.169}$$

and

$$\mathcal{U}_6=(s+L+i)^2\Gamma\left(L+s\right)\Gamma\left(1+s\right)\left(\frac{\psi(-s)-\psi(1-s)}{s}\right)\left(\sigma\omega_P u\right)^{-s}. \tag{3.170}$$

That is

$$\lim_{s\to -(L+i)}\mathcal{U}_4=-\frac{\left(-1\right)^{L-1}}{i!\left(i+L\right)!}\left(\sigma\omega_P u\right)^{L+i}\log\left(\sigma\omega_P u\right), \tag{3.171}$$

while the limit of $\mathcal{U}_5$ can be expressed using [71, Eq. (06.14.06.0026.01)] as

$$\lim_{s\to -(L+i)}\mathcal{U}_5=\frac{\left(-1\right)^{L-1}\left[\psi(i+1)+\psi(L+i)\right]}{i!\left(i+L\right)!}\left(\sigma\omega_P u\right)^{L+i}, \tag{3.172}$$

whereas, the one of the term $\mathcal{U}_6$ can be expressed as

$$\lim_{s\to -(L+i)}\mathcal{U}_6=\frac{\left(-1\right)^{L-1}\left(\sigma\omega_P u\right)^{i+L}}{i!\left(i+L\right)!}\left[\psi(L+i)-\psi(1+L+i)\right]. \tag{3.173}$$

Now, replacing (3.171), (3.172), and (3.173) into (3.167) and then substituting (3.165) and

(3.167) into (3.164), one can obtain

$$\mathcal{M}_2(u) = \frac{1}{u}\sum_{i=0}^{+\infty}\frac{(-1)^{L-1}}{i!\,(i+L)!}(\sigma\omega_P u)^{L+i}\left[\,-\log(\sigma\omega_P u)+\psi(i+1)+2\psi(L+k)-\psi(1+L+i)\,\right] + \frac{1}{u}\sum_{i=1}^{L-1}\frac{(-1)^{i-1}\,\Gamma(L-i)}{i!}(\sigma\omega_P u)^{i}. \tag{3.174}$$

In a similar manner to the previous computation performed for (3.163), the incomplete Meijer's G-function $\mathcal{J}(u)$ given in (3.82) can be expressed as sum of residues by considering the poles of second-order at $-L-i, i\in\mathbb{N}$ and the ones of first-order at $-i$, $1\leq i\leq L-1$. That is

$$\mathcal{J}(u) = \frac{1}{u}\sum_{i=0}^{+\infty}\frac{(-1)^{L-1}\,\Gamma(1+L+i,\phi)\,\mathcal{N}_i(u)}{i!\,(i+L)!\left(\frac{\omega_P u}{\lambda_{\mathrm{SP}}}\right)^{-(L+i)}} + \frac{1}{u}\sum_{i=1}^{L-1}\frac{(-1)^{i-1}\,\Gamma(L-i)\,\Gamma(1+i,\phi)\,(\omega_P u)^{i}}{i!\lambda_{\mathrm{SP}}^{i}},$$

where

$$\mathcal{N}_i(u) = -\log\left(\frac{\omega_P u}{\lambda_{\mathrm{SP}}}\right)+\psi(i+1)+2\psi(L+i)+\log(\phi)-\psi(1+i+L) + \frac{1}{\Gamma(1+L+i,\phi)}G_{2,3}^{3,0}\left(\phi\,\middle|\,\begin{matrix}-;1,1\\0,0,1+i+L;-\end{matrix}\right). \tag{3.175}$$

Now, by substituting (3.174) and (3.175) into (3.80) and (3.82), respectively, then by incorporating the final expressions of Ω_1 and Ω_2 into (3.125) and by considering only the first term in the infinite series and the case of $L>1$, the asymptotic expression of $\mathrm{SOP}_{2,i.i.d}$ is given by

$$\mathrm{SOP}_{2,i.i.d}\sim 1-\frac{1}{\delta}+\frac{\xi}{\delta\lambda_{\mathrm{RP}}\overline{\gamma}_P}\left(\,1+\tfrac{1-e^{-\phi}}{\Gamma(L)}(\mathcal{B}_1+\mathcal{B}_2)-\mathcal{B}_3\,\right), \tag{3.176}$$

where $\mathcal{B}_1$, $\mathcal{B}_2$, and $\mathcal{B}_3$ are defined in (3.138), (3.139), and (3.140), respectively.

Finally, substituting (3.141) and (3.162) into (3.18) yields (3.131), while replacing (3.144) and (3.176) into (3.18), we obtain (3.144), which concludes the proof. ■

Remark 4. *It can be noticed from (3.131) and (3.132) that the asymptotic expressions of* SOP

for both i.n.i.d and i.i.d cases with respect to $\overline{\gamma}_S$ can be obtained by replacing $\overline{\gamma}_P$ by $\sigma\overline{\gamma}_S$

$$\mathrm{SOP}_{i.n.i.d} \sim 1 - \frac{\mathcal{A}_1}{\delta} - \frac{\mathcal{A}_2}{\delta\sigma}\overline{\gamma}_S^{-1}, \tag{3.177}$$

and

$$\mathrm{SOP}_{i.i.d} \sim 1 - \frac{\mathcal{C}_1}{\delta} + \frac{\mathcal{C}_2 + \mathcal{D}_1}{\sigma\delta}\overline{\gamma}_S^{-1}. \tag{3.178}$$

Remark 5. *It is worth mentioning that the approximate expression given in (3.131) is an increasing function with respect to $\overline{\gamma}_P$ as the coefficient $\mathcal{A}_2$ is positive. In a similar manner, one can notice that the approximate* SOP *representation in (3.132) is a decreasing function in $\overline{\gamma}_P$ as the term $\frac{\mathcal{C}_2+\mathcal{D}_1}{\delta}$ is a positive real number.*

3.3.3 Numerical results and discussions

This section capitalizes on the derived analytic expressions and provides a thorough analysis of the corresponding results. To this end, illustrative numerical examples are presented and validated through extensive results from respective Monte Carlo simulations. The used parameters are set up as shown in Table 3.2. The parameters $\lambda_{\mathrm{SR}} = 0.5$ for i.i.d case and $\lambda_{\mathrm{SR}_k} = \beta + \frac{k}{10}$, $0 \leq k \leq \frac{L-1}{10}$ for i.n.i.d fading channels with β either equal to 0.1 or 0.5. The aim of the conducted simulation is to evaluate the impact of the MTIP at the P_{Rx}, the maximum transmit power of the source S, the fading severity parameters, the EH ratio θ, and the number of the relay antennas on the security performance of the system. The corresponding computer simulation has been performed by repeating the same experiments 10^6 times. From Figs. 3.6-3.11, we observe that the simulation results match perfectly the numerical results, which verifies the validity of the derived exact and asymptotic analytic expressions.

Figs. 3.6-3.9 depict the closed-form expressions of the SOP as a function of $\overline{\gamma}_P$ and $\overline{\gamma}_S$, respectively for various numbers of the relay's antennas for both i.n.i.d and i.i.d cases. It can be noticed that this probability decreases with the increasing values of either $\overline{\gamma}_P$ or $\overline{\gamma}_S$. This can be justified by the fact that the greater the $\overline{\gamma}_P$ and $\overline{\gamma}_S$, the greater the γ_R, γ_D, γ_{1E}, and γ_{2E}. Under the assumption of no significant difference between fading severity parameters of legitimate and wiretap channels, it follows from (3.7), (3.2.2), (3.9), and (3.58) that the increasing scale of γ_R and γ_D exceeds largely the one of γ_{1E} and γ_{2E} as the relay performs the MRC diversity

Table 3.2: Simulation parameters of contribution 3.

Parameter	value	Figures
λ_{SP}	0.1	All figures
λ_{RD}	0.3	All figures
λ_{SE}	0.2	All figures
λ_{RE}	0.4	All figures
λ_{RP}	0.5	All figures
R_S(bit/s/Hz)	1	All figures
$\bar{\gamma}_P$(dB)	10	All except Figs. 3.6 & 3.7
$\bar{\gamma}_S$ (dB)	10	All except Figs. 3.8 & 3.9
η	0.8	All figures
θ	0.5	All except Figs. 3.10-3.12

technique. In addition, when $\overline{\gamma}_P$ and $\overline{\gamma}_S$ exceed certain thresholds, the instantaneous powers P_S and P_R remain constant as stated in (1.1) and (3.48). As a consequence, the SOP remains constant as well. Furthermore, one can ascertain that the greater the parameters λ_{SR_k} the smaller the combined SNR at the relay. Consequently, the secrecy capacity at the first hop decreases as well, leading to a degradation of the system's security.

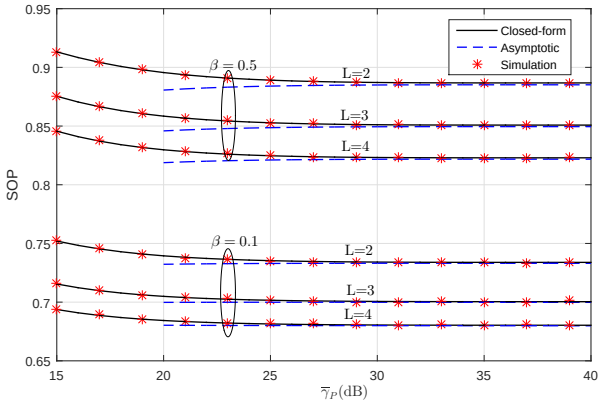

Figure 3.6: SOP versus $\overline{\gamma}_P$ for $\overline{\gamma}_S = 20$ dB and i.n.i.d Rayleigh fading channels.

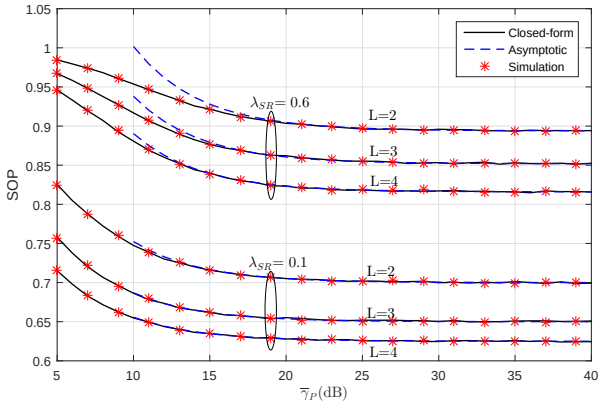

Figure 3.7: SOP versus $\overline{\gamma}_P$ for $\overline{\gamma}_S = 50$ dB and i.i.d Rayleigh fading channels.

Fig. 3.10 and Fig. 3.11 illustrate the SOP for the i.n.i.d and i.i.d cases versus the EH ratio θ for different numbers of the relay antennas, computed using (3.59), (3.60), (3.131), and (3.132). It can be observed that the SOP is a concave function of θ. Indeed, it can be seen from (3.2.2), (3.56), and (3.58) that as θ approaches 0, both γ_D and γ_{2E} tend to 0. Consequently, both C_{S_2} and C_S tend to 0, which leads to a higher value of the SOP. Similarly, according to (3.7) and (3.9), the greater the value of θ i.e., when it tends to 1, both γ_R and γ_{1E} tend to 0. Therefore,

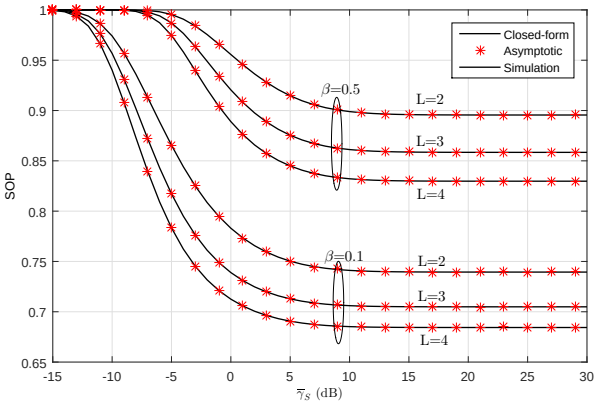

Figure 3.8: SOP versus $\overline{\gamma}_S$ for i.n.i.d Rayleigh fading channels.

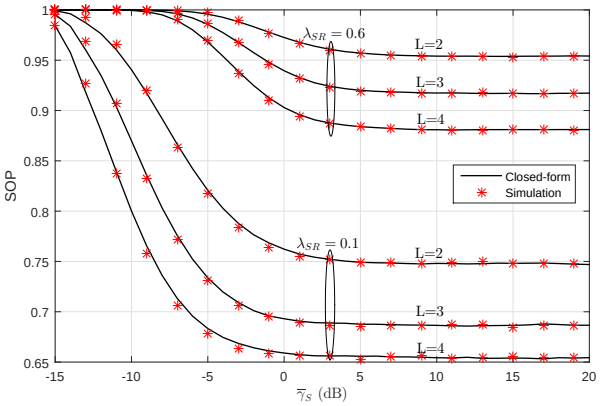

Figure 3.9: SOP versus $\overline{\gamma}_S$ for i.i.d Rayleigh fading channels.

both C_{1S} and C_S approach 0, and therefore the SOP increases accordingly.

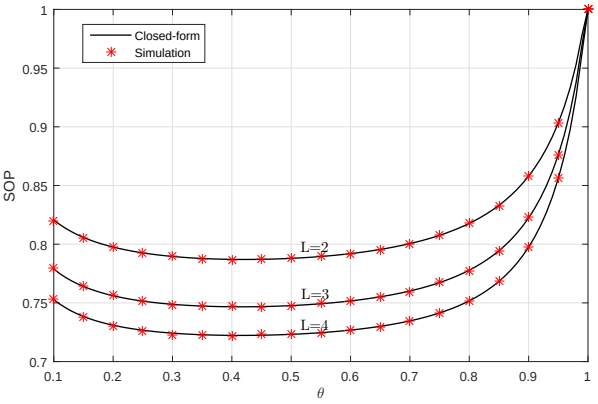

Figure 3.10: SOP versus θ for i.n.i.d Rayleigh fading channels $\overline{\gamma}_S = \overline{\gamma}_P =$ 10 dB for $\beta = 0.1$.

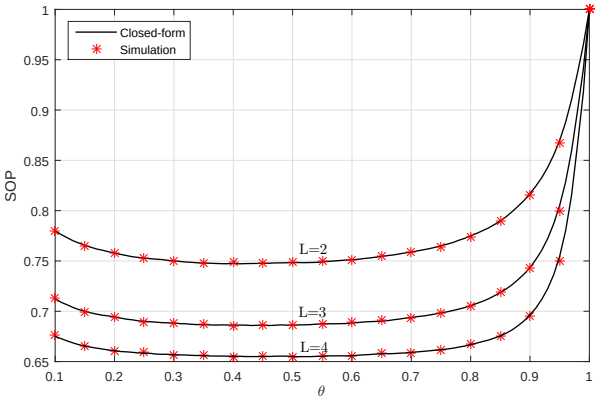

Figure 3.11: SOP versus θ for i.i.d Rayleigh fading channels $\overline{\gamma}_S = \overline{\gamma}_P =$ 10 dB for $\lambda_{\mathrm{SR}} = 0.1$.

Finally, Fig. 3.12 shows the SOP versus θ and $\overline{\gamma}_P$. Obviously, the parameters $\overline{\gamma}_P$ and θ admit certain values for which better security is achieved. For instance, one can infer that higher secrecy is achieved for $0.4 \leq \theta \leq 0.6$ and $\overline{\gamma}_P \geq 15$ dB. This constitutes a practical insight that is expected to be useful in the design of future EH based CR systems and networks.

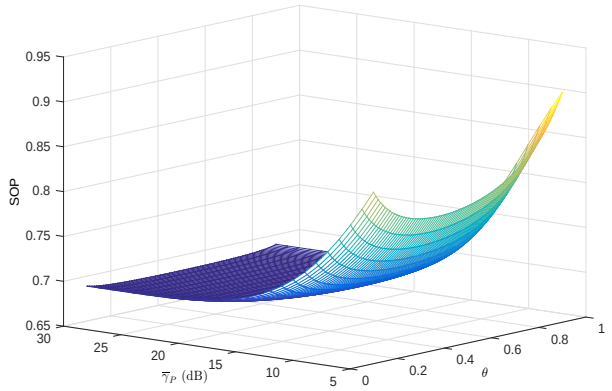

Figure 3.12: SOP versus θ and $\overline{\gamma}_P$ for i.n.i.d Rayleigh fading channels for $\overline{\gamma}_S = 10$ dB, $\beta = 0.1$, and $L = 4$.

3.4 Concluding remarks

PLS has been investigated , in this chapter, by considering two setups of a dual-hop EH-CRNs. In the first contribution, the rely was equipped with only one antenna and assumed to be located far from the PU and not causing any interference to it. In the second contribution, the rely was equipped with multiple antennas, performing MRC combining technique, and continuously adapting its transmit power to not interfere with the PU signals. In the first contribution of this chapter, closed-form expression for the sop was derived, whereas in the second contribution, both closed-form and asymptotic expressions were derived for the SOP by considering both i.n.i.d and i.i.d Rayleigh fading channels. For both setups, we investigated the impact of several parameters on the system's security performance. We showed that the security is improved for high tolerated interference power at the primary receiver as well as for high secondary users transmit power. Furthermore, better secrecy is achieved when the fraction of the harvested energy takes its values in the interval $[0.4, 0.6]$.

The current chapter studied the impact of EH on the secrecy performance of a dual-hop CRN. The next chapter investigates the impact of jamming signal on the secrecy performance of underlay CRNs.

Chapter 4

On the Secrecy Performance of a Jamming-based Underlay CRN

4.1 Introduction

4.1.1 Motivation

Recently, the PLS of CRNs has been the focus of many research works. For instance, non-cooperative CRNs were considered in [93–96], therein all receivers i.e., both destination and eavesdropper were assumed to be equipped with multiple antennas and perform MRC technique, while in [96], the source is also assumed to be a multi-antenna node performing transmit antenna selection. Also, in [94] the secrecy performance was investigated for both secondary and primary networks. Closed-form and asymptotic expressions for the SOP were derived under Nakagami-m [93, 96] and Rayleigh [94, 95] fading models.

The PLS of cooperative dual-hop CRNs was explored in [97–103]. Specifically, in [97] and [98], the communication was performed in the presence of only one eavesdropper attempting to overhear the communication channel, while multiple eavesdroppers were considered in [102] and [103]. Furthermore, In [97], optimal and suboptimal relay selection were analyzed while in [98] the relay that minimizes the SNR of the wiretap link was chosen. Besides, in [102], the most threatening eavesdropper is selected first according to the maximum SNR of the wiretap links between the source and the eavesdroppers. Next, the best relay minimizing the SNR at the selected eavesdropper is then chosen. In [103], the relay that maximizes the achievable

secrecy rate is selected. Under these conditions, closed-form and asymptotic expressions for the SOP and IP were derived over either Nakagami-m [97] or Rayleigh [98–103] fading channels.

The PLS of underlay EH-based CRNs have been investigated in [31–35]. Specifically, in [32–34], the energy-constrained nodes were harvesting energy fro the RF signals of the PU. The authors of [31], derived the upper and lower bounds probability of strictly positive secrecy capacity by considering that the destination node was harvesting energy from the source node and used the harvested energy to send a jamming signal to downgrade the eavesdropper's decoding capacity. In [32], the SOP was derived by considering a direct communication link where the source was equipped with multiple antennas and communicating with a multi-antenna destination in the presence of a multi-antenna eavesdropper. In [33], the IP was derived by considering that multiple SUs were communicating with a base station in the presence of multiple eavesdroppers. The authors of [34] investigated the PLS of an EH-based overlay CRN where the SUs harvest energy from the PU signals and act as relays between the PU transmitter and the PU receiver. In [35], the secrecy performance was investigated by considering a direct communication link where a secondary base station was communicating with a secondary receiver in the presence of multiple eavesdroppers. The eavesdroppers were assumed to be all legitimate users in the network that are also energy harvesters.

The PLS of non-orthogonal multiple access (NOMA)-based CRNs has been investigated in [106–108]. In [106], an overlay NOMA CRN was considered such that the SUs were assumed to be eavesdroppers, while the PLS of mmWave NOMA CRN was investigated in [107]. Closed-form expressions for the connection outage probability, SOP, and secrecy throughput were derived over Nakagami-m fading channels. In [108], zero-forcing-beamforming technique was used to secure communications in MIMO, NOMA-based CRN.

PLS analysis through the aid of a friendly jammer was discussed in [36, 37]. In [36], the IP was derived by considering multiple source-destination pairs communicating under eavesdropping attempts of only one eavesdropper, with the source cooperation aided opportunistic jamming. In [37], the SOP of dual-hop aided opportunistic jamming CRNs is investigated. In this work, one relay is selected to forward the information while another one is chosen to disrupt the eavesdropper by sending an artificial noise. Also, in the two aforementioned works, several selection policies of the friendly jammer were considered.

Concurrently, to the best of the authors' knowledge, very few research works have investigated the PLS of HSTCNs. The secrecy analysis of HSTCNs where the terrestrial secondary network is sharing the spectrum with a satellite system, acting as a primary network is examined in [109] by maximizing the SUs rate and considering various beamforming techniques. Distinctively, the authors in [110] dealt with the minimization of the total transmit power of numerous terrestrial base stations and onboard the satellite subject to the PU secrecy rate constraint. Later, the ASC and SOP of a downlink hybrid satellite-FSO cooperative system were derived in [111] by considering both amplify-and-forward and DF relaying protocols. Likewise, the authors of [27] investigated the PLS of a hybrid very high throughput satellite communication system with an FSO feeder link. Therein, a satellite combines the received data from multiple optical ground stations, performs a decoding process, regenerates the information signal, and forwards it to the end-user with zero-forcing precoding so that to cancel the interbeam interference at the receivers.

Although the above works have added new insights to the research field, only few works have considered the friendly jammer approach to improve the secrecy of a given CR communication system. Additionally, the existing jamming-based communication contributions neglected the power adaptation constraints of the SUs, despite that this condition is of paramount importance in order to avoid interference with PUs. Therefore, our aim is to investigate the impact of multiple techniques namely, jamming signal, spatial diversity, number of eavesdroppers, etc. on the overall system security of a CR communication system.

4.1.2 Contributions

The main contributions of this chapter are given as follows:

- Secrecy performance analysis of a direct-link jamming-based underlay CRN.
  - By considering the power adaptation constraint of SUs, a closed-form expression for the IP is derived for two scenarios: (i) presence and (ii) absence of a friendly jammer. These exact analytic results constitute the basis for the derivation of simpler, more tractable, and more insightful asymptotic expression.
  - We develop useful insights into the secrecy performance of the considered communication system. Specifically, we conclude that for a high number of eavesdroppers

and a low transmit power of the friendly jammer, the security performance of the system becomes the same for both scenarios.

- Secrecy performance analysis of a dual-hop jamming-based underlay CRN over Rayleigh fading channels.
  - Closed-form expression for the SOP is derived by considering the power adaptation constraint of the SUs as well as the presence of multiple eavesdroppers that are intercepting the transmitted data at both communication hops.
  - Differently from the previous works, we combine, in this contribution, two techniques (i) using a friendly jammer to enhance the security at the first hop, and (ii) considering a multi-antenna destination node that performs MRC technique to improve security at the second hop.
  - Deep useful insights into the secrecy performance of the considered communication system are given.
- Secrecy performance analysis of a dual-hop Jamming-based CR communication system with multi-antenna receivers over Nakagami-m fading channels.
  - The PLS of an underlay uplink dual-hop CRN operating under Nakagami-m fading environment is investigated by deriving closed-form and asymptotic expressions for the SOP of the overall system under two scenarios namely, (i) presence and (ii) absence of a friendly jammer.
  - Under the power adaptation constraint of the SUs, the joint impact of the friendly jammer's transmit power, multiple SUs with power adaptation constraint, number of eavesdroppers, number of diversity branches, MTIP at the PU receiver on the system's security is investigated.
  - We show that the system's security is enhanced in the presence of an important number of eavesdroppers by increasing the (i) SUs' transmit powers (ii) number of legitimate destination branches (iii) and MTIP.
- Secrecy performance analysis of a dual-hop jamming-based underlay cognitive hybrid satellite-terrestrial network.

- A novel expression for the IP of a dual-hop DF relaying in the presence of eavesdroppers at each hop is derived.
- Capitalizing on the above result, the IP expression of HSTCN is derived in closed-form for both the presence and absence of friendly jammer scenarios.
- The asymptotic expression for the IP in high SNR regime is also provided, based on it, the achievable diversity order is retrieved.
- Insightful discussions on the impact of different key parameters of HSTCN on its security are also provided. Specifically, we demonstrated that the system's secrecy can be enhanced by increasing (i) SU's transmit power, (ii) maximal tolerated interference power (MTIP) at PU, and (iii) average power of the downlink channel along with the satellite transmit power. Moreover, we demonstrated that under low source transmit power and low MTIP constraints, the friendly jammer does not enhance the system's secrecy.

4.1.3 Chapter's structure

The remainder of this chapter is organized as follows: Sections 2, 3 and 4 provide contributions on the PLS of 3 various setups, namely a direct-link jamming-based CR system subject to Rayleigh fading, a dual-hop jamming-based CR system subject to Rayleigh fading, and a dual-hop jamming-based CR system subject to Nakagami-m fading with multi-antenna receivers. For each contribution, system and channel model, secrecy performance analysis, and numerical results are provided. Section 5 concludes this chapter.

4.2 Contribution 4: Secrecy performance analysis of a direct-link jamming-based underlay CRN

4.2.1 System and channel model

We consider an uplink CRN, illustrated in Fig. 4.1, composed by multiple SUs $(S_i)_{i\leq N}$, multiple eavesdroppers $(E_k)_{k\leq M}$, one single-antenna secondary base station (B_s), one PU transmitter (PU_{Tx}), and one primary base station (PBS) (B_P). Multi-user scheduling is considered such

that, at the moment t, only one source (S_c) is selected according to the round-robbing scheduling algorithm for data transmission. Additionally, a jammer among the $N-1$ remaining sources is selected by the current transmitter to send an artificial noise (AN) that is added to the kth eavesdropper's signal. Indeed, the AN is considered as a signal designed in the null space of the legitimate channel i.e., $S_c - D$, and is transmitted to interfere with the eavesdroppers without affecting the legitimate destination. Similarly to [36], we consider that the AN is generated from a pseudo-random sequence. This sequence is known to the legitimate receiver while it is unknown to the eavesdroppers. Consequently, the destination is able to cancel out the AN while the eavesdroppers cannot.

For the sake of simplicity but without loss of generality, we denote the channel power gains by $g_q = |h_q|^2$ and their corresponding coefficients are λ_q, where $q = \{S_iB_S,\ S_iE_k,\ S_iB_P\}$. As the fading amplitudes for all links are Rayleigh distributed, it follows that the channel gains are exponentially distributed.

Moreover, under the power adaptation policy, the instantaneous SNR of the main channel $S_c - D$ and the wiretap link $S_c - E_k$ are given, respectively, by

$$\gamma_m^{(c)} = g_{S_cR} X_{S_c}, \tag{4.1}$$

and

$$\gamma_{e_k}^{(c,\epsilon J)} = \frac{g_{S_cE_k} X_{S_c}}{\epsilon g_{S_JE_k} X_{S_J} + 1}, \tag{4.2}$$

where

$$\epsilon = \begin{cases} 0 & : \text{without jammer} \\ 1 & : \text{with jammer} \end{cases}, \tag{4.3}$$

$$X_{S_c} = \min\left(\overline{\gamma}_{S_c}, \frac{\overline{\gamma}_P}{g_{S_cP}}\right), \tag{4.4}$$

and

$$X_{S_J} = \min\left(\overline{\gamma}_{S_J}, \frac{\overline{\gamma}_P}{g_{S_JP}}\right), \tag{4.5}$$

and $\overline{\gamma}_{S_c} = P_{S_c}^{\max}/N_0$, $\overline{\gamma}_{S_J} = P_{S_J}^{\max}/N_0$, $\overline{\gamma}_P = P_I/N_0$, with $P_{S_c}^{\max}$ and $P_{S_J}^{\max}$ denoting the maximal transmit power of S_c and S_J, respectively, while P_I accounts for the MTIP at PU_{Rx}, and N_0 is the variance of the additive white Gaussian noise, assumed the same, at each receiver.

It is worth mentioning that when P_I increases, the source nodes are able to use their maximal transmission power resulting in increasing the SNR at D, which leads the enhancement of the system's security.

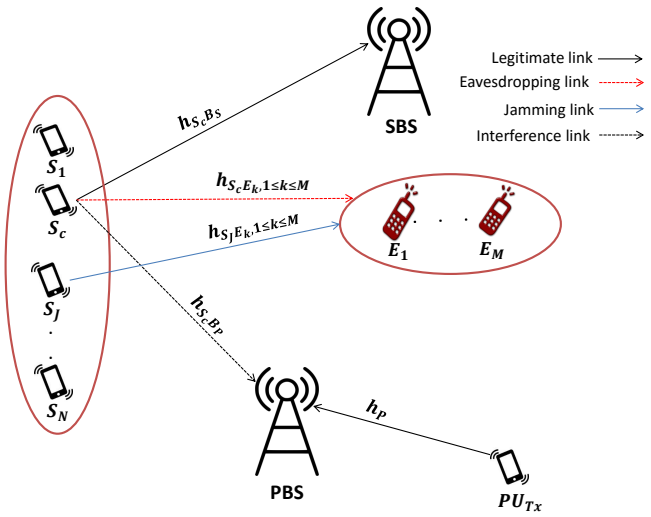

Figure 4.1: The considered direct-link jamming-based CRN.

4.2.2 Secrecy performance evaluation

In this section, the IP analysis of an underlay Uplink CRN is presented by considering the presence and absence of a friendly jammer. Similarly to [36], the IP of the considered CRN in the presence of a friendly jammer can be expressed as

$$P_{int} = \frac{1}{N(N-1)} \sum_{c=1}^{N} \sum_{\substack{J=1 \\ J \neq c}}^{N} P_{int}^{(c,J)}, \tag{4.6}$$

While the IP in the absence of a friendly jammer is expressed as

$$P_{int} = \frac{1}{N} \sum_{c=1}^{N} P_{int}^{(c)}, \tag{4.7}$$

For the considered system, the IP can be defined as the probability that at least one of the wiretap links capacities is above the legitimate one, namely

$$P_{int}^{(c,J)} = 1 - \prod_{k=1}^{M} \Pr\left(C_S^{(c,k,\epsilon J)} > 0\right), \tag{4.8}$$

and $C_S^{(c,\,k,\epsilon J)}$ denotes the secrecy capacity of the cth source E_k is intercepting the channel.

$$C_S^{(c,\,k,\epsilon J)} = \log_2\left(1+\gamma_m^{(c)}\right) - \log_2\left(1+\gamma_{e_k}^{(c,\epsilon J)}\right). \tag{4.9}$$

Remark 6. *It is worth mentioning that by considering identical parameters, the IPs given in (4.6) and (4.7) becomes the one of user c i.e.,* $P_{int}^{(c,J)}$.

Closed-form intercept probability

According to (4.6), in order to derive the IP of the considered system, we first have to determine the expression of $P_{int}^{(c,J)}$.

Theorem 4.2.1. *The IPs of cth source in presence and absence of a friendly jammer are given, respectively by*

$$P_{int}^{(c,J)} = 1 - \prod_{k=1}^{M}\left[1 - \lambda_{S_cD}\left(\frac{e^{-\varphi_J}}{\varpi_k^{(c)}} - \chi_c^{(k,J)}\left[\mathcal{M}_c^{(k,J)}\left[e^{-\varphi_J}-1\right] + e^{\theta_c^{(k,J)}-\varphi_J}\Delta_c^{(k,J)}\right]\right)\right], \tag{4.10}$$

and

$$P_{int}^{(c)} = 1 - \prod_{k=1}^{M}\left[\frac{\lambda_{S_cE_k}}{\lambda_{S_cE_k}+\lambda_{S_cD}}\right], \tag{4.11}$$

where

$\varphi_J = \lambda_{S_JP}\overline{\gamma}_P/\overline{\gamma}_{S_J}$, $\varpi_k^{(c)} = \lambda_{S_cE_k} + \lambda_{S_cD}$, $\varepsilon_c^{(k,J)} = \lambda_{S_JE_k}/\lambda_{S_cE_k}$, $\chi_c^{(k,J)} = \varepsilon_c^{(k,J)}/\overline{\gamma}_{S_J}$, $\theta_c^{(k,J)} = \varpi_k^{(c)}\chi_c^{(k,J)}$,

$$\mathcal{M}_c^{(k,J)} = G_{1,2}^{2,1}\left(\theta_c^{(k,J)}\middle|\begin{matrix}0;-\\0,0;-\end{matrix}\right),$$

$$\Delta_c^{(k,J)} = \left(A_1^{(c,k,J)}/\varphi_J - A_0^{(c,k,J)}\right),$$

$$A_v^{(c,k,J)} = \left(\varphi_J/\theta_c^{(k,J)}\right)^{v+1}\Omega_c^{(k,J)}, v\in\{0,1\},$$

$$\Omega_c^{(k,J)} = G_{2,2}^{2,2}\left(\varphi_J/\theta_c^{(k,J)}\middle|\begin{matrix}(0,0),(-v,\theta_c^{(k,J)});-\\(0,0),(0,0);-\end{matrix}\right),$$

Proof.

In the following, two cases are distinguished, namely the presence and absence of a friendly jammer.

- *Case 1: Presence of a jammer*

The IP corresponding to the links $S_c - D$ and $S_c - E_k$ can be expressed as

$$\begin{aligned} \Pr\left(C_S^{(c,k,J)} \leq 0\right) &= \Pr\left(g_{S_cD} \leq W_c^{(k,J)}\right) \\ &= \int_0^\infty F_{g_{S_cD}}(z)\, f_{W_c^{(k,J)}}(z)\, dz, \end{aligned} \tag{4.12}$$

where $W_c^{(k,J)} = g_{S_cE_k} / \left(Y_J^{(k)} + 1\right)$, $Y_J^{(k)} = g_{S_JE_k} X_J$, f_X and F_X denote the PDF and the CDF of the distribution X, respectively.

On the other hand, the CDF of $W_c^{(k,J)}$ is given by

$$F_{W_c^{(k,J)}}(\xi) = \int_0^\infty F_{g_{S_cE_k}}\left(\xi\left(z+1\right)\right) f_{Y_J^{(k)}}(z)\, dz, \tag{4.13}$$

where the CDF of $Y_J^{(k)}$ is expressed as

$$\begin{aligned} F_{Y_J^{(k)}}(\vartheta) &= \Pr\left(\min\left(\overline{\gamma}_{S_J}, \frac{\overline{\gamma}_P}{g_{S_JP}}\right) g_{S_JE_k} \leq \vartheta\right) \\ &= \underbrace{\Pr\left(\overline{\gamma}_{S_J} g_{S_JE_k} \leq \vartheta, \overline{\gamma}_{S_J} \leq \frac{\overline{\gamma}_P}{g_{S_JP}}\right)}_{\mathcal{I}_1^{(k,J)}} + \underbrace{\Pr\left(\frac{g_{S_JE_k}}{g_{S_JP}} \leq \frac{\vartheta}{\overline{\gamma}_P}, \overline{\gamma}_{S_J} > \frac{\overline{\gamma}_P}{g_{S_JP}}\right)}_{\mathcal{I}_2^{(k,J)}}. \end{aligned} \tag{4.14}$$

The first term $\mathcal{I}_1^{(k,J)}$ can be rewritten as

$$\begin{aligned} \mathcal{I}_1^{(k,J)} &= F_{g_{S_JE_k}}\left(\frac{\vartheta}{\overline{\gamma}_{S_J}}\right) F_{g_{S_JP}}\left(\frac{\overline{\gamma}_P}{\overline{\gamma}_{S_J}}\right) \\ &= \left(1 - e^{-\frac{\lambda_{S_JE_k}\vartheta}{\overline{\gamma}_{S_J}}}\right)\left(1 - e^{-\varphi_J}\right). \end{aligned} \tag{4.15}$$

while the second term $\mathcal{I}_2^{(k,J)}$ can be re-expressed as

$$\begin{aligned}\mathcal{I}_2^{(k,J)} &= \int_{\frac{\overline{\gamma}_P}{\overline{\gamma}_{S_J}}}^{\infty} f_{g_{S_JP}}(y) \int_0^{\frac{\vartheta}{\overline{\gamma}_P} y} f_{g_{S_JE_k}}(x) dxdy \\ &= \int_{\frac{\overline{\gamma}_P}{\overline{\gamma}_{S_J}}}^{\infty} f_{g_{S_JP}}(y) F_{g_{S_JE_k}}\left(\frac{\vartheta}{\overline{\gamma}_P} y\right) dxdy \\ &= e^{-\varphi_J} - \frac{e^{-\varphi_J\left(\vartheta\varrho_k^{(J)}+1\right)}}{\vartheta\varrho_k^{(J)}+1}, \end{aligned} \tag{4.16}$$

with $\varrho_k^{(J)} = \lambda_{S_JE_k}/\lambda_{S_JP}\overline{\gamma}_P$.

By replacing (4.15) and (4.16) into (4.14), we get the CDF of $Y_J^{(k)}$ as

$$F_{Y_J^{(k)}}(\vartheta) = 1 - e^{-\varphi_J\varrho_k^{(J)}\vartheta}\left(1 - e^{-\varphi_J}\right) - \frac{e^{-\varphi_J\left(\vartheta\varrho_k^{(J)}+1\right)}}{\varrho_k^{(J)}\vartheta+1}. \tag{4.17}$$

It follows by using the integration by part and substituting (4.17) into (4.13) that

$$\begin{aligned} F_{W_c^{(k,J)}}(\xi) &= 1 - \xi\int_0^{\infty} f_{g_{S_cE_k}}(\xi(z+1)) F_{Y_J^{(k)}}(z)\, dz \\ &= 1 - \Xi_k^{(c)}(\xi)\left[\ \tfrac{1}{\xi} + \tfrac{e^{-\varphi_J}-1}{\mu_c^{(k,J)}} - \lambda_{S_cE_k} e^{-\varphi_J}\Theta_c^{(k,J)}(z)\ \right], \end{aligned} \tag{4.18}$$

where $\Xi_k^{(c)}(\xi) = \xi e^{-\xi\lambda_{S_cE_k}}$, $\Theta_c^{(k,J)}(z) = \int_0^{\infty} \frac{e^{-\beta_c^{(k,J)}z}}{\varrho_k^{(J)}z+1}dz$, $\beta_c^{(k,J)} = \lambda_{S_cE_k}\mu_c^{(k,J)}$, and $\mu_c^{(k,J)} = \frac{\varphi_J\varrho_k^{(J)}}{\lambda_{S_cE_k}}+\xi$.

Now, making use of Eqs. (07.34.03.0456.01) (07.34.21.0088.01) of [71], the term $\Theta_c^{(k,J)}$ is given by

$$\Theta_c^{(k,J)} = \frac{1}{\varrho_k^{(J)}} G_{3,2}^{1,3}\left(\frac{\varrho_k^{(J)}}{\beta_c^{(k,J)}}\,\middle|\, \begin{matrix} 0,1,1;- \\ 1;0 \end{matrix}\right), \tag{4.19}$$

On the other hand, the Meijer's G-function obtained in (4.19) can be reduced to

$$\begin{aligned} G_{2,3}^{3,1}\left(\frac{\beta_c^{(k,J)}}{\varrho_k^{(J)}}\,\middle|\, \begin{matrix} 0;1 \\ 1,0,0;- \end{matrix}\right) &= \frac{1}{2\pi j}\int_{\mathcal{C}} \frac{\Gamma^2(s)\Gamma(1-s)}{\left(\frac{\beta_c^{(k,J)}}{\varrho_k^{(J)}}\right)^s} ds \\ &= G_{1,2}^{2,1}\left(\frac{\beta_c^{(k,J)}}{\varrho_k^{(J)}}\,\middle|\, \begin{matrix} 0;- \\ 0,0;- \end{matrix}\right), \end{aligned} \tag{4.20}$$

where $\mathcal{C}$ represents a complex contour of integration ensuring the convergence of the Mellin-Barnes integral.

Now, substituting (4.19) and (4.20) into (4.18) yields

$$F_{W_c^{(k,J)}}(\xi) = 1 - e^{-\lambda_{S_cE_k}\xi}\left[1 + \Upsilon_c^{(k,J)}(\xi)\right], \tag{4.21}$$

where

$$\Upsilon_c^{(k,J)}(\xi) = \frac{\xi\left(e^{-\varphi_J}-1\right)}{\chi_c^{(k,J)}+\xi} - \frac{\xi\lambda_{S_cE_k}}{\varrho_k^{(J)}} e^{-\varphi_J} G_{1,2}^{2,1}\left(\varphi_J + \frac{\varphi_J}{\chi_c^{(k,J)}}\xi \,\middle|\, \begin{matrix} 0;- \\ 0,0;- \end{matrix}\right). \tag{4.22}$$

By using the integration by parts and incorporating (4.21) into (4.12), we obtain

$$\begin{aligned} \Pr\left(C_S^{(c,k,J)} \le 0\right) &= 1 - \int_0^\infty f_{\,g_{S_cD}}(z)\, F_{W_c^{(k,J)}}(z)\, dz, \\ &= \lambda_{S_cD}\left[\frac{1}{\varpi_k^{(c)}} + \mathcal{I}_3^{(c,k,J)}\right]. \end{aligned} \tag{4.23}$$

The term $\mathcal{I}_3^{(c,k,J)} = \int_0^\infty e^{-\varpi_k^{(c)}z}\Upsilon_c^{(k,J)}(z)\,dz$ can be rewritten using (4.22) as

$$\mathcal{I}_3^{(c,k,J)} = \left(e^{-\varphi_J}-1\right)\Phi_1^{(c,k,J)} - \frac{\lambda_{S_cE_k}}{\varrho_k^{(J)}} e^{-\varphi_J}\Phi_2^{(c,k,J)}, \tag{4.24}$$

with

$$\begin{aligned} \Phi_1^{(c,k,J)} &= \int_0^\infty \frac{z e^{-\varpi_k^{(c)}z}}{\chi_c^{(k,J)}+z} dz \\ &= \frac{1}{\varpi_k^{(c)}} - \chi_c^{(k,J)} G_{1,2}^{2,1}\left(\theta_c^{(k,J)} \,\middle|\, \begin{matrix} 0;- \\ 0,0;- \end{matrix}\right), \end{aligned} \tag{4.25}$$

and

$$\begin{aligned} \Phi_2^{(c,k,J)} &= \int_0^\infty \frac{z}{e^{\varpi_k^{(c)}z}} G_{1,2}^{2,1}\left(\varphi_J + \frac{\varphi_J}{\chi_c^{(k,J)}}z \,\middle|\, \begin{matrix} 0;- \\ 0,0;- \end{matrix}\right) dz \\ &= \frac{\left(\chi_c^{(k,J)}\right)^2}{\varphi_J} e^{\theta_c^{(k,J)}}\left[\frac{A_1^{(c,k,J)}}{\varphi_J} - A_0^{(c,k,J)}\right], \end{aligned} \tag{4.26}$$

where the two functions $\left(A_v^{(c,k,J)}\right)_{v=0,1}$ are defined by

$$\begin{aligned} A_v^{(c,k,J)} &= \int_{\varphi_J}^{\infty} y^v e^{-\frac{\theta_c^{(k,J)}}{\varphi_J} y} G_{1,2}^{2,1}\left(y \left| \begin{matrix} 0;- \\ 0,0;- \end{matrix} \right. \right) dy \\ &= \frac{\eta_k^{v+1}}{2\pi j} \int_{\mathcal{C}} \Gamma^2(s)\,\Gamma(1-s)\,\Gamma\left(\varsigma_v, \theta_c^{(k,J)}\right) (\eta_k)^{-s}\, ds, \end{aligned} \tag{4.27}$$

where $\eta_k = \varphi_J/\theta_c^{(k,J)}$, and $\varsigma_v = v + 1 - s$.

Finally, by replacing (4.27) into (4.26) alongside incorporating (4.25), and (4.26) into (4.24), and using (4.8), we get (4.10).

- *Case 2: Absence of jammer*

Under this assumption, one can arrive at

$$\begin{aligned} \Pr\left(C_S^{(c,k)} \leq 0\right) &= \int_0^{\infty} F_{g_{S_cD}}(z) f_{g_{S_cE_k}}(z)\, dz \\ &= 1 - \frac{\lambda_{S_cE_k}}{\lambda_{S_cE_k} + \lambda_{S_cD}}. \end{aligned} \tag{4.28}$$

Substituting (4.28) into (4.8), we get the expression of IP given in (4.11), which concludes the proof of Theorem 4.2.1. ■

Remark 7. *It can be noticed that the IP in the presence of friendly jammer is independent from $\overline{\gamma}_{S_c}$, whereas the one in absence of jammer signal depends only on the fading parameters. Particularly, for identical fading parameters, IP is reduced to $P_{int}^{(c)} = 1 - \left(\frac{1}{2}\right)^M$. Therefore, for a high number of eavesdroppers, the system may become vulnerable to eavesdroppers' attacks.*

Asymptotic intercept probability

It can be noticed from (4.10) that the closed-form expression of the IP depends on the average SNRs $\overline{\gamma}_P$ and $\overline{\gamma}_{S_J}$. Consequently, the asymptotic expression for the IP can be derived for high SNR regime by considering either $\overline{\gamma}_P \to \infty$ or $\overline{\gamma}_{S_J} \to \infty$. Analogously to [95], we assume that $\overline{\gamma}_P$ is proportional to $\overline{\gamma}_{S_J}$ i.e., $\sigma = \overline{\gamma}_P/\overline{\gamma}_{S_J}$.

Theorem 4.2.2. *The Asymptotic expression for the IP of the considered communication system*

subject to flat Rayleigh fading channels can be expressed as

$$P_{int}^{(c,J)} \sim 1 - \prod_{k=1}^{M} \left[1 - \lambda_{S_c D} \left(1 + \frac{e^{-\varphi_J}}{\varphi_J} \right) \frac{\varepsilon_c^{(k,J)}}{\overline{\gamma}_{S_J}} \log\left(\overline{\gamma}_{S_J} \right) \right]. \tag{4.29}$$

Proof.

In order to derive the asymptotic expression for the IP, the residues theorem is used to approximate the Meijer G-function.

First, by using the Maclaurin series and performing some algebraic manipulations, the term Φ_2 in (4.26) can be approximated for high values of $\overline{\gamma}_{S_J}$ as

$$\begin{aligned} \Phi_2^{(c,k,J)} &\sim \frac{1}{2\pi j} \int_0^{\infty} z e^{-\varpi_k^{(c)} z} \int_C \Gamma^2(s)\, \Gamma(1-s) \left(\frac{\varphi_J z}{\chi_c^{(k,J)}} \right)^{-s} \left(1 - \frac{\chi_c^{(k,J)}}{z} s \right) ds dz \\ &\sim \frac{1}{\left(\varpi_k^{(c)} \right)^2} \Upsilon_1(\upsilon) - \frac{\chi_c^{(k,J)}}{\varpi_k^{(c)}} \Upsilon_2(\upsilon), \end{aligned} \tag{4.30}$$

where $\Upsilon_1(\upsilon) = G_{2,2}^{2,2}\left(\upsilon \left| \begin{matrix} 1,1; - \\ 1,2; - \end{matrix} \right. \right)$, $\Upsilon_2(\upsilon) = G_{2,2}^{2,2}\left(\upsilon \left| \begin{matrix} 0,1; - \\ 1,1; - \end{matrix} \right. \right)$, and $\upsilon = \chi_c^{(k,J)} \varpi_k^{(c)} / \varphi_J$.
The terms $\Upsilon_1(\upsilon)$ and $\Upsilon_2(\upsilon)$ given in (4.317) can be written in terms of complex integral as

$$\Upsilon_1(\upsilon) = \frac{1}{2\pi j} \int_{\mathcal{C}_1} \Gamma(1+s)\, \Gamma(2+s)\, \Gamma^2(-s)\, \upsilon^{-s} ds, \tag{4.31}$$

and

$$\Upsilon_2(\upsilon) = \frac{1}{2\pi j} \int_{\mathcal{C}_2} \Gamma^2(1+s)\, \Gamma(1-s)\, \Gamma(-s)\, \upsilon^{-s} ds. \tag{4.32}$$

By considering the left half plans of both $\mathcal{C}_1$ and $\mathcal{C}_2$, it can be noticed that (4.31) has simple pole at -1 and admits poles of second order at $-l-2$, $l \in \mathbb{N}$, while (4.32) has poles of second order at $-l-1$, $l \in \mathbb{N}$.

By making use of [105, Theorem 1.5], (4.31) is given by

$$\Upsilon_1(\upsilon) = \lim_{s \to -1} (s+1)\, \Gamma(1+s)\, \Gamma(2+s)\, \Gamma^2(-s)\, \upsilon^{-s} + \sum_{l=0}^{\infty} \lim_{s \to -(l+2)} \frac{\partial \mathcal{G}_1(s, \upsilon)}{\partial s}, \tag{4.33}$$

where

$$\mathcal{G}_1(s,\upsilon) = (s+l+2)^2\,\Gamma^2(1+s)\,(s+1)\,\Gamma^2(-s)\,\upsilon^{-s}. \tag{4.34}$$

It is evident that, the first term in (4.33) is equal to υ , while the partial derivative of $\mathcal{G}_1(s,\upsilon)$ with respect to s is given by

$$\frac{\partial \mathcal{G}_1(s,\upsilon)}{\partial s} = \mathcal{T}_1 + \mathcal{T}_2 + \mathcal{T}_3, \tag{4.35}$$

with

$$\mathcal{T}_1 = -(s+l+2)^2\,\Gamma^2(1+s)\,(s+1)\,\Gamma^2(-s)\,\upsilon^{-s}\log(\upsilon), \tag{4.36}$$

$$\mathcal{T}_2 = 2(s+l+2)\,\Gamma^2(1+s)\,[1+(s+l+2)\,\psi(1+s)]\,(s+1)\,\Gamma^2(-s)\,\upsilon^{-s}, \tag{4.37}$$

and

$$\mathcal{T}_3 = (s+l+2)^2\,\Gamma^2(1+s)\,\Gamma^2(-s)\,[1-2(s+1)\,\psi(-s)]\,\upsilon^{-s}. \tag{4.38}$$

The limit of $\mathcal{T}_1$ is expressed as

$$\lim_{s\to-(l+2)} \mathcal{T}_1 = (l+1)\,\upsilon^{l+2}\log(\upsilon). \tag{4.39}$$

On the other hand, the limit of $\mathcal{T}_2$ can be expressed using [71, Eq. (06.14.06.0026.01)] as follows

$$\lim_{s\to-(l+2)} \mathcal{T}_2 = -2(l+1)\,\psi(l+2)\,\upsilon^{l+2}, \tag{4.40}$$

while the limit of $\mathcal{T}_3$ is given by

$$\lim_{s\to-(l+2)} \mathcal{T}_3 = [1+2(l+1)\,\psi(l+2)]\,\upsilon^{l+2}. \tag{4.41}$$

By substituting (4.39), (4.40), and (4.41) into (4.33), we get

$$\Upsilon_1(\upsilon) = \upsilon + \sum_{l=0}^{\infty} \upsilon^{l+2}\,[(l+1)\log(\upsilon)+1]. \tag{4.42}$$

In the same manner to $\Upsilon_1(\upsilon)$, the term $\Upsilon_2(\upsilon)$ can be written using the residues theorem as

$$\Upsilon_2(\upsilon) = \sum_{l=0}^{\infty} (l+1)\,\upsilon^{l+1}\,[\psi(1+l) - \psi(2+l) - \log(\upsilon)]. \tag{4.43}$$

Using [71, Eq. (06.14.03.0001.01)], the term $\Upsilon_2(\upsilon)$ can be simplified as

$$\Upsilon_2(\upsilon) = \sum_{l=0}^{\infty} -(l+1)\,\upsilon^{l+1}\left[\frac{1}{l+1} + \log(\upsilon)\right]. \tag{4.44}$$

On the other hand, the MeijerG function given in (4.25) can be written in term of complex integral as

$$G_{1,2}^{2,1}\left(\kappa \,\middle|\, \begin{matrix} 0; - \\ 0, 0; - \end{matrix}\right) = \frac{1}{2\pi j}\int_{\mathcal{C}} \Gamma^2(s)\,\Gamma(1-s)\,\kappa^{-s} ds, \tag{4.45}$$

with $\kappa = \theta_c^{(k,J)}$.

It can be noticed that the above integrand function has poles of second order at $-l$, $l \in \mathbb{N}$. Hence, by using the residues theorem, (4.45) can be expressed as

$$G_{1,2}^{2,1}\left(\kappa \,\middle|\, \begin{matrix} 0; - \\ 0, 0; - \end{matrix}\right) = \sum_{l=0}^{\infty} \lim_{s\to -l} \frac{\partial \mathcal{G}_2(s,\kappa)}{\partial s}, \tag{4.46}$$

with

$$\mathcal{G}_2(s,\kappa) = (s+l)^2\,\Gamma^2(s)\,\Gamma(1-s)\,\kappa^{-s}. \tag{4.47}$$

The partial derivative of $\mathcal{G}_2(s,\upsilon)$ with respect to s is given by

$$\frac{\partial \mathcal{G}_2(s,\kappa)}{\partial s} = (s+l)\,\Gamma^2(s)\,\Gamma(1-s)\,\kappa^{-s}\left[-(s+l)\log(\kappa) + 2\left[1 + (s+l)\,\psi(s)\right] - (s+l)\,\psi(1-s)\right]. \tag{4.48}$$

By making use of [71, Eq. (06.14.06.0026.01)], the limit of (4.48) can be expressed as

$$\lim_{s\to -l} \frac{\partial \mathcal{G}_2(s,\kappa)}{\partial s} = \frac{\kappa^l}{l!}\left[\psi(1+l) - \log(\kappa)\right]. \tag{4.49}$$

Now, replacing (4.49) into (4.46), yields

$$G_{1,2}^{2,1}\left(\kappa \,\middle|\, \begin{matrix} 0; - \\ 0, 0; - \end{matrix}\right) = \sum_{l=0}^{\infty} \frac{\kappa^l}{l!}\left[\psi(1+l) - \log(\kappa)\right]. \tag{4.50}$$

Now, by substituting (4.42) and (4.43) into (4.317) and replacing (4.317) and (4.50) into (4.23)

and by considering only the first and second terms of the infinite sum, we get

$$\Pr\left(C_S^{(c,\,k,J)} \leq 0\right) \sim \lambda_{S_cD}\left[1+\frac{e^{-\varphi_J}}{\varphi_J}\right]\frac{\varepsilon_c^{(k,J)}}{\overline{\gamma}_{S_J}}\log\left(\overline{\gamma}_{S_J}\right). \tag{4.51}$$

Finally, by replacing (4.51) into (4.8) we get the asymptotic expression for $P_{int}^{(c,J)}$ given in (4.29). ■

4.2.3 Numerical results and discussions

In this section, the derived IP expression is validated through corresponding Monte-Carlo simulation by generating 10^6 exponentially distributed random values. The considered simulation parameters are given in Table. 4.1. We clearly see from the obtained figures that the analytical results perfectly match the simulation results.

Table 4.1: Simulation parameters of contribution 4.

Parameter	λ_q	M	N	$\overline{\gamma}_P$ (dB)
value	0.5	4	2	10

Figs. 4.2 and 4.3 show the IP as a function of $\overline{\gamma}_P$ for various values of $\overline{\gamma}_{S_J}$ and M, respectively. As it can be seen, the greater $\overline{\gamma}_P$ and $\overline{\gamma}_{S_J}$, the smaller the IP. According to (4.1), when $\overline{\gamma}_P$ increases the SNR of the main link increases as well. This leads to the improvement of the main link capacity and consequently the system's secrecy capacity enhances, which ensure secure transmission. Moreover, in the absence of a jammer, the IP remains constant, for a fixed number of eavesdroppers, regardless of the average SNR $\overline{\gamma}_P$ because as shown in (4.11) the IP depends only on the channel coefficients. Additionally, Fig. 2 shows that for $M = 4$, a better secrecy is achieved for high values of $\overline{\gamma}_{S_J}$. Indeed, it can be seen from (4.2) that SNR at the eavesdroppers decreases as long as $\overline{\gamma}_{S_J}$ increases. Consequently, the wiretap link capacity decreases, which leads to the enhancement of the system's security.

Fig. 4.4 depicts the IP as a function of the number of eavesdroppers M for various values of $\overline{\gamma}_{S_J}$ by considering the case of the presence and absence of a friendly jammer. As one can see, as the number of eavesdroppers increases the probability of intercepting communication increases as well. Moreover, it can be also noticed that when $\overline{\gamma}_{S_J}$ is significantly small i.e., $\overline{\gamma}_{S_J} \leq -2$ dB and $M \geq 10$, the friendly jammer does not contribute to improving the security

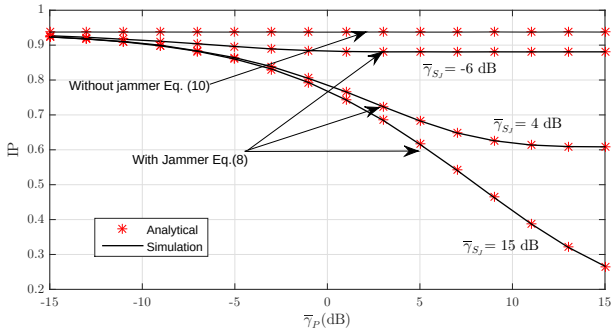

Figure 4.2: IP versus $\overline{\gamma}_P$.

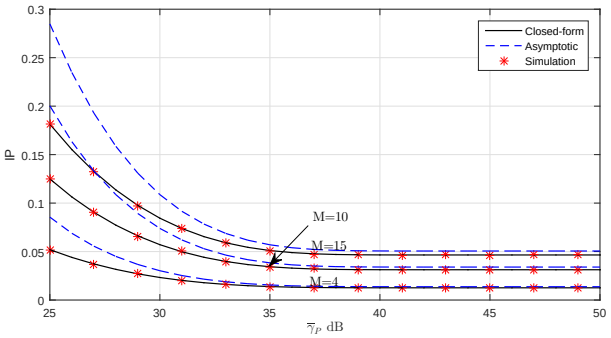

Figure 4.3: IP versus $\overline{\gamma}_P$ for $\overline{\gamma}_{S_J} = 30$ dB.

of the system.

Fig. 4.5 depicts the IP versus $\overline{\gamma}_{S_J}$ and the number of eavesdroppers M. It is clearly seen that better security is achieved for a small number of eavesdroppers and high transmission power of the friendly jammer. However, for a high number of eavesdroppers, the presence of a friendly jammer with low power does not have any significant impact on the system's security as the IP tends to be high.

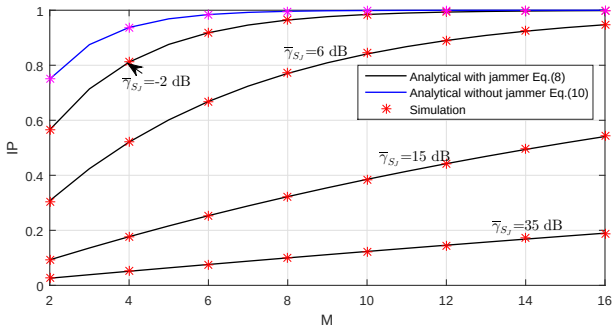

Figure 4.4: IP versus the number of eavesdroppers for $\overline{\gamma}_P = 25$dB.

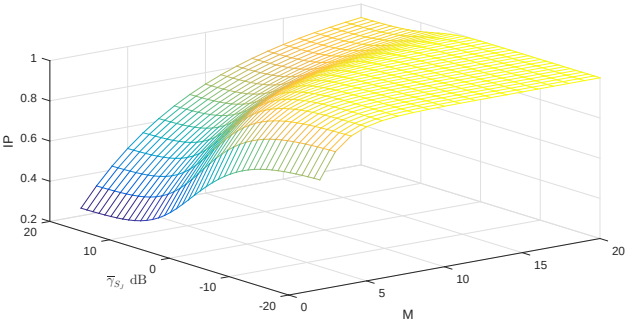

Figure 4.5: IP versus the number of eavesdroppers and $\overline{\gamma}_{S_J}$.

4.3 Contribution 5: Secrecy performance analysis of a dual-hop jamming-based underlay CRN

4.3.1 System and channel model

The considered dual-hop CRN, represented in Fig. 4.6, consists of multiple sources $(S_i)_{i=1,..,n}$, one relay R, multiple eavesdroppers $(E_k)_{k=1,..,m}$, one L-antennas destination D performing MRC diversity technique, one PU transmitter (PU_{Tx}), and one PU receiver (PU_{Rx}). In this scheme, all the nodes except D are assumed to be equipped with only one antenna. Moreover, we consider a multi-user scheduling such that, at the moment t, only one user is transmitting its data. We assume that the source nodes are taking rounds in accessing the spectrum and a friendly jammer S_J is randomly selected among $n-1$ source nodes in order to send an artificial noise to the eavesdroppers. We assume that the primary receiver PU_{Rx} and the relay R are able to cancel out that noise, while the eavesdroppers are not.

In this scheme, we are considering Rayleigh fading model for all links in which the channel gains are exponentially distributed. The channel coefficients of links $S_i \to R$, $R \to D$, $S_i \to E_k$, $R \to E_k$, $PU_{Tx} \to PU_{Rx}$, $R \to PU_{Rx}$, $S_i \to PU_{Rx}$ are denoted by h_{S_iR}, h_{RD}, $h_{S_iE_k}$, h_{RE_k}, h_P,h_{RP}, h_{S_iP}, respectively. The received signals at R, E_k at the first and second hop, D, and the primary receiver PU_{Rx} are, respectively, expressed as

$$y_R = \sqrt{P_{S_i}} h_{S_iR} x_{S_i} + n_R \; i = 1, .., n \tag{4.52}$$

$$y_{1E_k}^{(i)} = \sqrt{P_{S_i}} h_{S_iE_k} x_{S_i} + \epsilon \sqrt{P_{S_J}} h_{S_JE_k} x_{S_J} + n_{E_k}, \tag{4.53}$$
$$k = 1, .., m \; i = 1, .., n \; i \neq J$$

$$y_D = \sqrt{P_R} ||h_{RD}|| x_R + w_D n_D, \tag{4.54}$$

$$y_{2E_k} = \sqrt{P_R} h_{RE_k} x_r + n_E, k = 1, .., m \tag{4.55}$$

where

$$\epsilon = \begin{cases} 0, \text{ absence of jammer} \\ 1, \text{ presence of jammer} \end{cases},$$

and P_{S_i}, P_R, and P_{S_J} are the transmission power of S_i, R, and S_J, respectively. The transmitted signals of S_i, R, and S_J are x_{s_i}, x_R, and x_{S_j}, respectively. n_R, n_D, n_E, denote the additive white Gaussian noise at R, D, and E_k, respectively, $w_D = \frac{h_{RD}^{\dagger}}{||h_{RD}||}$, while h_{RD} denotes $L \times 1$ channel vector of the links R-$(D_j)_{j=1,..,L}$, and the symbol † denotes the transpose conjugate.

For the sake of simplicity, we denote the channel power gains by $g_q = |h_q|^2$ and their corresponding coefficients are λ_q where $q = \{S_iR,\ S_iE_k,\ S_iP,\ RD_j,\ RE_k,\ RP,\ P\}$. As the fading amplitudes of all links are Rayleigh distributed, it follows that the channel gains are exponentially distributed.

During transmission, the nodes S_i, S_J, and R have to set their transmission power in order to avoid causing harmful interference to the PUs. Thus, the transmission power of the source S_i, the jammer S_J, and the relay R can be, respectively, expressed as

$$P_{S_i} = \min\left(P_{S_i}^{\max},\ \frac{P_I}{g_{S_iP}}\right); i = 1, .., n, \tag{4.56}$$

and

$$P_R = \min\left(P_R^{\max},\ \frac{P_I}{g_{RP}}\right), \tag{4.57}$$

where $P_{S_i}^{\max}$, and $P_R^{\max}$ are the maximal transmit power at S_i, and R, respectively, while P_I accounts for the MTIP at PU_{Rx}. It is clearly seen from (4.56), and (4.57) that when P_I increases, the nodes S_i, S_J, and R will be allowed to use their maximal transmission power. Consequently, the SNR at both R and D will increase while the SNR at eavesdroppers will decrease leading to a system security improvement.

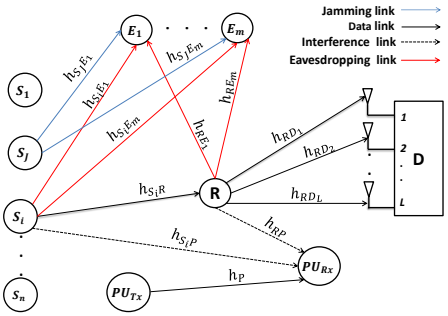

Figure 4.6: The considered dual-hop jamming-based CRN.

4.3.2 Secrecy performance evaluation

In this section, the SOP as performance metric is derived in its closed-form. To do so, we have to define first the expression of secrecy capacity. In our considered communication system, the secrecy capacity of the ith source when S_J is selected as a friendly jammer can be expressed by

$$C_s^{(i,J)} = \min_{k=1,..,m} \left(C_{1S}^{(i,k,J)}, C_{2S}^{(k)} \right), \tag{4.58}$$

where

- $C_{1S}^{(i,k,J)}$ denotes the secrecy capacity of the first link, i.e, the difference between the capacity of the main link $S_i - R$ and the one of the wiretap channel $S_i - E_k$ in the presence of the jammer S_J, and can be written as

$$\begin{aligned} C_{1S}^{(i,k,J)} &= \left[C_{1M}^{(i)} - C_{1E}^{(i,k,J)} \right]^+ \\ &= \begin{cases} \log_2 \left(\gamma_{1k}^{(i,J)} \right), \gamma_R^{(i)} > \gamma_{1E}^{(i,k,J)} \\ 0, \text{ elsewhere} \end{cases}, \end{aligned} \tag{4.59}$$

  where $\gamma_R^{(i)}$ and $\gamma_{1E}^{(i,k,J)}$ denote the instantaneous SNR at the relay R and the kth eavesdropper E_k, respectively, and are given as

$$\gamma_R^{(i)} = \frac{P_{S_i} g_{S_i R}}{N_R}, \tag{4.60}$$

$$\gamma_{1E}^{(i,k,J)} = \frac{P_{S_i} g_{S_i E_k}}{P_{S_J} g_{S_J E_k} + N_E}, \tag{4.61}$$

  and

$$\gamma_{1k}^{(i,J)} = \frac{1 + \gamma_R^{(i)}}{1 + \gamma_{1E}^{(i,k,J)}}. \tag{4.62}$$

- $C_{2S}^{(k)}$ is the secrecy capacity of the second hop, representing the difference between the capacity of the link $R - D$ and the one of the wiretap channel $R - E_k$

$$C_{2S}^{(k)} = \begin{cases} \log_2 \left(\gamma_{2k} \right), \gamma_D > \gamma_{2E}^{(k)} \\ 0, \text{ elsewhere} \end{cases}, \tag{4.63}$$

where

$$\gamma_{2k} = \frac{1+\gamma_D}{1+\gamma_{2E}^{(k)}}. \tag{4.64}$$

γ_D, and $\gamma_{2E}^{(k)}$ denote the instantaneous SNR of the main link $R-D$ and the channel $R-E_k$, respectively and are given as

$$\gamma_D = \frac{P_R \sum_{t=1}^{L} g_{RD_t}}{N_D}, \tag{4.65}$$

$$\gamma_{2E}^{(k)} = \frac{P_R g_{RE_k}}{N_E}, \tag{4.66}$$

Closed-form expression for the SOP

The SOP of the considered communication system can be expressed as

$$\text{SOP} = \frac{1}{n(n-1)} \sum_{i=1}^{n-1} \sum_{\substack{J=1 \\ J\neq i}}^{n} \text{SOP}_i^{(J)}, \tag{4.67}$$

where

$$\text{SOP}_i^{(J)} = \Pr\left(C_s^{(i,J)} < R_s\right), \tag{4.68}$$

It is clearly seen from (4.68) that as $C_s^{(i,J)}$ increases SOP decreases resulting in performance enhancement of the system. So, in order to investigate the system's security, it is sufficient to determine the CDF of $C_s^{(i,J)}$.

Substituting (4.58) into (4.68), yields

$$\begin{aligned} \text{SOP}_i^{(J)} &= 1 - \prod_{k=1}^{m} \Pr\left(\min(C_{1S}^{(i,k,J)}, C_{2S}^{(k)}) \geq R_s\right) \\ &= 1 - \prod_{k=1}^{m} \left[1 - F_{\gamma_{1k}^{(i,J)}}(\gamma)\right] \left[1 - F_{\gamma_{2k}}(\gamma)\right], \end{aligned} \tag{4.69}$$

where $\gamma = 2^{R_S}$.

One can see from (4.69) that the computation of $\text{SOP}_i^{(J)}$ requires the knowledge of the CDFs of both $\gamma_{1k}^{(i,J)}$ and γ_{2k}.

Theorem 4.3.1. *The CDFs of RVs $\gamma_{1k}^{(i,J)}$ and γ_{2k} are given by (4.70) and (4.71), respectively,*

$$F_{\gamma_{1k}^{(i,J)}}(\gamma) = 1 - \left\{ \left(1 - \lambda_{S_iR} N_R \gamma \Xi_{i,k}^{(J)}(\gamma)\right) e^{-\frac{\lambda_{S_iR} N_R (\gamma-1)}{P_{S_i}^{\max}}} \left(1 - \frac{e^{-\frac{\lambda_{S_iP} P_I}{P_{S_i}^{\max}}}}{\frac{\lambda_{S_iP} P_I}{\lambda_{S_iR} N_R (\gamma-1)} + 1}\right) \right\}, \tag{4.70}$$

and

$$F_{\gamma_{2k}}(\gamma) = 1 - \sum_{h=1}^{L} \prod_{\substack{l=1 \\ l \neq h}}^{L} \left(\frac{\lambda_{RD_l}}{\lambda_{RD_l} - \lambda_{RD_h}}\right) \frac{e^{-\frac{\lambda_{RD_h} N_D (\gamma-1)}{P_R^{\max}}}}{\frac{\lambda_{RD_h} N_D \gamma}{\lambda_{RE_k} N_E} + 1} \left[1 - \frac{e^{-\frac{\lambda_{RP} P_I}{P_R^{\max}}}}{\frac{\lambda_{RP} P_I}{\lambda_{RD_h} N_D (\gamma-1)} + 1}\right]. \tag{4.71}$$

where

$\Xi_{i,k}^{(J)}(\gamma) = \frac{e^{-\varphi_J}}{h_{i,k}} - \chi_{i,k}^{(J)} \left\{ \Upsilon_{i,k}^{(J)} \left[e^{-\varphi_J} - 1\right] - e^{\varpi_{i,k}^{(J)} - \varphi_J} \Lambda_{i,k}^{(J)} \right\}$, $\varphi_J = \frac{\lambda_{S_JP} P_I}{P_{S_J}^{\max}}$, $\chi_{i,k}^{(J)} = \frac{\lambda_{S_JE_k}}{\lambda_{S_iE_k} P_{S_J}^{\max}}$, $h_{i,k} = \lambda_{S_iE_k} N_E + \lambda_{S_iR} N_R \gamma$, $\Upsilon_{i,k}^{(J)} = G_{1,2}^{2,1}\left(\varpi_{i,k}^{(J)} \middle| \begin{matrix} 0; - \\ 0, 0; - \end{matrix}\right)$, $\varpi_{i,k}^{(J)} = \chi_{i,k}^{(J)} h_{i,k}$, $\Lambda_{i,k}^{(J)} = \frac{A_1^{(i,k,J)}}{\varphi_J} - A_0^{(i,k,J)}$, $A_p^{(i,k,J)} = \left(\beta_{i,k}^{(J)}\right)^{p+1} G_{2,2}^{2,2}\left(\beta_{i,k}^{(J)} \middle| \begin{matrix} (0,0), (-p, \varpi_{i,k}^{(J)}); - \\ (0,0), (0,0); - \end{matrix}\right)$, $\beta_{i,k}^{(J)} = \frac{\varphi_J}{\chi_{i,k}^{(J)} h_{i,k}}$.

Proof.

- **CDF of $\gamma_{1k}^{(i,J)}$**

The CDF of $\gamma_{1k}^{(i,J)}$ can be expressed as

$$\begin{aligned} F_{\gamma_{1k}^{(i,J)}}(\gamma) &= \Pr\left(P_{S_i}\left[\frac{g_{S_iR}}{N_R} - \gamma W_{i,k}^{(J)}\right] \leq \gamma - 1\right) \\ &= \Pr\left(\left(P_{S_i} \leq Z_{i,k}^{(J)} \text{ and } Z_{i,k}^{(J)} \geq 0\right) \text{or } Z_{i,k}^{(J)} \leq 0\right) \\ &= \int_0^{\infty} F_{P_{S_i}}(z) f_{Z_{i,k}^{(J)}}(z) dz + \int_{-\infty}^{0} f_{Z_{i,k}^{(J)}}(z) dz, \end{aligned} \tag{4.72}$$

where $W_{i,k}^{(J)} = \frac{g_{S_iE_k}}{P_{S_J} g_{S_JE_k} + N_E}$ and $Z_{i,k}^{(J)} = \frac{\gamma - 1}{\frac{g_{S_iR}}{N_R} - \gamma W_{i,k}^{(J)}}$. According to (4.72), it follows that the derivation of $F_{\gamma_{1k}^{(i,J)}}(\gamma)$ requires the knowledge of the CDFs of both P_{S_i} and $Z_{i,k}^{(J)}$. Doing some computations, the CDF of P_{S_i} can be easily shown to be given

$$F_{P_{S_i}}(z) = \begin{cases} 1 & : P_{S_i}^{\max} \leq z \\ F_{\frac{P_I}{g_{S_iP}}}(z) & : P_{S_i}^{\max} > z \end{cases}, \tag{4.73}$$

where the CDF of $\frac{P_I}{g_{S_iP}}$ can be obtained as

$$F_{\frac{P_I}{g_{S_iP}}}(z) = e^{-\lambda_{S_iP}\frac{P_I}{z}}. \tag{4.74}$$

On the other hand, the CDF of $Q_{i,k}^{(J)} = \dfrac{1}{Z_{i,k}^{(J)}}$ can be expressed for positive values of ψ as

$$\begin{aligned} F_{Q_{i,k}^{(J)}}(\psi) &= \Pr\left(g_{S_iR} \leq N_R\left[\psi\left(\gamma-1\right)+\gamma W_{i,k}^{(J)}\right]\right) \\ &= \int_0^\infty F g_{S_iR}\left(N_R\left[\psi\left(\gamma-1\right)+\gamma z\right]\right) f_{W_{i,k}^{(J)}}\left(z\right) dz. \end{aligned} \tag{4.75}$$

In order to derive $F_{Q_{i,k}^{(J)}}(\psi)$ we have to derive the CDF of the RV $W_{i,k}^{(J)}$

$$\begin{aligned} F_{W_{i,k}^{(J)}}\left(\xi\right) &= \Pr\left(g_{S_iE_k} \leq \xi\left(g_{S_JE_k}P_{S_J}+N_E\right)\right) \\ &= \int_0^\infty F_{g_{S_iE_k}}\left(\xi\left(z+N_E\right)\right) f_{P_{S_J}g_{S_JE_k}}\left(z\right) dz. \end{aligned} \tag{4.76}$$

By using integration by parts, we get

$$F_{W_{i,k}^{(J)}}\left(\xi\right) = 1 - \xi\int_0^\infty f_{g_{S_iE_k}}\left(\xi\left(z+N_E\right)\right) F_{P_{S_J}g_{S_JE_k}}\left(z\right) dz. \tag{4.77}$$

By definition, the CDF of the RV $P_{S_J}g_{S_JE_k}$ can be written as

$$F_{P_{S_J}g_{S_JE_k}}\left(z\right) = \underbrace{\Pr\left(g_{S_JE_k} \leq \frac{z}{P_{S_J}^{\max}}, \frac{P_I}{g_{S_JP}} \geq P_{S_J}^{\max}\right)}_{I_1^{(k,J)}} + \underbrace{\Pr\left(\frac{g_{S_JE_k}}{g_{S_JP}} \leq \frac{z}{P_I}, \frac{P_I}{g_{S_JP}} \leq P_{S_J}^{\max}\right)}_{I_2^{(k,J)}}$$

As the two RVs $g_{S_JE_k}$ and g_{S_JP} are independent, the first term $\mathcal{I}_1^{(k,J)}$ in (4.78) can be written as

$$\begin{aligned} \mathcal{I}_1^{(k,J)} &= \Pr\left(g_{S_JE_k} \leq \frac{z}{P_{S_J}^{\max}}\right)\Pr\left(g_{S_JP} \leq \frac{P_I}{P_{S_J}^{\max}}\right) \\ &= F_{g_{S_JE_k}}\left(\frac{z}{P_{S_J}^{\max}}\right) F_{g_{S_JP}}\left(\frac{P_I}{P_{S_J}^{\max}}\right), \end{aligned} \tag{4.78}$$

while, the second term $\mathcal{I}_2^{(k,J)}$ can be easily expressed as

$$\begin{aligned}\mathcal{I}_2^{(k,J)} &= \int_{\frac{P_I}{P_{S_J}^{\max}}}^{\infty} f_{g_{S_JP}}(y) \int_0^{\frac{z}{P_I}y} f_{g_{S_JE_k}}(x)dxdy \\ &= e^{-\varphi_J} - \frac{e^{-\varphi_J\left(z\varrho_k^{(J)}+1\right)}}{z\varrho_k^{(J)}+1},\end{aligned} \tag{4.79}$$

where $\varrho_k^{(J)} = \frac{\lambda_{S_JE_k}}{\lambda_{S_JP}P_I}$. Then, by plugging (4.149) and (4.79) into (4.78) we obtain

$$F_{P_{S_J}g_{S_JE_k}}(\vartheta) = 1 + e^{-\varphi_J\varrho_k^{(J)}\vartheta}\left(e^{-\varphi_J}-1\right) - \frac{e^{-\varphi_J\left(\vartheta\varrho_k^{(J)}+1\right)}}{\vartheta\varrho_k^{(J)}+1}. \tag{4.80}$$

Now, the CDF of $W_{i,k}^{(J)}$ can be obtained by incorporating (4.80) into (4.77), as

$$F_{W_{i,k}^{(J)}}(\xi) = 1 - e^{-\lambda_{S_iE_k}\xi N_E}\left[1 + \frac{\lambda_{S_iE_k}\xi\left(e^{-\varphi_J}-1\right)}{\varphi_J\varrho_k^{(J)}+\lambda_{S_iE_k}\xi} - \frac{\xi\lambda_{S_iE_k}e^{-\varphi_J}}{\varrho_k^{(J)}}\underbrace{\int_0^{\infty}\frac{e^{-\varrho_k^{(J)}\delta_{i,k}^{(J)}z}}{z+\frac{1}{\varrho_k^{(J)}}}dz}_{\mathcal{I}_3^{(i,k,J)}}\right], \tag{4.81}$$

where $\delta_{i,k}^{(J)} = \frac{\varphi_J\varrho_k^{(J)}+\lambda_{S_iE_k}\xi}{\varrho_k^{(J)}}$.

Making use of [71, Eq. (07.34.03.0456.01)] alongside [71, Eq. (07.34.21.0088.01)], we have

$$\begin{aligned}\mathcal{I}_3^{(i,k,J)} &= \delta_{i,k}^{(J)}\int_0^{\infty} G_{2,2}^{1,2}\left(z\left|\begin{matrix}1,1;-\\1;0\end{matrix}\right.\right)e^{-\delta_{i,k}^{(J)}z}dz \\ &= G_{3,2}^{1,3}\left(\frac{1}{\delta_{i,k}^{(J)}}\left|\begin{matrix}0,1,1;-\\1;0\end{matrix}\right.\right).\end{aligned} \tag{4.82}$$

Furthermore,

$$G_{3,2}^{1,3}\left(\frac{1}{\delta_{i,k}^{(J)}}\middle|\begin{matrix}0,1,1;-\\1;0\end{matrix}\right)=G_{2,3}^{3,1}\left(\delta_{i,k}^{(J)}\middle|\begin{matrix}0;1\\1,0,0;-\end{matrix}\right)$$
$$=\frac{1}{2\pi j}\int_{\mathcal{C}}\frac{\Gamma(s+1)\Gamma^2(s)\Gamma(1-s)}{\Gamma(s+1)}\left(\delta_{i,k}^{(J)}\right)^{-s}ds$$
$$=G_{1,2}^{2,1}\left(\delta_{i,k}^{(J)}\middle|\begin{matrix}0;-\\0,0;-\end{matrix}\right), \tag{4.83}$$

with and $\mathcal{C}$ represents a complex contour of integration ensuring the convergence of the Mellin-Barnes integral.

Then, by performing the substitution (4.82) into (4.81) yields

$$F_{W_{i,k}^{(J)}}(\xi)=1-e^{-\lambda_{S_iE_k}\xi N_E}\left[1+\frac{\lambda_{S_iE_k}\xi\left(e^{-\varphi_J}-1\right)}{\varphi_J\varrho_k^{(J)}+\lambda_{S_iE_k}\xi}-\frac{\xi\lambda_{S_iE_k}e^{-\varphi_J}}{\varrho_k^{(J)}}G_{1,2}^{2,1}\left(\varphi_J+\frac{\varphi_J\xi}{\chi_{i,k}^{(J)}}\middle|\begin{matrix}0;-\\0,0;-\end{matrix}\right)\right], \tag{4.84}$$

It follows, by substituting (4.84) into (4.75) that

$$F_{Q_{i,k}^{(J)}}(\psi)=1-e^{-\phi_i(\psi)}\left(1-\lambda_{S_iR}N_R\gamma\Xi_{i,k}^{(J)}(\gamma)\right), \tag{4.85}$$

where

$$\Xi_{i,k}^{(J)}(\gamma)=\int_0^\infty e^{-h_{i,k}z}dz+\left(e^{-\varphi_J}-1\right)\Theta_{1J}^{(i,k)}-\frac{\varphi_Je^{-\varphi_J}}{\chi_{i,k}^{(J)}}\Theta_2^{(i,k,J)}, \tag{4.86}$$

$$\Theta_{1J}^{(i,k)}=\int_0^\infty\frac{ze^{-h_{i,k}z}}{\chi_{i,k}^{(J)}+z}dz, \tag{4.87}$$

$$\Theta_{2J}^{(i,k)}=\int_0^\infty ze^{-h_{i,k}z}G_{1,2}^{2,1}\left(\varphi_J\left(1+\frac{z}{\chi_{i,k}^{(J)}}\right)\middle|\begin{matrix}0;-\\0,0;-\end{matrix}\right)dz, \tag{4.88}$$

and

$$\phi_i(\psi)=\lambda_{S_iR}N_R\psi(\gamma-1). \tag{4.89}$$

The term $\Theta_{1J}^{(i,k)}$ can be expressed as

$$\begin{aligned}\Theta_{1J}^{(i,k)} &= \int_0^\infty e^{-h_{i,k}z}dz - \chi_{i,k}^{(J)}\int_0^\infty \frac{e^{-h_{i,k}z}}{\chi_{i,k}^{(J)}+z}dz \\ &= \frac{1}{h_{i,k}} - \chi_{i,k}^{(J)} G_{1,2}^{2,1}\left(h_{i,k}\chi_{i,k}^{(J)}\left|\begin{matrix}0;-\\0,0;-\end{matrix}\right.\right),\end{aligned} \tag{4.90}$$

while the term $\Theta_{2J}^{(i,k)}$ can be rewritten, using a change of variable, as

$$\begin{aligned}\Theta_{2J}^{(i,k)} &= \frac{\chi_{i,k}^{(J)}}{\varphi_J}e^{\chi_{i,k}^{(J)}h_{i,k}}\int_{\varphi_J}^\infty\left(\frac{y}{\varphi_J}-1\right)e^{-\frac{\chi_{i,k}^{(J)}h_{i,k}}{\varphi_J}y}G_{1,2}^{2,1}\left(y\left|\begin{matrix}0;-\\0,0;-\end{matrix}\right.\right)dy \\ &= \eta_{i,k}^{(J)}\left[\frac{A_1^{(i,k,J)}}{\varphi_J} - A_0^{(i,k,J)}\right],\end{aligned} \tag{4.91}$$

where $\eta_{i,k}^{(J)} = \frac{\chi_{i,k}^{(J)}}{\varphi_J}e^{\chi_{i,k}^{(J)}h_{i,k}}$, and the function $\left(A_p^{(i,k,J)}\right)_{p=0,1}$ is defined by

$$\begin{aligned}A_p^{(i,k,J)} &= \int_{\varphi_J}^\infty y^p e^{-\frac{\chi_{i,k}^{(J)}h_{i,k}}{\varphi_J}y}G_{1,2}^{2,1}\left(y\left|\begin{matrix}0;-\\0,0;-\end{matrix}\right.\right)dy \\ &= \frac{1}{2\pi j}\int_{\mathcal{C}}\Gamma^2(s)\,\Gamma(1-s)\,ds\int_{\varphi_J}^\infty y^{p-s}e^{-\frac{\chi_{i,k}^{(J)}h_{i,k}}{\varphi_J}y}dy \\ &= \frac{\left(\beta_{i,k}^{(J)}\right)^{p+1}}{2\pi j}\int_{\mathcal{C}}\Gamma^2(s)\,\Gamma(1-s)\,\Gamma\left(\varsigma_{p,s},\varpi_{i,k}^{(J)}\right)\left(\beta_{i,k}^{(J)}\right)^{-s}ds,\end{aligned} \tag{4.92}$$

where $\varsigma_{p,s} = p+1-s$. Then, by substituting (4.92) into (4.91) alongside (4.90), we get the expression of the function $\Xi_{i,k}^{(J)}(\gamma)$ defined above.

In contrast, the CDF of $Z_{i,k}^{(J)}$ is expressed in terms of the one of its inverse as

$$F_{Z_{i,k}^{(J)}}(x) = 1 - F_{Q_{i,k}^{(J)}}\left(\frac{1}{x}\right) + F_{Q_{i,k}^{(J)}}(0). \tag{4.93}$$

By using (4.85), the CDF of $Z_{i,k}^{(J)}$ can be rewritten as

$$F_{Z_{i,k}^{(J)}}(x) = e^{-\frac{\lambda_{S_iR}N_R(\gamma-1)}{x}}(1-\lambda_{S_iR}N_R\gamma\Xi_{i,k}^{(J)}(\gamma)) + \lambda_{S_iR}N_R\gamma\Xi_{i,k}^{(J)}(\gamma). \tag{4.94}$$

Then, by performing the appropriate substitutions in (4.72), we obtain (4.70).

Remark 8. *For the scenario without any jammer source and by performing some computation we can get easily the CDF at the first hop as*

$$F_{\gamma_{1k}^{(i)}}(\gamma) = 1 + \frac{e^{-\Phi_i}}{\frac{\lambda_{S_iR}N_R\gamma}{\lambda_{S_iE_k}N_E}+1}\left[\frac{\Phi_i e^{-\Omega_i}}{\Omega_i+\Phi_i}-1\right], \tag{4.95}$$

where $\Omega_i = \frac{\lambda_{S_iP}P_I}{P_{S_i}^{\max}}$ *and* $\Phi_i = \frac{\lambda_{S_iR}N_R(\gamma-1)}{P_{S_i}^{\max}}$.

- **CDF of γ_{2k}**

Using (4.66), the CDF of γ_{2k} is given as

$$\begin{aligned} F_{\gamma_{2k}}(\gamma) &= \Pr\left(P_R\left[\frac{Y_{RD}}{N_D}-\frac{\gamma g_{RE_k}}{N_E}\right]\leq\gamma-1\right) \\ &= \Pr\left(P_R\leq V_{R,k}, V_{R,k}\geq 0\right)+\Pr\left(V_{R,k}\leq 0\right) \\ &= \int_0^{\infty} F_{P_R}(z)f_{V_{R,k}}(z)dz+\int_{-\infty}^{0} f_{V_{R,k}}(z), \end{aligned} \tag{4.96}$$

where $Y_{RD}=\sum_{v=1}^{L} g_{RDv}$, and $V_{R,k}=\frac{\gamma-1}{\left(\frac{Y_{RD}}{N_D}-\gamma\frac{g_{RE_k}}{N_E}\right)}$.

In a similar manner, we have to derive first the CDF of the RV $V_{R,k}=\frac{1}{U_{R,k}}$.

$$\begin{aligned} F_{U_{R,k}}(\vartheta) &= \Pr\left(Y_{RD}\leq N_D\left(\vartheta\left(\gamma-1\right)+\gamma\frac{g_{RE_k}}{N_E}\right)\right) \\ &= \int_0^{\infty} F_{Y_{RD}}\left(\theta(z)\right)f_{g_{RE_k}}\left(z\right)dz, \end{aligned} \tag{4.97}$$

where $\theta(z)=N_D\left(\vartheta\left(\gamma-1\right)+\gamma\frac{z}{N_E}\right)$.

According to [104], the CDF of Y_{RD} in the case of i.n.i.d RVs can be expressed as

$$F_{Y_{RD}}(x)=\sum_{h=1}^{L}\psi_h\left(1-e^{-\lambda_{RD_h}x}\right), \tag{4.98}$$

where $\psi_h=\prod_{\substack{l=1\\l\neq h}}^{L}\left(\frac{\lambda_{RD_l}}{\lambda_{RD_l}-\lambda_{RD_h}}\right)$.

By substituting the PDF of the exponential RV and (4.98) into (4.97), the CDF of $U_{R,k}$ can be derived as

$$F_{U_{R,k}}(\vartheta)=\sum_{h=1}^{L}\psi_h\left(1-\frac{e^{-\lambda_{RD_h}N_D\vartheta(\gamma-1)}}{\frac{\lambda_{RD_h}N_D\gamma}{\lambda_{RE_k}N_E}+1}\right). \tag{4.99}$$

Table 4.2: Simulation parameters of contribution 5.

Parameter	λ_q	m	n	R_S	N_R
value	0.5	2	2	1	2
Parameter	N_D	N_E	$P_{S_i}^{max}$	P_R^{max}	$P_{S_J}^{max}$
value	2	2	8	8	8

Similarly to (4.93), and making use of (4.99) yields

$$F_{Z_{R,k}}(x) = 1 - \sum_{h=1}^{L} \psi_h \frac{\left(1 - e^{-\frac{\lambda_{RD_h} N_D(\gamma-1)}{x}}\right)}{\frac{\lambda_{RD_h} N_D \gamma}{\lambda_{RE_k} N_E} + 1}. \tag{4.100}$$

As the CDF of P_R can be expressed similarly to the one of P_{S_i} given by (4.73) and (4.74), the CDF of γ_{2k} can be now rewritten as

$$F_{\gamma_{2k}}(\gamma) = \int_0^{P_R^{\max}} F_{\frac{P_I}{g_{RP}}}(t) f_{V_{R,k}}(t)\, dt + \underbrace{\int_{P_R^{\max}}^{\infty} f_{V_{R,k}}(t)\, dt + \int_{-\infty}^{0} f_{V_{R,k}}(t)\, dt}_{=1-\int_0^{P_R^{\max}} f_{V_{R,k}}(t)dt}, \tag{4.101}$$

Finally, by substituting CDF of $\frac{P_I}{g_{RP}}$, that is similarly to (4.74), and (4.100) into (4.101), we obtain (4.71) which concludes the proof of Theorem 4.3.1. ■

4.3.3 Numerical results and discussions

In this section, we present the analytical and the simulation results for the considered CRN. The setting parameters of the simulation experiment are summarized in Table 4.2 where the powers are given in dBW.

As seen in Figs. 4.7-4.9, all analytical and simulation curves are perfectly matched over the entire ranges of the considered parameters.

Fig. 4.7 shows the SOP as a function of the secrecy rate R_s for various values of destination's antennas number. It can clearly be seen that the SOP increases with the increasing values of R_s, as also noticed by (4.68). This can be interpreted by the fact that when a high secrecy rate is adopted for a better performance, it is less likely to achieve a perfect secure transmission. Furthermore, the security is enhanced when using multiple antennas at the destination instead of employing only a single one. For instance, for $R_s = 1$ bit/s/Hz we have SOP$\simeq$ 0.85 and

SOP= 0.94 for $L = 4$ and $L = 2$, respectively.

The SOP versus the transmission power of the selected jammer $P_{S_J}^{\max}$ is illustrated in Fig. 4.8 for various values of branches number L at the node D. It can be noticed that, the higher $P_{S_J}^{\max}$ the smaller the SOP and therefore the system security becomes more reliable. This can be construed as increasing $P_{S_J}^{\max}$ leads to a decrease of eavesdroppers' SNRs as it can be seen in (4.61). Consequently, the wiretap link capacity decreases as well leading to the improvement of the first hop secrecy capacity. Additionally, increasing the number of antennas at the destination enhances the SNR as shown in (4.65) leading to the enhancement of the main link capacity i.e., $R - D$, and consequently the secrecy performance gets better.

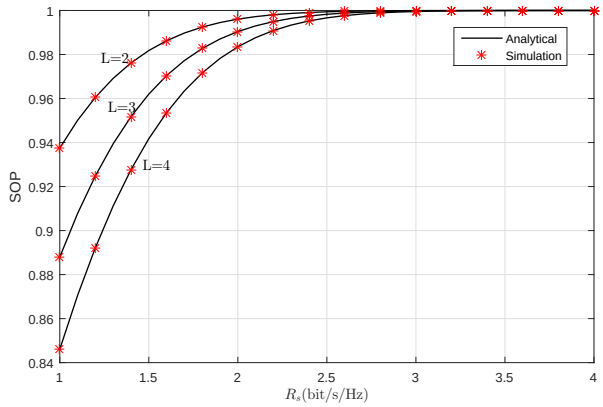

Figure 4.7: SOP versus secrecy rate for different numbers of antenna branches at the destination.

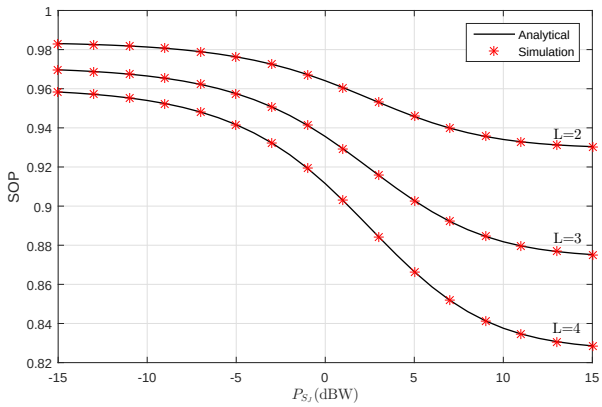

Figure 4.8: SOP versus maximum transmission power of the jammer S_J for different numbers of antennas at the destination.

Fig. 4.9 depicts the SOP versus P_I for different scenarios namely (i) either absence or presence of a friendly jammer and (i) single and multiple antennas destination. It can be noticed that the greater the P_I, the smaller the SOP. This can be justified, from (4.56) and (4.57), as increasing P_I above certain threshold, push the sources as well as the relay to transmit with their maximal powers. Also, it is clearly seen that a better secrecy is achieved when using a friendly jammer at the first hop and a destination with multiple antennas. Moreover, it can be noticed that the scenario with absence of jammer and L antennas destination ($L > 2$) is better than the one with presence of friendly jammer and a single antenna destination.

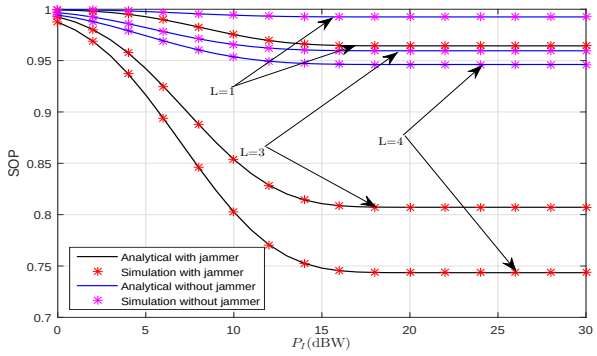

Figure 4.9: SOP versus P_I at PU_{Rx} for different numbers of antennas at the destination.

4.4 Contribution 6: Secrecy performance analysis of a dual-hop Jamming-based CR communication system with multi-antenna receivers

4.4.1 System and channel model

The considered two-hops CRN, represented in Fig. 4.10, consists of multiple sources $(S_i)_{i=1,..,N}$, one L_R-antennas relay R, multiple L_{E_k}-antennas eavesdroppers $(E_k)_{k=1,..,M}$, one destination D equipped with L_D antennas, one PU transmitter (P_{Tx}), and one PU receiver (P_{Rx}). For the sake of simplicity, we assume that the relay receives the transmitted signals from S_i on the L_R antennas and uses only one antenna to forward the message to D. Moreover, we consider multi-user scheduling such that, at any given moment, only one user is transmitting its data. Also, the source nodes are taking rounds in accessing the spectrum and a friendly jammer S_J is randomly selected among $N-1$ remaining nodes to send an artificial noise. This latter can be canceled by legitimate nodes, while E_k cannot mitigate it, leading to an increase in the secrecy capacity. Similarly to [36], we assume that a friendly jammer generates an artificial noise using a pseudo-random sequence that is known to the legitimate users which allows them to cancel out this noise, while this sequence remains unknown to the illegitimate ones. To this end, the main aim of this work is to investigate the impact of a friendly jammer, legitimate, and wiretap channels' average SNRs, MTIP as well as the spatial diversity at both the relay and the end-user on the secrecy performance of the considered communication system. In this scheme, Nakagami-m fading model is considered for all links. The fading amplitudes of links

$S_i \to R$, $R \to (D_t)_{1\leq t\leq L_D}$, $S_i \to E_k$, $R \to E_k$, $R \to P_{Rx}$, $S_i \to P_{Rx}$ are denoted by h_q where $q = \{S_iR,\ RD_t, S_iE_k,\ RE_k,\ RP,\ S_iP\}$. Consequently, the channel gains $g_q = |h_q|^2$ are Gamma distributed with PDF and CDF are given by

$$f_{g_q}(x) = \frac{\lambda_q^{m_q}}{\Gamma(m_q)} x^{m_q-1} e^{-\lambda_q x}, \tag{4.102}$$

$$F_{g_q}(x) = \frac{\gamma(m_q, \lambda_q x)}{\Gamma(m_q)}, \tag{4.103}$$

where $\lambda_q = \dfrac{m_q}{\Omega_q}$, m_q and Ω_q denote the fading severity and the average channel power gain, respectively. For a positive number m_q, the above CDF can be written as [67, Eq. (8.352.1)]

$$F_{g_q}(x) = 1 - e^{-\lambda_q x} \sum_{k=0}^{m_q-1} \frac{\lambda_q^k x^k}{k!}. \tag{4.104}$$

The received signals at R, E_k at both hops, and D are given, respectively, by

$$y_R^{(i)} = \sqrt{P_{S_i}} ||\mathbf{h}_{S_iR}|| x_{S_i} + \mathbf{w}_{S_iR}\mathbf{n}_R,\ i = 1, .., N, \tag{4.105}$$

$$y_{1E_k}^{(i)} = \sqrt{P_{S_i}} ||\mathbf{h}_{S_iE_k}|| x_{S_i} + \epsilon\sqrt{P_{S_J}} ||\mathbf{h}_{S_JE_k}|| x_{S_J} + \mathbf{w}_{S_iE_k}\mathbf{n}_{E_k}, \tag{4.106}$$
$$k = 1, .., M,\ i = 1, .., N,\ J \neq i,$$

$$y_{2E_k} = \sqrt{P_R} ||\mathbf{h}_{RE_k}|| x_R + \mathbf{w}_{RE_k}\mathbf{n}_{E_k}, k = 1, .., M, \tag{4.107}$$

$$y_D = \sqrt{P_R} ||\mathbf{h}_{RD}|| x_R + \mathbf{w}_{RD}\mathbf{n}_D, \tag{4.108}$$

with

$$\epsilon = \begin{cases} 0,\ \text{Absence of a jammer} \\ 1,\ \text{Presence of a jammer} \end{cases}.$$

Here, P_n and x_n denote the transmit power and signal from the node n, respectively where $n = \{S_i, R\}$, $\mathbf{w}_q = \frac{\mathbf{h}_q^\dagger}{||\mathbf{h}_q||}$, $q = \{S_iR, S_iE_k, RE_k, RD\}$, while $\mathbf{h}_q$ denotes $L_n \times 1$, channel vector of the links S_i-R, S_i-E_k, R-D, $\dagger$ denotes the transpose conjugate, and $||.||$ represents the Frobenius norm. Also, $\mathbf{n}_R$, $\mathbf{n}_D$, and $\mathbf{n}_{E_k}$, denote the $N_n \times 1$ additive white Gaussian noise vector at R, D, and E_k, respectively. For the sake of simplicity, all noise power vectors' components are

considered equal N_0.

Throughout the transmission process, both S_i, and R have to adapt their transmit powers so as to avoid causing harmful interference to the PUs. Thus, the transmit power of the source and the relay R taking into consideration the maximum constraint power can be, respectively, expressed as

$$P_{S_i} = \min\left(P_{S_i}^{max}, \frac{P_I}{g_{S_iP}}\right); i = 1, .., N, \tag{4.109}$$

and

$$P_R = \min\left(P_R^{max}, \frac{P_I}{g_{RP}}\right), \tag{4.110}$$

where $P_{S_i}^{max}$ and P_R^{max} denote the maximum transmit power at S_i, and R, respectively, while P_I accounts for the maximum tolerated interference power at P_{Rx}.

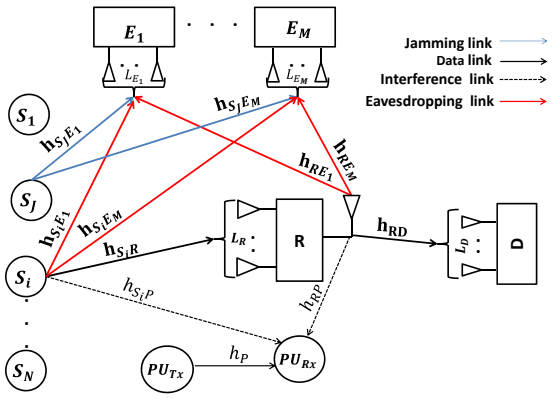

Figure 4.10: The considered dual-hop Jamming-based CRN.

4.4.2 Secrecy performance evaluation

In this section, the SOP is derived as performance metric. To do so, we have to define first the expression of the secrecy capacity. In our considered system, the secrecy capacities in the case of presence and absence of a friendly jammer are given, respectively, by

$$C_s^{(i,J)} = \min_{k=1,..,M}\left(C_{1S}^{(i,k,J)}, C_{2S}^{(k)}\right), \tag{4.111}$$

$$C_s^{(i)} = \min_{k=1,..,M}\left(C_{1S}^{(i,k)}, C_{2S}^{(k)}\right), \tag{4.112}$$

where

- $C_{1S}^{(i,k,J)}$ and $C_{1S}^{(i,k)}$ denote the secrecy capacities at the first hop, i.e., the difference between the capacity of the main link $S_i - R$ and the one of the wiretap channel $S_i - E_k$ in the presence and absence of a friendly jammer, respectively, and can be written as

$$C_{1S}^{(i,k,J)} = \begin{cases} \log_2\left(\dfrac{1+\gamma_R^{(i)}}{1+\gamma_{1E}^{(i,k,J)}}\right), \gamma_R^{(i)} > \gamma_{1E}^{(i,k,J)} \\ 0, \text{ elsewhere} \end{cases}, \tag{4.113}$$

$$C_{1S}^{(i,k)} = \begin{cases} \log_2\left(\dfrac{1+\gamma_R^{(i)}}{1+\gamma_{1E}^{(i,k)}}\right), \gamma_R^{(i)} > \gamma_{1E}^{(i,k)} \\ 0, \text{ elsewhere} \end{cases}, \tag{4.114}$$

  where $\gamma_R^{(i)}$ denotes the instantaneous SNR at R, while $\gamma_{1E}^{(i,k,J)}$ and $\gamma_{1E}^{(i,k)}$ stand for the SNRs at the eavesdropper E_k in the presence and absence of a friendly jammer, respectively, and are given by

$$\gamma_R^{(i)} = \min\left(\overline{\gamma}_{S_i}, \frac{\overline{\gamma}_I}{g_{S_iP}}\right) \sum_{u=1}^{L_R} g_{S_iR_u}, \tag{4.115}$$

$$\gamma_{1E}^{(i,k,J)} = \frac{\min\left(\overline{\gamma}_{S_i}, \frac{\overline{\gamma}_I}{g_{S_iP}}\right) \sum_{u=1}^{L_{E_k}} g_{S_iE_k^{(u)}}}{\min\left(\overline{\gamma}_{S_J}, \frac{\overline{\gamma}_I}{g_{S_JP}}\right) \sum_{u=1}^{L_{E_k}} g_{S_JE_k^{(u)}} + 1}, \tag{4.116}$$

$$\gamma_{1E}^{(i,k)} = \min\left(\overline{\gamma}_{S_i}, \frac{\overline{\gamma}_I}{g_{S_iP}}\right) \sum_{u=1}^{L_{E_k}} g_{S_iE_k^{(u)}}, \tag{4.117}$$

  and $\overline{\gamma}_{S_i} = P_{S_i}^{max}/N_0$, $\overline{\gamma}_I = P_I/N_0$, and $\overline{\gamma}_{S_J} = P_{S_J}^{max}/N_0$.

- $C_{2S}^{(k)}$ is the secrecy capacity of the second hop, representing the difference between the capacity of the link $R - D$ and the one of the wiretap channel $R - E_k$

$$C_{2S}^{(k)} = \begin{cases} \log_2\left(\dfrac{1+\gamma_D}{1+\gamma_{2E}^{(k)}}\right), \gamma_D > \gamma_{2E}^{(k)} \\ 0, \text{ elsewhere} \end{cases}, \tag{4.118}$$

  where γ_D, and $\gamma_{2E}^{(k)}$ denote the instantaneous SNR of the main link $R-D$ and the channel

$R - E_k$, respectively and are given as

$$\gamma_D = \min\left(\overline{\gamma}_R, \frac{\overline{\gamma}_I}{g_{RP}}\right) \sum_{t=1}^{L_D} g_{RD_t}, \tag{4.119}$$

$$\gamma_{2E}^{(k)} = \min\left(\overline{\gamma}_R, \frac{\overline{\gamma}_I}{g_{RP}}\right) \sum_{u=1}^{L_{E_k}} g_{RE_k^{(u)}}, \tag{4.120}$$

with $\overline{\gamma}_R = P_R^{\max}/N_0$.

Remark 9.

- *One can see from (4.115) and (4.116), that the PHY layer security at the first hop in the presence of a friendly jammer can be enhanced by increasing separately $\overline{\gamma}_I$, $\overline{\gamma}_{S_i}$, or $\overline{\gamma}_{S_J}$. Indeed, the increasing scale of the SNR at the relay exceeds the one of the kth eavesdropper as a jamming signal is added to the one received by E_k. However, in the absence of a friendly jammer, one can see from (4.115) and (4.117) that only the impact of legitimate and wiretap channels' parameters can make the distinction between the two associated SNRs. Consequently, the smaller λ_{S_iR}, the greater the secrecy capacity and then the security gets improved.*

- *From (4.119) and (4.120), it can be noticed that increasing either $\overline{\gamma}_R$ or $\overline{\gamma}_I$ enhances more the capacity of the legitimate link as D performs the MRC technique. Additionally, increasing the number of antennas at the receiver increases the SNR at D. Consequently, the system's security gets enhanced as well.*

Closed-form expression for the SOP

For the considered system, the N sources are taking rounds in accessing the spectrum then one jammer is randomly selected among the $N-1$ remaining sources. The SOP if there is no jamming, can be expressed as

$$\text{SOP} = \frac{1}{N} \sum_{i=1}^{N} \text{SOP}^{(i)}, \tag{4.121}$$

while in the presence of a jammer, it becomes

$$\text{SOP} = \frac{1}{N(N-1)} \sum_{i=1}^{N} \sum_{\substack{J=1 \\ J \neq i}}^{N} SOP^{(i,J)}, \tag{4.122}$$

where $\text{SOP}^{(i)}$ and $\text{SOP}^{(i,J)}$ account for SOP of the system linking S_i with D in the presence of eavesdroppers, and in the absence and presence of the Jth friendly jammer, respectively. The SOP of the considered system stands for the probability that at least one of the secrecy capacities falls below a predefined secrecy rate R_s, namely

$$\begin{aligned} \text{SOP}^{(i,J)} &= 1 - \prod_{k=1}^{M} \Pr\left(\min(C_{1S}^{(i,k,J)}, C_{2S}^{(k)}) \geq R_s\right) \\ &= 1 - \prod_{k=1}^{M} \left[1 - \text{SOP}_1^{(i,k,J)}\right] \left[1 - \text{SOP}_2^{(k)}\right], \end{aligned} \tag{4.123}$$

and

$$\text{SOP}^{(i)} = 1 - \prod_{k=1}^{M} \left[1 - \text{SOP}_1^{(i,k)}\right] \left[1 - \text{SOP}_2^{(k)}\right], \tag{4.124}$$

where $\text{SOP}_1^{(i,k,J)}$ and $\text{SOP}_1^{(i,k)}$ stand for the secrecy capacities at the first hop in the presence and absence of a friendly jammer, respectively, and $\text{SOP}_2^{(k)}$ represents the secrecy capacity at the second hop. One can see from (4.123) and (4.124) that the computation of SOP requires the knowledge of $\text{SOP}_1^{(i,k,J)}$, $\text{SOP}_1^{(i,k)}$, and $\text{SOP}_2^{(k)}$ as well.

Remark 10. *As* $\text{SOP}_1^{(i,k,J)}$, $\text{SOP}_1^{(i)}$, *and* $\text{SOP}_2^{(k)}$ *are between* 0 *and* 1, *it is worth mentioning that the greater is* M, *the greater is* SOP *(approaches 1), and then the system becomes vulnerable to eavesdropping attack.*

Theorem 4.4.1. *The closed-form expressions of* $\text{SOP}_1^{(i,k,J)}$, $\text{SOP}_1^{(i,k)}$, *and* $\text{SOP}_2^{(k)}$ *under Nakagami-*

m fading model are given by (4.125), (4.126), and (4.127), respectively,

$$\begin{aligned}\mathrm{SOP}_1^{(i,k,J)} &= 1 - \frac{\gamma\left(m_{S_iP}, \varphi_{S_i}\right)\Gamma\left(L_R m_{S_iR}, \frac{\sigma_i \xi_{S_iR}}{\overline{\gamma}_I}\right) + \mathcal{M}_3\left(\frac{\xi_{S_iR}}{\lambda_{S_iP}\overline{\gamma}_I}\right)}{\Gamma(L_R m_{S_iR})\Gamma\left(m_{S_iP}\right)} \\ &+ \frac{\gamma\alpha_i^{(k,J)}}{\Gamma\left(m_{S_iP}\right)} \sum_{h=0}^{L_{E_k} m_{S_iE_k}-1} \Omega_h^{(i,k)} \sum_{l=0}^{L_R m_{S_iR}-1} \frac{\Upsilon_l^{(i)}\left(\overline{\gamma}_I\right)^{-L_R m_{S_iR}+l+1}}{\left(\varpi_i^{(k)}\right)^{L_{E_k} m_{S_iE_k}+l-h}} \\ &\times \left[\frac{\gamma\left(m_{S_iP}, \varphi_{S_i}\right) e^{-\frac{\sigma_i \xi_{S_iR}}{\overline{\gamma}_I}}}{\sigma_i^{-L_R m_{S_iR}+l+1}} + \frac{\lambda_{S_iP}^{m_{S_iP}}\Gamma\left(m_{S_iP} + L_R m_{S_iR} - l - 1, \varphi_{S_i} + \frac{\sigma_i \xi_{S_iR}}{\overline{\gamma}_I}\right)}{\left(\lambda_{S_iP} + \frac{\xi_{S_iR}}{\overline{\gamma}_I}\right)^{m_{S_iP}+L_R m_{S_iR}-l-1}}\right] \\ &\times \left[\gamma\left(m_{S_JP}, \varphi_J\right)\mathcal{M}_1^{(h,l)}\left(\varpi_i^{(k)}\theta_i^{(k,J)}\right) + \mathcal{M}_2^{(h,l)}\left(\frac{\varsigma_i^{(k,J)}\varpi_i^{(k)}}{\overline{\gamma}_I}\right)\right]. \end{aligned} \tag{4.125}$$

$$\begin{aligned}\mathrm{SOP}_1^{(i,k)} &= 1 - \frac{\lambda_{S_iR}^{L_R m_{S_iR}}\gamma\overline{\gamma}_I^{-L_R m_{S_iR}}}{\Gamma\left(L_{E_k} m_{S_iE_k}\right)\Gamma(L_R m_{S_iR})\Gamma\left(m_{S_iP}\right)} \\ &\times \sum_{l=0}^{L_R m_{S_iR}-1} \frac{\Upsilon_l^{(i)}\overline{\gamma}_I^{l+1}}{\left(\gamma\lambda_{S_iR}\right)^{l+1}} G_{2,2}^{1,2}\left(\frac{\lambda_{S_iE_k}}{\lambda_{S_iR}\gamma}\middle| \begin{matrix} -l, 1; - \\ L_{E_k} m_{S_iE_k}; 0 \end{matrix}\right) \\ &\times \left[\frac{\gamma\left(m_{S_iP}, \varphi_{S_i}\right) e^{-\frac{\sigma_i \xi_{S_iR}}{\overline{\gamma}_I}}}{\sigma_i^{-L_R m_{S_iR}+l+1}} + \frac{\lambda_{S_iP}^{m_{S_iP}}\Gamma\left(m_{S_iP} + L_R m_{S_iR} - l - 1, \varphi_{S_i} + \frac{\sigma_i \xi_{S_iR}}{\overline{\gamma}_I}\right)}{\left(\lambda_{S_iP} + \frac{\xi_{S_iR}}{\overline{\gamma}_I}\right)^{m_{S_iP}+L_R m_{S_iR}-l-1}}\right]. \end{aligned} \tag{4.126}$$

and

$$\begin{aligned}\mathrm{SOP}_2^{(k)} &= 1 - \frac{\lambda_{RD}^{L_D m_{RD}}\overline{\gamma}_I^{-L_D m_{RD}}}{\Gamma\left(L_{E_k} m_{RE_k}\right)\Gamma(L_D m_{RD})\Gamma(m_{RP})} \sum_{j=0}^{L_D m_{RD}-1} \frac{\mathcal{B}_j \overline{\gamma}_I^{j+1}}{\lambda_{RD}^{j+1}} G_{2,2}^{1,2}\left(\frac{\lambda_{RE_k}}{\lambda_{RD}\gamma}\middle| \begin{matrix} -j, 1; - \\ L_{E_k} m_{RE_k}; 0 \end{matrix}\right) \\ &\times \left[\frac{e^{-\frac{\delta \xi_{RD}}{\overline{\gamma}_I}}\gamma\left(m_{RP}, \varphi_R\right)}{\delta^{-L_D m_{RD}+j+1}} + \frac{\lambda_{RP}^{m_{RP}}\Gamma\left(L_D m_{RD} + m_{RP} - j - 1, \varphi_R + \frac{\delta \xi_{RD}}{\overline{\gamma}_I}\right)}{\left(\frac{\xi_{RD}}{\overline{\gamma}_I} + \lambda_{RP}\right)^{L_D m_{RD}+m_{RP}-j-1}}\right]. \end{aligned} \tag{4.127}$$

where $\varpi_i^{(k)} = \gamma\lambda_{S_iR} + \lambda_{S_iE_k}$, $\sigma_i = \overline{\gamma}_I/\overline{\gamma}_{S_i}$, $\delta = \overline{\gamma}_I/\overline{\gamma}_R$, $\gamma = 2^{R_S}$, $\theta_i^{(k,J)} = \lambda_{S_JE_k}/\left(\overline{\gamma}_{S_J}\lambda_{S_iE_k}\right)$, $\varphi_J = \lambda_{S_JP}\overline{\gamma}_I/\overline{\gamma}_{S_J}$, $\varsigma_i^{(k,J)} = \lambda_{S_JE_k}/\left(\lambda_{S_JP}\lambda_{S_iE_k}\right)$, $\varphi_R = \lambda_{RP}\overline{\gamma}_I/\overline{\gamma}_R$, $\varphi_{S_i} = \lambda_{S_iP}\overline{\gamma}_P/\overline{\gamma}_{S_i}$,

$$\mathcal{M}_1^{(h,l)}(z) = G_{2,3}^{2,2}\left(z\middle| \begin{matrix} -h, 1; - \\ \mu_{i,k}^{(h,l)}, L_{E_k} m_{S_JE_k}; 0 \end{matrix}\right), \tag{4.128}$$

$$\mathcal{M}_2^{(h,l)}(z) = G_{3,3}^{2,3}\left(z \left| \begin{array}{c} (1-m_{S_JP},\varphi_J),(1,0),(-h,0);- \\ (L_{E_k}m_{S_JE_k},0),\left(\mu_{i,k}^{(h,l)},0\right);(0,0) \end{array} \right.\right), \tag{4.129}$$

$$\mu_{i,k}^{(h,l)} = L_{E_k}m_{S_iE_k} - h + l, \tag{4.130}$$

$$\xi_v = \lambda_v(\gamma-1); v = \{S_iR, RD\}, \tag{4.131}$$

$$\mathcal{M}_3(z) = G_{2,2}^{2,1}\left(z \left| \begin{array}{c} (1-m_{S_iP},\varphi_{S_i});(1,0) \\ (0,0),(L_Rm_{S_iR},0);- \end{array} \right.\right), \tag{4.132}$$

$$\Omega_h^{(i,k)} = \binom{L_{E_k}m_{S_iE_k}-1}{h}\lambda_{S_iE_k}^{L_{E_k}m_{S_iE_k}-h-1}, \tag{4.133}$$

$$\alpha_i^{(k,J)} = \frac{\beta_k^{(J)}\lambda_{S_iR}^{L_Rm_{S_iR}}}{\Gamma(L_{E_k}m_{S_iE_k})\Gamma(L_Rm_{S_iR})}, \tag{4.134}$$

$$\beta_k^{(J)} = \frac{1}{\Gamma(L_{E_k}m_{S_JE_k})\Gamma(m_{S_JP})}, \tag{4.135}$$

$$\Upsilon_l^{(i)} = \binom{L_Rm_{S_iR}-1}{l}\gamma^l(\gamma-1)^{L_Rm_{S_iR}-1-l}, \tag{4.136}$$

$$\mathcal{B}_{n_1} = \binom{L_Dm_{RD}-1}{n_1}(\gamma-1)^{L_Dm_{RD}-1-n_1}. \tag{4.137}$$

Proof.

- **Expression of SOP at the first hop**

The SOP at the first hop in the absence and presence of a friendly jammer is given, respectively, by

$$\mathrm{SOP}_1^{(i,k)} = 1 - \gamma\int_{x=0}^{\infty} f_{g_{S_iP}}(x)\Xi_2^{(i,k)}(x)\,dx, \tag{4.138}$$

and

$$\mathrm{SOP}_1^{(i,k,J)} = 1 - \gamma\int_{x=0}^{\infty} f_{g_{S_iP}}(x)\Xi_1^{(i,k,J)}(x)\,dx, \tag{4.139}$$

where (4.138) and (4.139) hold by using integration by parts on [38, Eq. (33)] , with

$$\Xi_1^{(i,k,J)}(x) = \int_0^{\infty} f_{\gamma_R^{(i)}|g_{S_iP}=x}(\gamma y+\gamma-1)\,F_{\gamma_{1E}^{(i,k,J)}|g_{S_iP}=x}(y)dy, \tag{4.140}$$

and

$$\Xi_2^{(i,k)}(x) = \int_0^\infty f_{\gamma_R^{(i)}|g_{S_iP}=x}(\gamma y + \gamma - 1)\, F_{\gamma_{1E}^{(i,k)}|g_{S_iP}=x}(y)dy, \tag{4.141}$$

and γ is being defined in Theorem 4.4.1.

The CDF of $\gamma_R^{(i)}$ for a given g_{S_iP} can be expressed as

$$\begin{aligned} F_{\gamma_R^{(i)}|g_{S_iP}=x}(z) &= \Pr\left(\min\left(\overline{\gamma}_{S_i}, \frac{\overline{\gamma}_I}{x}\right)\mathcal{E}_{S_iR} \le z\right) \\ &= F_{\mathcal{E}_{S_iR}}\left(\frac{z}{\Phi(x)}\right), \end{aligned} \tag{4.142}$$

where $\mathcal{E}_{S_iR} = \sum_{u=1}^{L_R} g_{S_iR_u}$, $\Phi(x) = \overline{\gamma}_{S_i}$ for $x \le \overline{\gamma}_I/\overline{\gamma}_{S_i}$ and $\Phi(x) = \overline{\gamma}_I/x$ for $x > \overline{\gamma}_I/\overline{\gamma}_{S_i}$.

SOP at the first hop with the absence of a jamming signal

The conditional CDF of $\gamma_{1E}^{(i,k)}$ can be expressed as

$$\begin{aligned} F_{\gamma_{1E}^{(i,k)}|g_{S_iP}=x}(y) &= \Pr\left(\min\left(\overline{\gamma}_{S_i}, \frac{\overline{\gamma}_I}{x}\right)\mathcal{E}_{S_iE_k} \le y\right) \\ &= F_{\mathcal{E}_{S_iE_k}}\left(\frac{y}{\Phi(x)}\right). \end{aligned} \tag{4.143}$$

where $\mathcal{E}_{S_iE_k} = \sum_{u=1}^{L_R} g_{S_iE_k^{(u)}}$.

It is worth mentioning that for i.i.d Nakagami-m channels, $\mathcal{E}_{S_iR}$ and $\mathcal{E}_{S_iE_k}$ are Gamma distributed with shape and scale parameters $L_R m_{S_iR}$ and λ_{S_iR}, $L_{E_k} m_{S_iE_k}$ and $\lambda_{S_iE_k}$, respectively.

Using Eqs. (06.06.26.0004.01) and (07.34.21.0088.01) of [71], and substituting (4.142) and (4.143) into (4.141)yields

$$\begin{aligned} \Xi_2^{(i,k)}(x) = &\frac{\lambda_{S_iR}^{L_R m_{S_iR}} e^{-\frac{\xi_{S_iR}}{\Phi(x)}}}{\Phi^{L_R m_{S_iR}}(x)\,\Gamma(L_{E_k} m_{S_iE_k})\,\Gamma(L_R m_{S_iR})} \sum_{l=0}^{L_R m_{S_iR}-1} \Upsilon_l^{(i)} \\ &\times \left(\frac{\lambda_{S_iR}\gamma}{\Phi(x)}\right)^{-l-1} G_{2,2}^{1,2}\left(\frac{\lambda_{S_iE_k}}{\lambda_{S_iR}\gamma}\middle| \begin{matrix} -l, 1; - \\ L_{E_k} m_{S_iE_k}; 0 \end{matrix}\right), \end{aligned} \tag{4.144}$$

where $\Upsilon_l^{(i)}$ is defined in (4.136).

Now, replacing (4.144) into (4.138), one can obtain

$$\mathrm{SOP}_1^{(i,k)} = 1 - \frac{\lambda_{S_iR}^{L_R m_{S_iR}} \gamma}{\Gamma\left(L_{E_k} m_{S_iE_k}\right) \Gamma(L_R m_{S_iR})} \sum_{l=0}^{L_R m_{S_iR}-1} \frac{\Upsilon_l^{(i)}}{\left(\gamma \lambda_{S_iR}\right)^{l+1}} \mathcal{H}_1 G_{2,2}^{1,2}\left(\frac{\lambda_{S_iE_k}}{\lambda_{S_iR}\gamma} \middle| \begin{matrix} -l, 1; - \\ L_{E_k} m_{S_iE_k}; 0 \end{matrix} \right), \tag{4.145}$$

where

$$\begin{aligned} \mathcal{H}_1 &= \int_0^\infty \frac{f_{g_{S_iP}}(x) e^{-\frac{\xi_{S_iR}}{\Phi(x)}}}{\Phi^{L_R m_{S_iR}-l-1}(x)} dx \qquad (4.146) \\ &\overset{(a)}{=} \frac{\overline{\gamma}_I^{-L_R m_{S_iR}+l+1}}{\Gamma\left(m_{S_iP}\right)} \left[\frac{e^{-\frac{\sigma_i \xi_{S_iR}}{\overline{\gamma}_I}}}{\sigma_i^{-L_R m_{S_iR}+l+1}} \gamma\left(m_{S_iP}, \varphi_{S_i}\right) + \frac{\lambda_{S_iP}^{m_{S_iP}} \Gamma\left(L_R m_{S_iR} + m_{S_iP} - l - 1, \varphi_{S_i} + \frac{\xi_{S_iR}}{\overline{\gamma}_{S_i}}\right)}{\left(\lambda_{S_iP} + \frac{\xi_{S_iR}}{\overline{\gamma}_I}\right)^{L_R m_{S_iR} + m_{S_iP} - l - 1}} \right], \end{aligned}$$

where step (a) is obtained by replacing $\Phi(x)$ by its values, and performing some algebraic manipulations.

Now, incorporating (4.146) into (4.145), (4.126) is attained.

SOP at the first hop in the presence of a jamming signal

In the presence of a friendly jammer, the CDF of $\gamma_{1E}^{(i,k,J)}$ for a given g_{S_iP} is given by

$$F_{\gamma_{1E}^{(i,k,J)}|g_{S_iP}=x}(y) \overset{(a)}{=} \int_0^\infty F_{\mathcal{E}_{S_iE_k}}\left(\frac{y(t+1)}{\Phi(x)}\right) f_{W_k^{(J)}}(t)\, dt \tag{4.147a}$$

$$\overset{(b)}{=} 1 - \Psi_i^{(k)}(y) \sum_{h=0}^{L_{E_k} m_{S_iE_k}-1} \binom{L_{E_k} m_{S_iE_k} - 1}{h} \mathcal{V}^{(h)}(y), \tag{4.147b}$$

where $W_k^{(J)} = \min\left(\overline{\gamma}_{S_J}, \frac{\overline{\gamma}_P}{g_{S_JP}}\right) \mathcal{E}_{S_JE_k}$, $\mathcal{E}_{S_JE_k} = \sum_{u=1}^{L_{E_k}} g_{S_JE_k^{(u)}}$, $\mathcal{V}^{(h)}(y) = \int_0^\infty t^h e^{-\frac{y\lambda_{S_iE_k}}{\Phi(x)}t} F_{W_k^{(J)}}(t)\, dt$, $\Psi_i^{(k)}(y) = \frac{y f_{S_iE_k}\left(\frac{y}{\Phi(x)}\right)}{\Phi(x)}$. Here step (4.147a) holds using the definition (4.116), while step (4.147b) is obtained by using integration by parts alongside the Binomial formula for a positive integer $L_{E_k} m_{S_iE_k}$. Importantly, the derivation of the CDF of $\gamma_{1E}^{(i,k,J)}$ requires the one of $W_k^{(J)}$, given as

$$\begin{aligned} F_{W_k^{(J)}}(t) &= \Pr\left(\mathcal{E}_{S_JE_k} \le \frac{t}{\overline{\gamma}_{S_J}}, \frac{\overline{\gamma}_I}{g_{S_JP}} \ge \overline{\gamma}_{S_J}\right) + \Pr\left(\frac{\mathcal{E}_{S_JE_k}}{g_{S_JP}} \le \frac{t}{\overline{\gamma}_I}, \frac{\overline{\gamma}_I}{g_{S_JP}} \le \overline{\gamma}_{S_J}\right) \\ &= F_{\mathcal{E}_{S_JE_k}}\left(\frac{t}{\overline{\gamma}_{S_J}}\right) F_{g_{S_JP}}\left(\frac{\overline{\gamma}_I}{\overline{\gamma}_{S_J}}\right) + \mathcal{I}_1^{(k,J)}. \end{aligned} \tag{4.148}$$

where

$$\begin{aligned}\mathcal{I}_1^{(k,J)} &= \int_{\frac{\overline{\gamma}_I}{\overline{\gamma}_{S_J}}}^{\infty} f_{g_{S_JP}}(\nu)\, F_{\mathcal{E}_{S_JE_k}}\left(\frac{t}{\overline{\gamma}_I}\nu\right) d\nu \\ &\overset{(a)}{=} \frac{1}{2\pi j}\int_{\mathcal{L}_1} \frac{\Gamma(m_{S_JP}-s,\varphi_J)\,\Gamma(L_{E_k}m_{S_JE_k}+s)\,\Gamma(-s)}{\Gamma(1-s)\,(\kappa t)^s\left(\beta_k^{(J)}\right)^{-1}} ds \\ &= \beta_k^{(J)}\Delta_k^{(J)}(t),\end{aligned} \tag{4.149}$$

where $\mathcal{L}_1$ is a vertical line of integration chosen such as to separate the left poles of the above integrand function from the right ones, $\Delta_k^{(J)}(t) = G_{2,2}^{1,2}\left(\kappa t \middle| \begin{matrix}(1-m_{S_JP},\varphi_J),(1,0);-\\ (L_{E_k}m_{S_JE_k},0);(0,0)\end{matrix}\right)$, $\kappa = \lambda_{S_JE_k}/\lambda_{S_JP}\overline{\gamma}_I$, φ_J , and $\beta_k^{(J)}$ are defined in Theorem 4.4.1 and (4.135), respectively. Step (a) holds using [71, Eq. (06.06.26.0004.01)] alongside (4.102) and (4.103). As mentioned above, $\mathcal{E}_{S_JE_k}$ is also Gamma distributed with parameters $L_{E_k}m_{S_JE_k}$ and $\lambda_{S_JE_k}$.

Substituting (4.149) into (4.148), we get

$$F_{W_k^{(J)}}(t) = \beta_k^{(J)}\left[\ \gamma\left(L_{E_k}m_{S_JE_k}, \tfrac{\lambda_{S_JE_k}}{\overline{\gamma}_{S_J}}t\right) \times \gamma(m_{S_JP},\varphi_J) + \Delta_k^{(J)}(t)\ \right]. \tag{4.150}$$

Now, it remains to compute $\mathcal{V}^{(h)}(y)$ so as to evaluate (4.147b). Using (4.150), yields

$$\mathcal{V}^{(h)}(y) = \beta_k^{(J)}\left(\gamma(m_{S_JP},\varphi_J)\,\mathcal{T}_1^{(h)} + \mathcal{T}_2^{(h)}\right), \tag{4.151}$$

where

$$\begin{aligned}\mathcal{T}_1^{(h)} &= \int_0^{\infty} t^h e^{-\frac{y\lambda_{S_iE_k}}{\Phi(x)}t}\gamma\left(L_{E_k}m_{S_JE_k}, \frac{\lambda_{S_JE_k}}{\overline{\gamma}_{S_J}}t\right) dt \\ &\overset{(a)}{=} \int_0^{\infty} t^h e^{-\frac{y\lambda_{S_iE_k}}{\Phi(x)}t} G_{1,2}^{1,1}\left(\frac{\lambda_{S_JE_k}}{\overline{\gamma}_{S_J}}t \middle| \begin{matrix}1;-\\ L_{E_k}m_{S_JE_k};0\end{matrix}\right) dt \\ &\overset{(b)}{=} \left(\frac{\Phi(x)}{\lambda_{S_iE_k}y}\right)^{h+1}\Theta_1^{(h)}(y),\end{aligned} \tag{4.152}$$

with $\Theta_1^{(h)}(y) = G_{2,2}^{1,2}\left(\frac{\theta_i^{(k,J)}\Phi(x)}{y} \middle| \begin{matrix}-h,1;-\\ L_{E_k}m_{S_JE_k};0\end{matrix}\right)$ and $\theta_i^{(k,J)}$ is being defined in Theorem 4.4.1. The equality (a) and (b) follow by using Eqs. (06.06.26.0004.01) and (07.34.21.0088.01) of [71],

respectively.

On the other hand, the term $\mathcal{T}_2^{(h)}$ can be expressed as

$$\begin{aligned}\mathcal{T}_2^{(h)} &= \int_0^\infty t^h e^{-\frac{y\lambda_{S_iE_k}}{\Phi(x)}t}\Delta_k^{(J)}(t)\,dt \qquad (4.153)\\ &= \frac{1}{2\pi j}\left(\frac{\Phi(x)}{\lambda_{S_iE_k}y}\right)^{h+1}\int_{\mathcal{L}_2}\frac{\Gamma(1+h-s)\,\Gamma(-s)\,\Gamma(m_{S_JP}-s,\varphi_J)\,\Gamma(L_{E_k}m_{S_JE_k}+s)}{\Gamma(1-s)}\left(\frac{\eta}{y}\right)^{-s}ds\\ &= \left(\frac{\Phi(x)}{\lambda_{S_iE_k}y}\right)^{h+1}\Theta_2^{(h)}(y),\end{aligned}$$

where $\Theta_2^{(h)}(y) = G_{3,2}^{1,3}\left(\frac{\eta}{y}\,\middle|\,\begin{matrix}(\zeta_J,\varphi_J),(1,0),(-h,0);-\\ (L_{E_k}m_{S_JE_k},0);(0,0)\end{matrix}\right)$, $\eta = \frac{\varsigma_i^{(k,J)}\Phi(x)}{\overline{\gamma}_I}$, $\zeta_J = 1-m_{S_JP}$, and $\varsigma_i^{(k,J)}$ is being defined in Theorem 4.4.1.

Finally, the conditional CDF of $\gamma_{1E}^{(i,k,J)}$ can be expressed by substituting (4.152) and (4.153) into (4.151) and then replacing it into (4.147b), yields

$$F_{\gamma_{1E}^{(i,k,J)}|g_{S_iP}=x}(y) = 1-\Psi_i^{(k)}(y)\,\beta_k^{(J)}\sum_{h=0}^{L_{E_k}m_{S_iE_k}-1}\frac{\binom{L_{E_k}m_{S_iE_k}-1}{h}\Phi^{h+1}(x)}{(\lambda_{S_iE_k}y)^{h+1}}\left[\gamma(m_{S_JP},\varphi_J)\,\Theta_1^{(h)}(y)+\Theta_2^{(h)}(y)\right]. \qquad (4.154)$$

Now, the remaining last previous step in this proof consists of computing $\Xi_1^{(i,k,J)}(x)$. Indeed, by differentiating (4.142) and using (4.102) alongside with (4.154), (4.140) can be rewritten for a positive integer $L_Rm_{S_iR}$ as

$$\begin{aligned}\Xi_1^{(i,k,J)}(x) &= \frac{\Gamma\left(L_Rm_{S_iR},\frac{\xi_{S_iR}}{\Phi(x)}\right)}{\gamma\Gamma(L_Rm_{S_iR})}\alpha_i^{(k,J)}\sum_{h=0}^{L_{E_k}m_{S_iE_k}-1}\frac{\Omega_h^{(i,k)}e^{-\frac{\xi_{S_iR}}{\Phi(x)}}}{(\Phi(x))^{L_{E_k}m_{S_iE_k}+L_Rm_{S_iR}-h-2}} \qquad (4.155)\\ &\times\sum_{l=0}^{L_Rm_{S_iR}-1}\Upsilon_l^{(i)}\left[\gamma(m_{S_JP},\varphi_J)\,\mathcal{U}_1^{(h,l)}+\mathcal{U}_2^{(h,l)}\right],\end{aligned}$$

where ξ_{S_iR}, $\Omega_h^{(i,k)}$, $\alpha_i^{(k,J)}$, and $\Upsilon_l^{(i)}$ are defined in (4.131), (4.133), (4.134), (4.136), respectively, and

$$\mathcal{U}_a^{(h,l)} = \int_0^\infty y^{L_{E_k}m_{S_iE_k}+l-h-1}e^{-\frac{\varpi_i^{(k)}}{\Phi(x)}y}\Theta_a^{(h)}(y)\,dy,\ a=\{1,2\}, \qquad (4.156)$$

with $\varpi_i^{(k)}$ is being defined in Theorem 4.4.1.

The two above terms can be expressed as

$$\mathcal{U}_1^{(h,l)} = \left(\frac{\Phi\left(x\right)}{\varpi_i^{(k)}}\right)^{l+L_{E_k}m_{S_iE_k}-h} \mathcal{M}_1^{(h,l)}\left(\varpi_i^{(k)}\theta_i^{(k,J)}\right), \tag{4.157}$$

and

$$\begin{aligned}\mathcal{U}_2^{(h,l)} &= \left(\frac{\Phi\left(x\right)}{\varpi_i^{(k)}}\right)^{L_{E_k}m_{S_iE_k}+l-h} \frac{1}{2\pi j}\int_{\mathcal{L}_3} \frac{\Gamma\left(L_{E_k}m_{S_iE_k}+l-h+s\right)\Gamma\left(m_{S_JP}-s,\varphi_J\right)}{\Gamma\left(1-s\right)} \\ &\times \Gamma\left(L_{E_k}m_{S_JE_k}+s\right)\Gamma\left(-s\right)\Gamma\left(1+h-s\right)\left(\frac{\varsigma_i^{(k,J)}\varpi_i^{(k)}}{\overline{\gamma}_I}\right)^{-s} ds \\ &= \left(\frac{\Phi\left(x\right)}{\varpi_i^{(k)}}\right)^{L_{E_k}m_{S_iE_k}+l-h} \mathcal{M}_2^{(h,l)}\left(\frac{\varsigma_i^{(k,J)}\varpi_i^{(k)}}{\overline{\gamma}_I}\right),\end{aligned} \tag{4.158}$$

where $\mathcal{M}_1^{(h,l)}\left(.\right)$ and $\mathcal{M}_2^{(h,l)}\left(.\right)$ are defined in (4.128) and (4.250), respectively. Note that (4.157) follows relying on [71, Eq. (07.34.21.0088.01)].

Henceforth, substituting (4.157) and (4.158) into (4.155), yields

$$\begin{aligned}\Xi_1^{(i,k,J)}\left(x\right) &= \frac{\Gamma\left(L_Rm_{S_iR},\frac{\xi_{S_iR}}{\Phi(x)}\right)}{\gamma\Gamma(L_Rm_{S_iR})} - \alpha_i^{(k,J)} \sum_{h=0}^{L_{E_k}m_{S_iE_k}-1} \frac{\Omega_h^{(i,k)}e^{-\frac{\xi_{S_iR}}{\Phi(x)}}}{\left(\Phi\left(x\right)\right)^{L_{E_k}m_{S_iE_k}+L_Rm_{S_iR}-h-2}} \\ &\times \sum_{l=0}^{L_Rm_{S_iR}-1} \Upsilon_l^{(i)}\left(\frac{\Phi\left(x\right)}{\varpi_i^{(k)}}\right)^{L_{E_k}m_{S_iE_k}+l-h} \left[\begin{array}{c}\gamma\left(m_{S_JP},\varphi_J\right)\mathcal{M}_1^{(h,l)}\left(\varpi_i^{(k)}\theta_i^{(k,J)}\right) \\ +\mathcal{M}_2^{(h,l)}\left(\frac{\varsigma_i^{(k,J)}\varpi_i^{(k)}}{\overline{\gamma}_P}\right)\end{array}\right].\end{aligned} \tag{4.159}$$

Now, replacing (4.159) into (4.139), we obtain

$$\begin{aligned}\mathrm{SOP}_1^{(i,k,J)} &= 1 - \frac{\Lambda_1}{\Gamma(L_Rm_{S_iR})} + \gamma\alpha_i^{(k,J)} \sum_{h=0}^{L_{E_k}m_{S_iE_k}-1} \Omega_h^{(i,k)} \sum_{l=0}^{L_Rm_{S_iR}-1} \frac{\Upsilon_l^{(i)}\Lambda_2}{\left(\varpi_i^{(k)}\right)^{l+L_{E_k}m_{S_iE_k}-h}} \\ &\times \left[\gamma\left(m_{S_JP},\varphi_J\right)\mathcal{M}_1^{(h,l)}\left(\varpi_i^{(k)}\theta_i^{(k,J)}\right) + \mathcal{M}_2^{(h,l)}\left(\frac{\varsigma_i^{(k,J)}\varpi_i^{(k)}}{\overline{\gamma}_I}\right)\right],\end{aligned} \tag{4.160}$$

where

$$\begin{aligned}\Lambda_1 &= \int_0^\infty f_{g_{S_iP}}(x)\Gamma\left(L_Rm_{S_iR},\frac{\xi_{S_iR}}{\Phi\left(x\right)}\right)dx \\ &\overset{(a)}{=} \frac{1}{\Gamma\left(m_{S_iP}\right)}\left[\gamma\left(m_{S_iP},\varphi_{S_i}\right)\Gamma\left(L_Rm_{S_iR},\frac{\xi_{S_iR}}{\overline{\gamma}_{S_i}}\right) + \mathcal{M}_3\left(\frac{\xi_{S_iR}}{\lambda_{S_iP}\overline{\gamma}_P}\right)\right],\end{aligned} \tag{4.161}$$

and

$$\Lambda_2 = \int_0^\infty \frac{f_{g_{S_iP}}(x) e^{-\frac{\xi_{S_iR}}{\Phi(x)}}}{(\Phi(x))^{L_R m_{S_iR}-l-1}} dx \tag{4.162}$$
$$= \frac{\gamma(m_{S_iP}, \varphi_{S_i}) e^{-\frac{\xi_{S_iR}}{\overline{\gamma}_{S_i}}}}{\Gamma(m_{S_iP}) \overline{\gamma}_{S_i}^{L_R m_{S_iR}-l-1}} + \frac{\lambda_{S_iP}^{m_{S_iP}} \Gamma\left(m_{S_iP} + L_R m_{S_iR} - l - 1, \varphi_{S_i} + \frac{\xi_{S_iR}}{\overline{\gamma}_{S_i}}\right)}{\Gamma(m_{S_iP}) \overline{\gamma}_I^{L_R m_{S_iR}-l-1} \left(\lambda_{S_iP} + \frac{\xi_{S_iR}}{\overline{\gamma}_P}\right)^{m_{S_iP}+L_R m_{S_iR}-l-1}},$$

with $\mathcal{M}_3(.)$ is defined in (4.132). Equality (a) holds by replacing $\Phi(x)$ by their values along using [71, Eqs. (06.06.26.0005.01), (07.34.21.0088.01)]. By substituting (4.161) and (4.162) into (4.160), (4.125) is attained.

Expression of SOP at the second Hop

In like manner to $\text{SOP}_1^{(i,k)}$, $\text{SOP}_2^{(k)}$ can be expressed as

$$\text{SOP}_2^{(k)} = 1 - \gamma \int_0^\infty f_{g_{RP}}(x) \Xi_3^{(k)}(x) dx, \tag{4.163}$$

with

$$\Xi_3^{(k)}(x) = \int_0^\infty f_{\gamma_D|g_{RP}=x}(\gamma + \gamma y - 1) F_{\gamma_{2E}^{(k)}|g_{RP}=x}(y) dy. \tag{4.164}$$

One can notice from (4.164) that in order to calculate $\text{SOP}_2^{(k)}$, it is necessary to find first the conditional CDFs of γ_D and $\gamma_{2E}^{(k)}$ for a given g_{RP}.

Let's define $Y_{RD} = \sum_{t=1}^{L} g_{RD_t}$. In a similar manner to (4.142), the conditional CDFs of γ_D and $\gamma_{2E}^{(k)}$ are given, respectively, by

$$F_{\gamma_D|g_{RP}=x}(z) = F_{Y_{RD}}\left(\frac{z}{\mathcal{D}(x)}\right), \tag{4.165}$$

and

$$F_{\gamma_{2E}^{(k)}|g_{RP}=x}(y) = F_{\mathcal{E}_{RE_k}}\left(\frac{y}{\mathcal{D}(x)}\right), \tag{4.166}$$

where $\mathcal{E}_{RE_k} = \sum_{u=1}^{L_{E_k}} g_{RE_k^{(u)}}$, $\mathcal{D}(x) = \overline{\gamma}_R$ for $x \leq \overline{\gamma}_I/\overline{\gamma}_R$ and $\mathcal{D}(x) = \overline{\gamma}_I/x$ for $x > \overline{\gamma}_I/\overline{\gamma}_R$. It follows, in a similar manner to $\mathcal{E}_{S_iR}$, that $\mathcal{E}_{RE_k}$ is also Gamma distributed with parameters $L_{E_k} m_{RE_k}$ and λ_{RE_k}.

It is worthwhile that Y_{RD} is Gamma distributed for i.i.d Nakagami-m fading channels with shape and scale parameters $L_D m_{RD}$ and λ_{RD}, respectively. That is

$$\Xi_3^{(k)}(x) \overset{(a)}{=} \frac{\lambda_{RD}^{L_D m_{RD}} e^{-\frac{\xi_{RD}}{\mathcal{D}(x)}}}{\Gamma(L_D m_{RD})\Gamma\left(L_{E_k} m_{RE_k}\right)\left(\mathcal{D}(x)\right)^{L_D m_{RD}-1}} \times \sum_{n_1=0}^{L_D m_{RD}-1} \mathcal{B}_{n_1} \gamma^{n_1} \int_0^{\infty} y^{n_1} e^{-\frac{\lambda_{RD}\gamma}{\mathcal{D}(x)} y} \gamma\left(L_{E_k} m_{RE_k}, \frac{\lambda_{RE_k}}{\mathcal{D}(x)} y\right)$$
$$\overset{(b)}{=} \frac{\lambda_{RD}^{L_D m_{RD}} e^{-\frac{\xi_{RD}}{\mathcal{D}(x)}}}{\gamma\Gamma(L_D m_{RD})\Gamma\left(L_{E_k} m_{RE_k}\right)\mathcal{D}^{L_D m_{RD}-1}(x)} \times \sum_{n_1=0}^{L_D m_{RD}-1} \mathcal{B}_{n_1} \left(\frac{\mathcal{D}(x)}{\lambda_{RD}}\right)^{n_1+1} G_{2,2}^{1,2}\left(\frac{\lambda_{RE_k}}{\lambda_{RD}\gamma}\middle| \begin{matrix} -n_1, 1; - \\ L_{E_k} m_{RE_k}; 0 \end{matrix}\right), \tag{4.167}$$

where $\mathcal{B}_{n_1}$ is defined in (4.137). Note that step (a) holds by substituting (4.165) and (4.166) into (4.164), while equality (b) follows by using [71, Eqs. (06.06.26.0004.01), (07.34.21.0088.01)].

Substituting (4.167) into (4.163), yields

$$\mathrm{SOP}_2^{(k)} = 1 - \frac{\lambda_{RD}^{L_D m_{RD}}}{\Gamma\left(L_{E_k} m_{RE_k}\right)\Gamma(L_D m_{RD})} \sum_{n_1=0}^{L_D m_{RD}-1} \frac{\mathcal{B}_{n_1}}{\lambda_{RD}^{n_1+1}} \mathcal{J}_{n_1} G_{2,2}^{1,2}\left(\frac{\lambda_{RE_k}}{\lambda_{RD}\gamma}\middle| \begin{matrix} -n_1, 1; - \\ L_{E_k} m_{RE_k}; 0 \end{matrix}\right), \tag{4.168}$$

where

$$\mathcal{J}_{n_1} = \int_0^{\infty} f_{g_{RP}}(x)\left(\mathcal{D}(x)\right)^{-L_D m_{RD}+n_1+1} e^{-\frac{\xi_{RD}}{\mathcal{D}(x)}} dx \tag{4.169}$$
$$\overset{(a)}{=} \frac{1}{\Gamma(m_{RP})}\left[\frac{e^{-\frac{\xi_{RD}}{\overline{\gamma}_R}}\gamma\left(m_{RP}, \varphi_R\right)}{\overline{\gamma}_R^{L_D m_{RD}-n_1-1}} + \frac{\lambda_{RP}^{m_{RP}}\Gamma\left(\upsilon_{n_1}, \varphi_R + \frac{\xi_{RD}}{\overline{\gamma}_R}\right)}{\overline{\gamma}_I^{L_D m_{RD}-n_1-1}\left(\frac{\xi_{RD}}{\overline{\gamma}_I} + \lambda_{RP}\right)^{\upsilon_{n_1}}}\right],$$

where $\upsilon_{n_1} = L_D m_{RD} + m_{RP} - n_1 - 1$, φ_R is defined in Theorem 4.4.1. Here step (a) is obtained by replacing $\mathcal{D}(x)$ by its values and using (4.102) alongside with Eqs. (3.381.1) and (3.381.3) of [67].

By considering $\frac{\overline{\gamma}_I}{\overline{\gamma}_R} = \delta$ and substituting (4.169) into (4.168), one can obtain (4.127) which concludes the proof of Theorem 4.4.1. ■

Asymptotic expression for the SOP

In this section, we provide an asymptotic analysis of the derived closed-form expressions of the SOP. The expressions (4.125)-(4.127) can be approximated for high SNR regime by considering

$\overline{\gamma}_P \to \infty$.

Theorem 4.4.2. *The asymptotic expression of the* SOP *in the absence of a jammer is given by*

$$SOP^{(i)} \sim 1-\prod_{k=1}^{M}\mathcal{A}_{RE_k,RD,D}\left(1\right)\mathcal{A}_{S_iE_k,S_iR,R}\left(1\right)-\frac{1}{\overline{\gamma}_I}\sum_{k=1}^{M}\prod_{\substack{j=1\\j\neq k}}^{M}\mathcal{A}_{RE_j,RD,D}\left(1\right)\mathcal{A}_{S_iE_j,S_iR,R}\left(1\right)$$
$$\times\left(\mathcal{A}_{RE_k,RD,D}\left(1\right)\mathcal{A}_{S_iE_k,S_iR,S_i,R}+\mathcal{A}_{S_iE_k,S_iR,R}\left(1\right)\mathcal{A}_{RE_k,RD,R,D}\right), \tag{4.170}$$

While the asymptotic expressions of the SOP *in the presence of a jamming signal is expressed depending on various cases as follows*

- $L_R m_{S_iR} < L_{E_k} m_{S_J E_k}$

$$SOP^{(i,k,J)} \sim 1-\prod_{k=1}^{M}\mathcal{A}_{RE_k,RD,D}\left(1\right)-\frac{\sum_{k=1}^{M}\prod_{\substack{j=1\\j\neq k}}^{M}\mathcal{A}_{RE_j,RD,D}\left(1\right)}{\overline{\gamma}_I}\mathcal{A}_{RE_k,RD,R,D}\left(1-\mathcal{P}\left(S_iR\right)\mathcal{C}_1^{(i,k,J)}\right), \tag{4.171}$$

- $L_R m_{S_iR} > L_{E_k} m_{S_J E_k}$

$$SOP^{(i,k,J)} \sim 1-\prod_{k=1}^{M}\mathcal{A}_{RE_k,RD,D}\left(1\right)-\frac{\sum_{k=1}^{M}\prod_{\substack{j=1\\j\neq k}}^{M}\mathcal{A}_{RE_j,RD,D}\left(1\right)}{\overline{\gamma}_I}\mathcal{A}_{RE_k,RD,R,D}\left(1-\mathcal{P}\left(S_JE_k\right)\mathcal{C}_2^{(i,k,J)}\right), \tag{4.172}$$

- $L_R m_{S_iR} = L_{E_k} m_{S_J E_k} = 1$

$$SOP^{(i,J)} \sim 1-\prod_{k=1}^{M}\mathcal{A}_{RE_k,RD,D}\left(1\right)+\frac{\log\left(\overline{\gamma}_I\right)}{\overline{\gamma}_I}\sum_{k=1}^{M}\prod_{\substack{j=1\\j\neq k}}^{M}\mathcal{A}_{RE_j,RD,D}\left(1\right)\mathcal{A}_{RE_k,RD,D}\left(1\right)\mathcal{C}_3^{(i,k,J)}. \tag{4.173}$$

- $L_R m_{S_iR} = L_{E_k} m_{S_J E_k}$ *and* $L_{E_k} m_{S_J E_k} > 1$

$$SOP^{(i,J)} \sim 1-\prod_{k=1}^{M}\mathcal{A}_{RE_k,RD,D}\left(1\right)-\frac{1}{\overline{\gamma}_I}\sum_{k=1}^{M}\prod_{\substack{j=1\\j\neq k}}^{M}\mathcal{A}_{RE_j,RD,D}\left(1\right)\mathcal{A}_{RE_k,RD,R,D}, \tag{4.174}$$

where $\mathcal{P}\left(q\right)=1-sgn\left(L_v m_q-1\right)$, $q=\{S_iR, S_JE_k\}$, *sgn stands for sign function,*

$$\mathcal{A}_{e,c,v}\left(y\right)=\frac{1}{\Gamma\left(L_v m_e\right)\Gamma(m_c)}G_{2,2}^{1,2}\left(\frac{\lambda_e}{\lambda_c\gamma}\middle|\begin{matrix}-L_v m_c+y,1;-\\ L_v m_e;0\end{matrix}\right), e=\{S_iE_k, RE_k\}, \tag{4.175}$$

$$c=\{S_iR, RD\}, y=\{1,2\}, v=\{R,D\}$$

$$\mathcal{A}_{e,c,u,v} = \left\{ \begin{array}{c} \frac{\lambda_c(L_v m_c - 1)\mathcal{A}_{e,c,v}(2)}{\Gamma(m_{uP})} \left[\delta\gamma\left(m_{uP}, \varphi_u\right) + \frac{\Gamma(m_{uP}+1,\varphi_u)}{\lambda_{uP}}\right] \\ -\frac{\xi_c \mathcal{A}_{e,c,v}(1)}{\Gamma(m_{uP})} \left[\delta\left(\gamma\left(m_{uP}, \varphi_u\right) + \varphi_R^{m_{uP}-1} e^{-\varphi_u}\right) + \frac{m_{uP}}{\lambda_{uP}} \Gamma\left(m_{uP}, \varphi_u\right)\right] \end{array} \right\}, \tag{4.176}$$

$$u = \{S_i, R\}, v = \{R, D\}$$

$$\mathcal{C}_1^{(i,k,J)} = \left[\gamma\left(m_{S_iP}, \varphi_{S_i}\right) \sigma_i^{L_R m_{S_iR}} + \frac{\Gamma\left(m_{S_iP} + L_R m_{S_iR}, \varphi_{S_i}\right)}{\lambda_{S_iP}^{L_R m_{S_iR}}}\right] \frac{\xi_{S_iR}^{L_R m_{S_iR}}}{L_R m_{S_iR} \Gamma(L_R m_{S_iR}) \Gamma\left(m_{S_iP}\right)} \tag{4.177}$$

$$+ \gamma \alpha_i^{(k,J)} \sum_{l=0}^{L_R m_{S_iR}-1} \Upsilon_l \left[\frac{\gamma\left(m_{S_iP}, \varphi_{S_i}\right)}{\sigma_i^{-L_R m_{S_iR}+l+1}} + \frac{\Gamma\left(m_{S_iP} + L_R m_{S_iR} - l - 1, \varphi_{S_i}\right)}{\lambda_{S_iP}^{L_R m_{S_iR}-l-1}}\right]$$

$$\times \frac{\Gamma\left(L_{E_k} m_{S_JE_k} - l - 1\right) \Gamma\left(L_{E_k} m_{S_iE_k} + l + 1\right)}{(l+1)\,\Gamma\left(m_{S_iP}\right)}$$

$$\times \left[\gamma\left(m_{S_JP}, \varphi_J\right) \left(\frac{\delta \lambda_{S_JE_k}}{\lambda_{S_iE_k}}\right)^{l+1} + \Gamma\left(m_{S_JP} + l + 1, \varphi_J\right) \left(\varsigma_i^{(k,J)}\right)^{l+1}\right],$$

$$\mathcal{C}_2^{(i,k,J)} \sim \frac{\gamma^{L_R m_{S_iR}} \alpha_i^{(k,J)}}{L_{E_k} m_{S_JE_k}} \left[\begin{array}{c} \gamma\left(m_{S_JP}, \varphi_J\right) \left(\frac{\delta \lambda_{S_JE_k}}{\lambda_{S_iE_k}}\right)^{L_{E_k} m_{S_JE_k}} \\ + \Gamma\left(m_{S_JP} + L_{E_k} m_{S_JE_k}, \varphi_J\right) \left(\varsigma_i^{(k,J)}\right)^{L_{E_k} m_{S_JE_k}} \end{array}\right] \tag{4.178}$$

$$\times \sum_{h=0}^{L_{E_k} m_{S_iE_k}-1} \frac{\Omega_h^{(i,k)} \Gamma\left(L_{E_k} m_{S_iE_k} + L_R m_{S_iR} - L_{E_k} m_{S_JE_k} - h - 1\right) \Gamma\left(L_{E_k} m_{S_JE_k} + h + 1\right)}{\left(\varpi_i^{(k)}\right)^{L_{E_k} m_{S_iE_k} + L_R m_{S_iR} - L_{E_k} m_{S_JE_k} - h - 1}},$$

and

$$\mathcal{C}_3^{(i,k,J)} = \frac{\gamma^{L_R m_{S_iR}} \alpha_i^{(k,J)}}{\varpi^{L_R m_{S_iR} - L_{E_k} m_{S_JE_k}}} \left[\begin{array}{c} \gamma\left(m_{S_JP}, \varphi_J\right) \left(\frac{\delta \lambda_{S_JE_k}}{\lambda_{S_iE_k}}\right)^{L_{E_k} m_{S_JE_k}} \\ + \left(\varsigma_i^{(k,J)}\right)^{L_{E_k} m_{S_JE_k}} \Gamma\left(m_{S_JP} + L_{E_k} m_{S_JE_k}, \varphi_J\right) \end{array}\right] \tag{4.179}$$

$$\times \frac{(-1)^{L_{E_k} m_{S_JE_k} - L_R m_{S_iR}} \Gamma\left(L_{E_k} m_{S_iE_k} + L_{E_k} m_{S_JE_k}\right)}{L_{E_k} m_{S_JE_k}}.$$

Proof.

The residues theorem is used in order to find the approximate expressions of Meijer-G's function given in (4.125).

- **Asymptotic expression of** $SOP_1^{(i,k,J)}$

Case 1: Presence of a jammer

The Meijer-G's functions $\mathcal{M}_1^{(h,l)}(z)$ and $\mathcal{M}_2^{(h,l)}(z)$ defined in (4.128) and (4.250), respectively can be expressed in terms of complex integral as

$$\mathcal{M}_1^{(h,l)}(z) = \frac{1}{2\pi j}\int_{\mathcal{L}_3} \frac{\Gamma\left(L_{E_k} m_{S_J E_k} + s\right)\Gamma(1+h-s)\,\Gamma\left(L_{E_k} m_{S_i E_k} + l - h + s\right)\Gamma(-s)}{\Gamma(1-s)} z^{-s} ds, \tag{4.180}$$

and

$$\begin{aligned}\mathcal{M}_2^{(h,l)}(z) &= \frac{1}{2\pi j}\int_{\mathcal{L}_3} \frac{\Gamma\left(L_{E_k} m_{S_J E_k} + s\right)\Gamma(1+h-s)\,\Gamma\left(L_{E_k} m_{S_i E_k} + l - h + s\right)}{\Gamma(1-s)} \\ &\quad \times \Gamma(-s)\,\Gamma\left(m_{S_J P} - s, \varphi_J\right) z^{-s} ds.\end{aligned} \tag{4.181}$$

It is noteworthy that the conditions of [105, Theorem 1.5] are satisfied. That is, the two above functions can be written as an infinite sum of the poles belonging to the left half plan of $\mathcal{L}_3$. Furthermore, as the upper incomplete gamma function in (4.312) is always finite for $\varphi_J \neq 0$, it follows that the integrand functions of the two above equations have the same poles. Additionally, it is clearly seen that the order of the left poles depends on the values of $L_{E_k} m_{S_J E_k}$, $L_{E_k} m_{S_i E_k}$, h, and l. Owing to this fact, three cases can be distinguished:

- $-L_{E_k} m_{S_J E_k} < -L_{E_k} m_{S_i E_k} - l + h$: In this case, the two integrand functions given in (4.180) and (4.312) admit $-\chi_{h,l,r}$ with $\chi_{h,l,r} = L_{E_k} m_{S_i E_k} + l - h + r$ and $0 \leq r \leq L_{E_k} m_{S_J E_k} - L_{E_k} m_{S_i E_k} - l + h - 1$ as simple poles and $-\varrho_r$ with $\varrho_r = L_{E_k} m_{S_J E_k} + r$ and r natural number as poles of second-order.

- $-L_{E_k} m_{S_J E_k} > -L_{E_k} m_{S_i E_k} - l + h$: Under this condition, the aforementioned integrands have $-\varrho_r$ with $0 \leq r \leq L_{E_k} m_{S_i E_k} - L_{E_k} m_{S_J E_k} + l - h - 1$ as simple poles and $-\chi_{h,l,r}$ where $r \in \mathbb{N}$ as poles of second-order.

- $-L_{E_k} m_{S_J E_k} = -L_{E_k} m_{S_i E_k} - l + h$: Under this assumption, the two integrands admit only poles of second-order at $-\varrho_r$, $r \in \mathbb{N}$.

a. $-L_{E_k} m_{S_J E_k} < -L_{E_k} m_{S_i E_k} - \mathbf{l} + \mathbf{h}$

Relying on [105, Theorem 1.5], $\mathcal{M}_1^{(h,l)}(z)$ can be rewritten as series of residues at the afore-

mentioned poles

$$\mathcal{M}_1^{(h,l)}(z) = \sum_{r=0}^{\varrho_r-\chi_{h,l,r}-1} \lim_{s\to-\chi_{h,l,r}} Q_1(s,z) + \sum_{r=0}^{\infty} \lim_{s\to-\varrho_r} \frac{\partial Q_2(s,z)}{\partial s}, \tag{4.182}$$

where

$$Q_1(s,z) = (\chi_{h,l,r}+s)\,\frac{\Gamma(\chi_{h,l,r}-r+s)\,\Gamma(L_{E_k}m_{S_JE_k}+s)\,\Gamma(-s)\,\Gamma(1+h-s)}{\Gamma(1-s)} z^{-s}, \tag{4.183}$$

and

$$Q_2(s,z) = (\varrho_r+s)^2 \frac{\Gamma(L_{E_k}m_{S_iE_k}+l-h+s)\,\Gamma(L_{E_k}m_{S_JE_k}+s)\,\Gamma(-s)\,\Gamma(1+h-s)}{\Gamma(1-s)} z^{-s}. \tag{4.184}$$

Obviously, the limit of $Q_1(s,z)$ can be expressed as

$$\lim_{s\to-\chi_{h,l,r}} Q_1(s,z) = \frac{(-1)^r\,\Gamma(L_{E_k}m_{S_iE_k}+l+r+1)\,\Gamma(L_{E_k}m_{S_JE_k}-\chi_{h,l,r})}{r!\chi_{h,l,r}} z^{\chi_{h,l,r}}. \tag{4.185}$$

On the other hand, using [71, Eqs. (06.14.06.0026.01) and (06.14.16.0003.01)] the partial derivative of $Q_2(s,z)$ is given by

$$\frac{\partial Q_2(s,z)}{\partial s} = \frac{(s+\varrho_r)^2\Gamma(\chi_{h,l,r}-r+s)\,\Gamma(-s)\,\Gamma(L_{E_k}m_{S_JE_k}+s)\,\Gamma(1+h-s)}{\Gamma(1-s)\,z^s} \mathcal{G}^{(h,l,r)}(z,s), \tag{4.186}$$

where $\mathcal{G}^{(h,l,r)}(z,s) = -\log z + \psi(r+1) + \psi(\varrho_r-\chi_{h,l,r}+r+1) - \frac{1}{s} - \psi(1+h-s)$.

Replacing (4.186) and (4.185) into (4.182), yields

$$\begin{aligned}\mathcal{M}_1^{(h,l)}(z) = &\sum_{r=0}^{\varrho_r-\chi_{h,l,r}-1} \frac{(-1)^r\,\Gamma(L_{E_k}m_{S_JE_k}-\chi_{h,l,r})\,\Gamma(L_{E_k}m_{S_iE_k}+l+r+1)}{r!\chi_{h,l,r}} z^{\chi_{h,l,r}} \\ &+ \sum_{r=0}^{\infty} \frac{(-1)^{\varrho_r-\chi_{h,l,r}}\,\Gamma(h+\varrho_r+1)}{(-L_{E_k}m_{S_iE_k}+\varrho_r-l+h)!k!\varrho_r} z^{\varrho_r}\mathcal{G}^{(h,l,r)}(z,-\varrho_r).\end{aligned} \tag{4.187}$$

In similar manner, $\mathcal{M}_2^{(h,l)}(z)$ can be expressed as

$$\mathcal{M}_2^{(h,l)}(z) = \sum_{k=0}^{\varrho_r-\chi_{h,l,r}-1} \frac{(-1)^r \Gamma\left(L_{E_k} m_{S_i E_k} + l + r + 1\right)}{r! \chi_{h,l,r} z^{-\chi_{h,l,r}}} \Gamma\left(m_{S_J P} + \chi_{h,l,r}, \varphi_J\right) \Gamma\left(L_{E_k} m_{S_J E_k} - \chi_{h,l,r}\right)$$
$$+ \sum_{r=0}^{\infty} \frac{(-1)^{\varrho_r-\chi_{h,l,r}} \Gamma(1+h+\varrho_r)}{(-L_{E_k} m_{S_i E_k} + \varrho_r - l + h)! r! \varrho_r} z^{\varrho_r} \left\{ \begin{array}{c} \left[\mathcal{G}^{(h,l,r)}(z, -\varrho_r) - \log(\varphi_J)\right] \\ \times \Gamma\left(m_{S_J P} + \varrho_r, \varphi_J\right) - \mathcal{V}^{(r)}(\varrho_r) \end{array} \right\}, \tag{4.188}$$

where $\mathcal{V}^{(r)}(\varrho_r) = G_{2,3}^{3,0}\left(\varphi_J \left| \begin{array}{c} -; 1, 1 \\ 0, 0, m_{S_J P} + \varrho_r; - \end{array} \right. \right)$.

Interestingly, one can notice that $\varrho_r > \chi_{h,l,r}$ for $L_{E_k} m_{S_J E_k} > L_{E_k} m_{S_i E_k} + l - h$. Consequently, the second summation in the two above expressions can be ignored as z approaches 0, i.e.,

$$\mathcal{M}_1^{(h,l)}(z) \sim \frac{\Gamma\left(L_{E_k}(m_{S_J E_k} - m_{S_i E_k}) - l + h\right) \Gamma\left(L_{E_k} m_{S_i E_k} + l + 1\right)}{\left(L_{E_k} m_{S_i E_k} + l - h\right)} z^{L_{E_k} m_{S_i E_k} + l - h} \tag{4.189}$$

and

$$\mathcal{M}_2^{(h,l)}(z) \sim \frac{\Gamma\left(L_{E_k} m_{S_i E_k} + l + 1\right) \Gamma\left(L_{E_k}(m_{S_J E_k} - m_{S_i E_k}) - l + h\right)}{\left(L_{E_k} m_{S_i E_k} + l - h\right)}$$
$$\times \Gamma\left(m_{S_J P} + L_{E_k} m_{S_i E_k} + l - h, \varphi_J\right) z^{L_{E_k} m_{S_i E_k} + l - h}. \tag{4.190}$$

b. $-L_{E_k} m_{S_J E_k} > -L_{E_k} m_{S_i E_k} - \mathbf{l} + \mathbf{h}$

Analogously to the previous case, the integrals (4.180) and (4.312) can be computed relied on [105, Theorem 1.5] and [71, Eq. (06.14.16.0003.01)], respectively, as

$$\mathcal{M}_1^{(h,l)}(z) = \sum_{r=0}^{\chi_{h,l,r}-\varrho_r-1} \frac{\Gamma\left(L_{E_k} m_{S_i E_k} + l - h - \varrho_r\right) \Gamma(1+h+\varrho_r)}{r! \varrho_r (-1)^{-r} z^{-\varrho_r}} \tag{4.191}$$
$$+ \sum_{r=0}^{\infty} \frac{(-1)^{\chi_{h,l,r}-\varrho_r} \Gamma(1+h+\chi_{h,l,r})}{(\chi_{h,l,r} - L_{E_k} m_{S_J E_k})! r! \chi_{h,l,r}} z^{\chi_{h,l,r}}$$
$$\times \left\{ \psi(r+1) + \psi(-L_{E_k} m_{S_J E_k} + \chi_{h,l,r} + 1) - \psi(1 + L_{E_k} m_{S_i E_k} + l + r) + \frac{1}{\chi_{h,l,r}} - \log z \right\},$$

and

$$\mathcal{M}_2^{(h,l)}(z) = \sum_{r=0}^{\chi_{h,l,r}-\varrho_r-1} \frac{(-1)^r \Gamma\left(L_{E_k} m_{S_i E_k} + l - h - \varrho_r\right) \Gamma(1+h+\varrho_r)\, z^{\varrho_r} \Gamma\left(m_{S_J P} + \varrho_r, \varphi_J\right)}{r! \varrho_r}$$
$$+ \sum_{r=0}^{\infty} \frac{(-1)^{\chi_{h,l,r}-\varrho_r} \Gamma(1+h+\chi_{h,l,r})}{(\chi_{h,l,r}-\varrho_r)! r! \chi_{h,l,r} z^{-\chi_{h,l,r}}} \left[\mathcal{Z} - \mathcal{V}^{(r)}(\chi_{h,l,r})\right], \tag{4.192}$$

where

$$\mathcal{Z} = \Gamma\left(m_{S_J P} + \chi_{h,l,r}, \varphi_J\right) \begin{bmatrix} -\log z + \psi(r+1) + \psi(-L_{E_k} m_{S_J E_k} + \chi_{h,l,r} + 1) \\ -\psi(L_{E_k} m_{S_i E_k} + l - h + r) - \psi(L_{E_k} m_{S_i E_k} + l + r + 1) \\ +\psi(1+\chi_{h,l,r}) - \log(\varphi_J) \end{bmatrix}. \tag{4.193}$$

One can notice that as $\varrho_r < \chi_{h,l,r}$, $\mathcal{M}_1^{(h,l)}(z)$ and $\mathcal{M}_2^{(h,l)}(z)$ can be approximated when z tends to 0 by

$$\mathcal{M}_1^{(h,l)}(z) \sim \frac{\Gamma\left(L_{E_k} m_{S_i E_k} - L_{E_k} m_{S_J E_k} + l - h\right) \Gamma\left(L_{E_k} m_{S_J E_k} + h + 1\right)}{L_{E_k} m_{S_J E_k}} z^{L_{E_k} m_{S_J E_k}}, \tag{4.194}$$

and

$$\mathcal{M}_2^{(h,l)}(z) \sim \frac{\Gamma\left(L_{E_k} m_{S_J E_k} + h + 1\right) \Gamma\left(m_{S_J P} + L_{E_k} m_{S_J E_k}, \varphi_J\right)}{L_{E_k} m_{S_J E_k}}$$
$$\times \Gamma\left(L_{E_k} m_{S_i E_k} - L_{E_k} m_{S_J E_k} + l - h\right) z^{L_{E_k} m_{S_J E_k}}. \tag{4.195}$$

c. $-L_{E_k} m_{S_J E_k} = -L_{E_k} m_{S_i E_k} - l + h$

For this case, the two complex integrals given in (4.180) and (4.312) can be expressed by performing some algebraic operations as

$$\mathcal{M}_1^{(h,l)}(z) = \sum_{r=0}^{\infty} \frac{(-1)^{\varrho_r - \chi_{h,l,r}} \Gamma(1+h+\varrho_r)}{(-L_{E_k} m_{S_i E_k} + \varrho_r - l + h)! k! \varrho_r} z^{\varrho_r} \mathcal{G}^{(h,l,r)}(z, -\varrho_r), \tag{4.196}$$

and

$$\mathcal{M}_2^{(h,l)}(z) = \sum_{r=0}^{\infty} \frac{(-1)^{\varrho_r - \chi_{h,l,r}} \Gamma(1+h+\varrho_r)}{(\varrho_r - L_{E_k} m_{S_i E_k} - l + h)! r! \varrho_r} z^{\varrho_r}$$
$$\times \left\{ \left[\mathcal{G}^{(h,l,r)}(z) - \log(\varphi_J)\right] \Gamma\left(m_{S_J P} + \varrho_r, \varphi_J\right) - \mathcal{V}^{(r)}(\varrho_r) \right\}. \tag{4.197}$$

Again, $\mathcal{M}_1^{(h,l)}(z)$ and $\mathcal{M}_2^{(h,l)}(z)$ can be approximated as z approaches 0 by

$$\mathcal{M}_1^{(h,l)}(z) \sim \frac{(-1)^{L_{E_k} m_{S_J E_k} - L_R m_{S_i R}+1} \Gamma\left(L_{E_k} m_{S_i E_k} + L_{E_k} m_{S_J E_k}\right) z^{L_{E_k} m_{S_J E_k}} \log z}{L_{E_k} m_{S_J E_k}}, \tag{4.198}$$

and

$$\begin{aligned}\mathcal{M}_2^{(h,l)}(z) \sim & \frac{(-1)^{L_{E_k} m_{S_J E_k} - L_R m_{S_i R}+1} \Gamma\left(L_{E_k}\left(m_{S_i E_k} + m_{S_J E_k}\right)\right)}{L_{E_k} m_{S_J E_k}} \\ & \times \Gamma\left(m_{S_J P} + L_{E_k} m_{S_J E_k}, \varphi_J\right) z^{L_{E_k} m_{S_J E_k}} \log(z).\end{aligned} \tag{4.199}$$

Finally, the Meijer's G-function $\mathcal{M}_3(z)$ defined in (4.132) can be written in terms of complex integral as

$$\mathcal{M}_3(z) = \frac{1}{2\pi j} \int_{\mathcal{L}_4} \frac{\Gamma\left(L_R m_{S_i R} + s\right) \Gamma\left(m_{S_i P} - s, \varphi_{S_i}\right)}{s} z^{-s} ds. \tag{4.200}$$

It is worth mentioning that the conditions of [105] are applied also here. Thus, the above integrand function can be written as an infinite sum of the left poles in $\mathcal{L}_4$. Besides, that integrand admits only poles of the first order at 0 and $-L_R m_{S_i R} - r$, $r \in \mathbb{N}$. That is

$$\begin{aligned}\mathcal{M}_3(z) &= \Gamma\left(L_R m_{S_i R}\right) \Gamma\left(m_{S_i P}, \varphi_{S_i}\right) + \sum_{r=0}^{\infty} \frac{(-1)^{r+1} \Gamma\left(m_{S_i P} + L_R m_{S_i R} + r, \varphi_{S_i}\right)}{r!\left(L_R m_{S_i R} + r\right) z^{-L_R m_{S_i R} - r}} \\ &\overset{(a)}{\sim} \Gamma\left(L_R m_{S_i R}\right) \Gamma\left(m_{S_i P}, \varphi_{S_i}\right) - \frac{\Gamma\left(m_{S_i P} + L_R m_{S_i R}, \varphi_{S_i}\right)}{L_R m_{S_i R} z^{-L_R m_{S_i R}}},\end{aligned} \tag{4.201}$$

with step (a) follows by considering only the first term of the infinite summation when z tends to 0.

Finally, armed by [67, Eq. (8.354.2)] the upper incomplete Gamma given in (4.125) can be approximated for small values of z as

$$\Gamma\left(L_R m_{S_i R}, \frac{\sigma_i \xi_{S_i R}}{\overline{\gamma}_I}\right) \sim \Gamma\left(L_R m_{S_i R}\right) - \frac{1}{L_R m_{S_i R}} \left(\frac{\sigma_i \xi_{S_i R}}{\overline{\gamma}_I}\right)^{L_R m_{S_i R}}. \tag{4.202}$$

Interestingly, the $\mathrm{SOP}_1^{(i,k,J)}$ can finally be approximated in high SNR regime (i.e., $\overline{\gamma}_I \to \infty$) by considering three cases, namely $L_R m_{S_i R} < L_{E_k} m_{S_J E_k}$, $L_R m_{S_i R} > L_{E_k} m_{S_J E_k}$, and $L_R m_{S_i R} = L_{E_k} m_{S_J E_k}$.

- $L_R m_{S_i R} < L_{E_k} m_{S_J E_k}$

Substituting (4.189), (4.190), (4.201), and (4.202) into (4.125), and by considering $h = L_{E_k} m_{S_i E_k} - 1$, $\mathrm{SOP}_1^{(i,k,J)}$ can be approximated as

$$\mathrm{SOP}_1^{(i,k,J)} \sim \frac{\mathcal{C}_1^{(i,k,J)}}{\overline{\gamma}_I^{L_R m_{S_i R}}}, \tag{4.203}$$

where $\mathcal{C}_1^{(i,k,J)}$ is given in (4.177).

- $L_R m_{S_i R} > L_{E_k} m_{S_J E_k}$

Incorporating (4.194), (4.195), (4.201), and (4.202) into (4.125), and by considering $l = L_R m_{S_i R} - 1$, $\mathrm{SOP}_1^{(i,k,J)}$ can be approximated as

$$\mathrm{SOP}_1^{(i,k,J)} \sim \frac{\mathcal{C}_2^{(i,k,J)}}{\overline{\gamma}_I^{L_{E_k} m_{S_J E_k}}}, \tag{4.204}$$

where $\mathcal{C}_2^{(i,k,J)}$ is given in (4.178).

- $L_R m_{S_i R} = L_{E_k} m_{S_J E_k}$

Replacing (4.194), (4.195), (4.198), (4.199), (4.201), and (4.202) into (4.125), and by considering $l = L_R m_{S_i R} - 1$, $\mathrm{SOP}_1^{(i,k,J)}$ can be approximated as

$$SOP_1^{(i,k,J)} \sim \mathcal{C}_3^{(i,k,J)} \frac{\log\left(\overline{\gamma}_I\right)}{\overline{\gamma}_I^{L_{E_k} m_{S_J E_k}}}, \tag{4.205}$$

where $\mathcal{C}_3^{(i,k,J)}$ is given in (4.179).

Case 2: Absence of a Friendly Jammer

In order to derive the asymptotic expression of $\mathrm{SOP}_1^{(i,k)}$ given in (4.126), we need to approximate the upper incomplete Gamma function. One can ascertain by applying the Maclaurin series that

$$\Gamma\left(a, b + cz\right) \sim \Gamma\left(a, b\right) - czb^{a-1}e^{-b}, \tag{4.206}$$

as z tends to 0. By considering only the two cases i.e., $l = L_R m_{S_i R} - 1$ and $l = L_R m_{S_i R} - 2$ and performing some algebraic manipulations, one can obtain

Table 4.3: Simulation parameters of contribution 6.

Parameter	M	N	λ_{S_iR}	λ_{S_iP}	$\lambda_{S_iE_k}$
value	3	4	0.1	0.3	0.6
Parameter	λ_{RE_k}	λ_{RP}	λ_{RD}	m_{S_iR}	m_{S_iP}
value	0.6	0.2	0.1	2	3
Parameter	$m_{S_iE_k}$	m_{RD}	m_{RE_k}	m_{RP}	
value	5	2	4	3	

$$\mathrm{SOP}_1^{(i,k)} \sim 1 - \mathcal{A}_{S_iE_k,S_iR,R} - \frac{\mathcal{A}_{S_iE_k,S_iR,S_i,R}}{\overline{\gamma}_I}, \tag{4.207}$$

where $\mathcal{A}_{\bullet,\bullet,\bullet}$ and $\mathcal{A}_{\bullet,\bullet,\bullet,\bullet}$ are defined in (4.175) and (4.176), respectively.

- **Asymptotic expression of $\mathbf{SOP}_2^{(k)}$**

As $\mathrm{SOP}_1^{(i,k)}$ and $\mathrm{SOP}_2^{(k)}$ given in (4.126) and (4.127), respectively have the same shape, one can see that

$$\mathrm{SOP}_2^{(k)} \sim 1 - \mathcal{A}_{RE_k,RD} - \frac{\mathcal{A}_{RE_k,RD,R}}{\overline{\gamma}_I}, \tag{4.208}$$

Finally, replacing (4.203), (4.204), (4.205), and (4.208) into (4.123), one can get the expressions (4.171)-(4.174), respectively. Furthermore, substituting (4.207) and (4.208) into (4.124), (4.170) is attained which concludes the proof of Theorem 4.4.2. ■

4.4.3 Numerical results and discussions

In this section, we validate the derived analytical results through Monte Carlo simulation by generating 10^6 Gamma-distributed RVs. The setting parameters of the simulation are summarized in Table 4.3. Indeed, the values of fading severity parameter $m_\bullet$ have been chosen such that the wiretap channel is better than the legitimate one. Moreover, their values are taken integer in the range 2..5 similarly to [97] and [18]. On the other hand, the average SNR, which is inversely proportional to $\lambda_\bullet$, the legitimate link is considered better than the one of the wiretap channel. It is worthwhile that these parameters are associated with all figures except those indicating other values. As one can see in Figs. 4.11-4.16, all closed-form and simulation curves are perfectly matched for considered parameters' values.

Fig. 4.11 and Fig. 4.12 depict closed-form and asymptotic expressions for the SOP versus $\overline{\gamma}_I$ for various numbers of antennas' in both the presence and absence of a friendly jammer cases, respectively. As stated in remark 9, it can be noticed that the greater $\overline{\gamma}_I$, the smaller the SOP. Interestingly, above a certain threshold of $\overline{\gamma}_I$ the SOP becomes steady this can be obviously justified from (4.109) and (4.110) that above that threshold, both sources and relay will always transmit with their maximum powers. Consequently, the legitimate and wiretap capacities of each hop remain constant, leading to a constant value of SOP. Interestingly, by comparing the SOP values in the two aforementioned figures, one can ascertain that better secrecy is achieved by using a friendly jammer. In addition, the asymptotic curves are plotted under the considered fading severity values (i.e., $m_{S_iR} = 2$, $m_{S_JE_k} = 5$) from Eqs. (4.170)-(4.174). Clearly, the asymptotic curves match with the closed-form ones in high SNR regime.

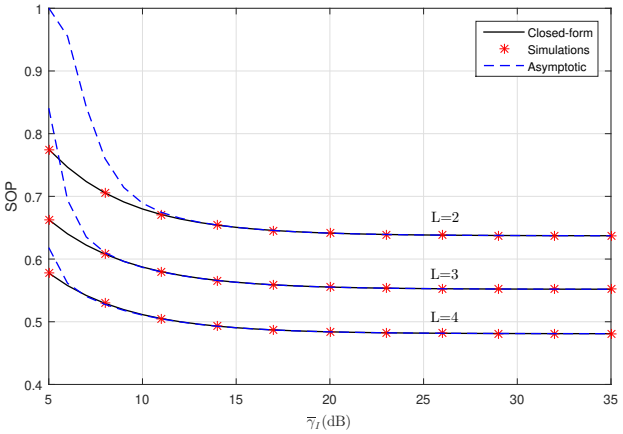

Figure 4.11: SOP versus $\overline{\gamma}_I$ for different numbers of antennas at the destination in the presence of a friendly jammer for $\eta = \sigma_i = \delta = 0.1$ and $L_R = L_{E_k} = L_D = L$.

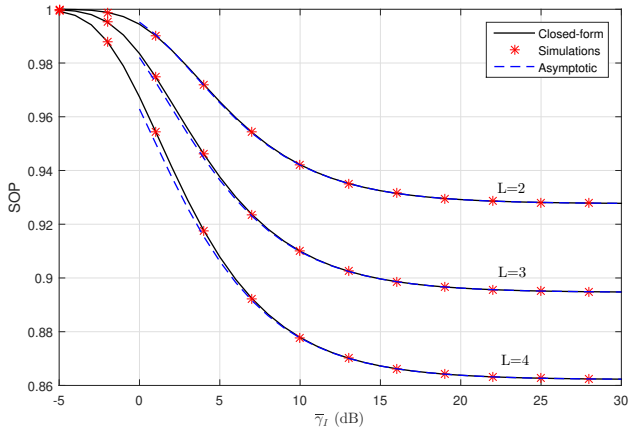

Figure 4.12: SOP versus $\overline{\gamma}_I$ in the absence of a friendly jammer for $\sigma_i = \delta = 0.1$ and $L_R = L_{E_k} = L_D = L$.

Fig. 4.13 illustrates the SOP versus $\overline{\gamma}_{S_J}$ for numerous numbers of branches' L_D at the receiver D. Again, as indicated in remark 9, one can realize that the higher $\overline{\gamma}_{S_J}$ and L_D, the smaller the SOP and therefore the system's security gets improved.

Fig. 4.14 and Fig. 4.15 show the SOP as a function of the number of eavesdroppers M for different values of $\overline{\gamma}_{S_J}$ and by considering both cases i.e., presence and absence of jammer. One can observe that the smaller $\overline{\gamma}_{S_J}$ or the greater M the worst is the system's secrecy

as highlighted in remark 9 and 10, respectively. In addition, introducing a jamming signal improves significantly the secrecy performance for high values of $\overline{\gamma}_{S_J}$ or in the presence of small numbers of eavesdroppers.

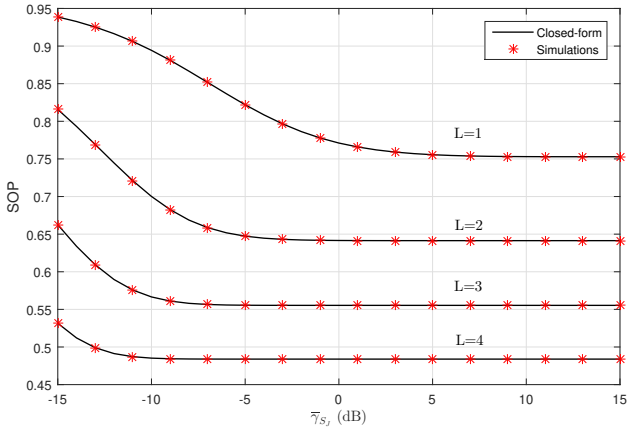

Figure 4.13: SOP versus $\overline{\gamma}_{S_J}$ for different numbers of antennas at the destination for $\overline{\gamma}_I = \overline{\gamma}_{S_i} = \overline{\gamma}_R = 20$ dB and $L_R = L_{E_k} = L_D = L$.

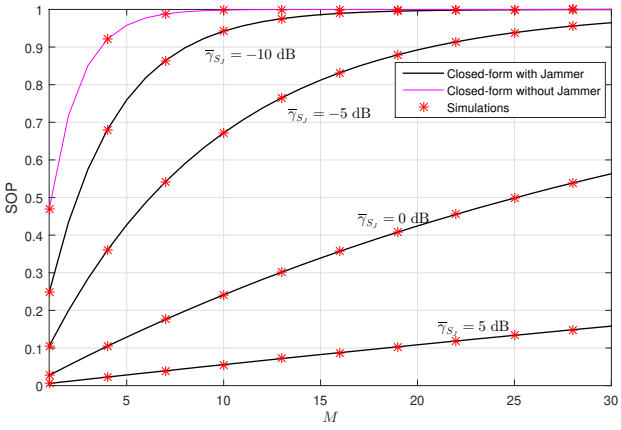

Figure 4.14: SOP versus number of eavesdroppers and different values $\overline{\gamma}_{S_J}$ for $L_D = 4$ and $\overline{\gamma}_I = \overline{\gamma}_{S_i} = \overline{\gamma}_R = 20$ dB.

Fig. 4.16 depicts the SOP as a function of the number of eavesdroppers by considering the presence and absence of a friendly jammer. It is worth mentioning that better security is obviously achieved for the case of presence of jammer and multi-antenna nodes, while the scenario of the absence of jammer and legitimate nodes equipped with a single antenna is the worst case. For this reason, our aim here is to investigate if the security gets enhanced when having artificial noise and legitimate nodes with a single antenna or the scenario of the absence of jammer and all legitimate nodes are equipped with multiple antennas. One can obviously notice that the system's security is improved when diversity is used at the legitimate nodes. Additionally, in the presence of an important number of eavesdroppers, the friendly jammer does not contribute to the enhancement of the system's security.

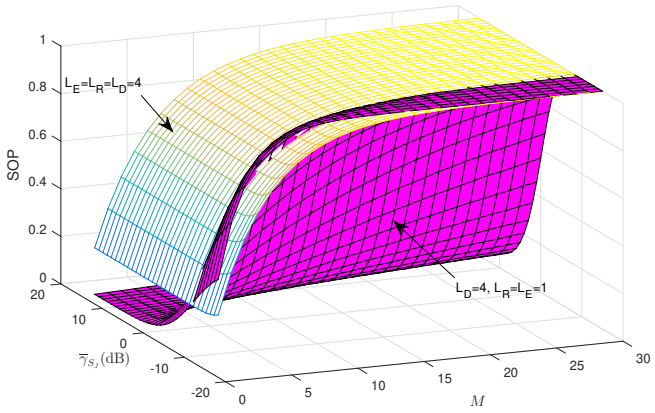

Figure 4.15: SOP versus number of eavesdroppers and $\overline{\gamma}_{S_J}$ for $\overline{\gamma}_I = \overline{\gamma}_{S_i} = \overline{\gamma}_R = 20$ dB.

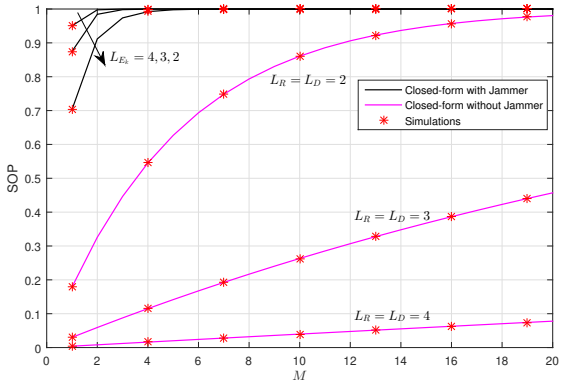

Figure 4.16: SOP versus the number of eavesdroppers in the presence and absence of friendly jammer and different numbers of antennas for $\overline{\gamma}_{S_J} = 20$ dB.

4.5 Contribution 7: Secrecy performance analysis of a dual-hop jamming-based underlay cognitive hybrid satellite-terrestrial network

4.5.1 System and channel model

We consider an underlay cognitive satellite system, presented in Fig. 4.17, consisting of two SU sources, namely a data source S, a jammer source S_J, satellite R that serves as a relay, one optical ground station D, two eavesdroppers E_1 and E_2 intercepting the communication at the first and the second hop, respectively, one primary transmitter PU_{T_x}, and one primary receiver PU_{R_x}. It is worth mentioning that the jamming signal sent by S_J can be canceled at the legitimate receiver (i.e. R), while the eavesdropper E_1 is not able to decode it. Without loss of generality, the source communicates with the optimal relay through an RF-link, while at the second hop R forwards data to D through an optical feeder link. The received signal at R and E_1 are, respectively, given by

$$y_R = \sqrt{P_S} x_S h_{SR} + n_R, \tag{4.209}$$

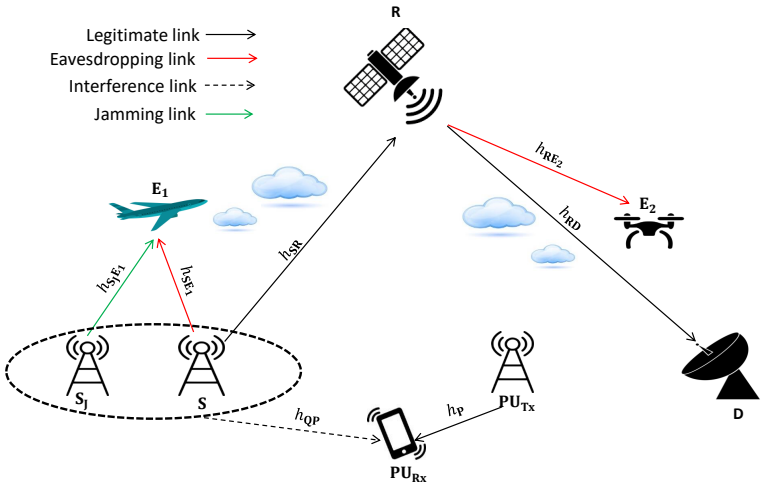

Figure 4.17: The considered HSTCN.

$$y_{E_1} = \sqrt{P_S} x_S h_{SE_1} + \varepsilon \sqrt{P_{S_J}} x_{S_J} h_{S_J E_1} + n_{E_1}, \tag{4.210}$$

while, the received signal at node $Z \in \{D, E_2\}$ is given by

$$y_Z = \sqrt{P_R \omega_Z} \left(\eta I_Z\right)^{\frac{r}{2}} x_R + n_Z, \tag{4.211}$$

where, ε is either equal to 0 or to 1 in absence or presence of artificial noise, respectively. I_Z is the irradiance of the link R-D, $\left(i.e., I_Z = I_Z^{(a)} I_Z^{(p)} I_Z^{(l)}\right)$ defined as the product of the irradiance fluctuation caused by atmospheric turbulence (i.e., $I_Z^{(a)}$), the pointing error due to the beam misalignment (i.e., $I_Z^{(p)}$), and the free-space path loss (FSPL) (i.e., $I_Z^{(l)}$), respectively. Of note, the latter irradiance can be expressed as $I_Z^{(l)} = I_t e^{-\phi d_Z}$, with I_t stands for the laser emittance. For simplicity reasons, the FSPL's irradiance is considered normalized to unity ($\phi = 0$). Furthermore, r refers to the detection technique index (i.e., $r = 1$ for coherent detection and $r = 2$ for direct detection).

To avoid interference with the PU signal, the SNR at R can be characterized as

$$\gamma_R = \min\left(\overline{\gamma}_S, \frac{\overline{\gamma}_I}{g_{SP}}\right) g_{SR}, \tag{4.212}$$

while the SNR at E_1 in the case of absence and presence of a friendly jammer are, respectively,

given by

$$\gamma_{E_1} = \mathcal{U}_S, \tag{4.213}$$

and

$$\gamma_{E_1}^{(J)} = \frac{\mathcal{U}_S}{\mathcal{U}_{S_J} + 1}, \tag{4.214}$$

where

$$\mathcal{U}_Q = \min\left(\overline{\gamma}_Q, \frac{\overline{\gamma}_I}{g_{QP}}\right) g_{QE_1},\ Q\ \in \{S, S_J\}, \tag{4.215}$$

$\overline{\gamma}_Q = P_Q^{\max}/N$, and $\overline{\gamma}_I = P_I/N$, with N presents the thermal power noise at the receivers, assumed identical.

Furthermore, the SNR at node $Z \in \{D, E_2\}$ can be straightforwardly expressed from (4.211) as

$$\gamma_Z = \frac{P_R \omega_Z \left(\eta I_Z\right)^r}{N}. \tag{4.216}$$

Given that the satellite R performs the DF protocol, the equivalent SNR of the end-to-end link is given by

$$\gamma_{eq} = \min\left(\gamma_R, \gamma_D\right). \tag{4.217}$$

All fading amplitudes are assumed to be independent and identically distributed (i.i.d). Specifically, the amplitudes of the terrestrial (i.e. S-PU$_{Rx}$ and S_J-PU$_{Rx}$) and uplink channels (i.e. S-R, S-E_1, and S_J-E_1) are Rayleigh and shadowed-Rician distributed, respectively. Therefore, the PDF and CDF of the channel gain corresponding to the latter channel can be characterized as given in (1.21) and (1.22), respectively.

On the other hand, as the atmospheric turbulence induced-fading with pointing error for the received optical beam is modeled with Gamma-Gamma distribution, the PDF and CDF of the SNR γ_Z are expressed, respectively as in (1.16) and (1.17).

4.5.2 Secrecy performance evaluation

In this section, we derive closed-form and asymptotic expressions for the IP defined in (1.35) such that the secrecy capacity of the system is defined in (1.31). Differently from the previous systems, we are considering in this contribution the presence of two eavesdroppers. Therefore,

the secrecy capacity at the second hop is given by

$$C_{2S} = \min\left(\log_2\left(\frac{1+\gamma_R}{1+\gamma_{E_2}}\right), \log_2\left(\frac{1+\gamma_D}{1+\gamma_{E_2}}\right)\right). \tag{4.218}$$

Remark 11. *One can see from (1.35) that the system's secrecy can be enhanced by increasing the SNRs at legitimate nodes (i.e., R and D) or decreasing the SNRs at the eavesdroppers at both hops. To this end, the system's secrecy is impacted by two main factors: (i) transmit power of the sources, and (ii) fading severity exhibited by different channels. Owing to that, it can be clearly noticed from (4.212) and (4.214) that increasing either* $\overline{\gamma}_I$ *or* $\overline{\gamma}_S$ *enhances the SNR at R, while increasing* $\overline{\gamma}_{S_J}$ *decreases the SNR at* E_1*. Particularly, the presence of a friendly jammer decreases this latter metric as can be ascertained in (4.214) and (4.213). Furthermore, above a certain threshold of either* $\overline{\gamma}_I$ *or* $\overline{\gamma}_S$*, both legitimate and eavesdropper SNRs depend exclusively of either* $\overline{\gamma}_S$ *or* $\overline{\gamma}_I$*, respectively as can be observed in (4.214)-(4.215). Consequently, the IP remains steady in both aforementioned cases. Likewise, it can be noticed from (4.216) that the capacities of the second-hop channels are affected by various parameters including the satellite's transmit power and the average powers of both LOS and multipath components of the downlink turbulence channel.*

New framework for the IP

In order to derive the closed-form and asymptotic expressions for the IP of the considered HSTCN, we have to provide first a framework for IP's evaluation of a dual-hop cognitive system in the presence of an eavesdropper at each hop when the relay performs the DF protocol. Next, both closed-form and asymptotic expressions of the IP for the considered system are provided under two scenarios, namely (i) absence, and (ii) presence of a friendly jamming signal.

Lemma 1. *For a dual-hop cognitive network-aided DF relaying protocol experiencing generalized fading models over the intercepting attempt of two wiretappers* E_1 *and* E_2 *at the first and the second hop, respectively, the* IP *can be evaluated as*

$$\text{IP} = 1 - \int_{u=0}^{\infty} f_{g_{SP}}(u)\, \mathcal{R}_1(u)\, du, \tag{4.219}$$

where

$$\mathcal{R}_1(u) = \int_{y=\gamma_{th}}^{\infty} \mathcal{J}_1(y,u)\, \mathcal{J}_2(y)\, dy, \tag{4.220}$$

$$\mathcal{J}_1(y,u) = f_{\gamma_R|g_{SP}=u}(y)\, F_{\gamma_{E_1}|g_{SP}=u}(y), \tag{4.221}$$

and

$$\mathcal{J}_2(y) = \int_{z=0}^{y} f_{\gamma_{E_2}}(z)\, F^c_{\gamma_D}(z)\, dz, \tag{4.222}$$

where $F^c_{\cdot}(.)$ denotes the complementary CDF.

Proof. Using equations (1.31), (1.32), (1.35), and (4.218), the IP can be rewritten as

$$\begin{aligned} \text{IP} &\overset{(a)}{=} \Pr(C_{\text{sec}} \leq 0 |\, \gamma_R > \gamma_{th}) \Pr(\gamma_R > \gamma_{th}) + \Pr(C_{\text{sec}} \leq 0 |\, \gamma_R < \gamma_{th}) \Pr(\gamma_R < \gamma_{th}) \\ &\overset{(b)}{=} \Pr(C_{\text{sec}} \leq 0 |\, \gamma_R > \gamma_{th}) \Pr(\gamma_R > \gamma_{th}) + \Pr(\gamma_R < \gamma_{th}), \end{aligned} \tag{4.223}$$

where step (a) is attained by using both total probability and Bayes' rules, while step (b) holds by noting that when $\gamma_R < \gamma_{th}$, the satellite R fails to decode the received message from S and therefore the communication could not be established between the source and the destination (i.e. $\gamma_D = \gamma_{E_2} = 0$). It follows that $C_{\text{sec}} = 0$ and consequently, $\Pr(C_{\text{sec}} \leq 0 |\, \gamma_R < \gamma_{th}) = 1$.

On the other hand, by considering that

$$\Pr(C_{\text{sec}} \leq 0 |\, \gamma_R > \gamma_{th}) = \Pr(\gamma_R > \gamma_{th}) - \Pr(C_{\text{sec}} > 0 |\, \gamma_R > \gamma_{th}), \tag{4.224}$$

Substituting (**??**) and (4.224) into (4.223), the IP can be rewritten as

$$\begin{aligned} \text{IP} &= 1 - \Pr(C_{\text{sec}} > 0, \gamma_R > \gamma_{th}), \\ &= 1 - \underbrace{\Pr(\gamma_R > \gamma_{E_1}, \gamma_R > \gamma_{E_2}, \gamma_D > \gamma_{E_2}, \gamma_R > \gamma_{th})}_{\mathcal{I}}. \end{aligned} \tag{4.225}$$

Obviously, the term $\mathcal{I}$ can be expressed as the sum of six different probabilities (i.e. $\mathcal{I} = \sum_{i=1}^{6} \mathcal{I}_i$ with $\mathcal{I}_i = \Pr(E_i, \gamma_D > \gamma_{E_2})$ where the events E_i are summarized in Table 4.4.

$$\mathcal{I}_1 = \int_0^{\infty} f_{g_{SP}}(u)\, du \int_{\gamma_{th}}^{\infty} F_{\gamma_{E_1}|g_{SP}=u}(y) \left[\begin{array}{c} f_{\gamma_R|g_{SP}=u}(y) \int_{\gamma_{th}}^{y} f_{\gamma_{E_2}}(z)\, F^c_{\gamma_D}(z)\, dz \\ -F^c_{\gamma_R|g_{SP}=u}(y)\, f_{\gamma_{E_2}}(y)\, F^c_{\gamma_D}(y) \end{array} \right] dy. \tag{4.226}$$

Table 4.4: Events for $\mathcal{I}$.

	Event		*Event*
E_1	$\gamma_R > \gamma_{E_1} > \gamma_{E_2} > \gamma_{th}$	E_4	$\gamma_R > \gamma_{th} > \gamma_{E_1} > \gamma_{E_2}$
E_2	$\gamma_R > \gamma_{E_2} > \gamma_{E_1} > \gamma_{th}$	E_5	$\gamma_R > \gamma_{E_2} > \gamma_{th} > \gamma_{E_1}$
E_3	$\gamma_R > \gamma_{th} > \gamma_{E_2} > \gamma_{E_1}$	E_6	$\gamma_R > \gamma_{E_1} > \gamma_{th} > \gamma_{E_2}$

$$\mathcal{I}_2 = \int_0^\infty f_{g_{SP}}(u)\,du \int_{\gamma_{th}}^\infty F^c_{\gamma_R|g_{SP}=u}(z)\, f_{\gamma_{E_2}}(z)\, F^c_{\gamma_D}(z) \left[F_{\gamma_{E_1}|g_{SP}=u}(z) - F_{\gamma_{E_1}|g_{SP}=u}(\gamma_{th})\right] dz. \tag{4.227}$$

$$\mathcal{I}_3 = \int_0^\infty F^c_{\gamma_R|g_{SP}=u}(\gamma_{th})\, f_{g_{SP}}(u) \int_0^{\gamma_{th}} F_{\gamma_{E_1}|g_{SP}=u}(y)\, f_{\gamma_{E_2}}(y)\, F^c_{\gamma_D}(y)\, dudy. \tag{4.228}$$

$$\mathcal{I}_4 = \int_0^\infty F^c_{\gamma_R|g_{SP}=u}(\gamma_{th})\, f_{g_{SP}}(u) \int_0^{\gamma_{th}} f_{\gamma_{E_2}}(z)\, F^c_{\gamma_D}(z) \left[F_{\gamma_{E_1}|g_{SP}=u}(\gamma_{th}) - F_{\gamma_{E_1}|g_{SP}=u}(z)\right] dudz. \tag{4.229}$$

$$\mathcal{I}_5 = \int_0^\infty F_{\gamma_{E_1}|g_{SP}=u}(\gamma_{th})\, f_{g_{SP}}(u) \left[\int_{\gamma_{th}}^\infty f_{\gamma_{E_2}}(x)\, F^c_{\gamma_D}(x) - \int_{\gamma_{th}}^\infty F_{\gamma_R|g_{SP}=u}(x)\, f_{\gamma_{E_2}}(x)\, F^c_{\gamma_D}(x)\right] dudx. \tag{4.230}$$

$$\mathcal{I}_6 = \int_0^\infty f_{g_{SP}}(u) \int_{\gamma_{th}}^\infty f_{\gamma_R|g_{SP}=u}(x) \left[F_{\gamma_{E_1}|g_{SP}=u}(x) - F_{\gamma_{E_1}|g_{SP}=u}(\gamma_{th})\right] dxdu \times \int_0^{\gamma_{th}} f_{\gamma_{E_2}}(z)\, F^c_{\gamma_D}(z)\, dz. \tag{4.231}$$

Eqs. (4.226), (4.228), and (4.230) are obtained using integration by parts alongside some algebraic manipulations, while (4.227), (4.229), and (4.231) can be achieved by applying the basic definition of the CDF.

By performing a summation of (4.226)-(4.231) and substituting $\mathcal{I}$ into (4.225), (4.219) is attained, which concludes the proof of Lemma 1. ■

IP closed-form

Theorem 4.5.1. *The closed-form expressions for IP of the considered HSTCN under the considered fading models is given by (4.243), for both absence (i.e. $\mathcal{E} = A$) and presence (i.e. $\mathcal{E} = P$) of a friendly jamming, where*

$$e^{(Z,\tau)} = \frac{\Gamma\left(\alpha_Z - \xi_Z^2\right)\Gamma\left(\beta_Z - \xi_Z^2\right)}{\tau + \xi_Z^2}, \tag{4.232}$$

$$e^{(Z,\tau,k)}\left(x,y\right) = \frac{\left(-1\right)^k \Gamma\left(x-y-k\right)}{k!\left(\xi_Z^2 - y - k\right)\left(\tau + y + k\right)},\ \xi_Z^2 \neq y + k, \tag{4.233}$$

$$\mathcal{B}^{(n_1,n_2,n_3,p)} = \frac{\binom{n_2}{p}\phi_{S_J E_1}^{(n_1)}\phi_{SE_1}^{(n_2)}\phi_{SR}^{(n_3)}}{\upsilon_{S_J E_1}^{n_1+1}\upsilon_{SE_1}^{p}}, \tag{4.234}$$

$$\Psi_2^{(n_1,n_2,n_3,p,a,\tau)} = \frac{\varrho_D^{\tau}\left(\Upsilon_{E_2}\varrho_{E_2}\right)^a}{\zeta^{n_2+n_3-p+1+a+\tau}}\left[F_{g_{SP}}\left(\sigma_S\right)\mathcal{M}^{(n_1,n_2,n_3,p,a,\tau)} + \lambda_{SP}\sigma_S^{a+\tau}\mathcal{Y}^{(n_1,n_2,n_3,p,a,\tau)}\right], \tag{4.235}$$

$$\Psi_3^{(n_1,n_2,n_3,p,a,\tau)} = \frac{\varrho_D^{\tau}\left(\Upsilon_{E_2}\varrho_{E_2}\right)^a}{\zeta^{n_2+n_3-p+1+a+\tau}}\left[F_{g_{SP}}\left(\sigma_S\right)\Phi^{(n_1,n_2,n_3,p,a,\tau)} + \lambda_{SP}\sigma_S^{a+\tau}\mathcal{W}^{(n_1,n_2,n_3,p,a,\tau)}\right], \tag{4.236}$$

$$\theta = \mathcal{O}_D \times \mathcal{O}_{E_2}, \tag{4.237}$$

$$\varrho_Z = \frac{\overline{\gamma}_S}{\mu_1^{(Z)}}, \tag{4.238}$$

$$\sigma_Q = \frac{\overline{\gamma}_I}{\overline{\gamma}_Q}, \tag{4.239}$$

$$\epsilon_I = \frac{\gamma_{th}}{\overline{\gamma}_I}, \tag{4.240}$$

$$\chi = \frac{\upsilon_{S_J E_1}\zeta}{\upsilon_{SE_1}}, \tag{4.241}$$

$$\zeta = \upsilon_{SR} + \upsilon_{SE_1}, \tag{4.242}$$

$\tau \in \{0, q\}$, $q \in \{\xi_D^2, \alpha_D + k, \beta_D + k\}$, and $\mathcal{C}_s$ and $\mathcal{C}_w$ are two vertical lines of integration chosen so as to separate left poles of the integrand functions in (4.251) and (4.253), from the right ones.

$$\mathrm{IP}_{\mathcal{E}} = 1 - \frac{\xi_{E_2}^2\mathcal{D}_{\mathcal{E}}^{(0)}}{\Gamma\left(\alpha_{E_2}\right)\Gamma\left(\beta_{E_2}\right)} + \theta\left[\begin{array}{c} e^{(D,0)}\mathcal{D}_{\mathcal{E}}^{\left(\xi_D^2\right)} + \sum_{k=0}^{\infty} e^{(D,0,k)}\left(\beta_D,\alpha_D\right)\mathcal{D}_{\mathcal{E}}^{(\alpha_D+k)} \\ +e^{(D,0,k)}\left(\alpha_D,\beta_D\right)\mathcal{D}_{\mathcal{E}}^{(\beta_D+k)} \end{array}\right],\ \mathcal{E} \in \{A, P\} \tag{4.243}$$

$$\mathcal{D}_{A}^{(\tau)}=\Upsilon_{D}^{\tau}\Delta_{SE_{1}}\Delta_{SR}\sum_{n_{2}=0}^{m_{SE_{1}}-1}\sum_{n_{3}=0}^{m_{SR}-1}\frac{\phi_{SR}^{(n_{3})}\phi_{SE_{1}}^{(n_{2})}}{\upsilon_{SE_{1}}^{n_{2}+1}}\left[\begin{array}{c}e^{(E_{2},\tau)}\mathcal{N}_{1}^{\left(n_{2},n_{3},\xi_{E_{2}}^{2},\tau\right)}\\+\sum_{k=0}^{\infty}e^{(E_{2},\tau,k)}\left(\beta_{E_{2}},\alpha_{E_{2}}\right)\mathcal{N}_{1}^{\left(n_{2},n_{3},\alpha_{E_{2}}+k,\tau\right)}\\+\sum_{k=0}^{\infty}e^{(E_{2},\tau,k)}\left(\alpha_{E_{2}},\beta_{E_{2}}\right)\mathcal{N}_{1}^{\left(n_{2},n_{3},\beta_{E_{2}}+k,\tau\right)}\end{array}\right]. \tag{4.244}$$

$$\mathcal{D}_{P}^{(\tau)}=\Upsilon_{D}^{\tau}\Delta_{SR}\left[\begin{array}{c}\sum_{n_{3}=0}^{m_{SR}-1}\phi_{SR}^{(n_{3})}\Xi_{1}^{(n_{3},\tau)}-\Delta_{SE_{1}}\Delta_{S_{J}E_{1}}\sum_{n_{1}=0}^{m_{S_{J}E_{1}}-1}\sum_{n_{2}=0}^{m_{SE_{1}}-1}\sum_{p=0}^{n_{2}}\sum_{n_{3}=0}^{m_{SR}-1}\\\times\mathcal{B}^{(n_{1},n_{2},n_{3},p)}\left\{F_{g_{S_{J}P}}\left(\sigma_{S_{J}}\right)\Xi_{2}^{(n_{1},n_{2},n_{3},p,\tau)}+\Xi_{3}^{(n_{1},n_{2},n_{3},p,\tau)}\right\}\end{array}\right]. \tag{4.245}$$

$$\mathcal{N}_{1}^{(n_{2},n_{3},a,\tau)}=\frac{\varrho_{D}^{\tau}\left(\Upsilon_{E_{2}}\varrho_{E_{2}}\right)^{a}}{\upsilon_{SR}^{n_{3}+\tau+a+1}}\left[\begin{array}{c}F_{g_{SP}}\left(\sigma_{S}\right)G_{2,2}^{1,2}\left(\frac{\upsilon_{SE_{1}}}{\upsilon_{SR}}\middle|\begin{array}{c}(1,0),(-n_{3}-\tau-a,\epsilon_{I}\sigma_{S}\upsilon_{SR});-\\(n_{2}+1,0);(0,0)\end{array}\right)\\+\frac{\left(\lambda_{SP}\sigma_{S}\right)^{\tau+a}}{\left(2\pi j\right)^{2}}\int_{C_{s}}\frac{\Gamma(n_{2}+1+s)\Gamma(-s)}{\Gamma(1-s)}\left(\frac{\upsilon_{SE_{1}}}{\upsilon_{SR}}\right)^{-s}\\\times\int_{C_{w}}\frac{\Gamma(-\tau-a-w+1,\lambda_{SP}\sigma_{S})\Gamma(n_{3}+\tau+a+1-s+w)\Gamma(w)}{\Gamma(1+w)}\left(\frac{\epsilon_{I}\upsilon_{SR}}{\lambda_{SP}}\right)^{-w}dsdw\end{array}\right]. \tag{4.246}$$

$$\Xi_{1}^{(n_{3},\tau)}=e^{(E_{2},\tau)}\Psi_{1}^{\left(n_{3},\xi_{E_{2}}^{2},\tau\right)}+\sum_{k=0}^{\infty}e^{(E_{2},\tau,k)}\left(\beta_{E_{2}},\alpha_{E_{2}}\right)\Psi_{1}^{\left(n_{3},\alpha_{E_{2}}+k,\tau\right)}+e^{(E_{2},\tau,k)}\left(\alpha_{E_{2}},\beta_{E_{2}}\right)\Psi_{1}^{\left(n_{3},\beta_{E_{2}}+k,\tau\right)}. \tag{4.247}$$

$$\Psi_{1}^{(n_{3},a,\tau)}=\frac{\varrho_{D}^{\tau}\left(\Upsilon_{E_{2}}\varrho_{E_{2}}\right)^{a}}{\upsilon_{SR}^{n_{3}+\tau+a+1}}\left[\begin{array}{c}F_{g_{SP}}\left(\sigma_{S}\right)\Gamma\left(n_{3}+\tau+a+1,\epsilon_{I}\sigma_{S}\upsilon_{SR}\right)\\+\left(\sigma_{S}\lambda_{SP}\right)^{\tau+a}G_{2,2}^{2,1}\left(\frac{\upsilon_{SR}\epsilon_{I}}{\lambda_{SP}}\middle|\begin{array}{c}(\tau+a,\sigma_{S}\lambda_{SP});(1,0)\\(0,0),(n_{3}+\tau+a+1,0);-\end{array}\right)\end{array}\right]. \tag{4.248}$$

$$\begin{aligned}\Xi_{n}^{(n_{1},n_{2},n_{3},p,\tau)}&=e^{(E_{2},\tau)}\Psi_{n}^{\left(n_{1},n_{2},n_{3},p,\xi_{E_{2}}^{2},\tau\right)}+\sum_{k=0}^{\infty}e^{(E_{2},\tau,k)}\left(\beta_{E_{2}},\alpha_{E_{2}}\right)\Psi_{n}^{\left(n_{1},n_{2},n_{3},p,\alpha_{E_{2}}+k,\tau\right)}\\&+e^{(E_{2},\tau,k)}\left(\alpha_{E_{2}},\beta_{E_{2}}\right)\Psi_{n}^{\left(n_{1},n_{2},n_{3},p,\beta_{E_{2}}+k,\tau\right)},\ n\in\{2,3\}.\end{aligned} \tag{4.249}$$

$$\mathcal{M}^{(n_{1},n_{2},n_{3},p,a,\tau)}=G_{2,3}^{2,2}\left(\frac{\chi\sigma_{S_{J}}}{\overline{\gamma}_{I}}\middle|\begin{array}{c}(-p,0),(1,0);-\\(n_{1}+1,0),(n_{2}+n_{3}-p+1+\tau+a,\zeta\epsilon_{I}\sigma_{S});(0,0)\end{array}\right). \tag{4.250}$$

$$\begin{aligned}\mathcal{Y}^{(n_{1},n_{2},n_{3},p,a,\tau)}&=\frac{-\lambda_{SP}^{a+\tau-1}}{\left(2\pi j\right)^{2}}\int_{\mathcal{C}_{s}}\frac{\Gamma\left(n_{1}+1+s\right)\Gamma\left(1+p-s\right)}{s}\left(\frac{\chi\sigma_{S_{J}}}{\overline{\gamma}_{I}}\right)^{-s}\\&\times\int_{\mathcal{C}_{w}}\frac{\Gamma\left(n_{2}+n_{3}-p+1+\tau+a+s+w\right)\Gamma\left(1-a-\tau-w,\sigma_{S}\lambda_{SP}\right)}{w}\left(\frac{\zeta\epsilon_{I}}{\lambda_{SP}}\right)^{-w}dsdw.\end{aligned} \tag{4.251}$$

$$\Phi^{(n_1,n_2,n_3,p,a,\tau)} = G_{3,3}^{2,3}\left(\frac{\chi}{\lambda_{S_JP}\overline{\gamma}_I}\middle|\begin{matrix}(-p,0),(1,0),(0,\sigma_{S_J}\lambda_{S_JP});-\\(n_1+1,0),(n_2+n_3-p+1+\tau+a,\zeta\epsilon_I\sigma_S);(0,0)\end{matrix}\right). \tag{4.252}$$

$$\mathcal{W}^{(n_1,n_2,n_3,p,a,\tau)} = \frac{-\lambda_{SP}^{a+\tau-1}}{(2\pi j)^2}\int_{\mathcal{C}_s}\frac{\Gamma(n_1+1+s)\,\Gamma(1+p-s)\,\Gamma(1-s,\sigma_{S_J}\lambda_{S_JP})}{s}\left(\frac{\chi}{\lambda_{S_JP}\overline{\gamma}_I}\right)^{-s} \tag{4.253}$$

$$\times\int_{\mathcal{C}_w}\frac{\Gamma(n_2+n_3-p+1+a+\tau+s+w)\,\Gamma(1-a-\tau-w,\sigma_S\lambda_{SP})}{w}\left(\frac{\zeta\epsilon_I}{\lambda_{SP}}\right)^{-w}dsdw.$$

Proof. To prove the IP expression given in (4.243) in both the absence and presence of friendly jammer cases, it is mandatory to compute $\mathcal{J}_1(y,u)$, $\mathcal{J}_2(y)$, and $\mathcal{R}_1(u)$. As one can see from (4.221) and (4.222), to compute $\mathcal{J}_1(y,u)$ it is sufficient to derive the conditional CDFs of (4.212), (4.213) and (4.214), while $\mathcal{J}_2(y)$ can be attained using (1.21) and (1.22).

To do so, we start by computing the conditional CDF of γ_R for a given g_{SP} as follows

$$\begin{aligned}F_{\gamma_R|g_{SP}=u}(y) &= \Pr(\gamma_R\le y\,|g_{SP}=u)\\ &\overset{(a)}{=} F_{g_{SR}}\left(\frac{y}{\Omega(u)}\right),\end{aligned} \tag{4.254}$$

where $\Omega(u)=\overline{\gamma}_S$ if $u\le\sigma_S$ and $\Omega(u)=\frac{\overline{\gamma}_I}{u}$ if $u>\sigma_S$, with σ_S is defined in Theorem 4.5.1, and step (a) holds by using (4.212).

- **Absence of friendly jammer case.**

Using (4.213), the conditional CDF of γ_{E_1} for a given g_{SP} can be expressed as

$$\begin{aligned}F_{\gamma_{E_1}|g_{SP}=u}(y) &= \Pr\left(\min\left(\overline{\gamma}_S,\frac{\overline{\gamma}_I}{u}\right)g_{SE_1}\le y\right)\\ &= F_{g_{SE_1}}\left(\frac{y}{\Omega(u)}\right).\end{aligned} \tag{4.255}$$

Substituting (4.254) and (4.255) into (4.221), yields

$$\mathcal{J}_1(y,u) = \frac{1}{\Omega(u)}f_{g_{SR}}\left(\frac{y}{\Omega(u)}\right)F_{g_{SE_1}}\left(\frac{y}{\Omega(u)}\right). \tag{4.256}$$

Now, using (1.21) and (1.22), the term $\mathcal{J}_1(y,u)$ can be rewritten as

$$\mathcal{J}_1(y,u) = \frac{\Delta_{SE_1}\Delta_{SR}e^{-\frac{\upsilon_{SR}}{\Omega(u)}y}}{\Omega(u)} \sum_{n_2=0}^{m_{SE_1}-1} \frac{\phi_{SE_1}^{(n_2)}}{\upsilon_{SE_1}^{n_2+1}} \gamma_{inc}\left(n_2{+}1, \frac{\upsilon_{SE_1}}{\Omega(u)}y\right) \sum_{n_3=0}^{m_{SR}-1} \frac{\phi_{SR}^{(n_3)}}{\Omega^{n_3}(u)} y^{n_3}. \tag{4.257}$$

Next, the term $\mathcal{J}_2(y)$ given in (4.222) can be expressed as

$$\mathcal{J}_2(y) = F_{\gamma_{E_2}}(y) - \int_{z=0}^{y} f_{\gamma_{E_2}}(z)\, F_{\gamma_D}(z)\, dz. \tag{4.258}$$

By substituting (1.16) and (1.17) into (4.258), we get

$$\mathcal{J}_2(y) = F_{\gamma_{E_2}}(y) - \theta \int_{z=0}^{y} \frac{1}{z} G_{1,3}^{3,0}\left(\frac{\Upsilon_{E_2} z}{\mu_1^{(E_2)}}\middle| \begin{matrix} -;\xi_{E_2}^2+1 \\ \xi_{E_2}^2, \alpha_{E_2}, \beta_{E_2}; - \end{matrix}\right) G_{2,4}^{3,1}\left(\frac{\Upsilon_D z}{\mu_1^{(D)}}\middle| \begin{matrix} 1;\xi_D^2+1 \\ \xi_D^2, \alpha_D, \beta_D; 0 \end{matrix}\right) dz, \tag{4.259}$$

where θ is defined in Theorem 4.5.1.

To compute (4.259), we can express one of the two Meijer's G-functions as an infinite sum of the respective integrand's residues evaluated at the appropriate poles [105, Theorem 1.5]. That is,

$$G_{2,4}^{3,1}\left(y\middle| \begin{matrix} 1-\tau;\xi_Z^2+1 \\ \xi_Z^2, \alpha_Z, \beta_Z; -\tau \end{matrix}\right) = e^{(Z,\tau)} y^{\xi_Z^2} + \sum_{k=0}^{\infty} e^{(Z,\tau,k)}(\beta_Z, \alpha_Z)\, y^{\alpha_Z+k} + \sum_{k=0}^{\infty} e^{(Z,\tau,k)}(\alpha_Z, \beta_Z)\, y^{\beta_Z+k}, \tag{4.260}$$

where $\tau = \{0, q\}$, q takes a value in the set $\{\xi_D^2, \alpha_D + k, \beta_D + k\}$, $e^{(Z,\tau)}$, and $e^{(Z,\tau,k)}(.,.)$ are defined in Theorem 4.5.1.

Substituting (4.260) into (4.259), yields

$$\mathcal{J}_2(y) = F_{\gamma_{E_2}^{(k)}}(y) - \theta \begin{bmatrix} e^{(D,0)}\mathcal{P}(\xi_D^2, y) \\ +\sum_{k=0}^{\infty} e^{(D,0,k)}(\beta_D, \alpha_D)\, \mathcal{P}(\alpha_D + k, y) \\ +\sum_{k=0}^{\infty} e^{(D,0,k)}(\alpha_D, \beta_D)\, \mathcal{P}(\beta_D + k, y) \end{bmatrix}, \tag{4.261}$$

with

$$\mathcal{P}\left(q,y\right)=\left(\frac{\Upsilon_D}{\mu_1^{(D)}}\right)^q\int_0^y z^{q-1}G_{1,3}^{3,0}\left(\frac{\Upsilon_{E_2}z}{\mu_1^{(E_2)}}\middle|\begin{matrix}-;\xi_{E_2}^2+1\\ \xi_{E_2}^2,\alpha_{E_2},\beta_{E_2};-\end{matrix}\right)dz \tag{4.262}$$
$$\overset{(a)}{=}\left(\frac{\Upsilon_D y}{\mu_1^{(D)}}\right)^q G_{2,4}^{3,1}\left(\frac{\Upsilon_{E_2}y}{\mu_1^{(E_2)}}\middle|\begin{matrix}1-q;\xi_{E_2}^2+1\\ \xi_{E_2}^2,\alpha_{E_2},\beta_{E_2};-q\end{matrix}\right),$$

where step (a) follows using [71, Eq. 07.34.21.0003.01].

Replacing, (4.257) and (4.261) into (4.220), one can obtain

$$\mathcal{R}_1\left(u\right)=\frac{\xi_{E_2}^2\mathcal{L}_1^{(0)}\left(u\right)}{\Gamma\left(\alpha_{E_2}\right)\Gamma\left(\beta_{E_2}\right)}-\theta\left[\begin{matrix}e^{(D,0)}\mathcal{L}_1^{\left(\xi_D^2\right)}\left(u\right)\\ +\sum_{k=0}^{\infty}e^{(D,0,k)}\left(\beta_D,\alpha_D\right)\mathcal{L}_1^{(\alpha_D+k)}\left(u\right)\\ +\sum_{k=0}^{\infty}e^{(D,0,k)}\left(\alpha_D,\beta_D\right)\mathcal{L}_1^{(\beta_D+k)}\left(u\right)\end{matrix}\right], \tag{4.263}$$

where

$$\mathcal{L}_1^{(\tau)}\left(u\right)=\Delta_{SE_1}\Delta_{SR}\left(\frac{\Upsilon_D}{\mu_1^{(D)}}\right)^{\tau}\sum_{n_2=0}^{m_{SE_1}-1}\frac{\phi_{SE_1}^{(n_2)}}{\upsilon_{SE_1}^{n_2+1}}\sum_{n_3=0}^{m_{SR}-1}\frac{\phi_{SR}^{(n_3)}}{\Omega^{n_3+1}\left(u\right)}\int_{y=\gamma_{th}}^{\infty}y^{\tau+n_3}\gamma_{inc}\left(n_2{+}1,\frac{\upsilon_{SE_1}}{\Omega\left(u\right)}y\right)e^{-\frac{\upsilon_{SR}}{\Omega(u)}y} \tag{4.264}$$
$$\times\,G_{2,4}^{3,1}\left(\frac{\Upsilon_{E_2}y}{\mu_1^{(E_2)}}\middle|\begin{matrix}1-\tau;\xi_{E_2}^2+1\\ \xi_{E_2}^2,\alpha_{E_2},\beta_{E_2};-\tau\end{matrix}\right)dy.$$

Now, replacing (4.260) into (4.264), yields

$$\mathcal{L}_1^{(\tau)}\left(u\right)=\Delta_{SE_1}\Delta_{SR}\left(\frac{\Upsilon_D}{\mu_1^{(D)}}\right)^{\tau}\sum_{n_2=0}^{m_{SE_1}-1}\frac{\phi_{SE_1}^{(n_2)}}{\upsilon_{SE_1}^{n_2+1}}\sum_{n_3=0}^{m_{SR}-1}\frac{\phi_{SR}^{(n_3)}}{\Omega^{n_3+1}\left(u\right)} \tag{4.265}$$
$$\times\left[\begin{matrix}e^{(E_2,\tau)}\digamma_1^{\left(n_2,n_3,\xi_{E_2}^2,\tau\right)}\left(u\right)\\ +\sum_{k=0}^{\infty}e^{(E_2,\tau,k)}\left(\beta_{E_2},\alpha_{E_2}\right)\digamma_1^{\left(n_2,n_3,\alpha_{E_2}+k,\tau\right)}\left(u\right)\\ +\sum_{k=0}^{\infty}e^{(E_2,\tau,k)}\left(\alpha_{E_2},\beta_{E_2}\right)\digamma_1^{\left(n_2,n_3,\beta_{E_2}+k,\tau\right)}\left(u\right)\end{matrix}\right],$$

with

$$\digamma_1^{(n_2,n_3,a,\tau)}\left(u\right)=\left(\frac{\Upsilon_{E_2}}{\mu_1^{(E_2)}}\right)^a\int_{y=\gamma_{th}}^{\infty}y^{\tau+n_3+a}e^{-\frac{\upsilon_{SR}}{\Omega(u)}y}\gamma_{inc}\left(n_2{+}1,\frac{\upsilon_{SE_1}}{\Omega\left(u\right)}y\right)dy, \tag{4.266}$$

where a belongs to the set $\{\xi_{E_2}^2, \alpha_{E_2}+k, \beta_{E_2}+k\}$.

Using [71, Eq. (06.06.26.0004.01)], (4.266) can be expressed as

$$F_1^{(n_2,n_3,a,\tau)}(u) = \left(\frac{\Upsilon_{E_2}}{\mu_1^{(E_2)}}\right)^a \left(\frac{\Omega(u)}{\upsilon_{SR}}\right)^{l+1} G_{2,2}^{1,2}\left(\frac{\upsilon_{SE_1}}{\upsilon_{SR}}\middle|\begin{matrix}(1,0),(-l,\varsigma);-\\(n_2{+}1,0);(0,0)\end{matrix}\right), \tag{4.267}$$

with $l = n_3+\tau+a$ and $\varsigma = \frac{\gamma_{th}\upsilon_{SR}}{\Omega(u)}$.

Now, substituting (4.263) into (4.219), the IP in the absence of a friendly jammer can be written as

$$\mathrm{IP}_A = 1 - \frac{\xi_{E_2}^2 \mathcal{D}_A^{(0)}}{\Gamma(\alpha_{E_2})\Gamma(\beta_{E_2})} + \theta\left[\begin{matrix} e^{(D,0)}\mathcal{D}_A^{(\xi_D^2)} \\ +\sum_{k=0}^{\infty} e^{(D,0,k)}(\beta_D,\alpha_D)\,\mathcal{D}_A^{(\alpha_D+k)} \\ +\sum_{k=0}^{\infty} e^{(D,0,k)}(\alpha_D,\beta_D)\,\mathcal{D}_A^{(\beta_D+k)}\end{matrix}\right], \tag{4.268}$$

where

$$\mathcal{D}_A^{(\tau)} = \frac{\Upsilon_D^{\tau}}{\left(\mu_1^{(D)}\right)^{\tau}} \int_{u=0}^{\infty} f_{g_{SP}}(u)\,\mathcal{L}_1^{(\tau)}(u)\,du, \tag{4.269}$$

To compute (4.269), we need to replace $\Omega(u)$ by its values. Therefore, when $u \le \sigma_S$ the term $\mathcal{L}_1^{(\tau)}(u)$ becomes constant. Thus,

$$\mathcal{D}_A^{(\tau)} = \frac{\Upsilon_D^{\tau}}{\left(\mu_1^{(D)}\right)^{\tau}} \left[\mathcal{L}_2^{(\tau)}(\overline{\gamma}_S) F_{g_{SP}}(\sigma_S) + \lambda_{SP}\mathcal{L}_2^{(\tau)}(\overline{\gamma}_I)\right], \tag{4.270}$$

with $\mathcal{L}_2^{(\tau)}(\overline{\gamma}_I) = \int_{\sigma_S}^{\infty} e^{-\lambda_{SP}u}\mathcal{L}_1^{(\tau)}(u)\,du$.

The terms $\mathcal{L}_2^{(\tau)}(\overline{\gamma}_S)$ and $\mathcal{L}_2^{(\tau)}(\overline{\gamma}_I)$ can be obtained by replacing $\Omega(u) = \overline{\gamma}_S$ and $\Omega(u) = \frac{\overline{\gamma}_I}{u}$ in (4.265) and (4.267), respectively. Therefore, $\mathcal{L}_2^{(\tau)}(\overline{\gamma}_I)$ can be rewritten as

$$\mathcal{L}_2^{(\tau)}(\overline{\gamma}_I) = \Delta_{SE_1}\Delta_{SR}\left(\frac{\Upsilon_D}{\mu_1^{(D)}}\right)^{\tau} \sum_{n_3=0}^{m_{SR}-1} \frac{\phi_{SR}^{(n_3)}}{\overline{\gamma}_I^{n_3+1}} \sum_{n_2=0}^{m_{SE_1}-1} \frac{\phi_{SE_1}^{(n_2)}}{\upsilon_{SE_1}^{n_2+1}} \tag{4.271}$$
$$\times \left[\begin{matrix} e^{(E_2,\tau)}F_2^{\left(n_2,n_3,\xi_{E_2}^2,\tau\right)} \\ +\sum_{k=0}^{\infty} e^{(E_2,\tau,k)}\left(\beta_{E_2},\alpha_{E_2}\right) F_2^{\left(n_2,n_3,\alpha_{E_2}+k,\tau\right)} \\ +\sum_{k=0}^{\infty} e^{(E_2,\tau,k)}\left(\alpha_{E_2},\beta_{E_2}\right) F_2^{\left(n_2,n_3,\beta_{E_2}+k,\tau\right)}\end{matrix}\right],$$

where

$$\begin{aligned} F_2^{(n_2,n_3,a,\tau)} &= \left(\frac{\Upsilon_{E_2}}{\mu_1^{(E_2)}}\right)^a \int_{\sigma_S}^{\infty} e^{-\lambda_{SP}u} u^{n_3+1} F_1^{\left(n_2,n_3,\alpha_{E_2}+k,\tau\right)}(u)\, du \qquad (4.272)\\ &= \left(\frac{\overline{\gamma}_I}{\upsilon_{SR}}\right)^{\tau+n_3+a+1} \frac{1}{2\pi j} \int_{\mathcal{C}_s} \frac{\Gamma(n_2{+}1+s)\,\Gamma(-s)}{\Gamma(1-s)} \left(\frac{\upsilon_{SE_1}}{\upsilon_{SR}}\right)^{-s} \int_{\sigma_S}^{\infty} u^{-\tau-a} e^{-\lambda_{SP}u} \\ &\quad \times \Gamma(1+n_3+\tau+a-s, \epsilon_I \upsilon_{SR} u)\, ds du, \end{aligned}$$

where ϵ_I is defined in Theorem 4.5.1.

Using [71, Eq. (06.06.26.0005.01)], one obtains

$$\begin{aligned} F_2^{(n_2,n_3,a,\tau)} &= \left(\frac{\Upsilon_{E_2}}{\mu_1^{(E_2)}}\right)^a \left(\frac{\overline{\gamma}_I}{\upsilon_{SR}}\right)^{\tau+n_3+a+1} \frac{\lambda_{SP}^{a+\tau-1}}{(2\pi j)^2} \int_{\mathcal{C}_s} \frac{\Gamma(n_2{+}1+s)\,\Gamma(-s)}{\Gamma(1-s)} \left(\frac{\upsilon_{SE_1}}{\upsilon_{SR}}\right)^{-s} \qquad (4.273)\\ &\quad \times \int_{\mathcal{C}_w} \frac{\Gamma(-\tau-a-w+1, \lambda_{SP}\sigma_S)\,(\epsilon_I \upsilon_{SR})^{-w}\,\Gamma(\tau+n_3+a+1-s+w)}{w \lambda_{SP}^{-w}} dw ds, \end{aligned}$$

- **Presence of a friendly jammer**.

Using (4.214), the conditional CDF of $\gamma_{E_1}^{(J)}$ for a given g_{SP} can be expressed as

$$\begin{aligned} F_{\gamma_{E_1}^{(J)}|g_{SP}=u}(y) &= \Pr\left(\mathcal{U}_S \le y\left(\mathcal{U}_{S_J}+1\right)\right) \qquad (4.274a)\\ &= 1 - \frac{y}{\Omega(u)} \int_0^{\infty} f_{g_{SE_1}}\left(\frac{y(t+1)}{\Omega(u)}\right) F_{\mathcal{U}_{S_J}}(t)\, dt, \qquad (4.274b) \end{aligned}$$

where (4.274b) holds by using integration by parts.

On the other hand, the CDF of $\mathcal{U}_{S_J}$ is given by

$$\begin{aligned} F_{\mathcal{U}_{S_J}}(t) &= \Pr\left(\min\left(\overline{\gamma}_{S_J}, \frac{\overline{\gamma}_I}{g_{S_JP}}\right) g_{S_JE_1} \le t\right) \qquad (4.275)\\ &= F_{g_{S_JE_1}}\left(\frac{t}{\overline{\gamma}_{S_J}}\right) F_{g_{S_JP}}(\sigma_{S_J}) + \underbrace{\int_{\sigma_{S_J}}^{\infty} F_{g_{S_JE_1}}\left(\frac{t}{\overline{\gamma}_I} y\right) f_{g_{S_JP}}(y)\, dy}_{\mathcal{K}_1}. \end{aligned}$$

where σ_{S_J} is defined in Theorem 4.5.1.

Using (1.22) and [71, Eq. (06.06.26.0004.01)], the term $\mathcal{K}_1$ can be expressed as

$$\mathcal{K}_1 = \lambda_{S_JP}\Delta_{S_JE_1}\sum_{n_1=0}^{m_{S_JE_1}-1}\frac{\phi_{S_JE_1}^{(n_1)}}{\upsilon_{S_JE_1}^{n_1+1}}\int_{\sigma_{S_J}}^{\infty}e^{-\lambda_{S_JP}y}G_{1,2}^{1,1}\left(\frac{\upsilon_{S_JE_1}t}{\overline{\gamma}_I}y\middle|\begin{matrix}1;-\\ n_1+1;0\end{matrix}\right)dy \tag{4.276}$$
$$= \Delta_{S_JE_1}\sum_{n_1=0}^{m_{S_JE_1}-1}\frac{\phi_{S_JE_1}^{(n_1)}}{\upsilon_{S_JE_1}^{n_1+1}}G_{2,2}^{1,2}\left(\frac{\upsilon_{S_JE_1}t}{\overline{\gamma}_I\lambda_{S_JP}}\middle|\begin{matrix}(1,0),(0,\sigma_{S_J}\lambda_{S_JP});-\\ (n_1+1,0);(0,0)\end{matrix}\right).$$

Substituting (4.276) into (4.275), yields the CDF of $\mathcal{U}_{S_J}$

$$F_{\mathcal{U}_{S_J}}(t) = F_{g_{S_JE_1}}\left(\frac{t}{\overline{\gamma}_{S_J}}\right)F_{g_{S_JP}}(\sigma_{S_J})+\Delta_{S_JE_1}\sum_{n_1=0}^{m_{S_JE_1}-1}\frac{\phi_{S_JE_1}^{(n_1)}}{\upsilon_{S_JE_1}^{n_1+1}}G_{2,2}^{1,2}\left(\frac{\upsilon_{S_JE_1}t}{\overline{\gamma}_I\lambda_{S_JP}}\middle|\begin{matrix}(1,0),(0,\sigma_{S_J}\lambda_{S_JP});-\\ (n_1+1,0);(0,0)\end{matrix}\right). \tag{4.277}$$

Now, replacing (4.277) into (4.275), the CDF of γ_{E_1} can be expressed as

$$F_{\gamma_{E_1}^{(J)}|g_{SP}=u}(y) = 1-\frac{y\Delta_{SE_1}}{\Omega(u)}e^{-\frac{\upsilon_{SE_1}}{\Omega(u)}y}\sum_{n_2=0}^{m_{SE_1}-1}\frac{\phi_{SE_1}^{(n_2)}y^{n_2}}{\Omega^{n_2}(u)}\sum_{p=0}^{n_2}\binom{n_2}{p}\Delta_{S_JE_1} \tag{4.278}$$
$$\times\sum_{n_1=0}^{m_{S_JE_1}-1}\frac{\phi_{S_JE_1}^{(n_1)}}{\upsilon_{S_JE_1}^{n_1+1}}\left[F_{g_{S_JP}}(\sigma_{S_J})\mathcal{V}_1(y,u)+\mathcal{V}_2(y,u)\right]dt,$$

where

$$\mathcal{V}_1(y,u) = \int_0^{\infty}t^p e^{-\frac{\upsilon_{SE_1}y}{\Omega(u)}t}\gamma_{inc}\left(n_1+1,\frac{\upsilon_{S_JE_1}}{\overline{\gamma}_{S_J}}t\right)dt, \tag{4.279}$$

and

$$\mathcal{V}_2(y,u) = \int_0^{\infty}t^p e^{-\frac{\upsilon_{SE_1}y}{\Omega(u)}t}G_{2,2}^{1,2}\left(\frac{\upsilon_{S_JE_1}t}{\overline{\gamma}_I\lambda_{S_JP}}\middle|\begin{matrix}(1,0),(0,\sigma_{S_J}\lambda_{S_JP});-\\ (n_1+1,0);(0,0)\end{matrix}\right)dt, \tag{4.280}$$

Using [71, Eq.(07.34.21.0088.01)], the term $\mathcal{V}_1(y,u)$ can be expressed as

$$\mathcal{V}_1(y,u) = \left(\frac{\Omega(u)}{\upsilon_{SE_1}y}\right)^{p+1}G_{2,2}^{1,2}\left(\frac{\upsilon_{S_JE_1}\Omega(u)}{\upsilon_{SE_1}\overline{\gamma}_{S_J}y}\middle|\begin{matrix}-p,1;-\\ n_1+1;0\end{matrix}\right), \tag{4.281}$$

while the term $\mathcal{V}_2(y,u)$ can be evaluated as

$$\mathcal{V}_2(y,u) = \left(\frac{\Omega(u)}{\upsilon_{SE_1}y}\right)^{p+1}G_{3,2}^{1,3}\left(\frac{\upsilon_{S_JE_1}\Omega(u)}{\lambda_{S_JP}\upsilon_{SE_1}\overline{\gamma}_I y}\middle|\begin{matrix}(1,0),(0,\sigma_{S_J}\lambda_{S_JP}),(-p,0);-\\ (n_1+1,0);(0,0)\end{matrix}\right). \tag{4.282}$$

Replacing (4.281) and (4.282) into (4.278), and then substituting the obtained expression of $F_{\gamma_{E_1}|g_{SP}=u}(y)$ alongside (4.254) into (4.221), the term $\mathcal{J}_1(y,u)$ can be expressed as

$$\begin{aligned}\mathcal{J}_1(y,u) &= \Delta_{SR}\sum_{n_3=0}^{m_{SR}-1}\frac{\phi_{SR}^{(n_3)}y^{n_3}}{\Omega^{n3+1}(u)}e^{-\frac{\upsilon_{SR}}{\Omega(u)}y} - \Delta_{SR}\Delta_{S_JE_1}\Delta_{SE_1} \\ &\times \sum_{n_1=0}^{m_{S_JE_1}-1}\sum_{n_2=0}^{m_{SE_1}-1}\sum_{p=0}^{n_2}\sum_{n_3=0}^{m_{SR}-1}\frac{\mathcal{B}^{(n_1,n_2,n_3,p)}e^{-\frac{\zeta}{\Omega(u)}y}}{\Omega^{n_2+n_3-p+1}(u)}y^{n_2+n_3-p} \\ &\times \left[\begin{array}{c} F_{g_{S_JP}}(\sigma_{S_J})\,G_{2,2}^{1,2}\left(\frac{\upsilon_{S_JE_1}\Omega(u)}{\upsilon_{SE_1}\overline{\gamma}_{S_J}y}\middle|\begin{array}{c}-p,1;-\\ n_1+1;0\end{array}\right) \\ +G_{3,2}^{1,3}\left(\frac{\upsilon_{S_JE_1}\Omega(u)}{\lambda_{S_JP}\upsilon_{SE_1}\overline{\gamma}_I y}\middle|\begin{array}{c}(1,0),(0,\sigma_{S_J}\lambda_{S_JP}),(-p,0);-\\ (n_1+1,0);(0,0)\end{array}\right)\end{array}\right],\end{aligned} \tag{4.283}$$

where $\mathcal{B}^{(n_1,n_2,n_3,p)}$ is defined in Theorem 4.5.1.

Now, substituting (4.283) and (4.261) into (4.220), the term $\mathcal{U}_1(u)$ can be expressed as

$$\mathcal{U}_1(u) = \frac{\xi_{E_2}^2\mathcal{T}_1^{(0)}(u)}{\Gamma(\alpha_{E_2})\Gamma(\beta_{E_2})} - \theta\left[\begin{array}{c} e^{(D,0)}\mathcal{T}_1^{\left(\xi_D^2\right)}(u) \\ +\sum_{k=0}^{\infty}e^{(D,0,k)}(\beta_D,\alpha_D)\,\mathcal{T}_1^{(\alpha_D+k)}(u) \\ +\sum_{k=0}^{\infty}e^{(D,0,k)}(\alpha_D,\beta_D)\,\mathcal{T}_1^{\beta_D+k}(u)\end{array}\right], \tag{4.284}$$

where

$$\mathcal{T}_1^{(\tau)}(u) = \left(\frac{\Upsilon_D}{\mu_1^{(D)}}\right)^{\tau}\int_{y=\gamma_{th}}^{\infty}\frac{\mathcal{J}_1(y,u)}{y^{-\tau}}G_{2,4}^{3,1}\left(\frac{\Upsilon_{E_2}y}{\mu_1^{(E_2)}}\middle|\begin{array}{c}1-\tau;\xi_{E_2}^2+1\\ \xi_{E_2}^2,\alpha_{E_2},\beta_{E_2};-\tau\end{array}\right). \tag{4.285}$$

Using (4.283), the terms $\mathcal{T}_1^{(\tau)}(u)$ can be expressed as

$$\begin{aligned}\mathcal{T}_1^{(\tau)}(u) &= \Delta_{SR}\left(\frac{\Upsilon_D}{\mu_1^{(D)}}\right)^{\tau}\sum_{n_3=0}^{m_{SR}-1}\frac{\phi_{SR}^{(n_3)}\Theta_1^{(n_3,\tau)}(u)}{\Omega^{n3+1}(u)} - \Delta_{SR}\Delta_{S_JE_1}\Delta_{SE_1}\left(\frac{\Upsilon_D}{\mu_1^{(D)}}\right)^{\tau} \\ &\times \sum_{n_1=0}^{m_{S_JE_1}-1}\sum_{n_2=0}^{m_{SE_1}-1}\sum_{p=0}^{n_2}\sum_{n_3=0}^{m_{SR}-1}\frac{\mathcal{B}^{(n_1,n_2,n_3,p)}}{\Omega^{n_2-p+n_3+1}(u)}\left[F_{g_{S_JP}}(\sigma_{S_J})\,\Theta_2^{(n_1,n_2,n_3,p,\tau)}(u)+\Theta_3^{(n_1,n_2,n_3,p,\tau)}(u)\right],\end{aligned} \tag{4.286}$$

where

$$\Theta_1^{(n_3,\tau)}(u)=\int_{\gamma_{th}}^{\infty}\frac{e^{-\frac{\upsilon_{SR}}{\Omega(u)}y}}{y^{-n_3-\tau}}G_{2,4}^{3,1}\left(\frac{\Upsilon_{E_2}y}{\mu_1^{(E_2)}}\middle|\begin{matrix}1-\tau;\xi_{E_2}^2+1\\ \xi_{E_2}^2,\alpha_{E_2},\beta_{E_2};-\tau\end{matrix}\right)dy, \tag{4.287}$$

$$\begin{aligned}\Theta_2^{(n_1,n_2,n_3,p,\tau)}(u)=&\int_{\gamma_{th}}^{\infty}\frac{e^{-\frac{\zeta}{\Omega(u)}y}}{y^{-n_2-n_3+p-\tau}}G_{2,4}^{3,1}\left(\frac{\Upsilon_{E_2}y}{\mu_1^{(E_2)}}\middle|\begin{matrix}1-\tau;\xi_{E_2}^2+1\\ \xi_{E_2}^2,\alpha_{E_2},\beta_{E_2};-\tau\end{matrix}\right)\\ &\times G_{2,2}^{1,2}\left(\frac{\upsilon_{S_JE_1}\Omega(u)}{\upsilon_{SE_1}\overline{\gamma}_{S_J}y}\middle|\begin{matrix}-p,1;-\\ n_1+1;0\end{matrix}\right)dy,\end{aligned} \tag{4.288}$$

and

$$\Theta_3^{(n_1,n_2,n_3,p,\tau)}(u)=\int_{y=\gamma_{th}}^{\infty}\frac{e^{-\frac{\zeta}{\Omega(u)}y}}{y^{-n_2-n_3+p-\tau}}G_{3,2}^{1,3}\left(\frac{\upsilon_{S_JE_1}\Omega(u)}{\lambda_{S_JP}\upsilon_{SE_1}\overline{\gamma}_Iy}\middle|\begin{matrix}(1,0),(0,\sigma_{S_J}\lambda_{S_JP}),(-p,0);-\\ (n_1+1,0);(0,0)\end{matrix}\right) \tag{4.289}$$

$$\times G_{2,4}^{3,1}\left(\frac{\Upsilon_{E_2}y}{\mu_1^{(E_2)}}\middle|\begin{matrix}1-\tau;\xi_{E_2}^2+1\\ \xi_{E_2}^2,\alpha_{E_2},\beta_{E_2};-\tau\end{matrix}\right)dy,$$

Using (4.260), (4.287) can be expressed as

$$\begin{aligned}\Theta_1^{(n_3,\tau)}(u)=&e^{(E_2,\tau)}\Lambda_1^{\left(n_3,\xi_{E_2}^2,\tau\right)}(u)+\sum_{k=0}^{\infty}e^{(E_2,\tau,k)}\left(\beta_{E_2},\alpha_{E_2}\right)\Lambda_1^{\left(n_3,\alpha_{E_2}+k,\tau\right)}(u)\\ &+\sum_{k=0}^{\infty}e^{(E_2,\tau,k)}\left(\alpha_{E_2},\beta_{E_2}\right)\Lambda_1^{\left(n_3,\beta_{E_2}+k,\tau\right)}(u),\end{aligned} \tag{4.290}$$

where

$$\Lambda_1^{(n_3,a,\tau)}(u)=\left(\frac{\Upsilon_{E_2}}{\mu_1^{(E_2)}}\right)^a\left(\frac{\Omega(u)}{\upsilon_{SR}}\right)^{\tau+n_3+a+1}\Gamma\left(\tau+n_3+a+1,\frac{\gamma_{th}\upsilon_{SR}}{\Omega(u)}\right), \tag{4.291}$$

$g(a,u,\tau)=$ and $a=\{\xi_{E_2}^2,\alpha_{E_2}+k,\beta_{E_2}+k\}$.

Similarly to (4.290), (4.288) can be expressed as

$$\Theta_2^{(n_1,n_2,n_3,p,\tau)}(u)=e^{(E_2,\tau)}\mathcal{M}_1^{\left(n_1,n_2,n_3,p,\xi_{E_2}^2,\tau\right)}(u)+\sum_{k=0}^{\infty}\Lambda_2^{\left(\alpha_{E_2}+k\right)}(u,\beta_{E_2},\alpha_{E_2})+\sum_{k=0}^{\infty}\Lambda_2^{\left(\beta_{E_2}+k\right)}(u,\alpha_{E_2},\beta_{E_2}), \tag{4.292}$$

where

$$\Lambda_2^{(a)}(u,x,y)=e^{(E_2,\tau,k)}(x,y)\,\mathcal{M}_1^{(n_1,n_2,n_3,p,a,\tau)}(u), \tag{4.293}$$

$$\mathcal{M}_1^{(n_1,n_2,n_3,p,a,\tau)}(u)=\left(\frac{\Upsilon_{E_2}}{\mu_1^{(E_2)}}\right)^a\left(\frac{\Omega(u)}{\zeta}\right)^{\varkappa}\mathcal{H}_1(u), \tag{4.294}$$

with $\varkappa=n_2+n_3-p+1+a+\tau$, $\mathcal{H}_1(u)=G_{2,3}^{2,2}\left(\begin{matrix}\frac{\chi}{\overline{\gamma}_{S_J}}\\ \end{matrix}\middle|\begin{matrix}(-p,0),(1,0);-\\ (n_1{+}1,0),\left(\varkappa,\frac{\zeta\gamma_{th}}{\Omega(u)}\right);(0,0)\end{matrix}\right)$, and χ is defined in Theorem 4.5.1.

Analogously to (4.288) and (4.289), the term $\Theta_3^{(n_2,n_3,p)}(u)$ can be evaluated as

$$\Theta_3^{(n_1,n_2,n_3,p,\tau)}(u)=e^{(E_2,\tau)}\Phi_1^{\left(n_1,n_2,n_3,p,\xi_{E_2}^2,\tau\right)}(u)+\sum_{k=0}^{\infty}\Lambda_3^{\left(\alpha_{E_2}+k\right)}(u,\beta_{E_2},\alpha_{E_2})+\sum_{k=0}^{\infty}\Lambda_3^{\left(\beta_{E_2}+k\right)}(u,\alpha_{E_2},\beta_{E_2}), \tag{4.295}$$

where

$$\Lambda_3^{(a)}(u,x,y)=e^{(E_2,\tau,k)}(x,y)\,\Phi_1^{(n_1,n_2,n_3,p,a,\tau)}(u), \tag{4.296}$$

$$\Phi_1^{(n_1,n_2,n_3,p,a,\tau)}(u)=\left(\frac{\Upsilon_{E_2}}{\mu_1^{(E_2)}}\right)^a\left(\frac{\Omega(u)}{\zeta}\right)^{\varkappa}G_{3,3}^{2,3}\left(b\middle|\begin{matrix}(-p,0),(1,0),(0,c);-\\ (n_1{+}1,0),(\varkappa,v);(0,0)\end{matrix}\right). \tag{4.297}$$

where $b=\frac{\chi}{\lambda_{S_JP}\overline{\gamma}_I}$, $c=\ \sigma_{S_J}\lambda_{S_JP}$, and $v=\frac{\zeta\gamma_{th}}{\Omega(u)}$.

Now, the remaining last step in this proof consists of computing the expression for the IP in the presence of a friendly jammer by incorporating (4.284) into (4.219) as

$$\mathrm{IP}_P=1-\frac{\xi_{E_2}^2\mathcal{D}_P^{(0)}}{\Gamma(\alpha_{E_2})\Gamma(\beta_{E_2})}+\theta\left[\begin{matrix}e^{(D,0)}\mathcal{D}_P^{\left(\xi_D^2\right)}\\ +\sum_{k=0}^{\infty}e^{(D,0,k)}(\beta_D,\alpha_D)\,\mathcal{D}_P^{(\alpha_D+k)}\\ +\sum_{k=0}^{\infty}e^{(D,0,k)}(\alpha_D,\beta_D)\,\mathcal{D}_P^{(\beta_D+k)}\end{matrix}\right], \tag{4.298}$$

where

$$\mathcal{D}_P^{(\tau)}=\frac{\Upsilon_D^{\tau}}{\left(\mu_1^{(D)}\right)^{\tau}}\int_{u=0}^{\infty}f_{g_{SP}}(u)\,\mathcal{T}_1^{(\tau)}(u)\,du. \tag{4.299}$$

To compute (4.299), we need to replace $\Omega(u)$ by its values in (4.286). Therefore, when $u\leq\sigma_S$,

the term $\mathcal{T}_1^{(\tau)}(u)$ becomes constant. It follows that

$$\mathcal{D}_P^{(\tau)} = \frac{\mathcal{T}_2^{(\tau)}(\overline{\gamma}_S) F_{g_{SP}}(\sigma_S) + \lambda_{SP}\mathcal{T}_2^{(\tau)}(\overline{\gamma}_I)}{\left(\mu_1^{(D)}\right)^{\tau}}, \tag{4.300}$$

with $\mathcal{T}_2^{(\tau)}(\overline{\gamma}_I) = \int_{\sigma_S}^{\infty} e^{-\lambda_{SP}u}\mathcal{T}_1^{(\tau)}(u)$, while the term $\mathcal{T}_2^{(\tau)}(\overline{\gamma}_S)$ can be obtained by replacing $\Omega(u) = \overline{\gamma}_S$ in (4.286).

Also, to compute $\mathcal{T}_2^{(\tau)}(\overline{\gamma}_I)$, we need to replace $\Omega(u) = \frac{\overline{\gamma}_I}{u}$ in (4.286) and compute the following integrals

$$\mathcal{S}^{(n_3,a,\tau)} = \int_{\sigma_S}^{\infty} \frac{e^{-\lambda_{SP}u}}{u^{a+\tau}}\Gamma(\tau + n_3 + a + 1, \epsilon_I \upsilon_{SR} u)\, du, \tag{4.301}$$

$$\mathcal{Y}^{(n_1,n_2,n_3,p,a,\tau)} = \int_{\sigma_S}^{\infty} \frac{e^{-\lambda_{SP}u}}{u^{a+\tau}}\mathcal{M}_1^{(n_1,n_2,n_3,p,a,\tau)}(u)\, du, \tag{4.302}$$

and

$$\mathcal{W}^{(n_1,n_2,n_3,p,a,\tau)} = \int_{\sigma_S}^{\infty} \frac{e^{-\lambda_{SP}u}}{u^{a+\tau}}\Phi_1^{(n_1,n_2,n_3,p,a,\tau)}(u)\, du, \tag{4.303}$$

where ϵ_I is defined in Theorem 4.5.1.

Using [71, Eq. 06.06.26.0005.01], (4.301) can be expressed as

$$\mathcal{S}^{(n_3,a,\tau)} = \lambda_{SP}^{a+\tau-1} G_{2,2}^{2,1}\left(\frac{\epsilon_I \upsilon_{SR}}{\lambda_{SP}}\,\middle|\, \begin{matrix}(a+\tau, \lambda_{SP}\sigma_S);(1,0)\\ (0,0),(\tau+n_3+a+1,0);-\end{matrix}\right), \tag{4.304}$$

while (4.302) and (4.303) can be evaluated by replacing $\Omega(u) = \frac{\overline{\gamma}_I}{u}$ into (4.294) and (4.297), respectively, and calculating the following common integral

$$\begin{aligned}\mathcal{A}^{(n_1,n_2,n_3,p,\tau)} &= \int_{\sigma_S}^{\infty} u^{-a-\tau} e^{-\lambda_{SP}u}\Gamma(\varkappa + s, \epsilon_I\zeta u)\, du \\ &\overset{(a)}{=} \frac{1}{2\pi j}\int_{\mathcal{C}_w} \frac{\Gamma(w)\Gamma(\varkappa+s+w)}{\Gamma(1+w)}\left(\frac{\epsilon_I\zeta}{\lambda_{SP}}\right)^{-w} \frac{\Gamma(1-a-\tau-w, \sigma_S\lambda_{SP})}{\lambda_{SP}^{-a-\tau+1}} dw,\end{aligned} \tag{4.305}$$

where step (a) follows using [71, Eq. 06.06.26.0005.01].

Finally, substituting (4.305) into (4.302) and (4.303), one obtains (4.251) and (4.253) which concludes the proof of Theorem 4.5.1. ■

Asymptotic IP

In this subsection, we provide an asymptotic analysis of the derived closed-form expression for the IP in high SNR regime. It can be noticed from (4.250), (4.252), (4.251), and (4.253) that the expression for the IP can be approximated for high SNR values by considering $\overline{\gamma}_I \to \infty$.

Theorem 4.5.2. *The Asymptotic expression for the* IP *in the presence of a friendly jammer is given by (4.308), with*

$$\Psi_2^{(0,n_2,n_3,p,a,\tau)} = \sigma_{S_J} \mathcal{V}^{(n_2,n_3,p,a,\tau)}, \tag{4.306}$$

$$\Psi_3^{(0,n_2,n_3,p,a,\tau)} = \frac{\Gamma\left(2+n_1, \sigma_{S_J}\lambda_{S_JP}\right)}{\lambda_{S_JP}}\ \mathcal{V}^{(n_2,n_3,p,a,\tau)}, \tag{4.307}$$

and $\mathcal{V}^{(n_2,n_3,p,a,\tau)}$ is given by (4.311) as shown at the same aforementioned page.

$$\mathrm{IP}_P^{(\infty)} \sim 1 - \frac{\xi_{E_2}^2 \mathcal{D}_P^{(0,\infty)}}{\Gamma\left(\alpha_{E_2}\right)\Gamma\left(\beta_{E_2}\right)} + \theta \left[\begin{array}{c} e^{(D,0)} \mathcal{D}_P^{\left(\xi_D^2,\infty\right)} + \sum_{k=0}^{\infty} e^{(D,0,k)}\left(\beta_D, \alpha_D\right) \mathcal{D}_P^{(\alpha_D+i,\infty)} \\ + e^{(D,0,k)}\left(\alpha_D, \beta_D\right) \mathcal{D}_P^{(\beta_D+k,\infty)} \end{array} \right]. \tag{4.308}$$

$$\mathcal{D}_P^{(\tau,\infty)} = \Upsilon_D^{\tau} \Delta_{SR} \left[\begin{array}{c} \sum_{n_3=0}^{m_{SR}-1} \phi_{SR}^{(n_3)} \Xi_1^{(n_3,\tau)} - \Delta_{SE_1}\Delta_{S_JE_1} \sum_{n_2=0}^{m_{SE_1}-1} \sum_{p=0}^{n_2} \sum_{n_3=0}^{m_{SR}-1} \\ \times \left\{ F_{g_{S_JP}}\left(\sigma_{S_J}\right) \Xi_2^{(0,n_2,n_3,p,\tau)} + \Xi_3^{(0,n_2,n_3,p,\tau)} \right\} \mathcal{B}^{(n_1,n_2,n_3,p)} \end{array} \right]. \tag{4.309}$$

$$\begin{aligned} \Xi_n^{(0,n_2,n_3,p,\tau)} &= e^{(E_2,\tau)} \Psi_n^{\left(0,n_2,n_3,p,\xi_{E_2}^2,\tau\right)} + \sum_{k=0}^{\infty} e^{(E_2,\tau,k)}\left(\beta_{E_2}, \alpha_{E_2}\right) \Psi_n^{\left(0,n_2,n_3,p,\alpha_{E_2}+k,\tau\right)} \\ &\quad + e^{(E_2,\tau,k)}\left(\alpha_{E_2}, \beta_{E_2}\right) \Psi_n^{\left(0,n_2,n_3,p,\beta_{E_2}+k,\tau\right)},\ n \in \{2,3\}. \end{aligned} \tag{4.310}$$

$$\mathcal{V}^{(n_2,n_3,p,a,\tau)} = \frac{\chi \Gamma\left(2+p\right)}{\overline{\gamma}_I} \left[\begin{array}{c} F_{g_{SP}}\left(\sigma_S\right) \Gamma\left(n_2+n_3-p+\tau+a, \zeta\epsilon_I\sigma_S\right) \\ + \left(\lambda_{SP}\sigma_S\right)^{a+\tau} G_{2,2}^{2,1}\left(\frac{\zeta\epsilon_I}{\lambda_{SP}} \middle| \begin{array}{c} \left(a+\tau, \sigma_S\lambda_{SP}\right); (1,0) \\ (0,0), \left(n_2+n_3-p+\tau+a, 0\right); - \end{array} \right) \end{array} \right]. \tag{4.311}$$

Remark 12. *It is worth mentioning that the expression for the IP in the absence of a friendly jammer does not have an asymptotic expression as (4.244) is independent of* $\overline{\gamma}_I$.

Proof. One can clearly see from (4.243) and (4.245) that the asymptotic expression for the IP depends on approximating (4.249), which can be obtained by determining the asymptotic expansion of (4.235) and (4.236). To do so, the residues theorem is applied to find the asymptotic expressions of functions given in (4.250)-(4.253).

First, the functions given in (4.250) and (4.252) can be rewritten as Mellin-Barnes integrals as

$$\mathcal{M}^{(n_1,n_2,n_3,p,a,\tau)} = \frac{1}{2\pi j}\int_{\mathcal{C}} \frac{\Gamma\left(n_1+1+s\right)\Gamma\left(\varkappa+s,\zeta\epsilon_I\sigma_S\right)\Gamma\left(1+p-s\right)\Gamma\left(-s\right)}{\Gamma\left(1-s\right)}\left(\frac{\chi\sigma_{S_J}}{\overline{\gamma}_I}\right)^{-s} ds, \tag{4.312}$$

and

$$\begin{aligned}\Phi^{(n_1,n_2,n_3,p,a,\tau)} = \frac{1}{2\pi j}\int_{\mathcal{C}} &\frac{\Gamma\left(n_1+1+s\right)\Gamma\left(\varkappa+s,\zeta\epsilon_I\sigma_S\right)\Gamma\left(1+p-s\right)\Gamma\left(-s\right)}{\Gamma\left(1-s\right)} \\ &\times\Gamma\left(1-s,\sigma_{S_J}\lambda_{S_JP}\right)\left(\frac{\chi}{\lambda_{S_JP}\overline{\gamma}_I}\right)^{-s} ds,\end{aligned} \tag{4.313}$$

where $\varkappa = n_2+n_3-p+1+a+\tau$, and $\mathcal{C}_s$ is a vertical line of integration chosen such as to separate the left poles of the above integrand functions from the right ones,

It is noteworthy that the same complex contour, namely $\mathcal{C}_s$ can be used to evaluate both integrals as the upper incomplete Gamma function has no poles and both integrands have the same poles. Moreover, the conditions of [105, Theorem 1.5] hold. That is, the two above complex integrals can be written as an infinite sum of the poles belonging to the left half plan of $\mathcal{C}$. Furthermore, it is clearly seen that (4.312) and (4.313) both have same left poles $-n_1-1-k$, $k\in\mathbb{N}$. It follows that

$$\mathcal{M}^{(n_1,n_2,n_3,p,a,\tau)} = \sum_{k=0}^{\infty}\frac{(-1)^k\Gamma\left(2+p+n_1+k\right)\Gamma\left(\varkappa-n_1-1-k,\zeta\epsilon_I\sigma_S\right)}{k!\left(n_1+1+k\right)}\left(\frac{\chi\sigma_{S_J}}{\overline{\gamma}_I}\right)^{n_1+1+k}, \tag{4.314}$$

and

$$\begin{aligned}\Phi^{(n_1,n_2,n_3,p,a,\tau)} = \sum_{k=0}^{\infty}&\frac{(-1)^k\Gamma\left(2+p+n_1+k\right)\Gamma\left(\varkappa-n_1-1-k,\zeta\epsilon_I\sigma_S\right)}{k!\left(n_1+1+k\right)} \\ &\times\Gamma\left(2+n_1+k,\sigma_{S_J}\lambda_{S_JP}\right)\left(\frac{\chi}{\lambda_{S_JP}\overline{\gamma}_I}\right)^{n_1+1+k}.\end{aligned} \tag{4.315}$$

By considering only the first term of the infinite summation when $\overline{\gamma}_I \to \infty$, (4.314) and (4.315) can be asymptotically approximated by

$$\mathcal{M}^{(n_1,n_2,n_3,p,a,\tau)} \sim \frac{\Gamma\left(\varkappa - n_1 - 1 - k, \zeta\epsilon_I\sigma_S\right)\Gamma\left(2+p+n_1\right)}{n_1+1}\left(\frac{\chi\sigma_{S_J}}{\overline{\gamma}_I}\right)^{n_1+1}, \tag{4.316}$$

$$\Phi^{(n_1,n_2,n_3,p,a,\tau)} \sim \frac{\Gamma\left(2+n_1, \sigma_{S_J}\lambda_{S_JP}\right)\Gamma\left(2+p+n_1\right)\Gamma\left(\varkappa - n_1 - 1, \zeta\epsilon_I\sigma_S\right)}{n_1+1}\left(\frac{\chi}{\lambda_{S_JP}\overline{\gamma}_I}\right)^{n_1+1}. \tag{4.317}$$

In similar manner to (4.314) and (4.315), (4.251) and (4.253) can be, respectively, expressed as infinite sums as follows

$$\begin{aligned}\mathcal{Y}^{(n_1,n_2,n_3,p,a,\tau)} = \frac{\lambda_{SP}^{a+\tau-1}}{2\pi j}\int_{\mathcal{C}_w}\frac{\Gamma\left(1-a-\tau-w, \sigma_S\lambda_{SP}\right)}{w\left(\frac{\zeta\epsilon_I}{\lambda_{SP}}\right)^w} \\ \times\left[\begin{array}{c}\sum_{k=0}^{\infty}\frac{(-1)^k\Gamma(2+p+n_1+k)\Gamma(\varkappa+w-n_1-1-k)}{k!(n_1+1+k)}\left(\frac{\chi\sigma_{S_J}}{\overline{\gamma}_I}\right)^{n_1+1+k} \\ +\frac{(-1)^k\Gamma(n_1+1-\varkappa-w-k)\Gamma(1+p+\varkappa+w+k)}{k!(\varkappa+w+k)}\left(\frac{\chi\sigma_{S_J}}{\overline{\gamma}_I}\right)^{\varkappa+w+k}\end{array}\right]dw,\end{aligned} \tag{4.318}$$

and

$$\begin{aligned}\mathcal{W}^{(n_1,n_2,n_3,p,a,\tau)} = \int_{\mathcal{C}_w}\frac{\Gamma\left(1-a-\tau-w, \sigma_S\lambda_{SP}\right)}{w}\left(\frac{\zeta\epsilon_I}{\lambda_{SP}}\right)^{-w} \\ \times\left[\begin{array}{c}\sum_{k=0}^{\infty}\frac{(-1)^k\Gamma(2+p+n_1+k)\Gamma(\varkappa+w-n_1-1-k)\Gamma\left(2+n_1+k,\sigma_{S_J}\lambda_{S_JP}\right)}{k!(n_1+1+k)}\left(\frac{\chi}{\lambda_{S_JP}\overline{\gamma}_I}\right)^{n_1+1+k} \\ +\frac{(-1)^k\Gamma(n_1+1-\varkappa-w-k))\Gamma(1+p+\varkappa+w+k)\Gamma\left(1+\varkappa+w+k,\sigma_{S_J}\lambda_{S_JP}\right)}{k!(\varkappa+w+k)}\left(\frac{\chi}{\lambda_{S_JP}\overline{\gamma}_I}\right)^{\varkappa+w+k}\end{array}\right]dw,\end{aligned} \tag{4.319}$$

Subsequently, their asymptotic expression in high SNR regime can be straightforwardly obtained by taking the first term of the two above infinite summations as

$$\mathcal{Y}^{(n_1,n_2,n_3,p,a,\tau)} \sim \frac{\lambda_{SP}^{a+\tau-1}\Gamma\left(2+p+n_1\right)}{n_1+1}\left(\frac{\chi\sigma_{S_J}}{\overline{\gamma}_I}\right)^{n_1+1} G_{2,2}^{2,1}\left(\frac{\zeta\epsilon_I}{\lambda_{SP}}\middle|\begin{array}{c}\left(a+\tau, \sigma_S\lambda_{SP}\right);(1,0) \\ (0,0),(\varkappa-n_1-1,0);-\end{array}\right), \tag{4.320}$$

and

$$\mathcal{W}^{(n_1,n_2,n_3,p,a,\tau)} \sim \frac{\lambda_{SP}^{a+\tau-1}\Gamma\left(2+p+n_1\right)\Gamma\left(2+n_1,\sigma_{S_J}\lambda_{S_JP}\right)}{n_1+1}\left(\frac{\chi}{\lambda_{S_JP}\overline{\gamma}_I}\right)^{n_1+1} \times G_{2,2}^{2,1}\left(\frac{\zeta\epsilon_I}{\lambda_{SP}}\middle|\begin{matrix}(a+\tau,\sigma_S\lambda_{SP});(1,0)\\(0,0),(\varkappa-n_1-1,0);-\end{matrix}\right). \tag{4.321}$$

Lastly, substituting (4.316) alongside (4.320) and (4.317) along with (4.321) into (4.235) and (4.236), respectively, (4.306) and (4.307) are attained. This concludes the proof of Theorem 4.5.2. ■.

4.5.3 Numerical results and discussion

In this part, the derived analytical results are validated through Monte Carlo simulation by generating 10^6 random samples and setting the parameters are summarized in Table 4.5. The turbulence parameters of the FSO hops were generated based on OGS-satellite distance, wavelength, and aperture radius according to [65, Eqs. (4, 9-10)] and [**?**, Eqs. (8)]. The main point of note from Figures 4.18-4.24 is that all closed-form and simulation curves are perfectly matching for numerous system parameters' values, showing the high accuracy of our results.

Table 4.5: Simulation parameters of contribution 7.

Parameter	b_X	m_X	Ω_X	λ_{QP}	α_Z
Value	1.4	2	3	0.8	6.1096
Parameter	β_Z	ξ_Z	γ_{th}(dB)	$\overline{\gamma}_I$(dB)	$\overline{\gamma}_S$(dB)
Value	1.0794	1.1227	2	9	60
Parameter	$\overline{\gamma}_{S_J}$(dB)	μ_{E_2}(dB)	μ_D(dB)	η	ω_D
Value	10	20	40	0.7	0.7

Fig. 4.18 depicts the IP versus $\overline{\gamma}_I$ for various values of Ω_X. It is clearly seen that the greater $\overline{\gamma}_I$ is, the smaller the IP is. This can be justified from (4.212) by the fact that when the MTIP at the PU receiver increases, the SU is allowed to use its maximal transmit power, which contributes to the improvement of the system's secrecy.

Figures 4.19 and 4.20 show the IP versus $\overline{\gamma}_I$ and $\overline{\gamma}_S$, respectively, for various values of $\overline{\gamma}_{S_J}$. It can be ascertained that the IP decreases with the increase of $\overline{\gamma}_I$, $\overline{\gamma}_S$, and $\overline{\gamma}_{S_J}$ as explained in Remark 1. Also, it can be noticed that the presence of a friendly jammer improves the system's

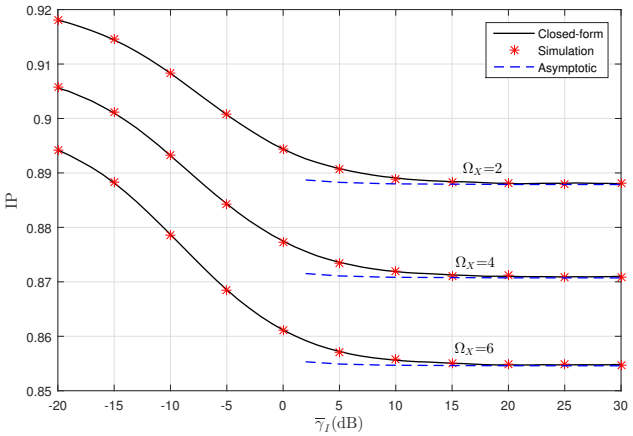

Figure 4.18: IP versus $\overline{\gamma}_I$ in the presence of a friendly jammer for different values of Ω_X, $\rho_D = 0.001$, $\rho_{E_2} = 0.01$, $\sigma_S = \sigma_{S_J} = 1$, $\epsilon_I = 0.1$, and $b_X = 4$.

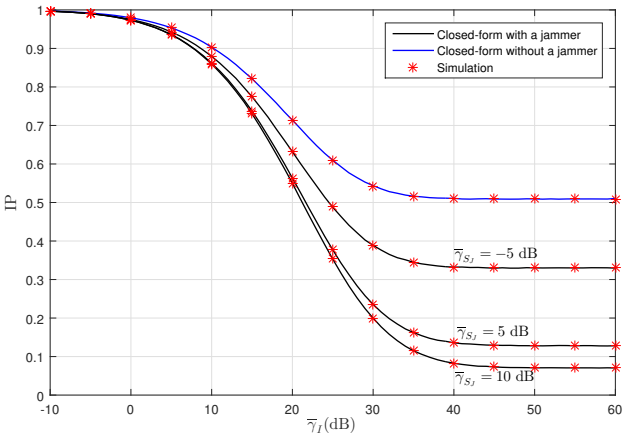

Figure 4.19: IP versus $\overline{\gamma}_I$ for different values of $\overline{\gamma}_{S_J}$.

secrecy per the same Remark. However, one can notice that for low values of $\overline{\gamma}_I$ and $\overline{\gamma}_S$, the friendly jammer does not contribute to the enhancement of the system's secrecy. In fact, it can be seen from (4.215) that the smaller $\overline{\gamma}_I$ and $\overline{\gamma}_S$ are, the smaller U_S is. Thus, it follows from (4.213) and (4.214) that both γ_{E_1} and $\gamma_{E_1}^{(J)}$ approach 0. Moreover, it can be observed that above certain thresholds of either $\overline{\gamma}_I$ or $\overline{\gamma}_S$, respectively, the IP becomes steady as discussed in Remark 1.

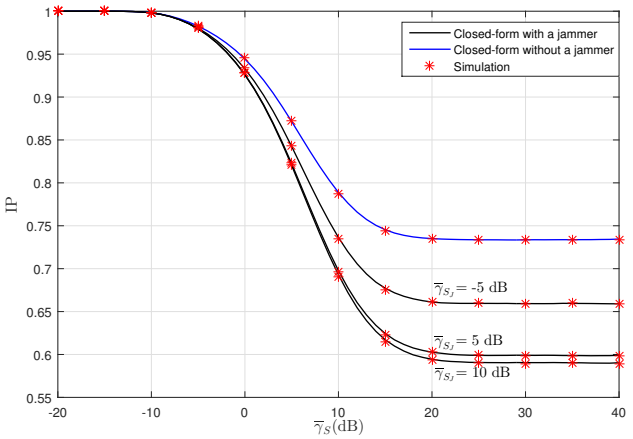

Figure 4.20: IP versus $\overline{\gamma}_S$ for different values of $\overline{\gamma}_{S_J}$.

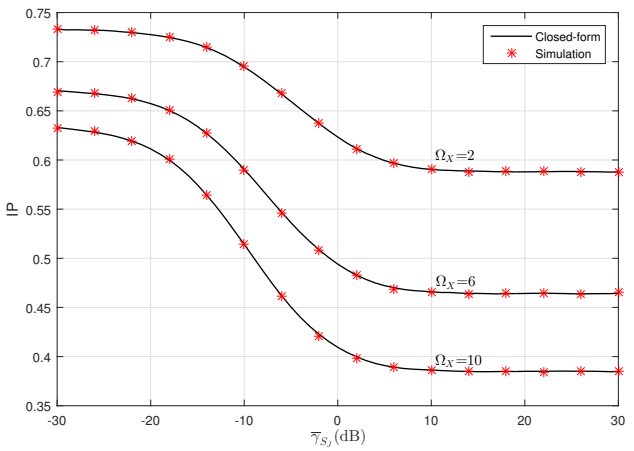

Figure 4.21: IP versus $\overline{\gamma}_{S_J}$ for different values of Ω_X.

Fig. 4.21 shows the IP versus $\overline{\gamma}_{S_J}$ for various values of Ω_X. As can be seen, the IP decreases with the increasing values of the $\overline{\gamma}_{S_J}$. This can be justified from (4.214) as increasing $\overline{\gamma}_{S_J}$

decreases the SNR at the eavesdropper which reduces the wiretap link capacity. Consequently, the secrecy capacity gets enhanced which results in an improvement of the system's secrecy.

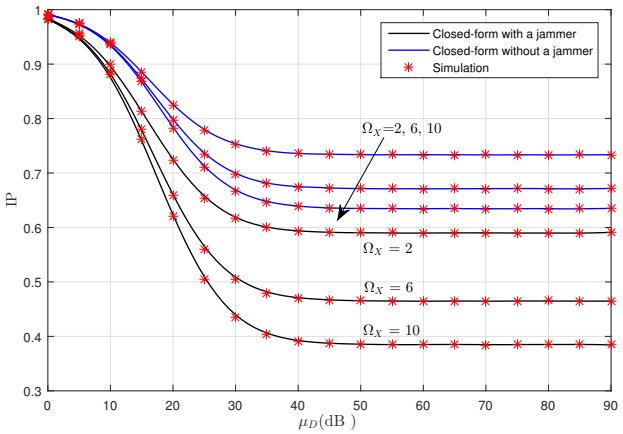

Figure 4.22: IP versus μ_D for different values of Ω_X.

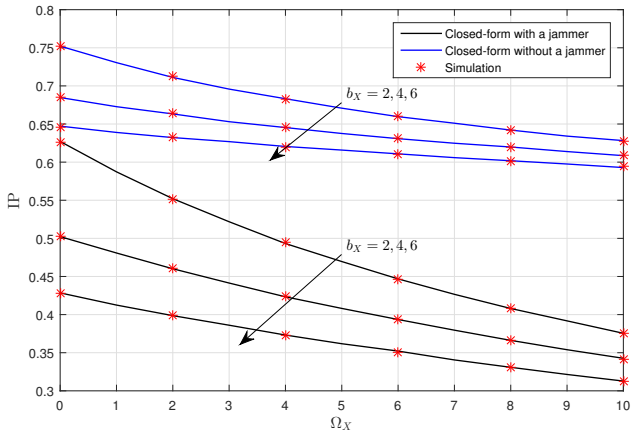

Figure 4.23: IP versus Ω_X for different values of b_X.

Fig. 4.22 illustrates the IP as a function of μ_D in the presence and absence of a friendly jammer for various values of Ω_X. The greater μ_D is, the greater the legitimate end-user SNR is, leading to the improvement of the system's secrecy. This behavior can be interpreted as increasing μ_D leads to the enhancement of the SNR at the destination which improves the legitimate link capacity accordingly.

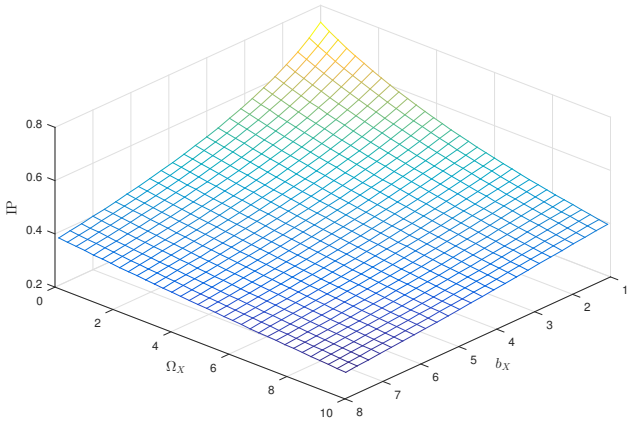

Figure 4.24: IP versus Ω_X and b_X in the presence of a friendly jammer.

Figures 4.23 and 4.24 depict the IP as a function of the average power of the LOS and multipath components in the presence and absence of a friendly jammer. These powers are assumed to be identical for all channels i.e., $\Omega_{SR} = \Omega_{SE_1} = \Omega_{S_JE_1}$, and $b_{SR} = b_{SE_1} = b_{S_JE_1}$.

One can ascertain that increasing the average powers of the LOS and multi-path components at the first hop result in an enhancement of the system's secrecy. Moreover, it is clearly seen that the presence of a friendly jammer is strengthening the system's secrecy. For instance, one can see that for $\Omega_X = 6$ and $b_X = 6$, IP equals 0.35 and 0.61 in the presence and absence of a friendly jammer, respectively.

4.6 Concluding remarks

A secrecy performance analysis was carried out by considering four jamming-based CR setups, namely: a single-hop and dual-hop communication systems over Rayleigh fading channels, dual-hop system with multiples antenna receivers over Nakagami-m fading channels, and a dual-hop HSCTNs. In the three contributions, we considered that multiple sources are taking rounds in transmitting their data in the presence of multiples eavesdroppers, while in the forth contribution one SU node was transmitting its data and another SU node was acting as a friendly jammer. Moreover, a new framework for the IP that considers the presence of two eavesdroppers was derived in the fourth contribution. For all contributions, we derived the IP and SOP by considering two scenarios, namely absence and presence of a friendly jammer and investigated the impact of several key parameters of the network on the system's security. The obtained results showed that the best secrecy is achieved in the presence of a small number of eavesdroppers when increasing the transmit power of the SUs', the number of antennas at the legitimate receiver and the MTIP at the PU as well. Interestingly, we showed that equipping the legitimate nodes by multiple antennas leads to a noticeable enhancement of the system's security rather than sending an artificial noise.

General Conclusion and Future Directions

Conclusions

In this dissertation, we investigated the physical layer security of CRNs by considering different system setups. Interestingly, the derived analytical results could serve as a touchstone for the deployment of futuristic power-limited CRNs.

Secrecy performance analysis of dual-hop CRNs was conducted in Chapter 2 by considering that the relay node is equipped with multiple antennas and performs MRC technique to process the received copies of the transmitted signal. Specifically, we derived the SOP as a performance metric over Nakagami-m fading model and we demonstrated that a better secrecy could be achieved when the tolerated interference power at the primary user as well as the number of the relay's antennas are increased.

In Chapter 3, the PLS of dual-hop EH-based CRNs was investigated over 2 schemes, namely single and multi-antenna relay where the relay is considered as energy-constrained node that was harvesting energy from the received SU signals. The SOP was derived for both contributions over Rayleigh fading model. In the first contribution closed-form expression for the SOP was derived by assuming that the relay is located far from the PU and thus did not need to perform power adaptation. In the second contribution, we derived both closed-form and asymptotic expressions under power adaptation constraint of the SU relay for both i.n.i.d and i.i.d fading channels which added another layer of complexity in terms of analytical computation.

Finally, Chapter 4 dealt with secrecy performance analysis of jamming-based-CRNs. In particular, four system setups were considered, namely direct-link underlay CRN, dual-hop CRNs such that only the destination is equipped with multiple antennas, dual-hop CRNs where all

receivers (i.e., eavesdroppers, relays, and destination) are equipped with multiple antennas, and dual-hop hybrid satellite-terrestrial cognitive radio network. In all contributions, performance metric was derived by considering two scenarios namely (i) presence and (ii) absence of a friendly jammer. In the first and fourth contributions, closed-form and asymptotic expressions for the IP were derived, whereas in the second contribution closed-form expression for the SOP was derived over Rayleigh fading, while exact and approximate expressions over Nakagami-m fading model were given for these metrics in the third one.

Perspectives

Although a solid investigation with regards to PLS of CRNs was conducted so far in the dissertation, we aim to pursue further research by combining multiple techniques so as to achieve higher secrecy. Some future potential research directions can be summarized as follows

- It is envisioned that leveraging NOMA techniques along with CRNs would have a tremendous potential to improve spectrum efficiency and the number of users to be served. Indeed, it has been shown that NOMA enables massive connectivity, and low transmission latency at the cost of the mutual interference and the implementation complexity of the receiver. Therefore, our aim is to investigate the secrecy performance of a dual-hop NOMA-based CRNs under the mutual interference constraints.

- Investigating the physical layer security of CRNs by considering more generalized analytical models for wireless impairments that encompass both multipath fading and shadowing. Additionally, we aim to investigate the impact of more techniques so as to enhance the overall system's security.

Bibliography

[1] J. Chapin and W. Lehr, "Mobile broadband growth, spectrum scarcity, and sustainable competition." TPRC, 2011.

[2] N. Ghasemi and S. Hosseini, "Comparison of smart grid with cognitive radio: Solutions to spectrum scarcity," in *2010 The 12th International Conference on Advanced Communication Technology (ICACT)*, vol. 1. IEEE, 2010, pp. 898–903.

[3] S. Priya and D. J. Inman, *Energy harvesting technologies*. Springer, 2009, vol. 21.

[4] X. Lu, P. Wang, D. Niyato, D. I. Kim, and Z. Han, "Wireless networks with rf energy harvesting: A contemporary survey," *IEEE Communications Surveys & Tutorials*, vol. 17, no. 2, pp. 757–789, 2014.

[5] J. Mitola, "Cognitive radio. an integrated agent architecture for software defined radio." *Doctor of Technology, Royal Inst. Technol. (KTH)*, 2002.

[6] Y. Saleem and M. H. Rehmani, "Primary radio user activity models for cognitive radio networks: A survey," *Journal of Network and Computer Applications*, vol. 43, pp. 1–16, 2014.

[7] M. Piñuela, P. D. Mitcheson, and S. Lucyszyn, "Ambient rf energy harvesting in urban and semi-urban environments," *IEEE Transactions on microwave theory and techniques*, vol. 61, no. 7, pp. 2715–2726, 2013.

[8] Y. Gu and S. Aissa, "Rf-based energy harvesting in decode-and-forward relaying systems: Ergodic and outage capacities," *IEEE Transactions on Wireless Communications*, vol. 14, no. 11, pp. 6425–6434, 2015.

[9] M. Bouabdellah, N. Kaabouch, F. El Bouanani, and H. Ben-Azza, "Network layer attacks and countermeasures in cognitive radio networks: A survey"," *Journal of Information Security and Applications*, vol. 38, pp. 40–49, 2018.

[10] M. R. Manesh, M. S. Apu, N. Kaabouch, and W.-C. Hu, "Performance evaluation of spectrum sensing techniques for cognitive radio systems," in *2016 IEEE 7th Annual Ubiquitous Computing, Electronics & Mobile Communication Conference (UEMCON)*. IEEE, 2016, pp. 1–7.

[11] I. F. Akyildiz, W.-Y. Lee, and K. R. Chowdhury, "Crahns: Cognitive radio ad hoc networks," *AD hoc networks*, vol. 7, no. 5, pp. 810–836, 2009.

[12] A. D. Wyner, "The wire-tap channel," *Bell system technical journal*, vol. 54, no. 8, pp. 1355–1387, 1975.

[13] Y. R. Ortega, P. K. Upadhyay, D. B. da Costa, P. S. Bithas, A. G. Kanatas, U. S. Dias, and R. T. de Sousa Junior, "Joint effect of jamming and noise on the secrecy outage performance of wiretap channels with feedback delay and multiple antennas," *Transactions on Emerging Telecommunications Technologies*, vol. 28, no. 11, p. e3191, 2017.

[14] B. Li, Y. Zou, J. Zhou, F. Wang, W. Cao, and Y.-D. Yao, "Secrecy outage probability analysis of friendly jammer selection aided multiuser scheduling for wireless networks," *IEEE Transactions on Communications*, vol. 67, no. 5, pp. 3482–3495, 2019.

[15] Y. Zhou, P. L. Yeoh, H. Chen, Y. Li, W. Hardjawana, and B. Vucetic, "Secrecy outage probability and jamming coverage of uav-enabled friendly jammer," in *2017 11th International Conference on Signal Processing and Communication Systems (ICSPCS)*. IEEE, 2017, pp. 1–6.

[16] H. Hui, A. L. Swindlehurst, G. Li, and J. Liang, "Secure relay and jammer selection for physical layer security," *IEEE Signal Processing Letters*, vol. 22, no. 8, pp. 1147–1151, 2015.

[17] Y. Zou, X. Wang, and W. Shen, "Optimal relay selection for physical-layer security in cooperative wireless networks," *IEEE journal on selected areas in communications*, vol. 31, no. 10, pp. 2099–2111, 2013.

[18] C. Zhong, T. Ratnarajah, and K.-K. Wong, "Outage analysis of decode-and-forward cognitive dual-hop systems with the interference constraint in nakagami-m fading channels," *IEEE Transactions on Vehicular Technology*, vol. 60, no. 6, pp. 2875–2879, 2011.

[19] Y. Liu, L. Wang, T. T. Duy, M. Elkashlan, and T. Q. Duong, "Relay selection for security enhancement in cognitive relay networks," *IEEE wireless communications letters*, vol. 4, no. 1, pp. 46–49, 2014.

[20] C. Kundu, S. Ghose, and R. Bose, "Secrecy outage of dual-hop regenerative multi-relay system with relay selection," *IEEE Transactions on Wireless Communications*, vol. 14, no. 8, pp. 4614–4625, 2015.

[21] V. N. Q. Bao, N. Linh-Trung, and M. Debbah, "Relay selection schemes for dual-hop networks under security constraints with multiple eavesdroppers," *IEEE transactions on wireless communications*, vol. 12, no. 12, pp. 6076–6085, 2013.

[22] Y. Zou, J. Zhu, X. Wang, and V. C. Leung, "Improving physical-layer security in wireless communications using diversity techniques," *IEEE Network*, vol. 29, no. 1, pp. 42–48, 2015.

[23] X. Chen, C. Zhong, C. Yuen, and H.-H. Chen, "Multi-antenna relay aided wireless physical layer security," *IEEE Communications Magazine*, vol. 53, no. 12, pp. 40–46, 2015.

[24] N. Yang, P. L. Yeoh, M. Elkashlan, R. Schober, and I. B. Collings, "Transmit antenna selection for security enhancement in MIMO wiretap channels," *IEEE Transactions on Communications*, vol. 61, no. 1, pp. 144–154, 2012.

[25] H. Lei, J. Zhang, K.-H. Park, P. Xu, Z. Zhang, G. Pan, and M.-S. Alouini, "Secrecy outage of max–min tas scheme in MIMO-NOMA systems," *IEEE Transactions on Vehicular Technology*, vol. 67, no. 8, pp. 6981–6990, 2018.

[26] L. Wang, M. Elkashlan, J. Huang, R. Schober, and R. K. Mallik, "Secure transmission with antenna selection in MIMO nakagami-m fading channels," *IEEE Transactions on Wireless Communications*, vol. 13, no. 11, pp. 6054–6067, 2014.

[27] E. Illi, F. El Bouanani, F. Ayoub, and M.-S. Alouini, "A PHY layer security analysis of a hybrid high throughput satellite with an optical feeder link," *IEEE Open Journal of the Communications Society*, 2020.

[28] J. Zhu, V. K. Bhargava, and R. Schober, "Secure downlink transmission in massive MIMO system with zero-forcing precoding," in *European Wireless 2014; 20th European Wireless Conference*. VDE, 2014, pp. 1–6.

[29] W. Zhang, J. Chen, Y. Kuo, and Y. Zhou, "Artificial-noise-aided optimal beamforming in layered physical layer security," *IEEE Communications Letters*, vol. 23, no. 1, pp. 72–75, 2018.

[30] A. Salem and K. A. Hamdi, "Secrecy analysis of amplify-and-forward relaying networks with zero forcing," *IET Communications*, vol. 11, no. 14, pp. 2181–2189, 2017.

[31] J. Zhang, G. Pan, and H.-M. Wang, "On physical-layer security in underlay cognitive radio networks with full-duplex wireless-powered secondary system," *IEEE Access*, vol. 4, pp. 3887–3893, 2016.

[32] H. Lei, M. Xu, I. S. Ansari, G. Pan, K. A. Qaraqe, and M.-S. Alouini, "On secure underlay MIMO cognitive radio networks with energy harvesting and transmit antenna selection," *IEEE Transactions on Green Communications and Networking*, vol. 1, no. 2, pp. 192–203, 2017.

[33] P. Yan, Y. Zou, and J. Zhu, "Energy-aware multiuser scheduling for physical-layer security in energy-harvesting underlay cognitive radio systems," *IEEE Transactions on Vehicular Technology*, vol. 67, no. 3, pp. 2084–2096, 2017.

[34] M. Li, H. Yin, Y. Huang, Y. Wang, and R. Yu, "Physical layer security in overlay cognitive radio networks with energy harvesting," *IEEE Transactions on Vehicular Technology*, vol. 67, no. 11, pp. 11 274–11 279, 2018.

[35] A. Singh, M. R. Bhatnagar, and R. K. Mallik, "Secrecy outage of a simultaneous wireless information and power transfer cognitive radio system," *IEEE Wireless Communications Letters*, vol. 5, no. 3, pp. 288–291, 2016.

[36] Y. Zou, "Physical-layer security for spectrum sharing systems," *IEEE Transactions on Wireless Communications*, vol. 16, no. 2, pp. 1319–1329, 2016.

[37] Y. Liu, L. Wang, T. T. Duy, M. Elkashlan, and T. Q. Duong, "Relay selection for security enhancement in cognitive relay networks," *IEEE wireless communications letters*, vol. 4, no. 1, pp. 46–49, 2014.

[38] M. Bouabdellah, F. El Bouanani, and H. Ben-Azza, "Secrecy outage performance for dual-hop underlay cognitive radio system over nakagami-m fading," in *Proceedings of the 2nd International Conference on Smart Digital Environment*, 2018, pp. 70–75.

[39] M. Bouabdellah, F. El Bouanani, P. C. Sofotasios, S. Muhaidat, D. B. Da Costa, K. Mezher, H. Ben-Azza, and G. K. Karagiannidis, "Cooperative energy harvesting cognitive radio networks with spectrum sharing and security constraints," *IEEE Access*, vol. 7, pp. 173 329–173 343, 2019.

[40] M. Bouabdellah, F. El Bouanani, P. C. Sofotasios, D. B. da Costa, K. Mezher, H. Benazza, S. Muhaidat, and G. K. Karagiannidis, "Physical layer security for dual-hop swipt-enabled cr networks," in *2019 16th International Symposium on Wireless Communication Systems (ISWCS)*. IEEE, 2019, pp. 629–634.

[41] M. Bouabdellah, F. El Bouanani, and M.-S. Alouini, "A PHY layer security analysis of uplink cooperative jamming-based underlay CRNs with multi-eavesdroppers," *IEEE Transactions on Cognitive Communications and Networking*, vol. 6, no. 2, pp. 704–717, 2019.

[42] M. Bouabdellah, F. El Bouanani, P. C. Sofotasios, D. B. da Costa, H. Ben-Azza, K. Mezher, and S. Muhaidat, "Intercept probability of underlay uplink CRNs with multi-eavesdroppers," in *2019 IEEE 30th Annual International Symposium on Personal, Indoor and Mobile Radio Communications (PIMRC)*. IEEE, 2019, pp. 1–6.

[43] M. Bouabdellah, F. El Bouanani, D. B. da Costa, P. C. Sofotasios, H. Ben-Azza, K. A. Mezher, and S. Muhaidat, "On the secrecy analysis of dual-hop underlay multi-source crns with multi-eavesdroppers and a multi-antenna destination." in *2019 International Conference on Advanced Communication Technologies and Networking (CommNet)*, 2019, pp. 1–7.

[44] M. Bouabdellah and F. El Bouanani, "A PHY layer security of a jamming-based underlay cognitive hybrid satellite-terrestrial network," *IEEE Transactions on Cognitive Communications and Networking*. [Online]. Available: https://arxiv.org/abs/2009.13993

[45] T. Yucek and H. Arslan, "A survey of spectrum sensing algorithms for cognitive radio applications," *IEEE communications surveys & tutorials*, vol. 11, no. 1, pp. 116–130, 2009.

[46] L. Lu, X. Zhou, U. Onunkwo, and G. Y. Li, "Ten years of research in spectrum sensing and sharing in cognitive radio," *EURASIP journal on wireless communications and networking*, vol. 2012, no. 1, p. 28, 2012.

[47] P. Kolodzy and I. Avoidance, "Spectrum policy task force," *Federal Commun. Comm., Washington, DC, Rep. ET Docket*, vol. 40, no. 4, pp. 147–158, 2002.

[48] B. Wang and K. R. Liu, "Advances in cognitive radio networks: A survey," *IEEE Journal of selected topics in signal processing*, vol. 5, no. 1, pp. 5–23, 2010.

[49] N. Armi, M. Z. Yusoff, and N. M. Saad, "Cooperative spectrum sensing in decentralized cognitive radio system," in *Eurocon 2013*. IEEE, 2013, pp. 113–118.

[50] A. Ghasemi and E. S. Sousa, "Spectrum sensing in cognitive radio networks: requirements, challenges and design trade-offs," *IEEE Communications magazine*, vol. 46, no. 4, pp. 32–39, 2008.

[51] I. F. Akyildiz, W.-Y. Lee, M. C. Vuran, and S. Mohanty, "Next generation/dynamic spectrum access/cognitive radio wireless networks: A survey," *Computer networks*, vol. 50, no. 13, pp. 2127–2159, 2006.

[52] Ž. Tabaković, "A survey of cognitive radio systems," *Post and Electronic Communications Agency, Jurišićeva*, vol. 13, 2011.

[53] S. Haykin, "Cognitive radio: brain-empowered wireless communications," *IEEE journal on selected areas in communications*, vol. 23, no. 2, pp. 201–220, 2005.

[54] M. El Tanab and W. Hamouda, "Resource allocation for underlay cognitive radio networks: A survey," *IEEE Communications Surveys & Tutorials*, vol. 19, no. 2, pp. 1249–1276, 2016.

[55] O. Altrad, S. Muhaidat, A. Al-Dweik, A. Shami, and P. D. Yoo, "Opportunistic spectrum access in cognitive radio networks under imperfect spectrum sensing," *IEEE Transactions on Vehicular Technology*, vol. 63, no. 2, pp. 920–925, 2013.

[56] A. Ali and W. Hamouda, "Low power wideband sensing for one-bit quantized cognitive radio systems," *IEEE Wireless Communications Letters*, vol. 5, no. 1, pp. 16–19, 2015.

[57] L. Giupponi and C. Ibars, "Distributed cooperation in cognitive radio networks: Overlay versus underlay paradigm," in *VTC Spring 2009 - IEEE 69th Vehicular Technology Conference*, 2009, pp. 1–6.

[58] M. Uysal and H. Nouri, "Optical wireless communications—an emerging technology," in *2014 16th international conference on transparent optical networks (ICTON)*. IEEE, 2014, pp. 1–7.

[59] I. S. Ansari, F. Yilmaz, and M.-S. Alouini, "Performance analysis of free-space optical links over Málaga-$\mathcal{M}$ turbulence channels with pointing errors," *IEEE Trans. Wireless Commun.*, vol. 15, no. 1, pp. 91–102, Jan. 2016.

[60] E. Zedini, I. S. Ansari, and M.-S. Alouini, "Performance analysis of mixed nakagami-m and Gamma–Gamma dual-hop fso transmission systems," *IEEE Photonics Journal*, vol. 7, no. 1, pp. 1–20, 2014.

[61] M. Bouabdellah, F. El Bouanani, and H. Ben-Azza, "Hybrid very high throughput satellites: Potential, challenges, and research directions," in *Proceedings of the 8th IEEE International Conference on Communications and Networking (ComNet)*, 2020.

[62] Z. Ghassemlooy, W. Popoola, and S. Rajbhandari, *Optical wireless communications: system and channel modelling with Matlab®*. CRC press, 2019.

[63] H. G. Sandalidis, "Performance of a laser earth-to-satellite link over turbulence and beam wander using the modulated Gamma–Gamma irradiance distribution," *Applied optics*, vol. 50, no. 6, pp. 952–961, 2011.

[64] L. C. Andrews and R. L. Phillips, "Laser beam propagation through random media." SPIE, 2005.

[65] H. Kaushal, G. Kaddoum, V. K. Jain, and S. Kar, "Experimental investigation of optimum beam size for fso uplink," *Optics communications*, vol. 400, pp. 106–114, 2017.

[66] F. Dios, J. A. Rubio, A. Rodríguez, and A. Comerón, "Scintillation and beam-wander analysis in an optical ground station-satellite uplink," *Applied optics*, vol. 43, no. 19, pp. 3866–3873, 2004.

[67] A. Jeffrey and D. Zwillinger, *Table of integrals, series, and products*. Elsevier, 2007.

[68] J. Ma, K. Li, L. Tan, S. Yu, and Y. Cao, "Performance analysis of satellite-to-ground downlink coherent optical communications with spatial diversity over Gamma–Gamma atmospheric turbulence," *Applied optics*, vol. 54, no. 25, pp. 7575–7585, 2015.

[69] H. Kaushal and G. Kaddoum, "Optical communication in space: Challenges and mitigation techniques," *IEEE communications surveys & tutorials*, vol. 19, no. 1, pp. 57–96, 2016.

[70] A. A. Farid and S. Hranilovic, "Outage capacity optimization for free-space optical links with pointing errors," *Journal of Lightwave technology*, vol. 25, no. 7, pp. 1702–1710, 2007.

[71] I. W. Research, *Mathematica Edition: version 11.3*. Champaign, Illinois: Wolfram Research, Inc., 2018.

[72] A. Goldsmith, *Wireless communications*. Cambridge university press, 2005.

[73] M. K. Simon and M.-S. Alouini, *Digital communication over fading channels*. John Wiley & Sons, 2005, vol. 95.

[74] M. V. Jamali and H. Mahdavifar, "Uplink non-orthogonal multiple access over mixed rf-fso systems," *IEEE Transactions on Wireless Communications*, vol. 19, no. 5, pp. 3558–3574, 2020.

[75] P. M. Shankar, *Fading and shadowing in wireless systems*. Springer, 2017.

[76] A. F. Molisch, *Wireless communications*. John Wiley & Sons, 2012, vol. 34.

[77] H. Kim, *Wireless communications systems design*. John Wiley & Sons, 2015.

[78] E. Basar, M. Di Renzo, J. De Rosny, M. Debbah, M.-S. Alouini, and R. Zhang, "Wireless communications through reconfigurable intelligent surfaces," *IEEE Access*, vol. 7, pp. 116 753–116 773, 2019.

[79] M. Z. Win and J. H. Winters, "Analysis of hybrid selection/maximal-ratio combining in rayleigh fading," in *1999 IEEE International Conference on Communications (Cat. No. 99CH36311)*, vol. 1. IEEE, 1999, pp. 6–10.

[80] G. L. Stüber and G. L. Stèuber, *Principles of mobile communication*. Springer, 1996, vol. 2.

[81] P. Grover and A. Sahai, "Shannon meets tesla: Wireless information and power transfer," in *2010 IEEE international symposium on information theory*. IEEE, 2010, pp. 2363–2367.

[82] X. Zhou, R. Zhang, and C. K. Ho, "Wireless information and power transfer: Architecture design and rate-energy tradeoff," *IEEE Transactions on communications*, vol. 61, no. 11, pp. 4754–4767, 2013.

[83] R. Zhang and C. K. Ho, "MIMO broadcasting for simultaneous wireless information and power transfer," *IEEE Transactions on Wireless Communications*, vol. 12, no. 5, pp. 1989–2001, 2013.

[84] G. Pan, H. Lei, Y. Yuan, and Z. Ding, "Performance analysis and optimization for swipt wireless sensor networks," *IEEE Transactions on Communications*, vol. 65, no. 5, pp. 2291–2302, 2017.

[85] A. A. Nasir, X. Zhou, S. Durrani, and R. A. Kennedy, "Relaying protocols for wireless energy harvesting and information processing," *IEEE Transactions on Wireless Communications*, vol. 12, no. 7, pp. 3622–3636, 2013.

[86] X. Mou and H. Sun, "Wireless power transfer: Survey and roadmap," in *2015 IEEE 81st Vehicular Technology Conference (VTC Spring)*. IEEE, 2015, pp. 1–5.

[87] J. Fakidis, S. Videv, S. Kucera, H. Claussen, and H. Haas, "Indoor optical wireless power transfer to small cells at nighttime," *Journal of Lightwave Technology*, vol. 34, no. 13, pp. 3236–3258, 2016.

[88] Y. Alsaba, S. K. A. Rahim, and C. Y. Leow, "Beamforming in wireless energy harvesting communications systems: A survey," *IEEE Communications Surveys & Tutorials*, vol. 20, no. 2, pp. 1329–1360, 2018.

[89] L. R. Varshney, "Transporting information and energy simultaneously," in *2008 IEEE International Symposium on Information Theory*. IEEE, 2008, pp. 1612–1616.

[90] X. Zhou, L. Song, and Y. Zhang, *Physical layer security in wireless communications*. Crc Press, 2013.

[91] E. Illi, F. El Bouanani, D. B. Da Costa, F. Ayoub, and U. S. Dias, "Dual-hop mixed rf-uow communication system: A PHY security analysis," *IEEE Access*, vol. 6, pp. 55 345–55 360, 2018.

[92] H. Lei, Z. Dai, I. S. Ansari, K.-H. Park, G. Pan, and M.-S. Alouini, "On secrecy performance of mixed rf-fso systems," *IEEE Photonics Journal*, vol. 9, no. 4, pp. 1–14, 2017.

[93] N.-P. Nguyen, T. L. Thanh, T. Q. Duong, and A. Nallanathan, "Secure communications in cognitive underlay networks over nakagami-m channel," *Physical Communication*, vol. 25, pp. 610–618, 2017.

[94] H. Tran, G. Kaddoum, F. Gagnon, and L. Sibomana, "Cognitive radio network with secrecy and interference constraints," *Physical Communication*, vol. 22, pp. 32–41, 2017.

[95] M. Elkashlan, L. Wang, T. Q. Duong, G. K. Karagiannidis, and A. Nallanathan, "On the security of cognitive radio networks," *IEEE Transactions on Vehicular Technology*, vol. 64, no. 8, pp. 3790–3795, 2014.

[96] H. Lei, C. Gao, I. S. Ansari, Y. Guo, Y. Zou, G. Pan, and K. A. Qaraqe, "Secrecy outage performance of transmit antenna selection for MIMO underlay cognitive radio systems over nakagami-m channels," *IEEE Transactions on Vehicular Technology*, vol. 66, no. 3, pp. 2237–2250, 2016.

[97] H. Lei, H. Zhang, I. S. Ansari, Z. Ren, G. Pan, K. A. Qaraqe, and M.-S. Alouini, "On secrecy outage of relay selection in underlay cognitive radio networks over nakagami-m fading channels," *IEEE Transactions on Cognitive Communications and Networking*, vol. 3, no. 4, pp. 614–627, 2017.

[98] K. Ho-Van and T. Do-Dac, "Analysis of security performance of relay selection in underlay cognitive networks," *IET Communications*, vol. 12, no. 1, pp. 102–108, 2017.

[99] Y. Liu, L. Wang, T. T. Duy, M. Elkashlan, and T. Q. Duong, "Relay selection for security enhancement in cognitive relay networks," *IEEE wireless communications letters*, vol. 4, no. 1, pp. 46–49, 2014.

[100] M.-N. Nguyen, N.-P. Nguyen, D. B. Da Costa, H.-K. Nguyen, and R. T. De Sousa, "Secure cooperative half-duplex cognitive radio networks with k-th best relay selection," *IEEE Access*, vol. 5, pp. 6678–6687, 2017.

[101] T. Zhang, Y. Huang, Y. Cai, and W. Yang, "Secure transmission in spectrum sharing relaying networks with multiple antennas," *IEEE Communications Letters*, vol. 20, no. 4, pp. 824–827, 2016.

[102] J. Ding, Q. Yang, and J. Yang, "Secrecy outage probability of minimum relay selection in multiple eavesdroppers df cognitive radio networks," in *2016 IEEE 83rd Vehicular Technology Conference (VTC Spring)*. IEEE, 2016, pp. 1–5.

[103] H. Sakran, M. Shokair, O. Nasr, S. El-Rabaie, and A. El-Azm, "Proposed relay selection scheme for physical layer security in cognitive radio networks," *Iet Communications*, vol. 6, no. 16, pp. 2676–2687, 2012.

[104] S. Nadarajah, "A review of results on sums of random variables," *Acta Applicandae Mathematicae*, vol. 103, no. 2, pp. 131–140, 2008.

[105] A. A. Kilbas, *H-transforms: Theory and Applications*. CRC Press, 2004.

[106] Z. Xiang, W. Yang, G. Pan, Y. Cai, and Y. Song, "Physical layer security in cognitive radio inspired NOMA network," *IEEE Journal of Selected Topics in Signal Processing*, vol. 13, no. 3, pp. 700–714, 2019.

[107] Y. Song, W. Yang, Z. Xiang, B. Wang, and Y. Cai, "Secure transmission in mmwave NOMA networks with cognitive power allocation," *IEEE Access*, vol. 7, pp. 76 104–76 119, 2019.

[108] N. Nandan, S. Majhi, and H.-C. Wu, "Secure beamforming for MIMO-NOMA-based cognitive radio network," *IEEE Communications Letters*, vol. 22, no. 8, pp. 1708–1711, 2018.

[109] K. An, M. Lin, J. Ouyang, and W.-P. Zhu, "Secure transmission in cognitive satellite terrestrial networks," *IEEE Journal on Selected Areas in Communications*, vol. 34, no. 11, pp. 3025–3037, 2016.

[110] W. Lu, T. Liang, K. An, and H. Yang, "Secure beamforming and artificial noise algorithms in cognitive satellite-terrestrial networks with multiple eavesdroppers," *IEEE Access*, vol. 6, pp. 65 760–65 771, 2018.

[111] Y. Ai, A. Mathur, M. Cheffena, M. R. Bhatnagar, and H. Lei, "Physical layer security of hybrid satellite-fso cooperative systems," *IEEE Photonics Journal*, vol. 11, no. 1, pp. 1–14, 2019.

Appendices

Appendix A: Accepted and submitted papers

- **Journal papers**

[J.1] M. Bouabdellah, N. Kaabouch, F. El Bouanani, and H. Ben-Azza, "Network Layer Attacks and Countermeasures in Cognitive Radio Networks: A Survey," *Journal of Information Security and Applications*, vol. 38, pp. 40-49, 2018.

[J.2] M. Bouabdellah, F. El Bouanani, P. C. Sofotasios, S. Muhaidat, D. B. Da Costa, K. Mezher, H. Ben-Azza, and G. K. Karagiannidis, "Cooperative Energy Harvesting Cognitive Radio Networks with Spectrum Sharing and Security Constraints," *IEEE Access*, vol. 7, pp. 173 329-173 343, 2019.

[J.3] M. Bouabdellah, F. El Bouanani, and M.-S. Alouini, "A PHY layer security analysis of uplink cooperative jamming-based underlay CRNs with multi-eavesdroppers," *IEEE Transactions on Cognitive Communications and Networking*, vol. 6, no. 2, pp. 704-717, 2019.

[J.4] M. Bouabdellah and F. El Bouanani, "A PHY layer security of a jamming-based underlay cognitive hybrid satellite-terrestrial network," *IEEE Transactions on Cognitive Communications and Networking*. [Online]. Available: https://arxiv.org/abs/2009.13993

- **Conference Papers**

[C.1] M. Bouabdellah, F. El Bouanani, and H. Ben-Azza, "Secrecy Outage Performance for Dual-hop Underlay Cognitive Radio System over Nakagami-m Fading," *in Proceedings of the 2nd International Conference on Smart Digital Environment (ICSDE)*, 2018, pp. 70-75.

[C.2] M. Bouabdellah, F. El Bouanani, and H. Ben-Azza, "Secrecy Outage Probability in Cognitive Radio Networks Subject to Rayleigh Fading Channels," *in Proceedings of the Inter-*

national Conference on Advanced Communication Technologies and Networking (CommNet). IEEE, 2018, pp. 1-5.

[C.3] M. Bouabdellah, F. El Bouanani, D. B. da Costa, P. C. Sofotasios, H. Ben-azza, K. Mezher, S. Muhaidat, "On the Secrecy Analysis of Dual-Hop Underlay Multi-Source CRNs with Multi-Eavesdroppers and a Multi-Antenna Destination", *in Proceedings of the International Conference on Advanced Communication Technologies and Networking (CommNet).* IEEE, 2019, 1-7.

[C.4] M. Bouabdellah, F. El Bouanani, P. C. Sofotasios, D. B. da Costa, K. Mezher, H. Benazza, S. Muhaidat, and G. K. Karagiannidis, "Physical Layer Security for Dual-hop Swipt-Enabled CR Networks," *in Proceedings of the 16th International Symposium on Wireless Communication Systems (ISWCS).* IEEE, 2019, pp. 629-634.

[C.5] M. Bouabdellah, F. El Bouanani, P. C. Sofotasios, D. B. da Costa, H. Ben-Azza, K. Mezher, and S. Muhaidat, "Intercept Probability of Underlay Uplink CRNs with Multieavesdroppers," *in Proceedings of the 30th Annual International Symposium on Personal, Indoor and Mobile Radio Communications (PIMRC).* IEEE, 2019, pp. 1-6.

[C.6] M. Bouabdellah, E. Illi, F. El Bouanani, M.-S. Alouini, "Hybrid Very High Throughput Satellites: Potential, Challenges, and Research Directions", *in Proceedings of the 8th IEEE International Conference on Communications and Networking (ComNet).* IEEE, 2020.